

Self-Organized Pattern Formation in Geological Soft Matter

Julyan H. E. Cartwright

*Instituto Andaluz de Ciencias de la Tierra,
CSIC, 18100 Armilla, Granada,
Spain**

*Instituto Carlos I de Física Teórica y Computacional,
Universidad de Granada, 18071 Granada,
Spain*

Charles S. Cockell

*School of Physics and Astronomy,
University of Edinburgh, Edinburgh,
UK*

Lucas Goehring

*School of Science and Technology,
Nottingham Trent University,
Nottingham NG11 8NS,
UK*

Silvia Holler

*Cellular Computational and Biology Department,
CIBIO, Laboratory for Artificial Biology,
University of Trento,
Via Sommarive 9, Povo, 38123,
Italy*

Sean F. Jordan

*Atlantic Technological University, Sligo,
Ireland*

Pamela Knoll

*School of Physics and Astronomy,
University of Edinburgh, Edinburgh,
UK*

Electra Kotopoulou

*Laboratoire Écologie,
Systématique et Évolution,
Université Paris-Saclay,
France*

Corentin C. Loron

*School of Physics and Astronomy,
University of Edinburgh, Edinburgh,
UK*

Sean McMahon

*School of Physics and Astronomy,
University of Edinburgh, Edinburgh,
UK*

Stephen W. Morris

*Department of Physics,
University of Toronto,
60 St. George St.,
Toronto, ON, Canada,*

M5S 1A7

Anna Neubeck

*Department of Earth Sciences,
Uppsala University, Uppsala,
Sweden*

Carlos Pimentel

*Departamento de Mineralogía y Petrología,
Facultad de Ciencias Geológicas,
Universidad Complutense de Madrid, 28040 Madrid,
Spain[†]*

C. Ignacio Sainz-Díaz

*Instituto Andaluz de Ciencias de la Tierra,
CSIC, 18100 Armilla, Granada,
Spain*

Noushine Shahidzadeh

*University of Amsterdam,
Institute of Physics-Van der Waals-Zeeman Institute,
Science Park 904,
1098 XH Amsterdam,
The Netherlands*

Piotr Szymczak

*Institute of Theoretical Physics,
Faculty of Physics,
University of Warsaw,
Poland[‡]*

(Dated: Draft version 2.6 of December 30, 2024.)

Geological materials are often seen as the antithesis of soft; rocks are hard. However, during the formation of minerals and rocks, all the systems we shall discuss, indeed geological materials in general, pass through a stage where they are soft. This occurs either because they are at a high temperature—igneous or metamorphic rock—or because they are at a lower temperature but in the presence of water—sedimentary rock. For this reason it is useful to introduce soft-matter concepts into the geological domain. There is a universality in the diverse instances of geological patterns that may be appreciated by looking at the common aspect in their formation of having passed through a stage as soft matter.

CONTENTS

I. Introduction	3	H. Glasses	8
II. Soft matter	3	I. Viscoelastic and viscoplastic materials	8
III. Physical types of geological soft matter	5	J. Granular media	9
A. Gels	5	IV. Mesoscale self-organized pattern-forming systems in geology	10
B. Polymers	5	A. Mineral dendrites	10
C. Foams	5	B. Agates	13
D. Colloids	6	C. Opals	21
E. Liquid crystals	6	D. Target patterns	21
F. Membranes	7	E. Orbicular granitoid rocks	22
G. Emulsions	7	F. Striped flint	22
		G. Banded sphalerite	23
		H. Foliation in gneiss	25
		I. Zebra rock	25
		J. Zebra textures	27
		K. Porphyroblasts and spiral garnets	27
		L. Geodes	30
		M. Concretions and nodules	30
		N. Thunder eggs	31

* julyan.cartwright@csic.es

† cpimentelguerra@geo.ucm.es

‡ piotrek@fuw.edu.pl

O. Gold nuggets	31
P. Desert roses and other efflorescence structures	33
Q. Dry salt lakes and convection	36
R. Salt weathering, honeycomb weathering, and tafoni	38
S. Stalactites and icicles	38
T. Stylolites	41
U. Solution pipes, wormholes, and replacement fingers	41
V. Mud volcanoes, pockmarks and seeps	46
W. Hydrothermal vents	47
X. Fulgurites	49
Y. Seismites	50
Z. Menilites	52
AA. Clathrites	53
AB. Sedimentary crack patterns	53
AC. Basalt columns	53
V. Physical mechanisms underlying geological self-organization	57
A. Reaction–diffusion systems	57
B. Liesegang patterns	59
C. Oscillatory zoning	60
D. Fluid-flow instabilities and convective processes	61
E. Rayleigh–Bénard convection	61
F. Rayleigh–Taylor instability	62
G. Kelvin–Helmholtz instability	63
H. Bénard–Marangoni convection	63
I. Capillary flow and coffee-ring instabilities	63
J. Saffman–Taylor instability, viscous fingering and reactive-infiltration instability	64
K. Chaotic advection	66
L. Osmotic processes	67
M. Diffusion-limited aggregation	68
N. Piezoelectricity	69
O. Ostwald ripening	69
P. Fracture processes	70
VI. Summary and outlook	71
Acknowledgments	72
References	72

I. INTRODUCTION

Pattern formation occurs at all scales in our universe, from the very largest of the large-scale structures of the cosmos, to the very smallest, how quarks organize themselves within atomic nuclei. In this review, we concentrate on the millimeter to meter scale, the mesoscale in which the forces at play are not acting on the chemistry of individual atoms, molecules and crystals, but on mesoscopic structures that emerge. In this sense, what we are interested in here is in the realm of soft matter, the subfield of condensed matter comprising systems in which forces acting are of the magnitude of thermal fluctuations. A defining characteristic of soft matter is the mesoscopic scale of physical structures that emerge from self-organization and self-assembly. The structures are much larger than the microscopic scale, the arrangement of atoms and molecules, and yet are much smaller than the macroscopic, overall scale of the material.

The structures that we describe here are seen in rocks, which during their formation all passed through a stage in which they were deformed or structurally altered by

thermal or mechanical stresses of the magnitude of thermal fluctuations. They are all instances of geological soft matter.

Although there is a whole slew of physics books dedicated to self organization and pattern formation, this information is not set in front of geologists. However, there are few exceptions to this rule. The first of these is Peter Ortoleva’s book *Geochemical Self-Organization* (Ortoleva, 1994), which, though written on an important topic, is so mathematically involved that few geoscientists are able to get through it. The second work which touches this subject was the book *Growth, Dissolution and Pattern Formation in Geosystems* (Jamtveit and Meakin, 1999), which was followed by the review article *Sculpting of Rocks by Reactive Fluids* (Jamtveit and Hammer, 2012). In our view, this is much closer to what a review on pattern formation aimed at the geoscience community should look like. However, it is strongly focused on dissolution and precipitation processes in rocks mediated by fluid flow. Although many geological processes have this nature, there is a vast group of phenomena that escapes this framework.

A closely related, soft-matter-oriented article is *Soft Matter Physics of the Ground Beneath Our Feet*, by Voigtländer *et al.* (2024), which focuses on exactly what its title suggests: soil and sediment physics, which are, and remain, soft matter. However, our focus is somewhat different; we examine patterns often found in hard rocks that were once soft, and we argue that this initial softness is crucial for understanding their genesis and structure.

The recent advances in soft matter physics have revealed numerous new processes that provide critical insights into long-standing puzzles in geological pattern formation. These developments offer a fresh perspective, potentially unlocking key mechanisms behind the dynamics of mesoscale patterns in Earth’s systems by linking them to the stage when they were soft. This focus on soft matter introduces novel insights that go beyond the scope of previous reviews, addressing complexities in geological phenomena that have long resisted explanation.

Our aim is that soft-matter physicists with an interest in geological applications will find this review of use. At the same time, we aspire to indicate to geologists the range of mechanisms in soft-matter physics that are involved in geological self organization.

II. SOFT MATTER

Soft matter is a relatively young field of condensed matter physics (De Gennes, 1992). But what is soft matter? Common examples are complex fluids, gels, liquid crystals, polymers, foams, and colloids. What these have in common is that the material properties are not based directly on the molecular-scale structure, but on mesoscopic structures that self organize in the system.

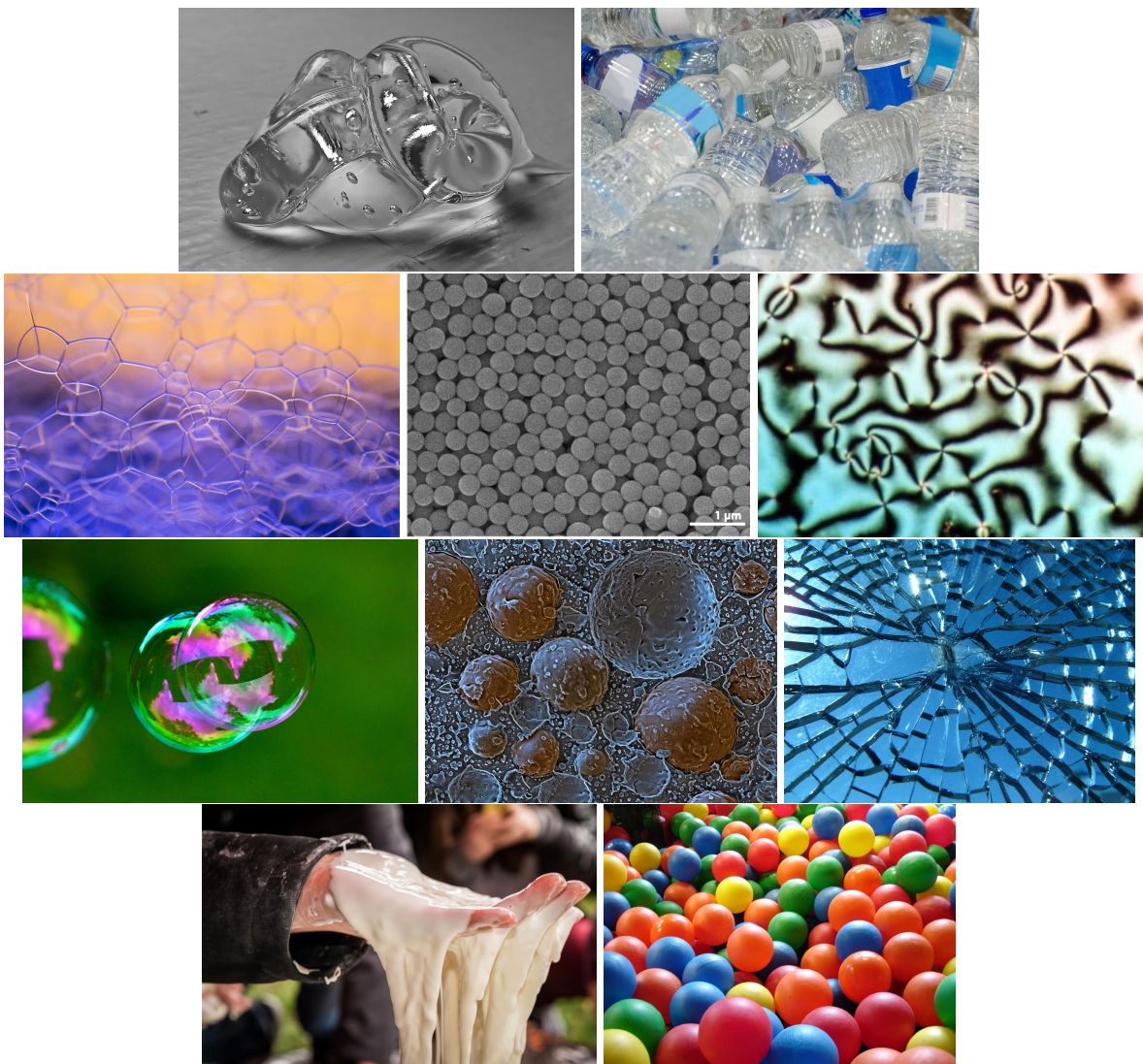


FIG. 1 Examples of soft matter: gel (image: Steve Johnson; CC-BY-2.0), polymer (public domain), foam (AdaptaLux; CC-BY-2.0), colloid (Yasrena, CC-BY-SA-4.0), liquid crystal (Minutemen, CC-BY-SA-2.5), membrane (public domain), emulsion (BASF, CC-BY-NC-ND-2.0), glass (Jef Poskanzer, CC-BY-2.0), viscoelastic material (image: Victor Wong, CC BY-SA 2.0) granular medium (image: Julie Kertesz, CC-BY-2.0).

A number of definitions have been suggested to delineate the field: that soft matter is soft; that it's a complex liquid; that the building blocks are intermediate in size between atoms and the system size; that forces between the building blocks are of the magnitude of thermal fluctuations; that soft matter shows a large response to weak forces. All of these definitions seek to characterize systems in which mesoscopic, intermediate-scale structures self organize and self assemble and can display a sensitive spatial dependence on the initial conditions that is similar to the temporal sensitive dependence that nonlinear chaotic systems experience. All of these definitions also work reasonably well to differentiate soft matter from traditional solid-state condensed matter like metals, semi-

conductors, superconductors, etc. That is to say, all of these give a cutoff at the small scale, but what about a cutoff at larger length-scales?

At large scales, things are less clear. Patterns form in condensed matter up to the large-scale structure of the universe. And the building blocks of those patterns—stars in a galaxy, galaxies in a cluster, etc—are effectively intermediate in scale. In this sense, it would suggest that there is no upper limit. Then, in the geological sciences, the whole of geomorphology might be viewed as soft matter, being deformable and sensitive to collective effects. Indeed, this has been argued (Jerolmack and Daniels, 2019). For example in landscape erosion, relatively weak forces, acting over longish times, make dramatic changes



FIG. 2 Geological gels: these geological materials most probably went through a gel stage in their formation. Agate-filled geode, Brazil (image: James St. John; CC-BY-2.0). Flint, Poland (image: Ra'ike; CC BY-SA 3.0). Gray chert, Knox County, Ohio, USA (image: James St. John; CC-BY-2.0).

to the system. It is clear that this time-scale is different to that the pioneers of the field had in mind. They were thinking of relatively short time scales over which soft materials deform while geology deals with exceedingly long time-scales over which weak forces can make substantial changes. And of course, the mesoscale can be a wide range in geology. Not just in geology, but in the whole of physics, all condensed matter is soft at a large enough length- and time-scale.

We argue that it is valid to accept all of these large-scale phenomena, at least as soft systems, as opposed to soft materials. Nevertheless, doing so opens up the field so much that it is in danger of becoming a catch-all. Here, then, we take an operational definition, that soft matter is what one encounters being studied in soft-matter groups and discussed at soft-matter conferences (Fig. 1). Of course, softness may seem a peculiar idea in the case of rocks, which are pretty hard, so not easily deformed by thermal fluctuations. However, they were soft when they were formed, and they became hard after; i.e., all of these patterns formed through deformation, diffusion or flow in a liquid or gel medium that later solidified. In the following, we consider some common, and overlapping, classes of soft matter systems and see where the geological phenomena fit into these categories as geological soft matter. As Evans *et al.* (2019) put it, “predicting the structure and dynamics of such complex phases of matter from the constituent building blocks and their interactions defines soft-matter science”.

III. PHYSICAL TYPES OF GEOLOGICAL SOFT MATTER

Let us review some common types of soft matter and note instances in which they are found in geology. Note that these types overlap, so that many examples can fall into several of these categories.

A. Gels

A gel is formed of a network of particles suspended in a fluid medium. Agates (Sec. IV.B), flints (Sec. IV.F), and cherts passed through a gel stage during formation (Howard and Rabinovitch, 2018; Oehler, 1976) (Fig. 2). Dendrites from viscous fingers, likewise (Langer, 1989). Basalt columns (Sec. IV.AC) form from a molten lava cooling and cracking (Mallet, 1875; Spry, 1962) near the glass transition temperature (Goehring and Morris, 2008; Ryan and Sammis, 1981), so are both soft and fluidic. Gold dendrites in rocks have been shown to have been formed in silica gel (Monecke *et al.*, 2023). Silica gels may play a role in earthquakes through weakening faults (Borhara and Onasch, 2020; Kirkpatrick *et al.*, 2013).

B. Polymers

A polymer is formed of large macromolecules having repeating subunits. Some minerals in the earth’s crust, aluminosilicate such as clays, quartz, feldspar, and amphiboles, have polymeric atomic structures and thus are instances of geological polymers (Fig. 3). There is a field of research into geopolymers, however in this literature these are generally synthetic, rather than naturally occurring materials, but composed, typically, of aluminosilicates (Davidovits, 1994). There are also petroleum-based geopolymers (Kim *et al.*, 2006).

C. Foams

A foam has gas bubbles dispersed in a liquid or solid. Geological foams (Fig. 4) include bubbly types of lava/magma, such as pumice and scoria (Jaupart and Vergnolle, 1989; Pal, 2003; Vasseur *et al.*, 2020). Pumice is a light and porous volcanic rock that forms when molten lava is rapidly cooled and solidified. The rapid cooling of the lava traps gas bubbles within the rock,



FIG. 3 Geological polymers: Crocidolite, blue asbestos, an amphibole mineral (image: Edgar Vonk; CC-BY-NC-SA-2.0).

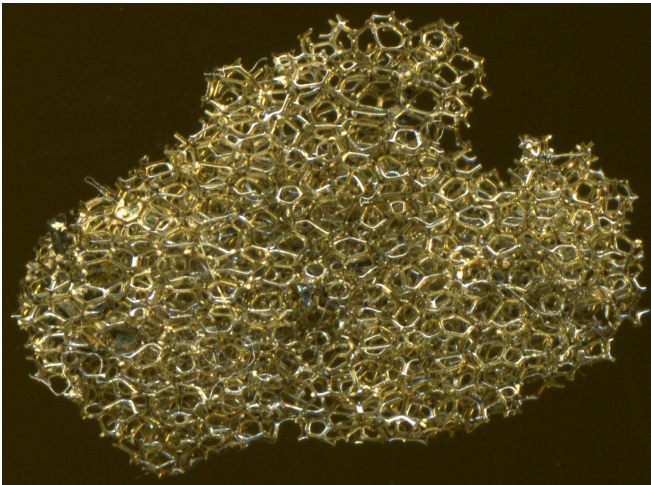


FIG. 4 Geological foam: Reticulite, 1.8 centimeters across, from the Holocene of Hawaii (image: James St. John; CC-BY-2.0).

creating a foam-like structure. Amygdaloidal basalts are the result of the bubbles infilling with secondary minerals from fluid flow (Morris, 1930).

D. Colloids

A colloid has a dispersed phase of particles of one substance suspended in a continuous phase of another substance. Silica and clay minerals are colloidal materials, containing mesoscale (say $\sim 1\text{--}1000$ nm) particles in solution (Yariv and Cross, 1979) (Fig. 5).

Clays are composed of fine-grained minerals, often less than 2 micrometers in size, making them colloidal in na-

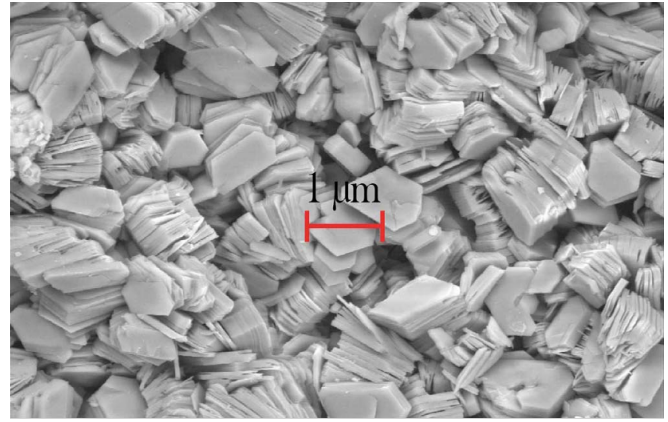


FIG. 5 Geological colloids: phyllosilicates (image: Paedona; CC-BY-SA-4.0).

ture. As colloids, clay particles are small enough to remain suspended in a liquid like water due to Brownian motion, and they possess a large surface area relative to their volume. This high surface area imparts clays with significant surface charge, which influences their interaction with surrounding water molecules and ions. The colloidal nature of clays leads to various important properties i) High plasticity: When mixed with water, clays can deform easily, which is why they are used in ceramics and pottery. ii) Swelling behavior: Some clays, like montmorillonite, can absorb water and swell, which is critical in applications such as drilling muds and as barriers in landfills. iii) Adsorption capacity: Due to their charged surfaces, clays can adsorb ions and organic molecules from solutions, making them useful in environmental cleanup and as catalysts.

Clay minerals, such as montmorillonite or kaolinite, are important colloidal materials in soil and sedimentary rocks. They have a layered structure and can form colloidal suspensions due to their small particle size and surface charge. Colloidal silica, also known as silica gel, can be found in various geological settings, including hydrothermal systems, sedimentary environments, and volcanic ash deposits. Opals (Sec. IV.C) are colloidal crystals of silica nanospheres (Jones *et al.*, 1964). Colloidal iron and manganese oxides often occur in soils, sediments, and weathering profiles. They contribute to the coloration of rocks and play a role in the transport and sequestration of trace elements. Colloidal gold nanoparticles are thought to play a significant role in ore formation (Saunders, 2022).

E. Liquid crystals

A liquid crystal is formed when solid particles within a liquid self-organize into periodic structures owing to their mutual interactions. Suspensions of mineral parti-

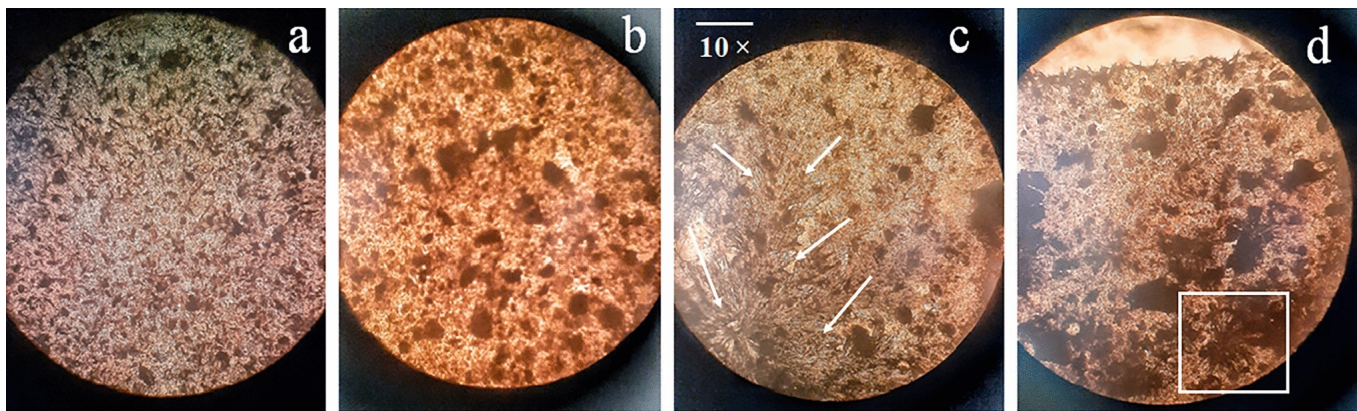


FIG. 6 Geological liquid crystals. POM images observed for 0.055 g of clay in different Na_2SO_4 solvent concentrations. (a) In 0.05 M Na_2SO_4 (b) In 0.1 M Na_2SO_4 (c) In 0.2 M Na_2SO_4 , showing lyotropic aggregates with nematic phase; (d) In 0.2 M Na_2SO_4 , showing lyotropic nematic micelle formation in the lower right corner (image: Neelamma *et al.* (2022)).

cles were noted to be liquid crystals back in 1925 (Zöcher, 1925), and this field is now active in chemical and materials science (Davidson and Gabriel, 2005). Clays are an important geological instance of liquid crystals (Fig. 6). When dispersed in water at certain concentrations, the plate-like clay particles can align themselves in a way that creates ordered phases characteristic of liquid crystals owing to the anisotropic shape (non-spherical, usually flat) of clay particles and the interactions between them: In nematically ordered phases clay particles align along a common axis but do not have positional order. This is similar to the behavior of liquid crystals in display technologies. In more concentrated dispersions, clays can form smectic phases, layered structures, where the particles are arranged in parallel layers with both orientational and positional order. Liquid-crystal textures have been observed in laboratory experiments with aqueous gels of clays (Gabriel *et al.*, 1996; Michot *et al.*, 2006).

The liquid-crystalline behavior of clays is significant in both natural and industrial contexts. In sedimentary basins, the alignment of clay particles can affect the porosity and permeability of the rock, influencing fluid flow and the extraction of resources. In industrial processes, understanding the liquid crystal phases of clays can help in designing materials with specific mechanical or optical properties.

It has been proposed that zebra rock patterns (Sec. IV.I) may have originated as liquid crystals (Matiyevich *et al.*, 2003).

F. Membranes

A membrane is a two-dimensional surface that acts as a selective barrier, allowing some molecules, ions, etc to pass through while inhibiting others from doing so. Geological mineral membranes are found in clays

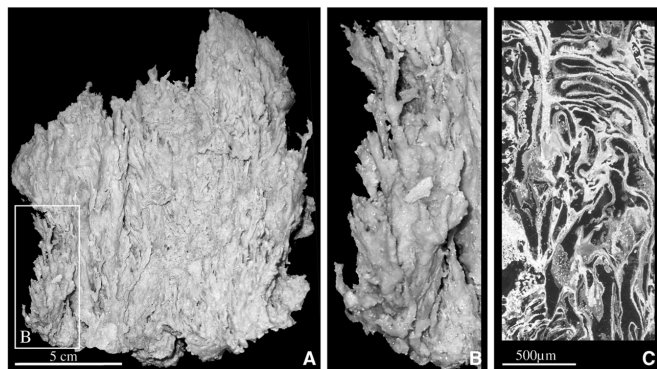


FIG. 7 Geological membranes. A–C progressively zooms in on mineral membranes at Lost City hydrothermal field. From Kelley *et al.* (2005).

(Fritz, 1986; Kharaka and Berry, 1973; Neuzil, 2000b), shales, siltstones, and zeolites, and in hydrothermal vents (Sec. IV.W) and fields (Barge *et al.*, 2015a; Russell *et al.*, 1994) (Fig. 7). These mineral membranes can be semipermeable, allowing only the solvent and not all solute species to pass, leading to osmotic pressures in a geological setting where fluids and semipermeable media interact, affecting fluid flow, chemical transport, and the formation of minerals and deposits.

G. Emulsions

An emulsion consists of droplets of one liquid dispersed in another. Like foams, emulsions are found in magmas (Gogoi and Saikia, 2019), and may be preserved in events such as meteorite impacts (Zieg and Marsh, 2005). Another example is oil shale (Cunningham-Craig, 1916), which forms from an emulsion of kerogen, a precursor to oil, and water-based clay minerals. Over millions



FIG. 8 Geological emulsion: oil shale from the Mahogany Zone of the Green River Formation, Colorado, USA (image: Georgialh; CC-BY-SA-3.0).



FIG. 9 Geological glass: gray obsidian (image: James St. John; CC-BY-2.0).

H. Glasses

A glass is an amorphous, that is, non-crystalline, solid. So-called natural glasses have been used by man long before humans learned to make synthetic glass (Cicconi and Neuville, 2019). Geological glasses can be igneous, metamorphic, or sedimentary (Heide and Heide, 2011). Obsidian is a volcanic glass that forms when felsic (silica-rich) lava cools rapidly with minimal crystal growth. It is usually dark-colored, with a glassy texture, and can contain small gas bubbles or mineral inclusions. It can occasionally be patterned (Ma *et al.*, 2001) (Fig. 9). Tektites are glassy objects that are formed during meteorite impacts. They are created when the intense heat and pressure from the impact turn surrounding rocks and soil into molten glass, which then solidifies into teardrop-shaped objects. One instance to be discussed further below is that of fulgurites (Sec. IV.X). Fulgurites are formed when lightning strikes sandy soil or sandy near-surface sediments. The extreme heat generated by the lightning melts the sand, forming hollow glass tubes or branching structures (Pasek *et al.*, 2012).

I. Viscoelastic and viscoplastic materials

The study of the nonlinear rheology of geological materials dates back hundreds of years (Boswell, 1951) and

of years, the kerogen-water emulsion settles, undergoes pressure and temperature changes, and transforms into a solid, shale-like rock (Fig. 8).



FIG. 10 Geological viscoelasticity and viscoplasticity. Aphebian-aged marble showing plastic deformation (image: Mike Beaugard; CC-BY-2.0). Soft sediment deformation in exposed Dead Sea sediment, Israel, gives rise to a Kelvin-Helmholtz shear instability (image: Mark A. Wilson; CC-BY-SA-3.0).

has been investigated for its implications in tectonics and orogenesis (Biot, 1961). Rocks generally show viscoelastic and viscoplastic behavior (Fig. 10). Viscoelasticity is a property of materials that exhibit both viscous (fluid-like, without a fixed shape) and elastic (spring-like, recoverable) responses under deformation. This behavior is time-dependent, meaning that the material response varies depending on the rate and duration of applied stress. Quicksands are a well-known example of a viscoelastic material having complex behavior owing to shear thickening (Kadau *et al.*, 2009; Khaldoun *et al.*, 2005; Matthes, 1953). In rocks, viscoelastic behavior can be observed when the applied stress is within a certain range and the time period of stress is relatively short. In this case, rocks tend to deform partially elastically and partially viscously. The elastic component allows the rock partially to recover its original shape after the stress is released, while the viscous component leads to permanent deformation or creep. Viscoplasticity refers to the behavior of materials that exhibit both viscous (fluid-like, without a fixed shape) and plastic (inelastic, non-recoverable) responses when subjected to stress. Unlike viscoelasticity, viscoplasticity is not time-dependent, and the material response is dependent on the stress magnitude rather than the rate or duration of the applied stress. In rocks, viscoplastic behavior is observed when the stress level exceeds a certain threshold. At high stress levels, rocks deform permanently without elastic recovery. This plastic deformation is related to the breaking and rearrangement of grains or crystal structures within the rock, leading to permanent deformation. Viscoplastic behavior is commonly seen in geological processes such as folding, faulting, or flow of rock masses under high-pressure conditions. Flowing lava shows this behavior (Griffiths, 2000). Sinkhole formation has been modelled with a viscoelastic model (Shalev and Lyakhovskiy, 2012)

and dikes and diapirs investigated in viscoelastic rock (Rubin, 1993). Viscoplastic soils, such as clays, show pattern formation in the form of shrinkage cracks (Vevakis and Poulet, 2021). Viscoelastic and viscoplastic responses are seen to be of importance for compositional banding and foliation in rocks (Burnley, 2013).

J. Granular media

A granular medium is composed of solid grains that have frictional interactions so that they sometimes act like solids, and other times like fluids (Andreotti *et al.*, 2013). Many granular media are part of the soft-matter family (Gravish and I. Goldman, 2016), and it is clear that many geological systems involve such granular materials as sand, soil, that have properties of both solids and fluids, but also phenomena found in neither, such as jamming and avalanches (Zheng *et al.*, 2021). Granular media can be found in myriad geological environments (Fig. 11). All clastic sediments can be considered as granular media. Listing all the environments in which they accumulate would fill a book; to mention just a few instances, granular media are a major component of sedimentary rocks such as sandstone, conglomerate, and breccia formed from the accumulation and lithification of sand, gravel, or pebbles. Granular media are abundant in river channels, streams, and floodplains, transported by erosion and deposition processes, forming riverbeds, river bars, and river deltas. In aeolian environments such as deserts, granular media are prevalent. They include sand dunes, sand sheets, and desert pavements formed by the transport and deposition of sand particles. Deposits of granular media like sand, gravel, and till can be observed in glacial landscapes. These include moraines, eskers, kames, and drumlins that are formed by glacial erosion



FIG. 11 Geological granular media: sand dunes near Dakhla Oasis, Western Desert, Egypt (image: Vyacheslav Argenberg, CC-BY-2.0); travertine-cemented conglomerate (image: James St. John; CC-BY-2.0).

and deposition. During volcanic eruptions, granular media like ash, lapilli, and volcanic bombs are ejected and can accumulate both locally and over wider areas. These materials are commonly found in volcanic ash fall deposits and pyroclastic flows. Granular media are found in coastal zones in the form of beaches, barrier islands, sandbars, and offshore sediments. These features are shaped by wave and tidal action, as well as longshore currents. And granular media are present on the ocean floor, especially in areas where river sediments are transported and deposited. This includes features like submarine canyons, turbidite deposits, and abyssal plains.

IV. MESOSCALE SELF-ORGANIZED PATTERN-FORMING SYSTEMS IN GEOLOGY

There are found in geological settings notable examples of phenomena in which material is self-organized at the mesoscale. In this section we review prominent examples of mesoscale pattern-forming systems in geology.

A. Mineral dendrites

Two-dimensional mineral dendrites—black or red-brown deposits on the surfaces of limestones, sandstones, opals or agates—have intrigued people with their form—dendrite is from the Greek *dendritēs* ‘treelike’—for centuries. We can find mention of them as early as Pliny the Elder’s *Natural History* of 77 CE (Pliny the Elder, 77), but more detailed descriptions and classifications appeared with the rise of naturalism and mineral collecting in the early 18th century (Mylius, 1709; Scheuchzer, 1700); see Fig. 12 for a reproduction of a plate with dendrites in Mylius’ *Memorabilium Saxoniae Subterraneae* of 1709. The organic-like form of the den-

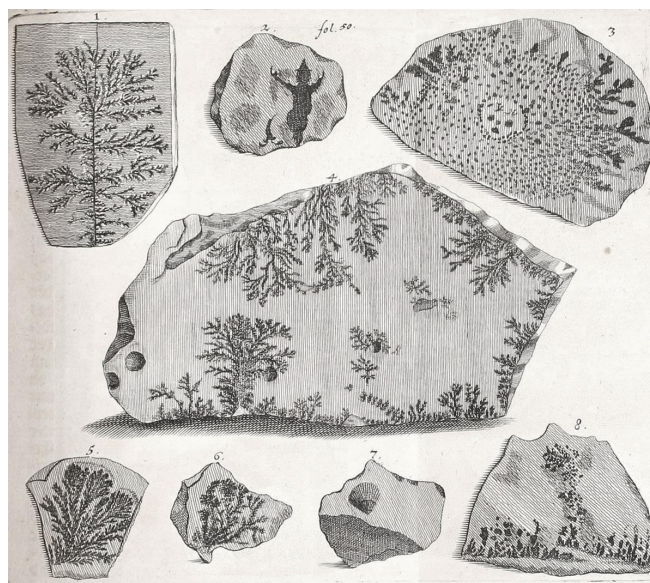


FIG. 12 Dendrite drawings in “*Memorabilium Saxoniae Subterraneae*” by Gotfried Friedrich Mylius (1709).

drites led some naturalists to the conviction that they are fossilized plants. However, by mid-18th century, they were pinpointed as patterns emerging as a result of physical processes. Some authors were even trying to recreate this process, for example, Emanuel Mendes da Costa in his *Natural History of Fossils* (Mendes da Costa, 1757) mentions that similar patterns can be created by inserting oil in between two sandstone plates and then pulling apart the plates, making this the first known experiment in viscous fingering (Sec. V.J). For a modern, detailed review of various geochemical types and shapes of mineral dendrites the reader is referred to the excellent paper by Van Straaten (1978).



FIG. 13 Quasi-2d dendrites in agate (A), and limestone (B–D). In B and C they originate from fractures, whereas in D there are multiple nucleation point. The image in (A) is by Chip Clark, Smithsonian Institution, public domain; (B) is by Jessica Rosenkrantz, published with permission of the author; (C) is from Adobe stock photography and (D) is by Dr. Jürg Alean, published with permission of the author.

Dendrites can be composed of various minerals, including manganese and iron oxides, copper, silver, and other metallic minerals. The most common are planar manganese and iron oxide dendrites formed along the bedding planes in limestones and sandstones, such as the ones shown in Fig. 13B–D. The bases of the dendrites are then usually associated with the intersections of the bedding planes with joints or other fractures, from where they grow in a direction perpendicular to that of the fracture at the starting point (cf. Fig. 13B–C). Interestingly, however, other forms also occur, which consist of a multitude of small, radial clusters, not connected to the base (cf., Fig. 13D).

Mineral dendrites are low-crystallinity products, with the absence of even short range three-dimensional pe-

riodic structure (García-Ruiz *et al.*, 1994), which suggests that they were formed by the precipitation of colloidal particles. This distinguishes them from crystalline dendrites often encountered in metallurgy (Trivedi and Kurz, 1994). Dendritic growth occurs at high supersaturation (highly concentrated solutions). The latter can be achieved in some environmental conditions via supercooling or evaporation in confinement. Crystalline dendrites are usually needle-like, with a significant control of the crystalline anisotropy and with thermal effects playing a key role during their formation. In the petrological context, such dendritic crystals often form as a result of magma crystallization in rapidly cooled rocks (Barbey *et al.*, 2019; Fowler *et al.*, 1989; Welsch *et al.*, 2013). Mineral dendrites, on the other hand,

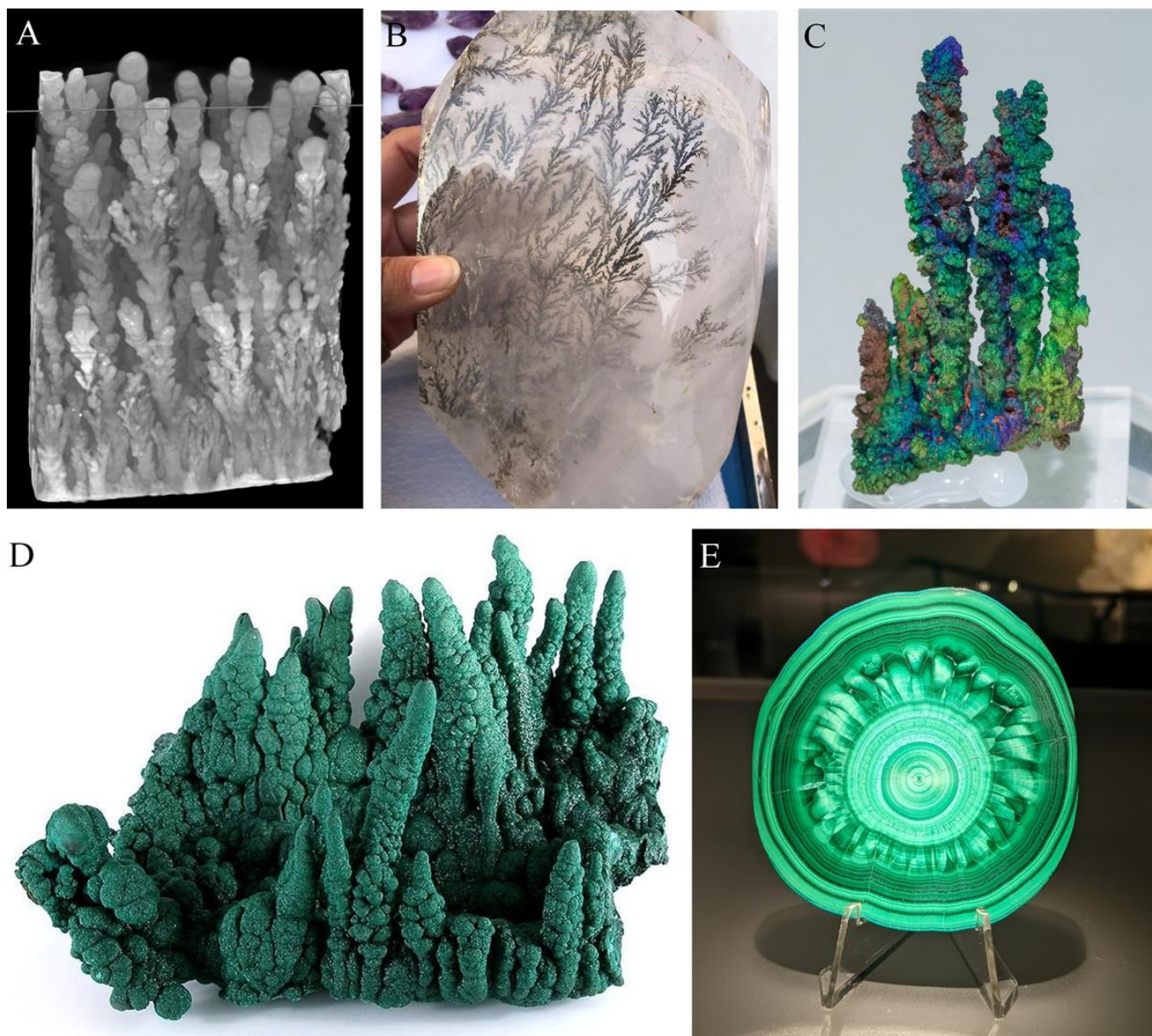


FIG. 14 Upper row: Three dimensional manganese oxide dendrites in zeolites (A) (Hou *et al.*, 2023) quartz (B). Lower row: columnar goethite (C) and malachite (D), and a cross section of a malachite column (E). The image in (B) is taken from Yuping Crystal Wholesale, reproduced with permission. The specimen and photo in (C) is from MVM (Minerals - Virtual Museum), reproduced with permission. The photo in (D) is by Robert M. Lavinsky, distributed under cc license. The photo in (E) is the property of Alfie Norville Gem & Mineral Museum of the University of Arizona, reproduced with permission.

have a branched, fractal structure which is strikingly similar to diffusion-limited aggregation (Witten Jr and Sander, 1981); Sec. V.M. This observation led Chopard *et al.* (1991) to propose a model in which two species (A and B) diffuse, forming species C which then aggregates, although the geochemical details of this process and the nature of the particles remain unspecified. This model has been extended by Hou *et al.* (2023). In their model, fluid pushes an oxygenated matrix pore fluid away from the joints and mixes with it, generating an

oversaturated Mn oxide solution. The resulting fern-like dendrites are made up a trunk, which grows very rapidly at the start of crystallization, followed by primary and secondary branches which grow in a more advanced state with slower growth rates. Laboratory studies on Mn oxide formation (Huang *et al.*, 2015; Li *et al.*, 2014) have confirmed that such conditions promote the initial growth of Mn-oxide nanoparticles. Such particles, once formed, diffuse through the rock matrix, and become attached to the Mn-oxide-coated joint, initiating an

dendrite growth. Dendrite formation would be then a nonstandard crystallization pathway, via particle attachment, which is increasingly recognized as an important and widespread type of crystal growth (Cöelfen and Antonietti, 2008; De Yoreo *et al.*, 2015). Hou *et al.* (2023) emphasize that the shape of the dendrite will also be a function of its interfacial energy as well as the concentration of the manganese oxide particles around it.

García-Ruiz *et al.* (1994) alternatively proposed that dendrites are the viscous fingering pattern (Sec. V.J) created when manganese-rich fluid infiltrated a fracture space filled with presumably much more viscous, oxygenated fluid, possibly a colloidal suspension. In essence, this mechanism aligns with da Costa’s 1757 conjecture (Mendes da Costa, 1757). Interestingly—and frustratingly—both models, DLA and viscous fingering, give rise to patterns of the same fractal dimension, around 1.70, as they are in the same universality class (Mathiesen *et al.*, 2006), thus geometric attributes of these patterns are insufficient for discerning the correct physical growth process. Other arguments invoked in this discussion are the lack of manganese outside the dendrites, which is easier to explain in terms of a viscous fingering model, unless one assumes that the DLA mechanism is highly effective in clearing the entire bedding plane of MnO particles formed in the space outside the dendrites (García-Ruiz *et al.*, 1994). On the other hand, viscous fingering cannot easily explain the formation of isolated dendrites, not connected to the main joint, as in Fig. 13D or banding structures, like the ones in Fig. 13A. Additionally, one can raise a mass conservation issue. Manganese concentrations in dendrites are much higher than those in Mn-bearing groundwater solutions, thus a large volume of solution, significantly larger than the volume of the visible pattern, is needed to create a dendrite.

In contrast to the quasi-2D planar dendrites growing along the bedding planes, internal dendrites are fully three-dimensional structures (Fig. 14), which start from fissures and penetrate into the porous rock (Hou *et al.*, 2023; Potter and Rossman, 1979; Van Straaten, 1978). Some of these dendrites are composed of manganese and iron oxides, just like their 2D counterparts, but there is also an interesting class of precious metal dendrites—self-organized gold, silver and their alloy electrum—, which occur, in particular, in ultrahigh-grade gold “bonanza” veins (Monecke *et al.*, 2023; Saunders, 2022; Saunders and Burke, 2017; Schoenly and Saunders, 1993) and are thus economically important. Two models of their formation have been proposed. The first one is the particle attachment model, in which dendrites form by accretion of colloidal gold or silver particles (Saunders, 1994; Saunders *et al.*, 2020). This is similar in spirit to the particle attachment growth model of the manganese oxide dendrites described above, with the only difference being that gold/silver particles are not produced locally, but are formed deep in the hydrothermal system and then

carried up by the fluid to the epithermal setting. An alternative mechanism for the growth of gold dendrites, following a classical crystallization pathway based on ion addition, was proposed by Monecke *et al.* (2023). See also Sec. IV.O.

As is often the case in earth sciences, a similar appearance of the structure does not necessarily imply a similar genesis. The three-dimensional dendrites growing in a zeolite matrix, as shown in Fig. 14A, are similar in appearance to some of the free-standing stalagmite-like forms of minerals, such as goethite (Fig. 14C) or malachite (Fig. 14D), which form in rock cavities from slowly dripping solutions. This might suggest a growth mechanism similar to that of stalactites, as discussed in Section IV.S, although in the latter, CO₂ degassing is important, which does not have a clear parallel in malachite, goethite, and other columnar forms. Instead, they are most probably formed by an evaporative growth mechanism (Keller, 1990), although other mechanisms, involving reaction-diffusion self-organization, were also invoked (Papineau, 2020). It is worth noting that, in contrast to agates (Sec. IV.B), malachite can be formed in the laboratory by evaporative growth, with patterns virtually indistinguishable from the natural ones (Balitsky *et al.*, 1987; Petrov *et al.*, 2013).

B. Agates

Agates (Fig. 15) are a banded type of chalcedony, which is a cryptocrystalline form of silica. They are renowned for their stunning appearance, characterized by unique, translucent layers of multiple colors. The term ‘agate’ originates from the Greek word *akhátes*, referring to a river in Sicily where agates were commonly found. Agates form in cavities created by gaseous bubbles trapped in erupted lavas, which eventually become filled with silica. While the characteristic layered structures lining the walls are perhaps the most well-known features of agates, other interesting patterns also require explanation, such as the horizontal, parallel layers known as ‘Uruguay banding’ and infiltration channels: bulbous structures that develop near the boundary of the agate-containing amygdule (see Fig. 21). The origin of colors in agate is linked to the presence of pigments on one side and variations in crystallite size and microstructure (including water content) on the other, as noted by (Götze *et al.*, 2020). The most common colors in agate are white, grey, and blue. White agate bands are associated with the presence of thick, plate-like crystallites, which can totally reflect incident light, while the surrounding clear areas contain globular crystallites that allow a portion of white light to be transmitted. The blue color is caused by the dispersion of light on the microparticles (Tyndall effect). On the other hand, the color pigments are mostly iron and manganese oxides and hydroxides, responsible



FIG. 15 Agates and their banded patterns. (A) Black River Agate (photo by Matthew Wood, reproduced with permission), (B) Lake Superior agate with a smoky quartz exterior and carnelian center with mineral spherulites (photo by Karen Brzys, Gitche Gumee Museum/Agatelady Rock Shop, Grand Marais, MI, USA, www.agateladyrockshop.com, reproduced with permission), (C) Laguna Agate, Mexico (Smithsonian Museum, distributed under CC license) (D) Crazy Lace Agate, Mexico (photo by James St. John, distributed under CC license) (E) Laguna Agate (Conejeros Claim), from Chihuahua, Mexico (specimen from Hannes Holzmann collection, photographed by Albert Russ, reproduced with permission. and (F) Botswana agate from near Bobanong, Botswana (photo by Takehiro Toge, distributed under CC license)

for red and yellow colorations. This results in a wide range of colors and patterns, making each agate distinct and visually appealing.

Importantly, there is more to the agate pattern than what is visible to the naked eye; microscopic studies reveal a much finer banded structure with alternating layers of defect-rich chalcedony and macrocrystalline quartz (Cady *et al.*, 1998; French *et al.*, 2013; Frondel, 1985; Heaney and Davis, 1995), as illustrated in Fig. 16. The banding in Fig. 16 has a wave-length in the range of approximately $100\mu\text{m}$, but similar oscillatory zonation in defect concentration has been reported at the length-scale of a $0.5\text{--}5\mu\text{m}$ (Frondel, 1978; Heaney and Davis, 1995; Jones, 1952), clearly visible in a cross-polarized light (Fig. 17A). The change of refractive index along these produces a rainbow-like display of colors in iris agates (Fig. 17B). Note that zones with iris banding exist in nearly every agate, although they are often concealed by pigmentation.

The microscopic images strongly suggest that microcrystalline chalcedony fibers nucleate on the cavity walls and grow inward towards the center of the cavity. Initially, there is spherulitic growth, with the fibers radiat-

ing outward from separate nucleation points at the edges of the system. Soon, a common banding is formed, running equidistant to the cavity walls (Götze *et al.*, 2020; Landmesser, 1984). The underlying spherulitic structure is particularly striking when observed in cross-polarized light (Fig. 16B and 18C), which shows the chains of quartz crystals of similar orientation growing from different nucleation points.

The debate surrounding the genesis of agate is both challenging and contentious, primarily due to the lack of a genuine lab synthesis that replicates natural agate formations. As a result, numerous theories and approaches have emerged, many of which contradict each other. Consequently, debates about the origin of agate remain as heated today as they were in the 19th century, when most of the agate-genesis models were first formulated. An unsurpassed review of these debates can be found in the paper by Landmesser (1984); more recent reviews can be found in Götze *et al.* (2020) and Moxon and Palyanova (2020).

In general, theories about the genesis of agate patterns can be divided into two broad classes based on what they consider to be the cause of the banding (Liesegang, 1910).

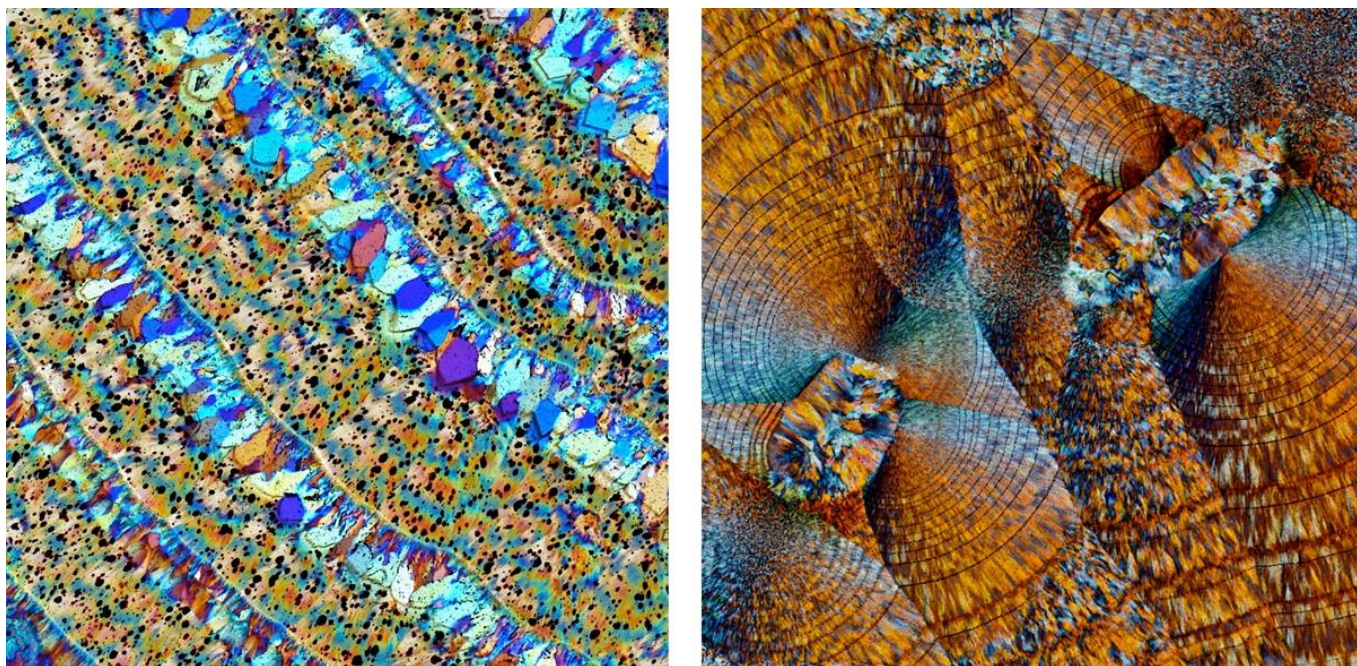


FIG. 16 A: Agate micro-banding with fibrous chalcedony interspersed with macrocrystalline quartz. B: Spherulitic pattern in an agate with chalcedony fibers radiating from the nucleation points on the rim of an agate. Photos courtesy of Prof. Bernardo Cesare, University of Padova, Italy

External rhythm models hypothesize that agate is an accumulation structure, its pattern reflecting alternating or periodic changes in environmental conditions. Agate, in this view, could be seen as a geological counterpart to the pseudo-mineral *fordite* (Fig. 19), an accumulation of enamel paint collected in hundreds of layers in automobile factories during lacquering (Hsu and Lucas, 2016; Nova *et al.*, 2021). However, questions remain about how this geological ‘lacquering process’ is carried out, including the temperature and form in which silica enters the cavity—here, numerous theories and ideas abound. Internal rhythm theories, on the other hand, link the formation of the agate structure to self-organization processes within the developing agate itself, treating it as a closed system. They usually assume that the agate was filled first by the gelatinous silica, and then a reaction-diffusion process of some kind took place which resulted in the formation of the banded pattern.

The first external rhythm theories were formulated in the 19th century. Haidinger (1848) hypothesized that agate patterns form where aqueous silica solutions seep into rock pores, precipitating on the cavity walls. This led to a debate about how the silica solution could enter the cavity after the layers had solidified. Noeggerath (1849) proposed infiltration channels as possible pathways for the solution, facilitating the continuous development of precipitate layers. On the other hand, Kenngott (1851) argued that the silica deposits in a gel state and only gradually hardens due to contraction, suggest-

ing that the deposition, while not yet solidified, remains permeable to seeping solutions.

The above models involve normal temperatures and pressures, but there are also several theories involving elevated temperatures. Reusch (1864) proposed that the cavities were repeatedly filled and then emptied due to intermittent hydrothermal activity in the rock. The solutions fill the cavities when driven upward by advancing steam; once the steam reaches the cavity, it empties again. Each infiltration produces a single layer of silica, again in a close resemblance to the car lacquering process. More recently, Harris (1989) based on oxygen isotope study of Jurassic agates concluded that the agate formation process involved periodic boiling of the hydrothermal solutions, with quartzine layers in agates forming from water vapor and the chalcedony layers crystallizing from liquid water. With each filling process, a fine layer of agate forms from the solution adhering to the cavity edge.

In external rhythm theories, agate, as an accumulation structure, should reflect the changing hydrogeological conditions. Returning to the comparison with *fordite*, one can reconstruct the colors of cars lacquered at a particular workstation by analyzing the successive layers. It is also expected that two *fordites*, created nearby, will have the same succession of stripes. However, this is not the case for agates; the banded structures of nearby agates are not correlated (Fig. 20), an argument frequently put forward against the external rhythm con-

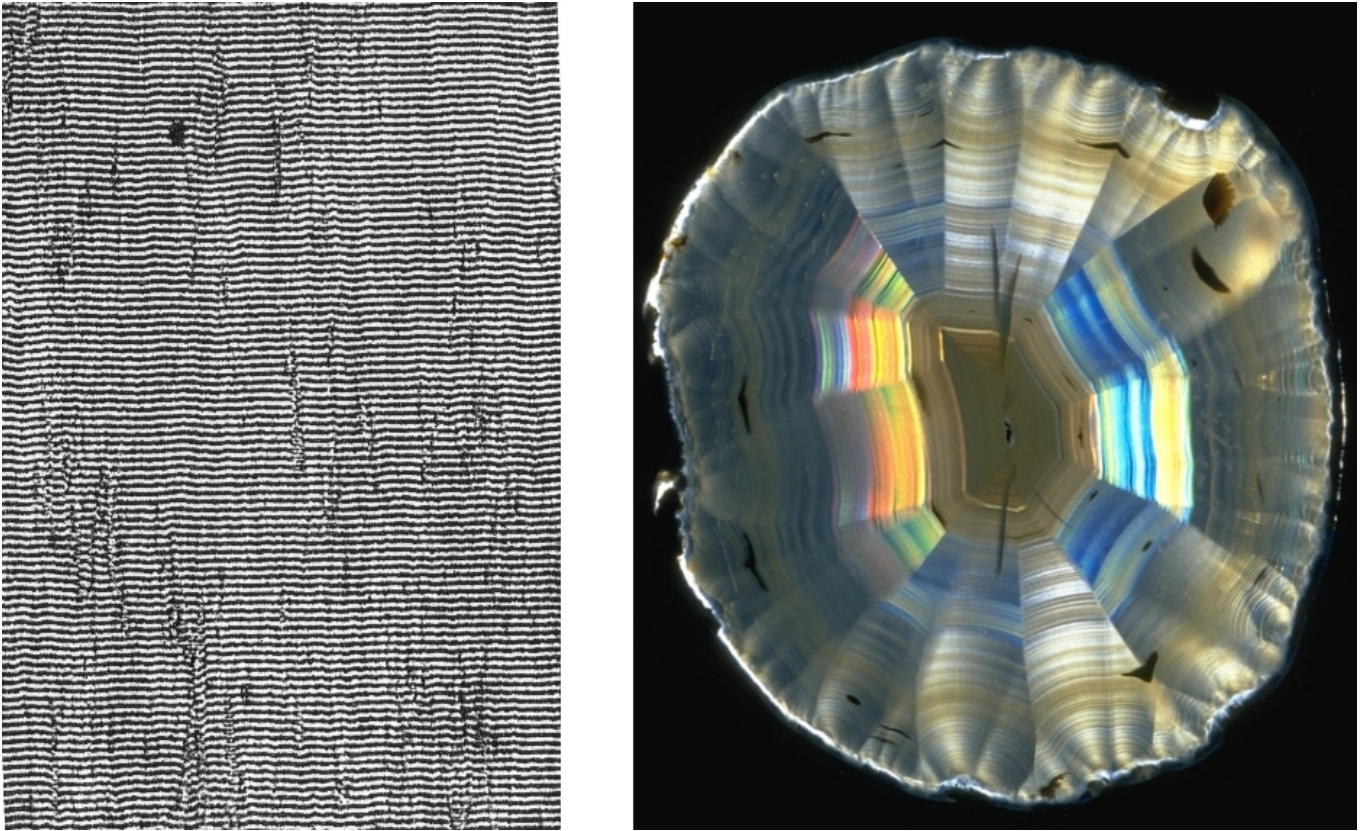


FIG. 17 A: Micron-scale banding in Iris Agate. The distance between the bands is $\sim 2\mu\text{m}$ (Jones, 1952). B: Iris agate produces a rainbow of colors in transmitted light. The photo in (B) is by Chip Clark, Smithsonian Institution, public domain.

cepts.

Among the internal rhythm theories, arguably the most famous is that proposed by Liesegang (1914), which links agate patterns to the banded structures that form when two components diffuse in a gel and react to form an insoluble precipitate (Fig. 19C and Sec. V.B). The similarity of patterns that can be created in this way to the agate banding is at first glance striking. However, a closer inspection reveals a number of important differences between these two systems, some of which were noted by Liesegang himself (Liesegang, 1914). Firstly, Liesegang patterns lack the sharp corners that are very characteristic of agate structures. Next, many structural defects are present in Liesegang rings, such as one ring splitting into two or being displaced in a direction perpendicular to the banding; these defects are absent in agates. Additionally, the distances between successive Liesegang rings obey a well-defined functional relationship (Jablczynski's Law (Jablczynski, 1926)) due to the diffusive nature of the underlying process, which is not seen in agates (Landmesser, 1984). Moreover, for the rings to form, reacting partners must diffuse in the gel, and it is difficult to definitively identify them in the case of agates, and even more challenging to associate their potential presence with the crystallite microstruc-

ture. Finally, as with other internal rhythm models, these models encounter a volume problem: the density of the gel is lower than that of the final chalcedony. As the gel dries, it would then shrink, always leaving an empty space in the center of the cavity. In real agates, this is sometimes the case, but we equally often find fully filled specimens. Additionally, in all actual experiments with Liesegang rings, the integrity of the banding is lost during the desiccation process, as the gels dehydrated and became cracked. Similar criticisms can be leveled against the model of Pabian and Zarins (1994) linking agate patterns with the Belousov-Zhabotinsky reaction (Sec. V.A) (although the reader will notice that this time the corners between the bands in Fig. 19D are sharp, resembling the agate pattern).

A more compelling internal rhythm theory was proposed by Wang and Merino (1990). The advantage of this model is that this time the self-organization process is directly linked to crystallization. According to Wang and Merino (1990), silica gel has the potential to crystallize in a patterned, repetitive manner. This is due to the acceleration of quartz crystallization by Al^{3+} cations, which accumulate at the growth front. The model suggests that fluctuations in the concentrations of trace elements could account for the alternating formation of chalcedony and

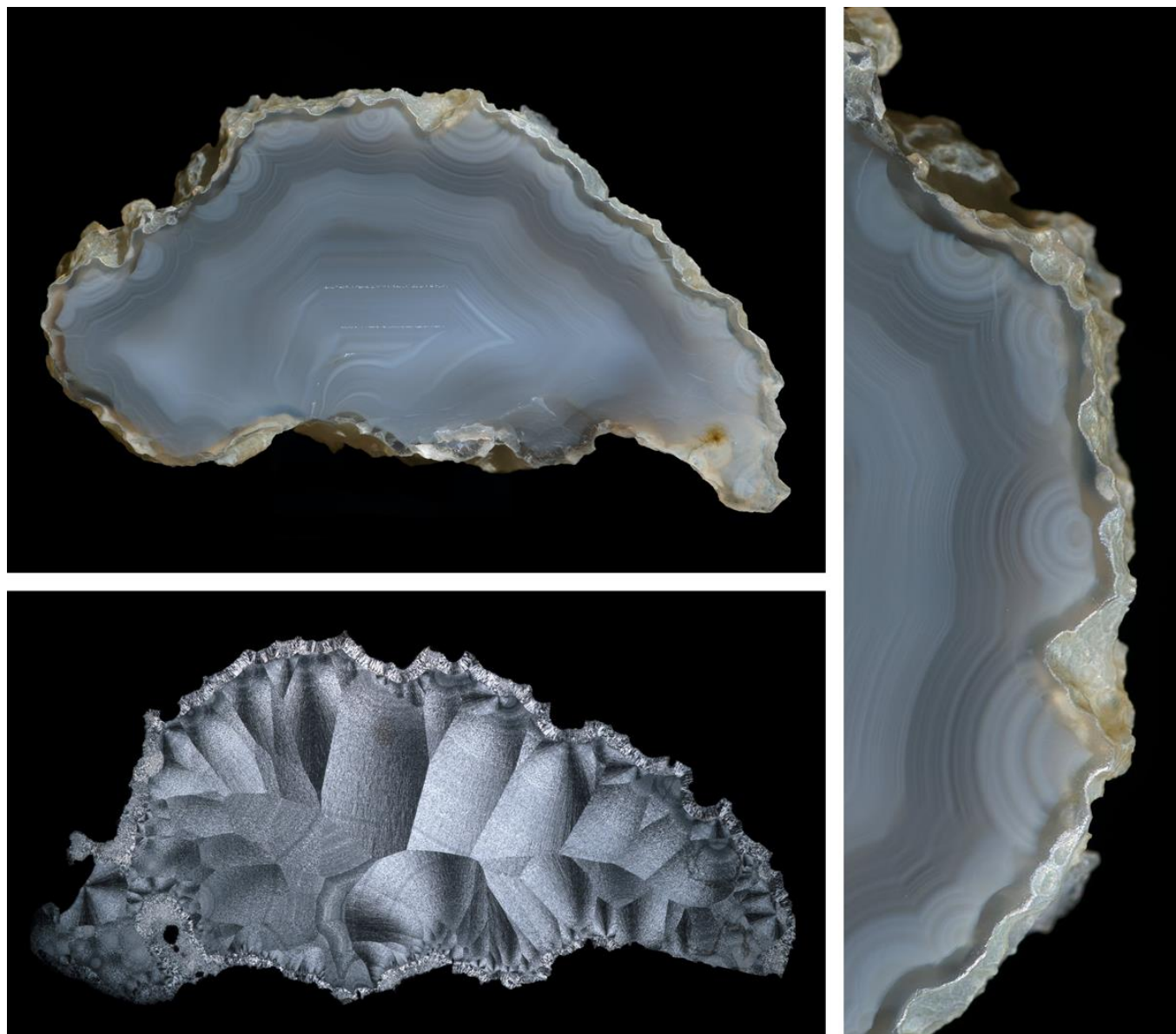


FIG. 18 Agate from Ashland, Oregon in plane light (A) and cross-polarized light (B). The inset on the right (C) shows the growth of spherulitic nuclei on the boundary of the agate. The photos are courtesy of A.C. Akhavan (quartzpage.de).

quartz bands, resulting in patterns similar to those depicted in Figs. 16 and 17.

The preceding models assumed that the precursor of an agate is a silica gel-filled cavity. Interestingly, there are also models that assume agates to be transformed glass droplets. The first model of this kind was proposed by Nacken (1948), inspired by his experimental observation that silica glass crystallizes into chalcedony and quartz while preserving its outer form when exposed to weak alkaline solutions at a temperature of approximately 400°C. Importantly, in this process, both the formation of spherulites at the edges of the system and the spontaneous development of a banded structure are ob-

served (Nacken, 1948; White and Corwin, 1961). Based on this, Nacken proposed that already during the magmatic stage, isolated molten silica droplets separated from the magma and rose upwards, acquiring a shape resembling ascending gas bubbles. With the influence of superheated water vapor, agates then develop from these glass droplets. In fact, the transformation process itself does not need to involve high temperatures, since the banding structure is known to appear in leached archaeological glass (Schalm *et al.*, 2011); see Fig. 19D.

However attractive the high-temperature models with a glassy precursor may sound, as pointed out by Landmesser (1984), such separation into pure glass does

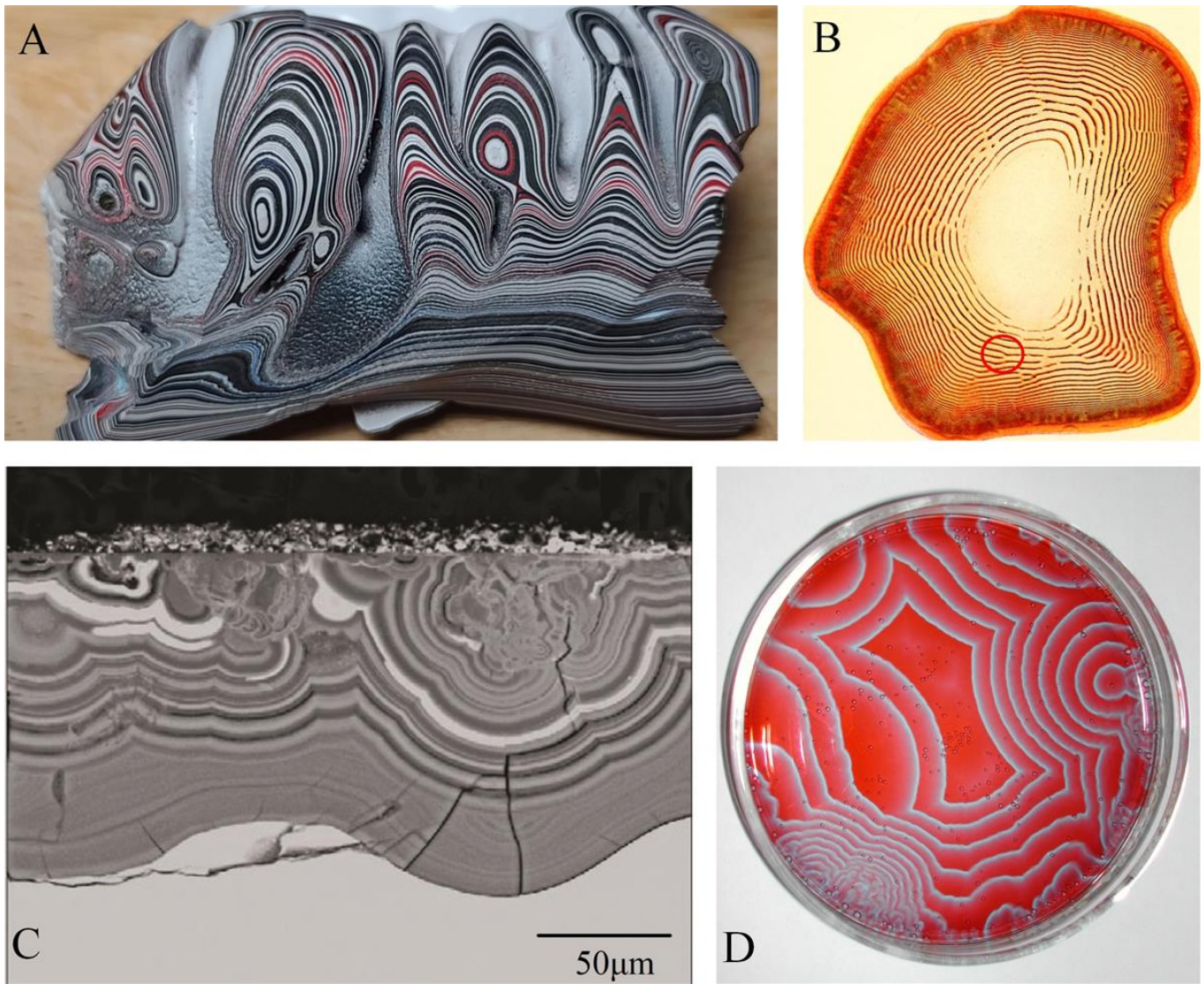


FIG. 19 Four banded patterns resembling agates: (A) Fordite, hardened enamel paint that has accumulated in hundreds of layers in automobile factories during the lacquering process. Image by Jeremy Cook (Willett Creek Agate Co.) distributed under CC BY-NC-SA 4.0 license. (B): A banded structure in a leached layer of an archaeological glass fragment from a 15th-century stained glass window (Schalm *et al.*, 2011). (C) Liesegang rings - periodic precipitation zones from supersaturated solutions in colloidal systems. The circle marks a defect in the structure. Adapted from (Farrington and Laufer, 1927) (D) Patterns arising in the Belousov-Zhabotinsky reaction (image by S. W. Morris).

not occur in multicomponent magma, even with small amounts of alkalis. Additionally, there have been cases identified where agates formed in carbonate cements, thus being separated from the magmatic rock. Furthermore, oxygen and hydrogen isotope analysis on Scottish agates by Fallick *et al.* (1985) demonstrated that their formation temperature was in the range of 50°C . In general, there is a growing consensus in the literature that agates form at temperatures below 100°C (Landmesser, 1984; Moxon and Palyanova, 2020).

One of the most significant issues with the internal rhythm models is that of volume preservation. Regard-

less of the assumptions made about the original filling of the cavity, whether it is a solution, gel, or glass, its density is not sufficiently high to generate enough silica to completely fill the entire cavity (Landmesser, 1984). In the case of a glass precursor, approximately 15% of the mass is missing, assuming the density of silica glass is 2.2 g/cm^3 and the density of chalcedony is 2.6 g/cm^3 . On the other extreme, if we suppose that silica precipitates from the solution under normal conditions with a solubility of about 100 mg/L , then we would require about 1700 liters of solution to fill a cavity with a 5 cm diameter.

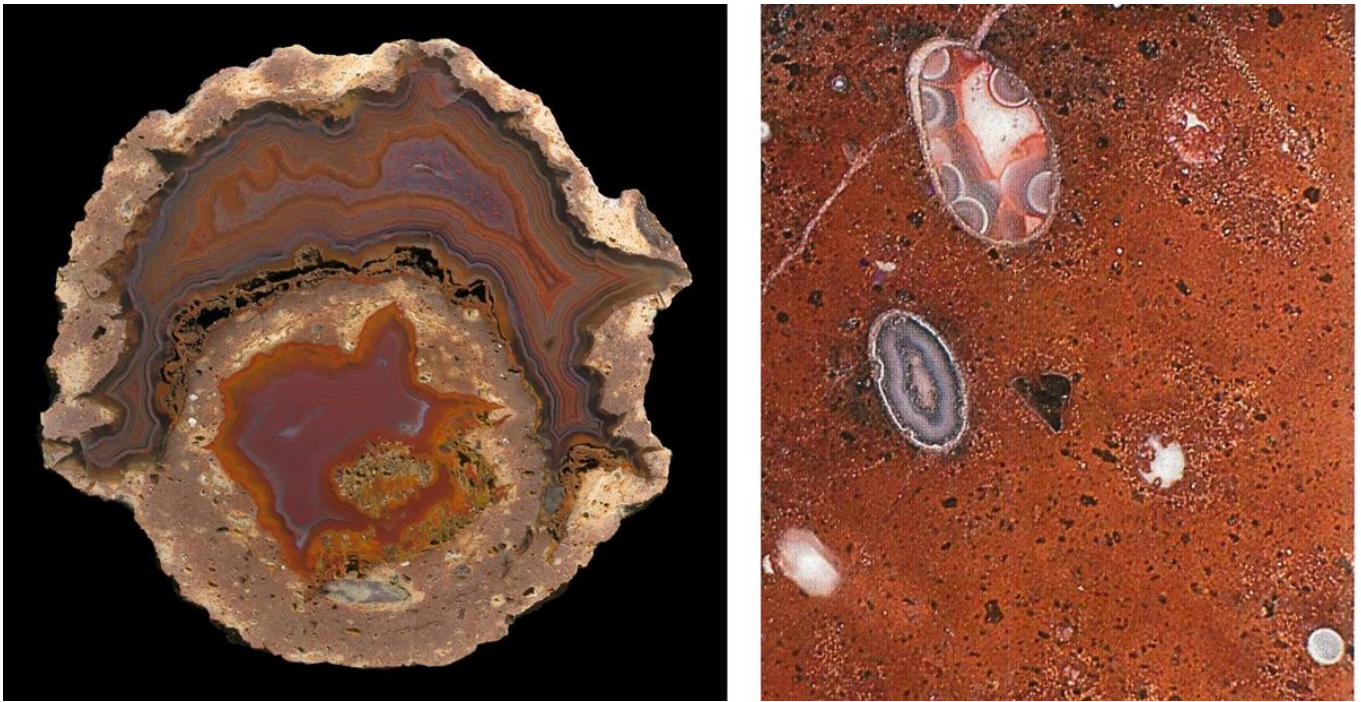


FIG. 20 Two nearby agates do not exhibit the same banding structure. A: a photograph by A.C. Akhavan, B: a photograph by Landmesser (1984).

It would thus seem that a successful agate formation theory should combine the self-organization characteristic of internal rhythm theories with a continuous supply of silica, typical for external rhythm theories. One such model was proposed by Heaney and Davis (1995), who hypothesized that the observed alternating crystallization of quartz and chalcedony in agate micro-banding is linked to varying degrees of silica saturation in the solution. Cavity fluids that are partially polymerized rapidly precipitate spherulitic chalcedony. If the depletion of silica near the fiber tips outpaces diffusion toward these tips, then the reduced activity of silica in the solution facilitates the progressively slower growth of larger crystals with fewer defects. Heaney and Davis (1995) assume that the crystallization proceeds directly from solution, other researchers suggest that the sol-gel transition takes place first (Götze *et al.*, 2020; Landmesser, 1984; Walger *et al.*, 2009).

As for the mechanism that sustains a continual flow of silica into the cavity, one obvious factor is the difference in solubility between the small pores and the large cavity space. Due to interfacial energy effects, the saturation concentration in small pores is considerably higher (Emmanuel and Berkowitz, 2007). This not only explains why silica precipitates in the cavities while keeping the small pores free, but also provides a chemical potential difference driving silica diffusion towards the cavity. However, this diffusion becomes hindered as the first chalcedony layers are formed. An interesting mechanism, which can

significantly speed up the process, is the ‘reverse osmotic pump’ concept proposed by Walger *et al.* (2009). Walger identifies the infiltration channels (Fig. 21) as potential entrance points for the silica solution, noting that they often correlate with fractures in the first chalcedony layer. The solution would then enter the cavity and precipitate on the walls, either as a gel or as a direct crystal layer. In any case, the pores in the wall-lining layers are too small for the partially polymerized silica to pass through, while still allowing water transport. This water then exits the system through the walls. In this way, solvent circulation in the system is sustained, with the solution entering through the infiltration channels and the solvent leaving through the walls. This is similar to the flow pattern in osmotic pumps (Theeuwes, 1975), but in a reversed direction. In osmotic pumps, the solvent is drawn through the porous walls and leaves the system, along with drugs, through a small orifice. As Walger points out, the presence of the flow in the infiltration channels hinders the precipitation there, leading to thinning out of the wall-lining layers and the formation of a characteristic onion-like shapes of the channels as observed in Fig. 21. It is important to note that there is not agreement in the literature about the role of these channels: some claim that they are the solution entry points (Kenngott, 1851; Noeggerath, 1849; Reusch, 1864; Walger *et al.*, 2009), pressure release valves (Goodchild, 1899; Schlossmacher, 1960) or gel deformation structures

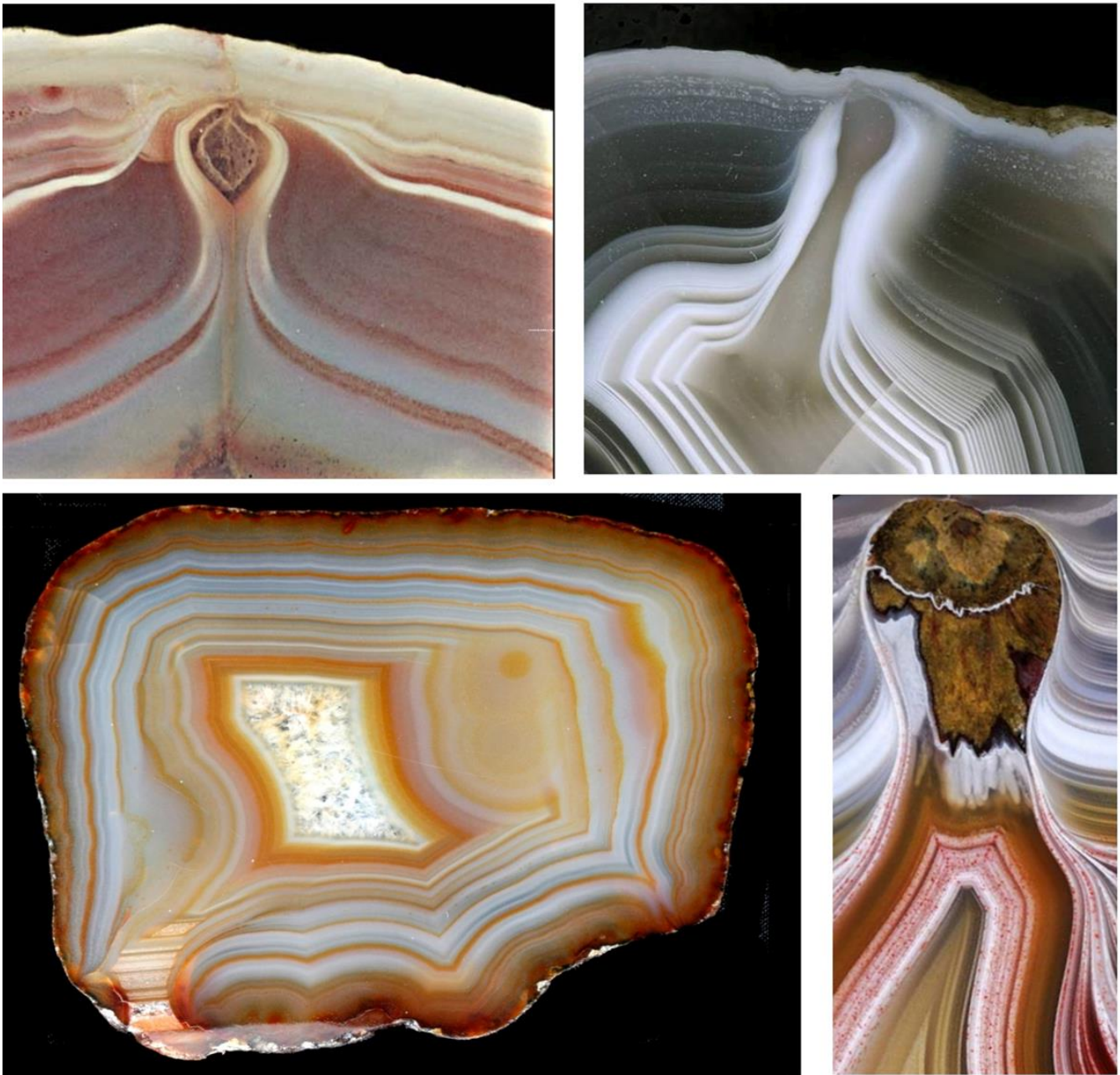


FIG. 21 Close-up views of infiltration channels in agates. (A) infiltration channel in an agate from Neuwald near Flonheim, Germany (Walger *et al.*, 2009), (B) infiltration channel in an agate from Scotland, UK (Jackson, 2003) (D) is by Karen Brzys, Gitche Gumee Museum/Agatelady Rock Shop, Grand Marais, MI, USA, www.agateladyrockshop.com, reproduced with permission.

(Götze *et al.*, 2020; Landmesser, 1984).

This necessarily brief overview of concepts regarding the genesis of agate shows the astonishing diversity of these concepts, rivaling the diversity of ideas about unifying forces in nature or dark energy in cosmology. Many of them explain certain aspects of agates, but usually not all, and unfortunately, none have resulted in the replication of agate-like pattern generation in the laboratory. However, it is evident that despite its appearance as a

hard rock, soft matter phenomena are underlying in the agate formation process. Initially, silica enters the amygdules either as a suspension or a gel. Following this, its deposition on the walls involves crystallization competing with diffusion, potentially influenced by fluid flow. Some theories argue that the deformation and stretching of the gel shape the infiltration channels, while others point to osmosis as central to agate formation. Although the formation of agates contains many unknowns, it is



FIG. 22 Cut and polished black opal from Lightning Ridge, Australia (image: Daniel Mekis; CC-BY-SA-3.0). Harlequin opal (image: Aisha Brown; CC-BY-SA-2.0). Zoned precious opal from the Pliocene of Idaho, USA (image: James St. John; CC-BY-2.0).

clear that the answer will ultimately be grounded in the physics of soft matter.

C. Opals

Opal, although considered a mineral for historical reasons by the International Mineralogy Association (IMA), is actually a mineraloid due to its amorphous (or amorphous mixed with paracrystalline components) nature. Even though opal is often referred to in general terms, there are four different types of opal (Curtis *et al.*, 2019; Gaillou *et al.*, 2008): opal-A (amorphous), which is subdivided into opal-AN (amorphous network) and opal-AG (amorphous gel); opal-CT (cristobalite-tridymite); and opal-C (cristobalite). Opal-C is a very rare phase in nature (Curtis *et al.*, 2019), so it has been little studied. Opal-A is often used as a synonym for opal-AG (Gaillou *et al.*, 2008).

In this review, we will focus on opal-AG, as it is the opal that is always formed by the self-organized aggregation of silica nanospheres (Curtis *et al.*, 2021; Gaillou *et al.*, 2008). In the case of opal-AN it does not present micro- or nano-structural features (Curtis *et al.*, 2021; Gaillou *et al.*, 2008); opal-C, as mentioned above, is uncommon and little studied; and opal-CT, which in addition to spherulitic morphologies, presents different forms of aggregation, can be formed by disoriented nanograins, nanograins in the form of fibers, nanograins in the form of plates or nanograins in the form of lepispheres (i.e., spheres composed of silica plates, with a morphology similar to desert roses) (Curtis *et al.*, 2021; Gaillou *et al.*, 2008).

The formation of opals from colloidal silica involves the self-assembly of tiny silica spheres, formed by addition of silica monomers or polymers, into a highly ordered, three-dimensional structure. The process begins

with the formation of colloidal silica particles in a supersaturated silica solution. These particles are typically in the nanometer size range and remain suspended in the solution due to their small size and the repulsive forces between them. Over time, these silica spheres begin to organize themselves into a regular, closely-packed lattice structure driven by the minimization of free energy in the system. The formation of a densely packed colloidal crystal has not yet been fully elucidated, there are two main theories, the older and classical one being sedimentation due to the force of gravity (Gaillou *et al.*, 2008; Iler, 1965; Norris *et al.*, 2004), while a more recent one holds that changes in solution conditions produce aggregation by electrostatic forces (Stewart *et al.*, 2010). The spaces between the packed silica spheres are gradually filled with silica gel which helps to stabilize the structure and cements the spheres together, leading to the formation of a solid, rigid material (Gaillou *et al.*, 2008).

The periodic arrangement of the silica spheres within the opal causes diffraction of light, which is responsible for the characteristic play of color observed in precious opals (Gaillou *et al.*, 2008). The entire process can take place over long geological time-scales or be accelerated in laboratory conditions. The specific conditions, such as temperature, pH, and solution composition, determine the final size of the silica spheres and the quality of the opal produced (Bogush *et al.*, 1988; Gao *et al.*, 2016; Liesegang and Milke, 2014; Stöber *et al.*, 1968).

D. Target patterns

Geological target patterns are seen in a wide variety of rock types; Fig. 23. We have already noted those in agates. Such patterns in rocks are often termed Liesegang rings or Liesegang patterns by geologists by analogy with the Liesegang patterns seen in laboratory precipitation

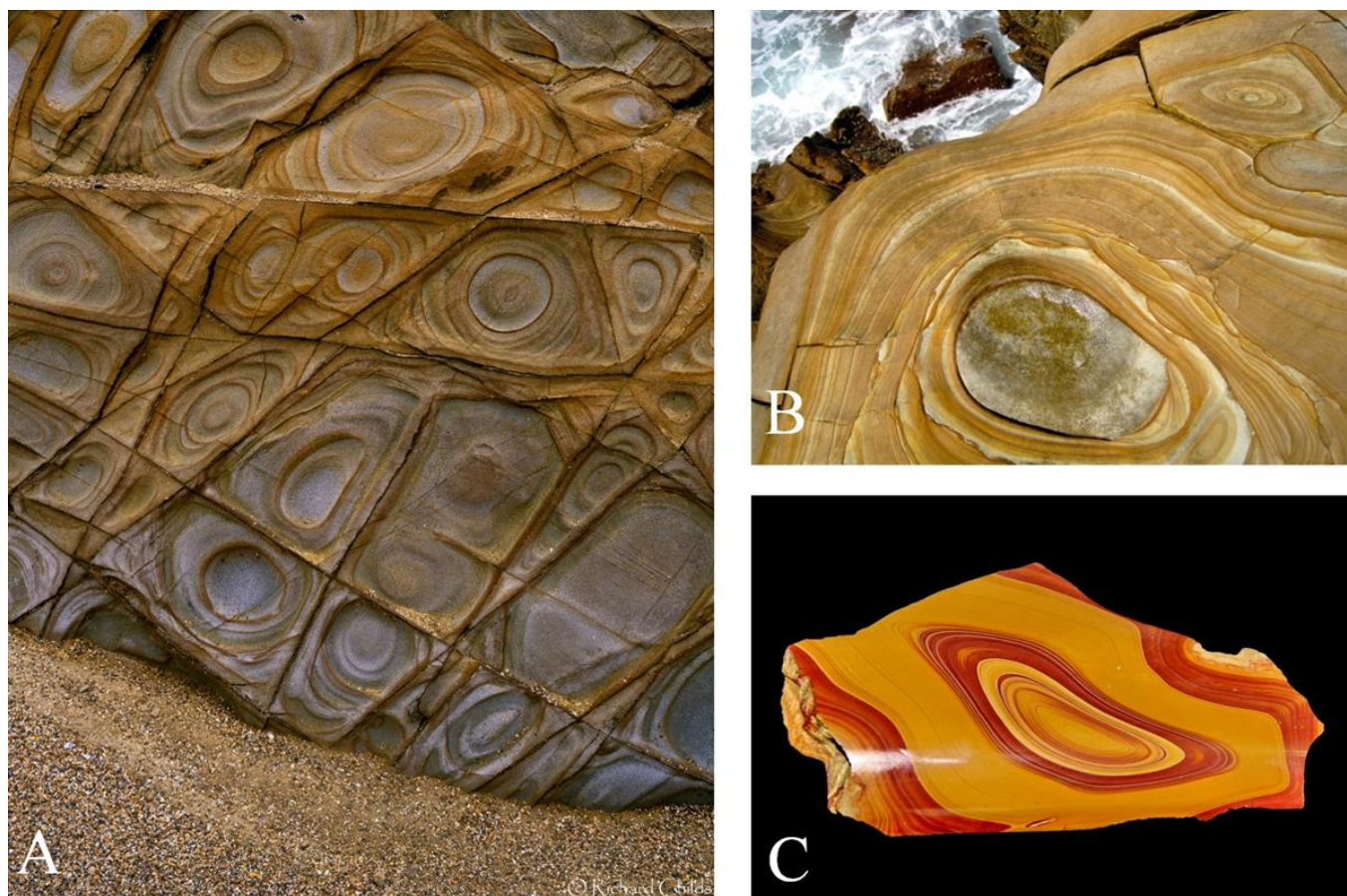


FIG. 23 Geological target patterns A: in sandstones at Bay Bude, England, B: at Bouddi National Park, New South Wales, Australia. C: in volcanosedimentary rock, Gobi desert. Photo (A) is by Richard Childs, reproduced with permission. Photo (B) is by Evelyn Ward, reproduced with permission. Photo (C) is by Dmitry Demezshko (distributed via imagegeo.egu.eu on the Creative Commons license)

experiments (Sec. V.B). Some geological target patterns may indeed be formed by a Liesegang mechanism (see the discussion regarding agates, Sec. IV.B), but it is not clear that all of them are, and, as we discuss below, there is a variety of physical-chemical mechanisms that can produce target patterns in soft matter. We insist on the need to preserve the term Liesegang rings for that particular physical-chemical mechanism.

E. Orbicular granitoid rocks

Orbicular granitoid rocks, or orbicules, Fig. 24, are uncommon rocks with local occurrence that have attracted the attention of geologists for at least a century (Sederholm, 1928). They are characterized by being formed by spheres with concentric shells, which are constituted of layers of mafic minerals, primarily phyllosilicate, and felsic minerals, predominantly quartz and feldspar (Ortoleva, 1994). These layers in turn are elongated crystals growing radial or tangential to the shells (Leveson, 1966;

Vernon, 1985). The origin of these shells seems to occur around a grain in a cooling magma chamber, although alternative theories about a metasomatic origin were posed in the past; see references in Vernon (1985). The diameter of these orbicular structures can vary between less than 5 cm (ultrabasic rocks), 5–10 cm (basic rocks) and up to 40 cm for granites (Lahti *et al.*, 2005). Finland is the country with the highest number of reported cases, although this kind of rocks can be found elsewhere.

F. Striped flint

Layered, banded, striped, or wave-like patterns are common in rocks and are related to the processes that form them. These patterns are common in sedimentary rocks, where layers form due to the gradual deposition of sediments over time. Each layer represents a different period of deposition, possibly reflecting changes in the environment, such as water flow, climate, or sediment sources.



FIG. 24 Orbicular granitoid rocks (images: kristallin.de; CC-BY-SA 3.0).

Nevertheless, the genesis of many patterns remains elusive. One of the most intriguing examples is the highly anisotropic, interference-like pattern of striped flint (Fig. 25), which resembles neither the sedimentary banding, nor target patterns or agate banded patterns. Surprisingly, petrographic, crystallographic and chemical analyses show very little difference between the bands except for the differences in pore distribution, with fewer and smaller pores in the darker bands (Migaszewski *et al.*, 2006).

Striped or banded flint (Fig. 25) was first described in the 19th century (Sowerby, 1804; Woodward, 1864). It is found in localities around the world, but the most well known is from Poland (Migaszewski *et al.*, 2022), where it occurs in Middle Oxfordian to Lower Kimmeridgian carbonate sediments at the north-eastern edge of the Świętokrzyskie Mountains. It belongs to a class of nodular cherts, occurring in nodules between few centimeters and 2 meters in diameter (Fig. 25B), commonly more or less flattened parallel to their horizontal axes and to the bedding of the host rock. The origin of silica forming nodular cherts (not only striped) is still under debate with some authors pointing to its hydrothermal origin (Migaszewski *et al.*, 2006), while others invoking a diagenetic alteration product of biogenic oozes (Knauth, 1994). The origin of nodular structure of cherts is also unknown, with "self-organization processes of enigmatic character" (McBride *et al.*, 1999) involved, and no theoretical framework predicts the sizes of the nodules and characteristic distances between them. As to the formation of nodule body itself, most often coupled dissolution-precipitation processes are considered (Knauth, 1994) with replacement of original limestone with silica on a volume-for-volume basis, analogous to petrified wood. Other theories assume that silica crystallized from a gel (Oehler and Schopf, 1971) or precipitated from solution cite (Mi-

gaszewski *et al.*, 2006).

Flint itself, not necessarily striped, also holds many mysteries. Flint is widespread as nodules in limestone, with size from a few centimeters to a few tens of centimeters. The nodules tend to be concentrated along bedding planes. They are believed to form by volume-for-volume replacement of calcium carbonate. It is not clear what controls this process, in particular what controls the sizes of the nodules and their spacing in what appears to be another example of self organization.

G. Banded sphalerite

Another example of a layered structure with an elusive origin is banded sphalerite, a prominent zinc ore, Fig. 26, which often has light colored ZnS rich cores surrounded by sub-mm nested, sequentially colored, bands of ZnS crystals that are arranged in cm-sized clusters (Katsev *et al.*, 2001).

In a similar fashion to the agate problem, both intrinsic and extrinsic mechanisms have been proposed to explain the formation of these patterns. In particular, the origin of banding was sought in pressure-temperature fluctuations, where shifts in these conditions during sphalerite formation alter the solubility of various elements. For instance, Zhu *et al.* (2018) demonstrate that sphalerite deposits show variations in zinc and sulfur isotopes, which correlate with changes in fluid temperatures over time. This results in the rhythmic deposition of sphalerite layers with slightly different compositions, contributing to band formation.

Other models (Cathles and Smith, 1983; Yardley *et al.*, 1991) suggest episodic fluid flow during hydrothermal mineralization, with long hiatuses separating periods of rapid crystallization. Variations in the concentration



FIG. 25 A, C, D: Striped flint specimens from Świętokrzyskie Mountains, Poland. B: Striped flint nodule at the limestone wall at the prehistoric flint mine in Krzmeionki Opatowskie, Poland. Images (A) and (B) are by Piotr Szymczak. Images (C) and (D) are by Ewa Siemońska (Museum of Minerals and Fossils in Święta Katarzyna, Poland)

of chemical elements in successive hydrothermal infiltrations can lead to alternating layers of different compositions, creating banding. A common criticism of these models is that attributing each of the tens or hundreds of thousands of layers to an episodic event, such as a crack-seal cycle, seems to violate the principle of Ockham's razor (Shore and Fowler, 1996).

Intrinsic models, on the other hand, suggest that the origin of the sphalerite banding is a process of self-organization and that it was formed in a single event of oscillatory zoning (Katsev *et al.*, 2001; Katsev and L'Heureux, 2001; L'Heureux, 2000; Oen *et al.*, 1980) (Sec. V.C). A pioneering model of this kind (Oen *et al.*, 1980) attributes oscillatory zoning in sphalerite to cyclic supersaturation and diffusion-controlled concentration gradients during crystallization. There is a feedback loop

here occurring during crystallization when two or more different cations compete for incorporation into a mineral structure. Initially, one cation is preferentially incorporated into the growing crystal while the other accumulates in the surrounding fluid. Once the concentration of the excluded cation reaches a threshold, it begins to be incorporated into the crystal, which results in a banding pattern (Benedetto *et al.*, 2005).

A somewhat more complex mechanism has been proposed by Katsev *et al.* (2001); Katsev and L'Heureux (2001); and L'Heureux (2000). Their model combines the effects of geochemical reactions, crystal growth, dissolution, and ripening under far-from-equilibrium conditions. An important role in the final formation of the banded structure is played by a self-propagating sequence of growth and dissolution events, known as coarsening



FIG. 26 Banded precipitation in hydrothermal ore deposition: Schalenblende and Zinblendes Pomorzany, Poland. Photo (A) is by Przemysław Budzyński, reproduced with permission. Photo (B) is by Piotr Szymczak.

waves (Boudreau, 1995; Feeney *et al.*, 1983). The mechanism here is a species of Ostwald ripening (Sec. V.O): as larger particles grow, they deplete the solute in their vicinity, causing smaller particles to dissolve and the solute to diffuse toward the larger particles. As shown in Boudreau (1995) and Feeney *et al.* (1983), this feedback mechanism leads to the formation of periodic structures or bands, which propagate as waves through the medium. These waves represent regions of alternating high and low particle concentration, coarsening over time as the system evolves toward a more stable state. Importantly, in the case of sphalerite patterns, this process can occur over geologically short time scales: although the formation of the entire centimeter-scale sphalerite cluster may take thousands of years, the band pattern itself is predicted to form on a time scale of months (Katsev *et al.*, 2001). This opens the possibility that intrinsic and extrinsic models work in conjunction, with intrinsic mechanisms responsible for sub-millimeter scale features and external conditions controlling centimeter-scale variability.

Finally, it is worth mentioning that sphalerite banding has also been linked to microbial activity (Kucha *et al.*, 2010), with microglobular sphalerite textures interpreted as fossil microbial mats of sulfate-reducing bacteria, as evidenced by sulfur isotope data.

H. Foliation in gneiss

Foliation or banding in gneiss refers to the distinct layering observed in this metamorphic rock, Fig. 27 (Passchier *et al.*, 2012). Gneiss is formed through the process of metamorphism, which involves the alteration of pre-existing rocks under high pressure and temperature conditions. During this process, the minerals within the

rock recrystallize and reorganize, leading to the development of a foliation. The foliation in gneiss is a result of the alignment of minerals or mineral layers parallel to the direction of pressure during metamorphism. This alignment gives gneiss its characteristic layered appearance, with alternating bands of different mineral compositions and colors. The banding is typically visible to the naked eye and can be straight or wavy. Foliation in gneiss can be classified into two main types: compositional and structural. Compositional foliation refers to the variation in mineral composition across the rock, creating bands of different minerals such as quartz, feldspar, and mica. Structural foliation, on the other hand, is related to the deformation of the rock during metamorphism, resulting in the alignment of mineral crystals or the development of preferred orientations. The presence of foliation in gneiss provides important information about its geological history and the conditions under which it formed. It indicates the intense pressure and temperature that the rock experienced during metamorphism. Additionally, the distinct layering in gneiss can be used to determine the direction and intensity of tectonic forces that acted on the rock.

I. Zebra rock

Before addressing zebra rocks and zebra textures (Sec. IV.J), it is necessary to explain that the name *zebra rocks* seems to be used in common parlance to refer to rocks that have bands of different colors. However, in the cases we are dealing with in this review, we will describe two very specific structures. The zebra rocks of Australia (the subject of this section) and the zebra textures, very characteristic of carbonate rocks (the subject of the section following this one).



FIG. 27 a) Gneiss foliation, Archean; Ennis Lake North roadcut, Madison County, Montana, USA; b) Chevron folds in gneiss, Precambrian; Medicine Bow Mountains, Wyoming, USA (image: James St. John; CC-BY-2.0).



FIG. 28 Zebra rock, from Kimberly, Western Australia (image: Coward *et al.* (2023)).

Zebra rocks, characterized by their alternating bands of light and dark hues, Fig. 28, are only found in Australia, in the Kimberly region of Western Australia (Coward *et al.*, 2023; Kawahara *et al.*, 2022; Larcombe, 1927). Although these bands are what gave the rock its name, other patterns, such as spots, pillars or rods, can also be observed. Zebra rocks are composed of a fine-grained form of sedimentary clay-rich siltstone, with the lighter bands containing mainly quartz and clay minerals and the darker bands being, in addition, enriched in iron oxides, i.e., hematite (Kawahara *et al.*, 2022; Retallack, 2021). What makes these rocks so curious, apart from the fact that they appear in only one very specific place, is the level of symmetry, regularity and morphological

pattern shown, which is unparalleled by any other (Coward *et al.*, 2023).

Furthermore, the geological processes that led to the formation of these rocks are not known, although several have been proposed from their first description in 1925 (Larcombe, 1925). In this review, we will mention those that seem to have become obsolete and briefly describe the formation processes that have been worked on in recent years. However, there seems to be a strong controversy about all of them.

The first hypothesis of the origin of these rocks was proposed by Larcombe (1925, 1927), who described how zebra rocks would have to have formed in deep, calm waters, far from land. Soon after, Trainer (1931) suggested

four possible origins for these zebra rocks: (1) original sedimentary banding followed by deformation, (2) crystallization of a fine grained flow rock, (3) infiltration into a white rock of iron-bearing solutions, and (4) leaching of the hematite from a red rock. However, currently, there are only three main hypotheses to explain the origin of these rocks: (1) hydrothermal alteration (Kawahara *et al.*, 2022), (2) acid sulfate soil weathering (Retallack, 2021), and (3) liquid crystals (Mattievich *et al.*, 2003).

The first mentioned process, i.e., formation by hydrothermal alteration, can be summarized in the following steps (Coward, 2022; Kawahara *et al.*, 2022): first, Fe²⁺-rich acidic hydrothermal fluids infiltrated into micaceous siltstones and shales. This fluid interacted with carbonate minerals, raising the pH and causing iron precipitation as Fe-oxyhydroxide at the reaction front. Continued diffusion of the Fe²⁺-bearing fluid led to successive neutralisation reactions, creating a rhythmic banding pattern. This hydrothermal fluid also altered other primary silicates in the bedrock, leading to the formation of secondary clay minerals. Over time, Fe-oxyhydroxide was converted to haematite as oxidation progressed.

The second mechanism mentioned relates the origin of the zebra rocks to the presence of ediacaric palaeosoils with iron oxides (Coward, 2022; Retallack, 2021). These palaeosoils were subsequently weathered by sulphate-bearing acid solutions, which washed the iron out of some of the soil horizons, changing their color from red to white.

The last process is the one in which its formation could be related to liquid crystal phases in the rock's mineral structure (Mattievich *et al.*, 2003). This theory stems from the observation that the banding patterns in zebra rocks resemble those seen in certain liquid crystal materials, which exhibit regular, repeating structures when undergoing phase changes. In the case of zebra rocks, it is hypothesized that liquid crystal-like behavior could have occurred in the minerals present during the rock's diagenesis or early lithification stages. During these stages, mineral-rich fluids could have flowed through the sedimentary siltstone, and under certain physical and chemical conditions, these minerals might have organized themselves into liquid crystal phases. The theory posits that as the minerals cooled and solidified, they could have preserved these liquid crystal patterns as alternating bands of dark (iron oxide-rich) and light (silica-rich) layers.

What most of the works seem to agree on is that the origin of these rocks is related to the presence of acid solutions, which altered the original host rock. The alternation of the bands, as well as the other patterns observed in these rocks, have been described as Liesegang patterns (Coward *et al.*, 2023; Coward, 2022; Liu *et al.*, 2023a; Loughnan and Roberts, 1990) (Sec. V.B).

J. Zebra textures

Zebra textures are very common in carbonate rocks occurring in various geological environments, such as Mississippi valley deposits and hydrothermal dolomite deposits (Fontbote and Gorzawski, 1990; Morrow, 2014; Wallace and Hood, 2018). In all these environments, the host rock is always a carbonate rock, while the mineralisation that will give the zebra texture can be carbonates (e.g., dolomite and magnesite) or other minerals (e.g., sphalerite or fluorite). These textures are characterized by a rhythmic alternation of light and dark bands of similar thickness. Generally, the bands are millimetric and, although they can be parallel to the stratification, most commonly the bands have a certain inclination (Wallace and Hood, 2018). These structures have been classified as examples of self-organized patterns (Fontboté, 1993; Merino *et al.*, 2006).

The origin of these textures has historically been described by three main mechanisms: dissolution (Fontbote and Gorzawski, 1990; Morrow, 2014), fracturing (Park, 1938; Swennen *et al.*, 2003), and metasomatism-replacement-recrystallisation (Kelka *et al.*, 2017; Lugli *et al.*, 2000). Other mechanisms have also been proposed on an ad hoc basis (Arne *et al.*, 1991; Krug *et al.*, 1996; Merino *et al.*, 2006). Recently, however, a theory for their origin has been proposed that combines the three main mechanisms. This theory, proposed by Wallace and Hood (2018), suggests that there are two processes occurring in close proximity: mineral replacement, and mineral dissolution and void generation. These two processes combined mean that in the hollows where the new crystals are growing, this growth can generate sufficient pressure to generate fractures. These fractures can then be dissolved and filled by new cement. The end result of all these processes is the formation of the banded structure.

K. Porphyroblasts and spiral garnets

Porphyroblasts (Fig. 30) are large mineral crystals that grow within a finer-grained matrix in metamorphic rocks. These crystals form during metamorphism, the process by which rocks change due to high temperature and pressure. Common minerals that grow as porphyroblasts include garnet, staurolite, and andalusite.

Porphyroblasts begin to form when specific minerals nucleate during metamorphism. As metamorphic conditions (temperature and pressure) increase, these minerals grow larger than the surrounding matrix due to differences in mineral stability and growth rates. Porphyroblasts often form in areas called reaction zones, where minerals become unstable and new, more stable minerals grow. The growth of porphyroblasts reflects the rock's chemical and physical evolution during metamorphism. As they grow, porphyroblasts can trap small fragments

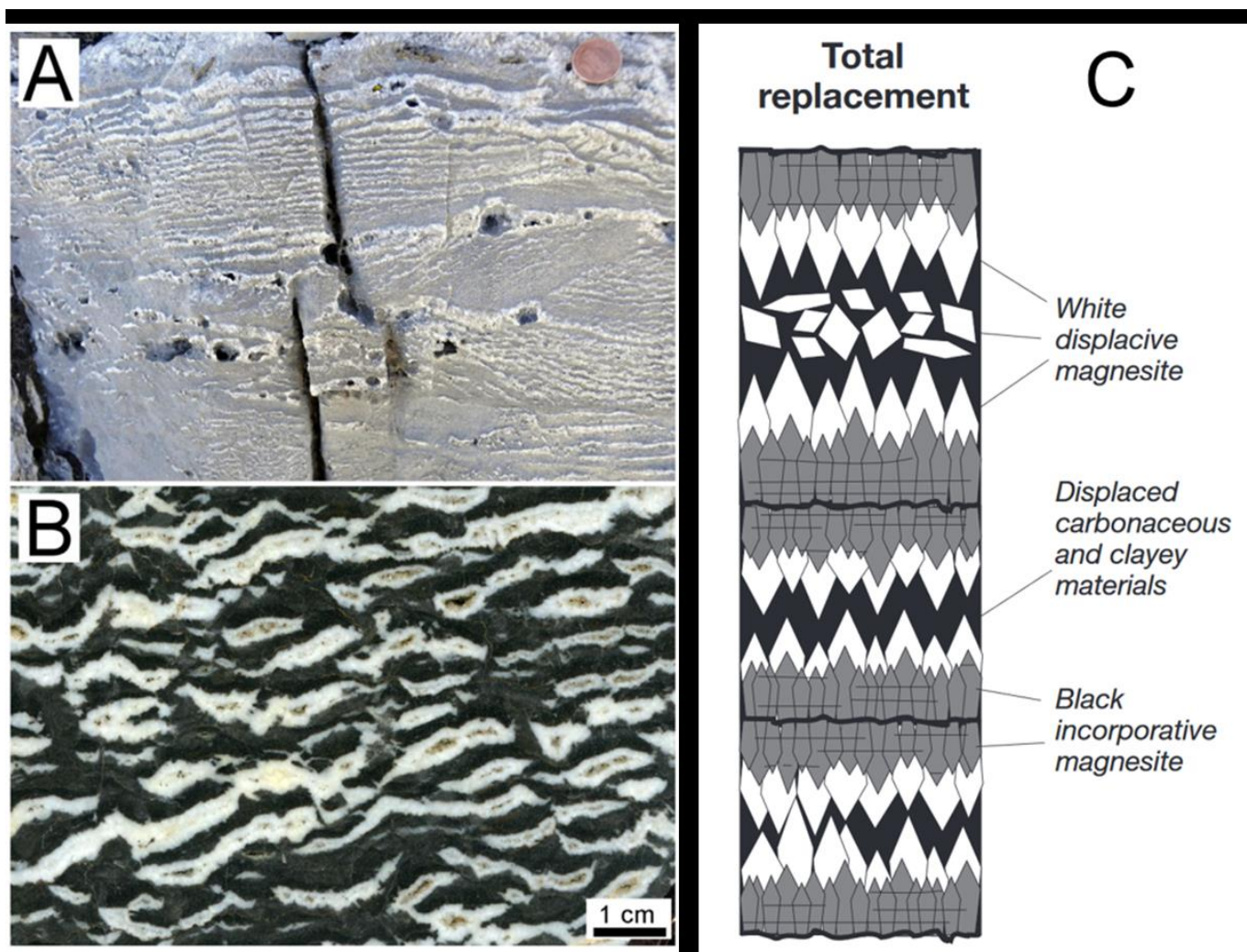


FIG. 29 (A) Zebra dolomite outcrop and (B) zebra dolomite polished hand specimen (images: Wallace and Hood (2018)). (C) Schematic representation of the zebra texture in Eugui magnesites, Spain (image: Lugli *et al.* (2000)).

of the surrounding rock, known as inclusions, preserving a record of the rock's history prior to their formation. During metamorphism, rocks are often subject to deformation, such as folding or shearing. This can cause porphyroblasts to rotate within the matrix. In some cases, porphyroblasts rotate due to the movement of the surrounding rock, such as in regions of simple shear, where the rock undergoes progressive deformation. The porphyroblasts act as relatively rigid bodies in the flowing matrix, leading to their rotation. Alternatively, in certain conditions, porphyroblasts may grow in such a way that they do not rotate significantly. Some garnet porphyroblasts exhibit spiral-shaped inclusion trails, known as spiral garnets or snowball garnets, which were once thought to indicate rotation. However, this spiral pattern could also form from progressive growth in a non-rotating environment where inclusions are entrained in the crystal as it grows.

There has been a long argument in geology about porphyroblast rotation (Bons *et al.*, 2009; Fay and Bell, 2008). The question about whether porphyroblasts rotate or not is clearly one that lies within the ambit of physics, in particular of fluid dynamics. A classical result in fluid dynamics shows that a sphere within a fluid that undergoes shear at a rate x will rotate by precisely half that amount: i.e., at a rate $x/2$. This has been used to argue that porphyroblasts must rotate as the rocks shear about them. However, that result is valid only within the realm of Newtonian fluids. Non-Newtonian fluids do not behave in this way, and rocks are not Newtonian fluids. For non-Newtonian fluids, Brunn 1976 and Gauthier *et al.* 1971 showed theoretically and experimentally that rotation rate is in fact the same for a non-Newtonian fluid as a Newtonian fluid, in the case of an isolated sphere in a second order fluid; i.e., for low shear rates. On the other hand, D'Avino 2008 performed simulations and Sni-

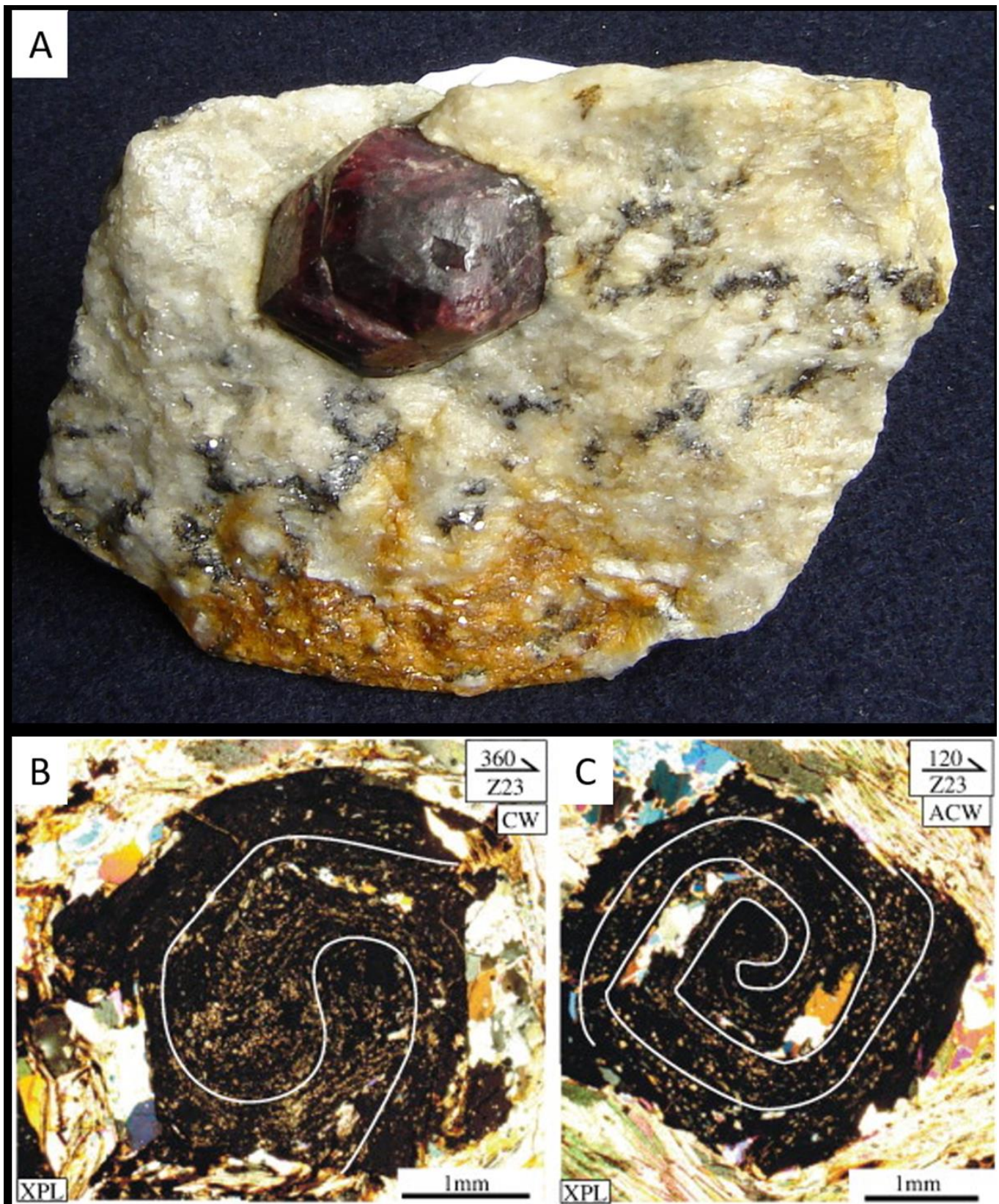


FIG. 30 A) Garnet porphyroblast (3 cm width) in a gneiss matrix (image: Eurico Zimbres (FGEL/UERJ) and Tom Epaminondas (mineral collector), CC-BY-SA). B-C) Crossed polars optical microscope images of spiral garnets showing (B) clockwise asymmetry and (C) anticlockwise asymmetry. (image: Shah *et al.* (2011)).

jkers et al. 2009 studied the question experimentally and found at higher shear rates slowing down compared to the Newtonian case. Michele et al. 1977 showed that for sufficiently high rates of shear, spherical particles of size 60–70 μm suspended within a non-Newtonian fluid formed string-like structures oriented in the direction of flow. They observed, moreover, that the particle rotation rate was much reduced to the Newtonian case; was yet lower when the spheres were closer, and practically vanished when the spheres lined up, as if the string of particles were a long rigid thread. Won & Kim 2004 and Scirocco et al. 2004 showed that the formation of these chains increases with the amount of shear thinning of the fluid and with the shear rate. Hwang et al. 2011 performed numerical simulations with several different non-Newtonian fluids and showed a transition in particle structures in a sequence: random, clustering, clustered string, and string formation, as the solvent viscosity lowers and the Weissenburg number increases. Thus the physics of non-Newtonian fluids shows a rotation of a single particle much less than in the Newtonian case, and the formation of strings of particles that behave as rigid structures. We may note the similarity of these string-like structures to the millipede structures of porphyroblasts (Bell and Bruce, 2007).

L. Geodes

Geodes (Fig. 31) are hollow, spherical or oval-shaped rock formations lined with inward-facing crystals or mineral deposits (Bassler, 1908; Rakovan, 2017). They can range in size from a few centimeters to over a meter in diameter. Geodes are commonly found in areas with volcanic activity and in sedimentary rock regions where water has caused dissolution of rocks, like limestone and shale. They form in a variety of geological environments, with the hollow interior often filled with minerals like quartz, amethyst, calcite, agate, and other silicate or carbonate minerals.

The formation of geodes occurs in two major stages: cavity creation and mineral deposition. Geodes begin as hollow cavities within rocks, which can form through several processes: In volcanic environments, molten lava can trap gas bubbles as it cools. These bubbles, or vesicles, form empty spaces within the solidifying rock. Over time, these cavities serve as the initial space for mineral deposition. In sedimentary environments, cavities can form due to the dissolution of minerals (e.g., limestone or gypsum) by water. Acidic groundwater can dissolve portions of the rock, leaving behind voids or hollows that become the basis for geode formation.

Once a cavity is formed, the second stage involves the deposition of minerals on the inner walls of the cavity. Groundwater or hydrothermal fluids, often rich in dissolved minerals, infiltrate the cavity. Over time, the min-

erals precipitate out of the solution and crystallize along the inner walls of the cavity. As mineral-laden water continues to flow through the cavity, crystals slowly grow inward. Depending on the local geochemistry, different minerals can form, creating colorful and varied geodes. Quartz is the most common mineral, but other varieties, such as amethyst (a purple form of quartz), calcite, and agate, are also common.

Geodes often display banding or layers of different minerals, as changes in water chemistry or temperature over time cause different minerals to be deposited sequentially. This can result in intricate patterns of colors and textures. Quartz geodes are the most common and feature clear or white quartz crystals lining the cavity. Some may also contain amethyst (purple quartz) or smoky quartz (gray-brown quartz). Calcite crystals are another frequent mineral found in geodes, often forming larger, more blocky crystals compared to quartz. Some geodes have a lining of banded agate, a type of chalcedony, which forms concentric layers of microcrystalline quartz around the inner walls.

M. Concretions and nodules

Concretions and nodules (Fig. 32) are both types of secondary mineral deposits found in sedimentary rocks, but they differ in terms of how they form and their internal structures (although it should be noted that this terminological distinction is not always applied consistently). Both are rounded or irregularly shaped mineral masses, typically harder than the surrounding rock, and they form in various geological settings.

Concretions (Marshall and Pirrie, 2013; Raiswell and Fisher, 2000; Seilacher, 2001) are hard, compact masses of mineral matter that form by the precipitation of minerals around a nucleus or core, typically in sedimentary rocks like sandstone, shale, or limestone. Concretions form when minerals precipitate from groundwater that moves through sediment. These minerals accumulate around a nucleus, which can be an organic object, like a fossil, shell, or plant fragment, or an inorganic particle, such as a grain of sand. As minerals continue to precipitate, the concretion grows outward, often developing a concentric layering. The growth occurs syndepositionally—during sediment deposition—or early diagenetically—soon after burial—before the surrounding sediment fully lithifies. Common minerals that precipitate to form concretions include calcite, silica (quartz or chalcedony), iron oxides (such as hematite), and siderite (iron carbonate). Concretions are often spherical or elliptical in shape, but they can also be irregular. They vary in size from a few centimeters to several meters across. Concretions often exhibit a radial or concentric internal structure, with mineral layers radiating out from the nucleus. This distinguishes them from nodules,



FIG. 31 Amethyst geode (image: Madeleinemcc, CC-BY-SA-3.0). Geode with aragonite, Bloomington, Indiana, USA (image: James St. John, CC-BY-2.0).

which lack this concentric growth pattern. Concretions are typically harder than the surrounding sedimentary rock, making them resistant to erosion. This often leads to their exposure as the surrounding rock erodes away.

Nodules (Boggs Jr, 2009) are mineral masses that form by replacement of the surrounding sediment or rock, rather than by mineral precipitation around a core. Unlike concretions, nodules do not have a clear concentric structure. Nodules form through a process called diagenetic replacement, where the original sedimentary material is replaced by minerals as groundwater circulates through the rock. This process often occurs post-deposition, after the sediment has already hardened into rock. Common minerals found in nodules include flint (a variety of microcrystalline quartz), chert, pyrite, phosphate, and gypsum. The replacement process can result in nodules that are chemically different from the surrounding rock. Nodules tend to be irregular in shape and are often found scattered within the host rock. They can vary significantly in size, similar to concretions, from small pebbles to large boulders. Nodules typically lack the concentric layering that concretions possess. Their internal structure is more uniform, often reflecting the mineral that replaced the original material. Nodules are often found in sedimentary rocks like limestone, chalk, and shale. For example, flint nodules are commonly found in chalk formations.

There has been some numerical modeling of the formation of these structures (Chan *et al.*, 2007).

N. Thunder eggs

Thunder eggs or lithophysae (Breitkreuz, 2013) are spherical or egg-shaped geological formations (Fig. 33)

that are typically found in rhyolitic volcanic rock (Roots, 1952). They can look externally similar to geodes (Sec. IV.L), but thunder eggs have distinct formation processes and internal structures. They are often filled with minerals like agate (Kile, 2002), quartz, chalcedony, or opal (Bryan, 1963).

Thunder eggs form in silicic volcanic rocks, particularly in rhyolite and tuff, during volcanic activity (Philpotts and Evans, 1991). Their formation can be broken down into two main stages: cavity formation and mineral deposition. Thunder eggs begin as spherical or subspherical cavities within solidified volcanic rock. These cavities generally form from trapped gas bubbles in the viscous lava or through shrinkage cracks as the lava cools and contracts. A further theory suggests that thunder eggs form due to a process called spherulitic growth, in which silicate minerals like quartz or feldspar crystallize in a radiating pattern from a central point, creating a ball-like structure. These structures may then develop voids or fractures that later become filled with minerals. After the cavities form, mineral-rich solutions, often silica-laden, percolate through the volcanic rock. Over time, chalcedony, agate, quartz, or opal precipitate from these solutions and fill the hollow centers of the thunder eggs.

O. Gold nuggets

Gold is a rare element, so how does it become concentrated into gold nuggets that pattern quartz veins (Fig. 34a) (Butt *et al.*, 2020; Craw and Lilly, 2016)?

During earthquakes, seismic pumping, which occurs due to pressure variations in fault zones, drives the circulation of hydrothermal fluids, in which gold may be present under high-temperature and high-pressure condi-

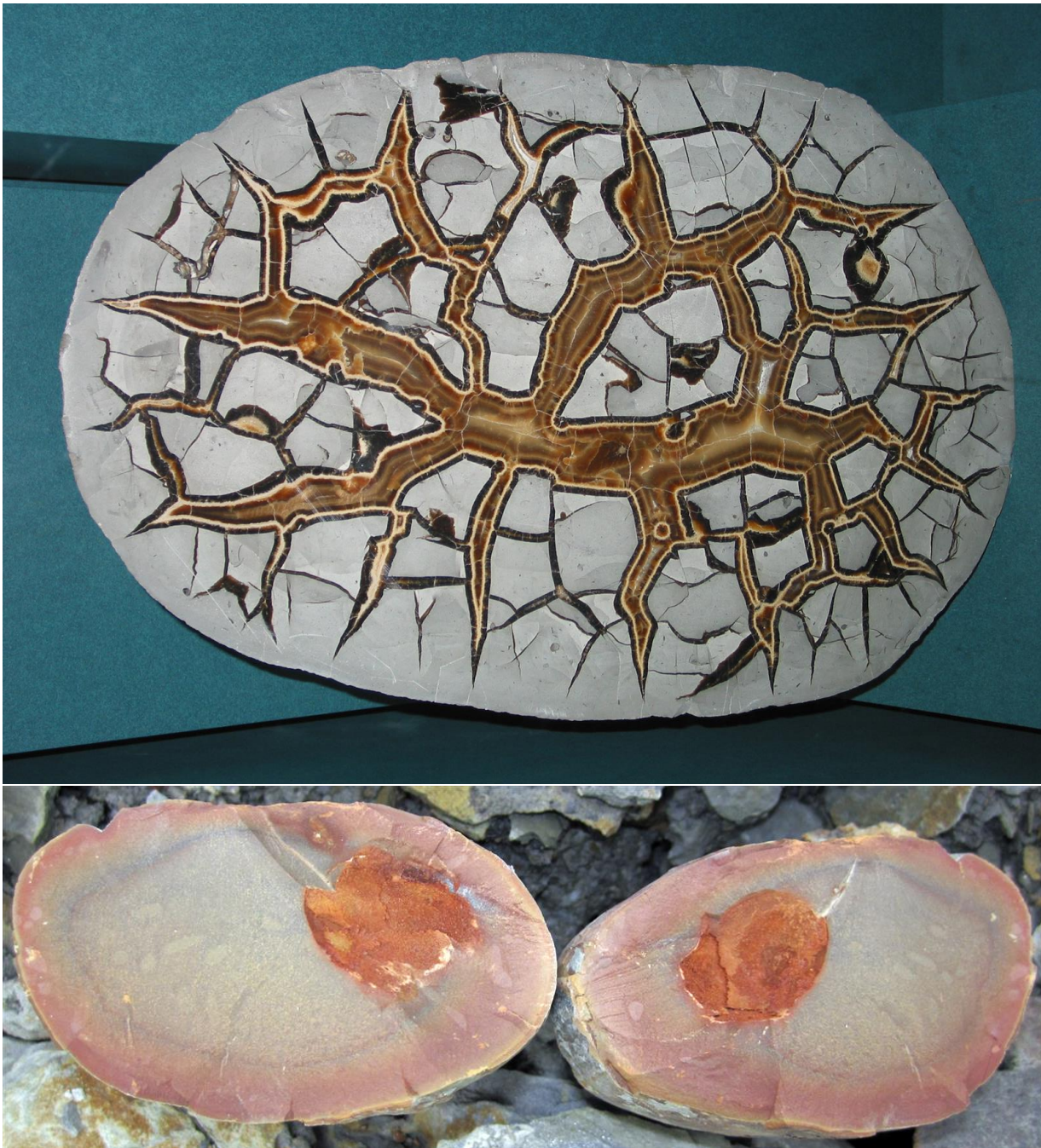


FIG. 32 Septarian concretion (image: Keith Pomakis, CC-BY-SA-2.5). Siderite (ironstone) nodule, Ohio, USA (image: James St. John, CC-BY-2.0).

tions. As faults experience repeated cycles of opening and closing during seismic and aseismic periods, cracks in the rock form and are gradually sealed in a so-called fault-valve mechanism. During these processes, gold from the circulating fluids can precipitate and accumulate within the faults. This mechanism leads to the episodic growth of gold veins or nuggets over time.

Quartz-rich rocks within fault zones can generate elec-

tric charges due to piezoelectric effects, particularly during deformation from seismic activities. These charges may influence the redox conditions within the fluid, potentially facilitating the reduction of dissolved gold to its solid state, leading to the precipitation of gold particles (Voisey *et al.*, 2024). Gold nanoparticles can aggregate to form larger structures in colloidal gold suspensions. This process is enhanced by the presence of carbon-rich fluids,

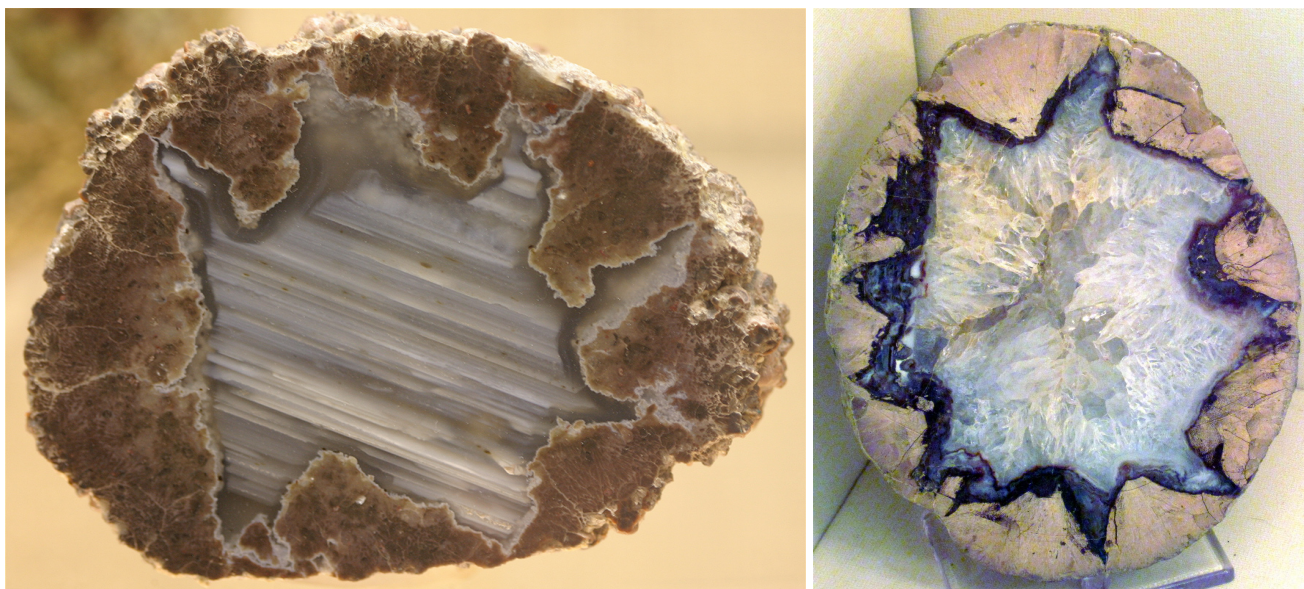


FIG. 33 Agate thunder egg (image: Cacophony, CC-BY-SA-3.0,2.5,2.0,1.0); quartz thunder egg, Oregon, USA (image: James St. John, CC-BY-2.0).

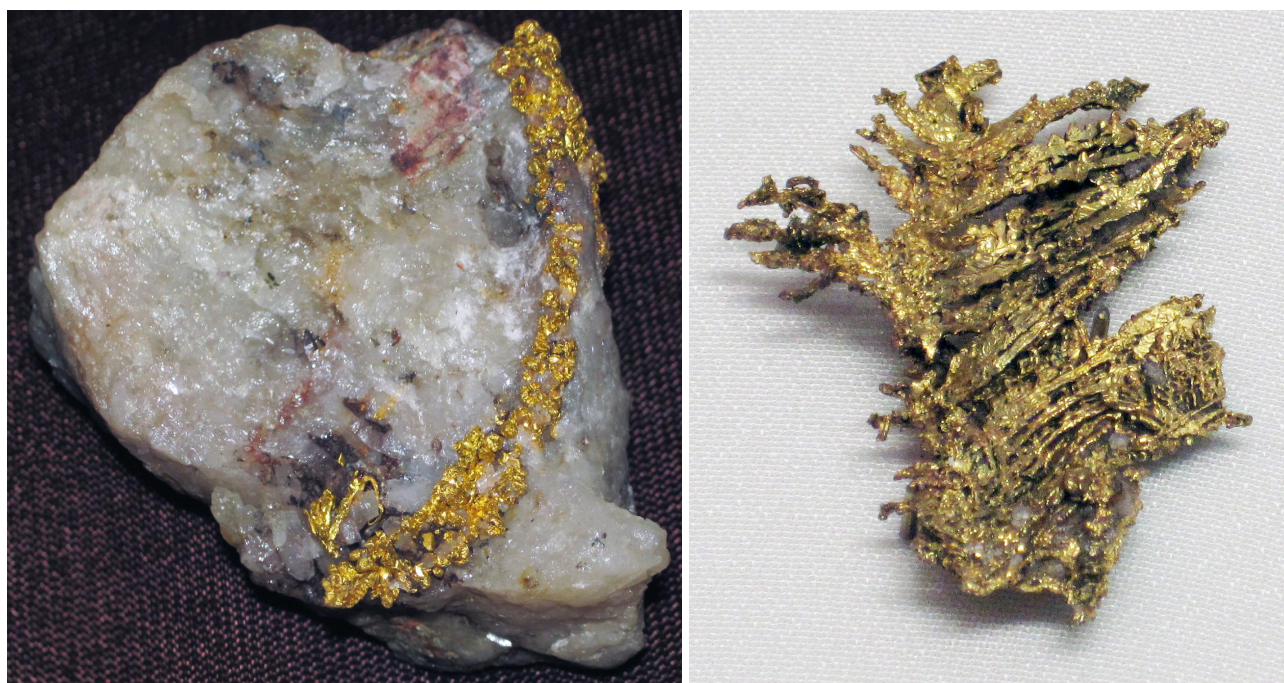


FIG. 34 Gold-quartz hydrothermal vein from Colorado, USA; dendritic gold nugget, California, USA (images: James St. John; CC-BY-2.0).

which stabilize the colloidal particles and lead to the formation of high-grade gold deposits. Diffusion-limited aggregation (Sec. V.M) represents one means by which gold particles grow in size, resulting in the dendritic, branched structures observed in natural gold nuggets (Fig. 34b).

P. Desert roses and other efflorescence structures

The presence of salts in natural environments can create spectacular landscapes but can also poses significant threats to ecosystems and historical artifacts (Cooke and Smalley, 1968; Pitman and Lauchli, 2002; Shahidzadeh-

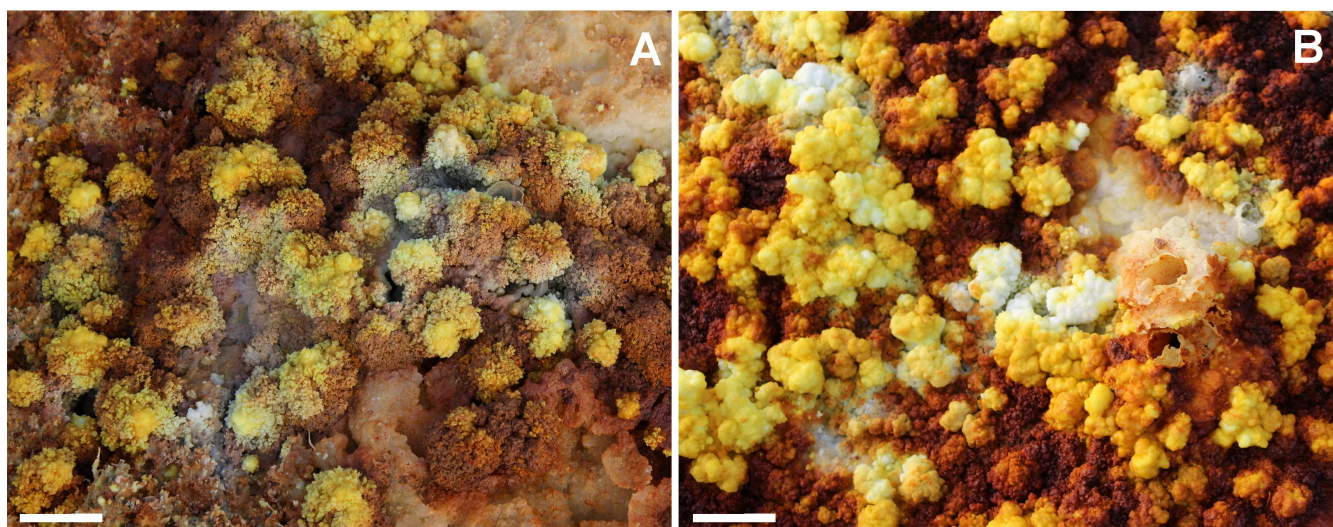


FIG. 35 Salt efflorescence at the acidic hydrothermal field of Dallol, Ethiopia (Kotopoulou *et al.*, 2019). Dendritic (A) and cauliflower (B) efflorescence of gypsum ($\text{CaSO}_4 \cdot 2\text{H}_2\text{O}$), sylvite (KCl), carnallite ($\text{KCl} \cdot \text{MgCl}_2 \cdot 6\text{H}_2\text{O}$), jarosite ($\text{KFe}_3(\text{SO}_4)_2(\text{OH})_6$) and iron-oxide minerals. Scale bar is 3 cm.

Bonn *et al.*, 2010). With environmental fluctuations such as rainfall or temperature and relative humidity changes, salt present in granular materials (consolidated or unconsolidated) such as stones or soil can dissolve and form salt solutions that can flow. Consequently, the salts can be transported and precipitate when the water will evaporate at the surface (Desarnaud *et al.*, 2015). This is the origin of salt creeping, a phenomenon in which salt crystals continue to precipitate far from an evaporating salt solution boundary (Hird and Bolton, 2016; Huang and Huang, 1976; Qazi *et al.*, 2019a; Washburn, 2002). Salt creeping can initiate and grow on flat surfaces but also on top of porous materials such as soil, sand and stones; this is called efflorescence (Fig. 35) (Desarnaud *et al.*, 2015; Qazi *et al.*, 2019b; Veran-Tissoires *et al.*, 2012). The latter can, for example, occur for ground water in soils or at salt lakes. Salt creeping can result in spectacular structures in natural environments, such as the formation of desert roses in arid regions, Fig. 36a–b, salt crystallization motifs near the Black and Dead Sea coasts. In addition, salt creep can lead to soil salinization, vegetation decline, and water quality issues, impacting biodiversity (Pitman and Lauchli, 2002).

Recent laboratory studies have shown that salt creeping is a general phenomenon that happens for different salts under conditions of low relative humidity, and is affected by the presence of impurities and other microcrystallites, that provide secondary nucleation sites near the evaporation front (Qazi *et al.*, 2019a). As salt crystals are wettable by their own salt solutions, such multiple nucleation sites provide a platform for a film of salt solution to spread even further over the newly formed microcrystallites, well beyond the initial evaporation front (Hird and

Bolton, 2016; Qazi *et al.*, 2019a). This in turn enlarges the evaporative area, which leads to a faster precipitation and so on, causing an exponential increase in the precipitating crystal mass in time. This self-amplifying process then results in spectacular three-dimensional crystal networks at macroscopic distances from the salt solution source. The microscopic analysis of the 3D network of such efflorescence reveals an internal porous structure of the crystalline salt network with a fractal structure characterized by a self-organized, self-similar arrangement of salt crystals, as we shall discuss in Sec. V.I.

Laboratory and field observations on different salts suggest that as different minerals have different crystalline structures reflecting the seven possible lattice structures, the macroscopic patterning is different between different salts. Desert roses typically consist of calcium sulfate (gypsum) or barium sulfate (barite) with sand grains (SiO_2) interspersed between the crystalline structures. When investigated in detail, desert roses reveal a spectacular self-organized structure: large petals, smaller petals in between these and even smaller ones between those, in a fractal organization. A close-up of the structure by SEM imaging, Fig. 36c-d, reveals that each petal itself is composed of parallel smaller leaflets crystals, emphasizing the universality of this pattern and the internal porous structure of the 3D salt network (Wijnhorst *et al.*, 2023). Because of its self-similar porous nature, this assembly of crystals structure in nature can grow up to 1 to 3 meters in height.

Salt creeping is therefore both universal and self-amplifying, typically initiated by the presence of salt crystals or impurities. It hinges on the formation of numerous crystallites under low humidity conditions, with

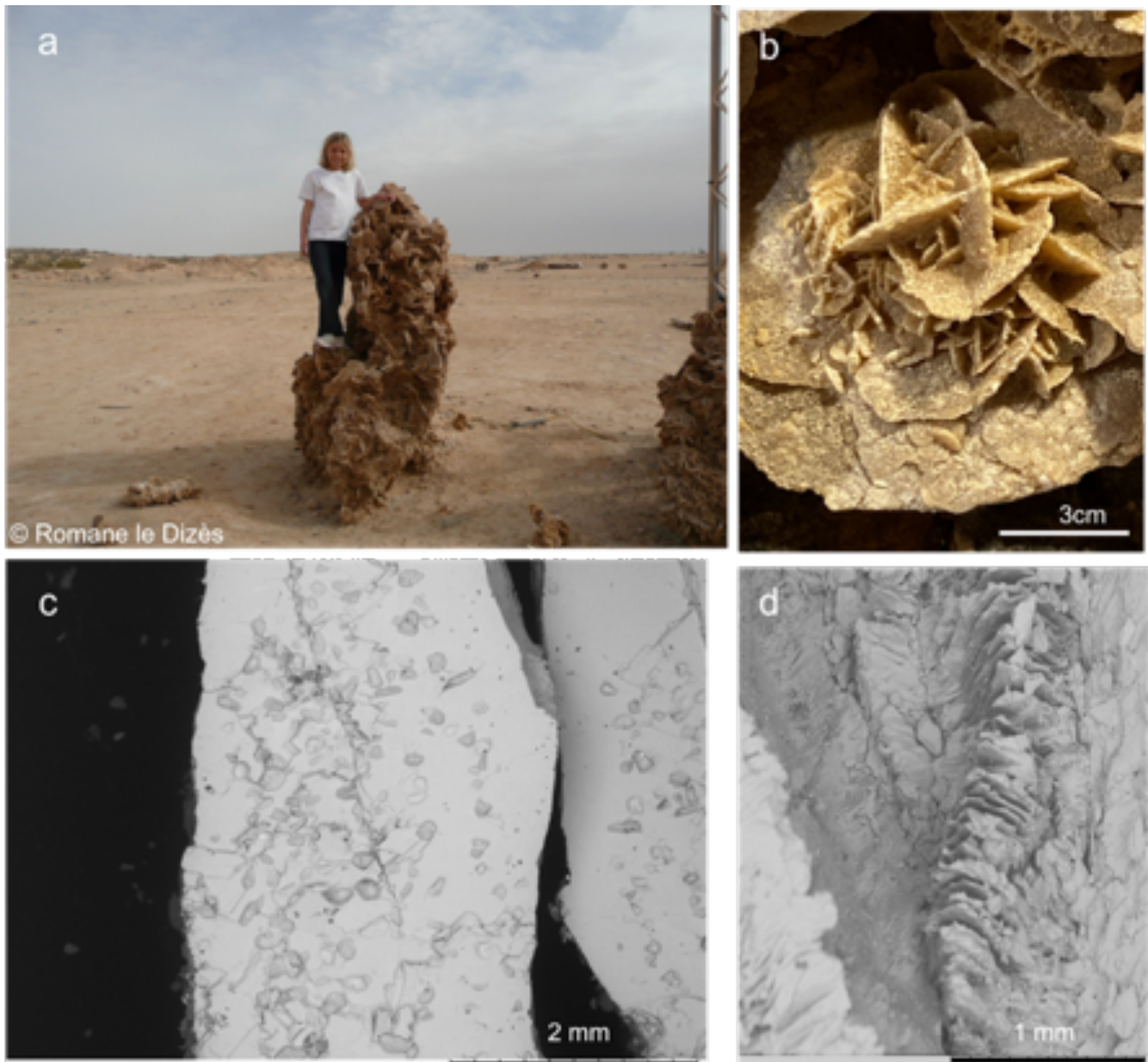


FIG. 36 Desert roses formed by crystallization at different scales. (a) typical structure of sand roses structure in the Moroccan desert arid region (image: courtesy of Romane le Dizès Castell). (b) a close up view of one desert Rose with its polycrystalline structure made of large and small petals. (c) SEM image of sand grains entrapped between two broken crystalline petals. (d) SEM image of the internal structure of one petal showing a self-organized crystallization at an even smaller scale. images b-d : ©copyright N.Shahidzadeh -UvA.

impurities often serving as nucleation centers or salt mixtures catalyzing this spectacular self-organized process. Addressing salt creep is vital for preserving our geo- and cultural heritage (Brocx and Semeniuk, 2010), calling for further research and interdisciplinary collaboration to develop sustainable solutions for their conservation. On the other hand, when salt crystallization occurs at the pore

scale within the porous materials it can induce weathering and damage outdoor historic and archeological sites such as Petra in Jordan (Heinrichs, 2008), or Pharaonic sandstones monuments in Luxor, Egypt (Fitzner *et al.*, 2003), and more generically our outdoor built cultural heritage. The impact of salt weathering will be discussed in more detail in Section IV.R.

Q. Dry salt lakes and convection

Dry salt lakes, also called evaporite pans, saline flats or playa are found in arid environments where evaporation of groundwater exceeds precipitation (Briere, 2000; Dixon, 2009; Lowenstein and Hardie, 1985). A common situation is a terminal valley with no outflow route for water, such as the case of Death Valley, California, shown in Fig. 37(a). Evaporites can develop from the decline and disappearance of a natural lake, like Owens Lake, Fig. 37(b), which dried up after the Owens River was diverted into aqueducts near Los Angeles (Bertenthal, 2021; Groeneveld *et al.*, 2010; Tyler *et al.*, 1997). Large natural evaporite pans are also found in arid basins including the Danakil salt plain, Ethiopia, Fig. 37(c). In coastal settings, similar features called sabkha can result from seawater evaporation, as in Fig. 37(d).

Striking patterns of closed polygonal shapes, bounded by narrow ridges, often appear to decorate the surface of dry lakes. Here, as groundwater evaporates over time, it leaves behind any dissolved salt that it had been carrying. These salts accumulate at the surface of the soil, forming into a solid salt crust, in which the patterns develop. Around the world, the patterns in dry salt lakes show a remarkable similarity. The polygons typically have a diameter of a few (1-10) meters, separated by 1-10 cm high ridges or raised features (Lasser *et al.*, 2023, 2020; Nield *et al.*, 2015). The surface patterns show dynamics on timescales of only a few months (Lasser *et al.*, 2023; Nield *et al.*, 2015).

Although beautiful, dry salt lakes produce mineral-rich dust through erosion (Klose *et al.*, 2019; Prospero, 2002), which is detrimental to air quality and human health and a major source of uncertainty in modelling climate sensitivity (Kok *et al.*, 2023). Changes in water use policy and climate are exacerbating these problems worldwide, as marginal saline lakes like the Dead Sea or Great Salt Lake are receding, leaving salt flats behind (Wurtsbaugh *et al.*, 2017). In this context, Owens Lake is seen as a case study for developing remediation strategy and dust control at dry lakes, given its situation as a man-made dry lake that was at one time the largest source of hazardous aerosols (PM-10) in the United States (Bertenthal, 2021).

Early interpretations of the polygonal patterns in the salt crusts of dry lakes focused on a range of mechanical instabilities of the surface crust itself, such as fracture (Krinsley, 1970) or buckling (Christiansen, 1963). However, more recently an appreciation of the hidden fluid dynamics of dry salt lakes has developed into an explanation of the remarkably well-ordered surface shapes of this pattern (Lasser *et al.*, 2021, 2023). Evaporite pans are maintained by evaporation of groundwater, and the groundwater table at active pans is usually very shallow, close enough to the surface to ensure good connection through capillary action (Briere, 2000; Lowenstein and Hardie, 1985; Tyler *et al.*, 1997). Dissolved salt concen-

trates in the groundwater near the surface, forming a boundary layer of salt-rich, heavy fluid. Measurements of the density and salinity of groundwater have demonstrated this layer, for example, in the upper ~ 1 m of Owens Lake (Lasser *et al.*, 2023; Tyler *et al.*, 1997). This scenario of heavy fluid resting atop a deep reservoir of less saline, and thus more buoyant, groundwater, is inherently unstable.

Since dry salt lakes occur in desert areas, thermal fluctuations might also be expected to contribute to their dynamics. In contrast to the more well-known double-diffusive fingering structures that produce stratification and ‘salt-fingers’ in the ocean (Huppert and Turner, 1981; Schmitt, 1995), however, thermal buoyancy does not appear to be relevant to dry lake convection: based on temperature logs and groundwater sampling at Owens Lake, the density contrast due to salinity is estimated to be two orders of magnitude larger than that caused by thermal expansion (Lasser *et al.*, 2021). A significant contribution, instead, might arise from the effects of temperature on the hydration states of some salts. For example, sodium sulfate can swell in volume by up to 300% when it changes from an anhydrous mineral (thenardite) to a hydrated state (mirabilite) (Flatt *et al.*, 2014). This phase transition occurs at temperatures and relative humidities routinely experienced in dry lake environments, but its effects on the salt crusts have not yet been explored.

The soil of a dry salt lake can be considered as a porous medium, saturated in water. Generally, density-driven convection in porous media is a well-studied topic, and the subject of several recent, detailed reviews (Hewitt, 2020; Nield and Bejan, 2017). In the context of a dry lake, evaporation occurs at the upper surface of the ground, and water is recharged from below from a distant reservoir. These boundary conditions lead to the problem of one-sided convection with a through-flow of fluid (Hewitt, 2020). It was first studied as the analogous but thermally-driven case of a geyser (Wooding, 1960), and later adapted to the setting of a dry salt lake (Wooding *et al.*, 1997a,b). In this model, the stability of the salt-rich, near surface boundary layer is related to a dimensionless Rayleigh number, Ra , which describes the balance between diffusive and advective effects. The Rayleigh number also gives the ratio of the speed at which a large heavy plume of fluid will fall under its own weight, to the speed of the upwards flow moving through the soil to replace water lost to evaporation. The steady-state boundary layer of the dry salt lake model is unstable to convection when Ra exceeds about 7 (Wooding, 1960). Analogue laboratory experiments in Hele-Shaw cells have confirmed this critical value for convection (Wooding *et al.*, 1997a), and explored the longer-term convective dynamics (Lasser *et al.*, 2023). Similarly, linear stability analyses have been made for an initially uniform lake, to investigate the time needed to build up a sufficiently thick boundary layer that will be unsta-

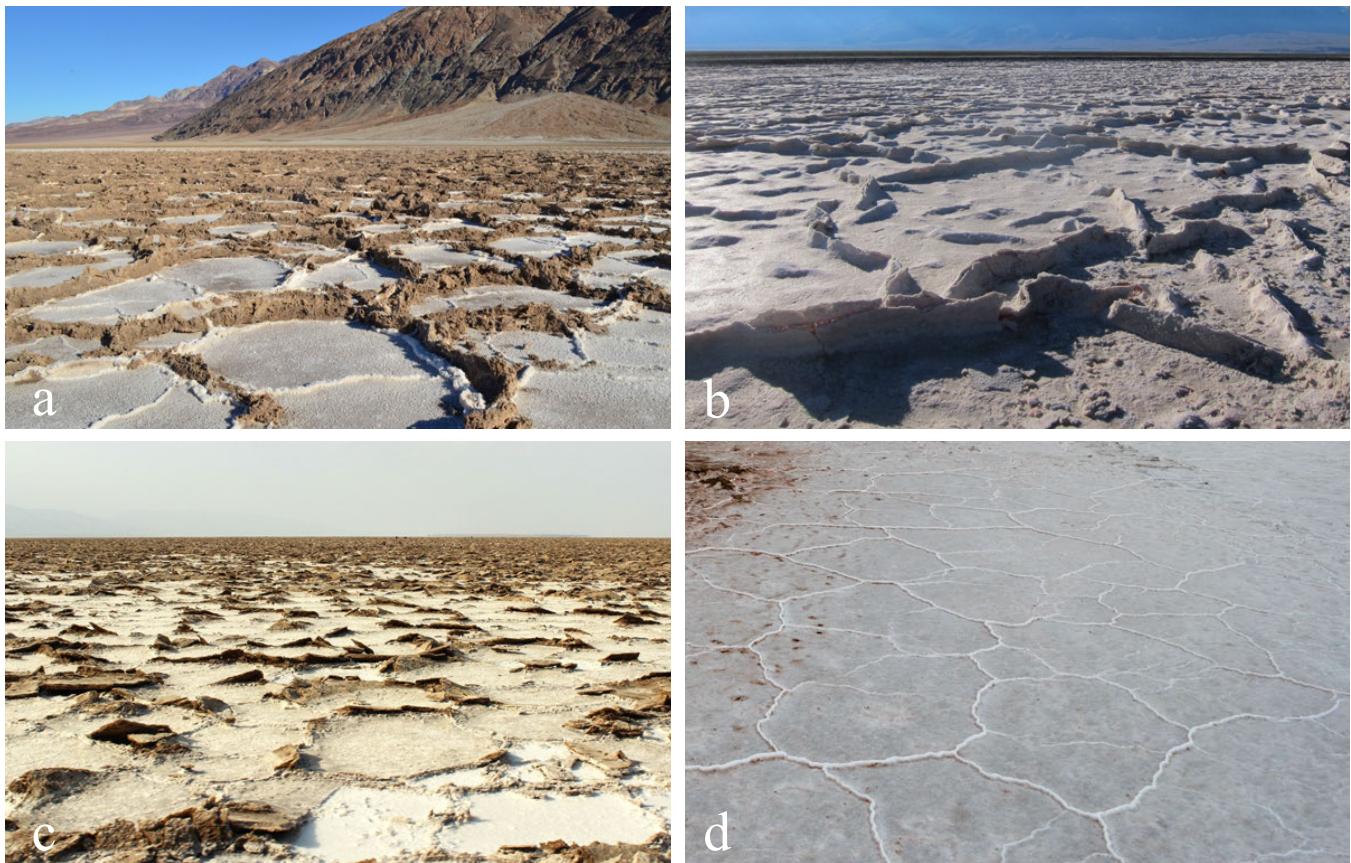


FIG. 37 Polygonal patterns of salt frequently appear in dry salt lakes and evaporite pans. Examples include at (a) Badwater Basin, Death Valley, California, (b) Owens Lake, California, (c) Danakil salt pan, Ethiopia and (d) the Skeleton Coast, Namibia. In all cases, a salt crust develops on the surface of the pan, with narrow raised ridges defining the edges of the polygons. (images: a,b,d: Lucas Goehring; c: Electra Kotopoulou.)

ble to convection (Bringedal *et al.*, 2022; Lasser *et al.*, 2021). At several dry lakes and sabkhas around the world, Rayleigh numbers have been estimated to be between about 100–100,000 (Lasser *et al.*, 2023; Van Dam *et al.*, 2009), showing that groundwater should be actively convecting at these sites. Indeed, large, heavy plumes of salt-rich water have been directly observed near the surface of sabkhas using electrical conductivity measurements (Stevens *et al.*, 2009; Van Dam *et al.*, 2009).

Simulations of the groundwater flows in dry salt lakes have shown that the pattern of the convective cells that develop near the surface of a modelled lakebed strongly resemble the patterns seen in natural salt crust (Lasser *et al.*, 2021, 2023). These models also predict that the typical size of convective features is governed by a characteristic scale given by the ratio of the diffusion constant of salts in the groundwater, to the volumetric evaporation rate. Since the typical diffusivity of salts in water is around 10^{-9} m/s², while the groundwater evaporation rates measured in active dry salt lakes are of order 0.1 mm/day (or 10^{-9} m/s), this scale is of order 1 meter in most cases, close to what is observed at places

like Badwater Basin, Owens Lake, and Sua Pan (Lasser *et al.*, 2023). Further, the models can predict rates of salt crust growth, by estimating the salt flux into the surface from a balance between advection and diffusion. In this context, the polygonal salt ridges should appear over downwelling sheets of salt-rich water, as has been confirmed by mapping out the groundwater salinity through direct sampling (Lasser *et al.*, 2023). Under the field conditions typical of Owens Lake, convective transport of salt has been estimated to contribute to growth rates about 1 mm/month, which is comparable to the growth rates observed at similar dry lakes in Botswana (Nield *et al.*, 2015). Since more salt should enter the crust above the salt-rich downwelling flows, these models also predict that salt ridges should grow about twice as fast as the rest of the crust (Lasser *et al.*, 2023).

As explored further in sections V.I and IV.P, the growth and internal structure of salt crusts can be quite complex. A better understanding of how water and salt move through the crust, and of the feedback between crust growth and local evaporation, are likely to be the next steps in further developing predictive models of dry



FIG. 38 Salt weathering: honeycomb / tafoni patterns (a) in the Le Grotte di Soprasasso, Bolognese Apennines, Italy (image: Elena Tartaglione; CC-BY-SA-4.0); (b) at Elgol, Isle of Skye, UK (image: Kalense; CC-BY-SA-3.0).

salt lakes. The effects of an unsaturated capillary fringe have also recently begun to be investigated (Liu *et al.*, 2023b), as have the effects of more efficient convective flows within any cracks in the ground, as might be caused for example by desiccation or a cycling of water availability (Ibne Haque *et al.*, 2024).

R. Salt weathering, honeycomb weathering, and tafoni

Salt weathering, haloclasty, honeycomb weathering, and tafoni, Fig. 38, are terms that describe a set of related geological processes and features. Salt weathering (Doehne, 2002; Wellman and Wilson, 1965), or haloclasty, is a physical weathering process in which salt crystals grow and expand within rock pores or fractures. This phenomenon is particularly common in arid and semi-arid regions where evaporation rates are high, and salt solutions can become concentrated, as well as in coastal environments where salt spray is present. In either case, brine penetrates a rock matrix. As it evaporates, it leaves behind salt crystals. As these crystals grow, their expansion exerts significant pressure on the rock matrix. Over time, this stress causes the rock to break apart, forming characteristic surface patterning.

Honeycomb or alveolar weathering is characterized by small, closely spaced cavities resembling a honeycomb pattern on rock surfaces (Mustoe, 1982; Rodriguez-Navarro *et al.*, 1999). It is often found in coastal and desert environments where salt spray or other saline moisture sources are present and is typically associated with sedimentary rocks, such as sandstones, which have high porosity. Salt weathering is generally thought to be a major physical mechanism involved in honeycomb weathering, albeit perhaps not the only one. Tafoni

are often rounded, cave-like features found on the surfaces of granular rocks such as sandstone, granite, and basalt. Tafoni structures can range from small pits to large hollowed-out spaces. There is no clear consensus on the threshold between tafoni and honeycomb weathering (Groom *et al.*, 2015). The two terms; it seems, are only differentiated on the basis of tafoni being larger. There are a number of modeling studies of honeycombs and tafoni (Huinink *et al.*, 2004). A Turing-type mechanism has been proposed for the formation of these honeycomb / tafoni features (McBride and Picard, 2004).

S. Stalactites and icicles

An *icicle* is the familiar elongated structure of ordinary ice that forms when water drips into freezing air from a point of support. Since ice formation requires the removal of latent heat, we can infer that heat transfer is most efficient at the fast growing tip and slower on the sides (Makkonen, 1988). The shape forms a substrate for the subsequent flow of water, some of which freezes while some drips off; the dripping water assists the heat transfer, causing faster growth at the tip. Very similar fluid mechanical transport is presumably involved in the formation of *stalactites*, which are calcium carbonate deposits that hang from roofs of caves. Here, the solid CaCO_3 is deposited when CO_2 comes out of solution (Camporeale and Ridolfi, 2012; Short *et al.*, 2005), but the water is not consumed. Both icicles and stalactites usually have a single dripping tip, but may sometimes develop multiple branches (Chen and Morris, 2011). Other common morphologies are also observed, such as sheet-like “drapery” formations in which the water flows only along a leading edge, or “flow stone”, in which water flows



FIG. 39 Icicles, hanging from the ceiling, and their rare cousins, the ice version of stalagmites, on the floor, in a lava tube cave in Iceland. The columnar jointing of the lava (Sec. IV.AC) can also be appreciated (image: Julyan Cartwright).

over a broad surface (Meakin and Jamtveit, 2010).

The suffix “-icle” has also been applied to other elongated structures, such as *snoticles* (also known as *snottites*), *brinicles* and *rusticles*. Snoticles (Macalady *et al.*, 2007) are drips of mucus-like microbial mats that hang from cave roofs, resembling small stalactites. Brinicles

(Testón-Martínez *et al.*, 2024) are ice structures that form on the underside of sea ice when plumes of dense, supercooled brine descends from channels in the ice, causing the surrounding sea water to freeze into an elongated pipe. Rusticles (Cullimore and Johnston, 2008) are long, iron-oxide rich structures that form on shipwrecks. Sub-

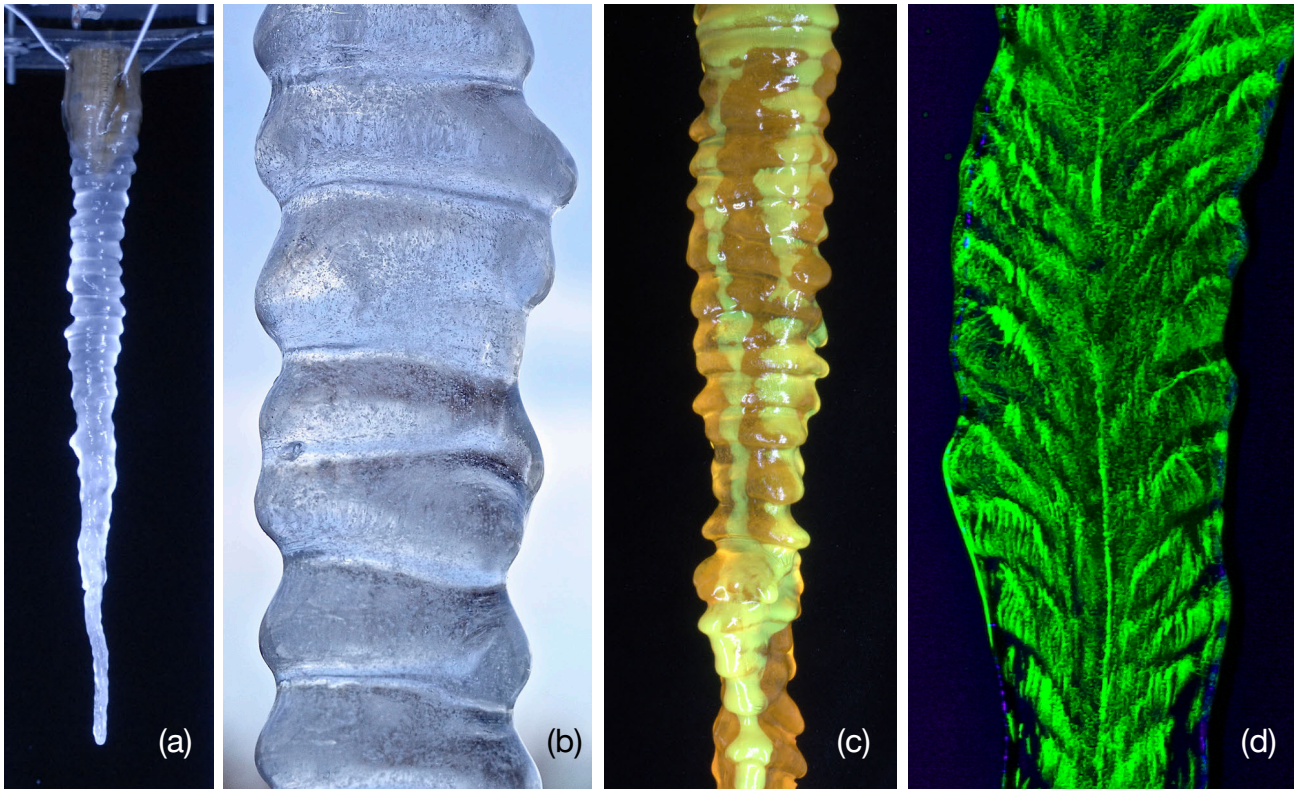


FIG. 40 Rippled icicles: (a) shows a lab-grown icicle from the *Icicle Atlas* (Chen *et al.*, 2006), made from distilled water with 320 ppm NaCl as an impurity. (b) shows a close up of the ripples on a natural icicle. In all cases, the ripple wave-length is close to 1 cm (image: S. W. Morris). (c) shows a lab-grown icicle with 519 ppm sodium fluorescein dye as the impurity. The dye glows green in the liquid phase, but appears orange when trapped in inclusions in the ice. The partial wetting of the surface is evident (Ladan and Morris, 2021). (d) shows a vertical section of a lab-grown icicle near 0C with 171 ppm sodium fluorescein. Here, the dye in the inclusions glows green. The chevron pattern of the inclusions tracks the slow upward motion of the ripples during growth. The chevrons have a substructure of crescents (Ladan and Morris, 2022).

merged, elongated pipe-like structures are also formed by some chemical gardens (Cartwright *et al.*, 2013).

In all cases, gravity- or buoyancy-driven fluid flows interact with the evolving shape, producing long, downward pointing structures. In addition to their overall pointy shape, icicles and stalactites may also exhibit ripple patterns about their circumference. These ripples have a near-universal wave-length of about 1 cm, independent of the growing conditions (Camporeale and Ridolfi, 2012; Chen and Morris, 2013; Ogawa and Furukawa, 2002; Ueno *et al.*, 2010). Examples of rippled icicles are shown in Fig. 40.

Unlike stalactites and most other formations, icicles are unusually amenable to laboratory study. Detailed experiments (Chen and Morris, 2011, 2013; Demmenie *et al.*, 2023; Ladan and Morris, 2021, 2022) have revealed a wealth of subtle phenomena. A crucial parameter in icicle morphology is the purity of the feed water. Icicles grown from ultrapure water (Demmenie *et al.*, 2023) have a “dripping candle” shape quite unlike that of natural icicles,

because the water descends in discrete sliding drops and hardly wets the ice at all. Even extremely low levels of impurity, far less than seawater, suffice to change the wetting properties of the ice surface and the overall morphology of the resulting icicle (Chen and Morris, 2011, 2013; Ladan and Morris, 2021). At moderate, but still very low, levels of impurity, ripples emerge on the surface of icicles (Chen and Morris, 2013), which are presumed to be due to a morphological instability. Even natural icicles which form from atmospheric precipitation may be impure enough to be in this regime (as in Fig. 40(b)). Ripples are observed to travel upward slightly during growth. As the impurity concentration is increased, ripples grow faster and to larger amplitude and eventually become disordered, but their wave-length always remains very close to 1 cm.

When a fluorescent dye is used as the impurity, it becomes possible to visualize the surface flow over the icicle (Ladan and Morris, 2021) and the fate of impurities trapped in the ice (Ladan and Morris, 2022). The most

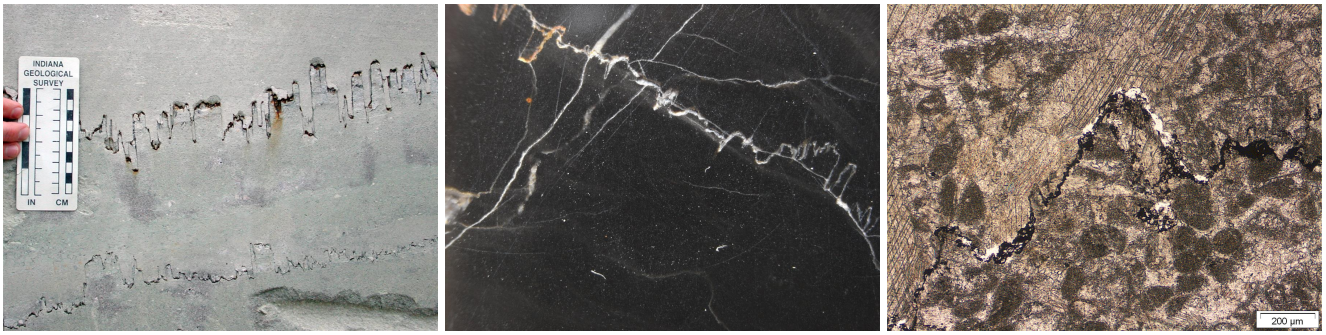


FIG. 41 (a) Macrostylolites in a limestone image: (Michael C. Rygel; CC-BY-SA-3.0). (b) Stylolites in Žarnov limestone, Slovakia (image: Lysippos; CC-BY-SA-3.0). (c) Irregular stylolite planes in a thin section of a packstone (clasts are microorganisms). Normal polarized light. Oehrlialk formation of the Axen nappe, Wellenberg, Switzerland (image: Woudloper; public domain).

well-formed ripples are found in an impurity concentration regime in which the ice is only partially wetted by the liquid phase, which descends in branching rivulets; see Fig. 40(c). At high concentrations (Demmenie *et al.*, 2023; Ladan and Morris, 2021), liquid coverage becomes complete and the ripples are very disordered. A substantial fraction of the impurity concentration ends up trapped in small liquid inclusions inside the ice; these inclusions are roughly spherical and $100\ \mu\text{m}$ in size. They form clusters that make a distinct pattern of chevrons following the peaks of the ripples (Ladan and Morris, 2022). Each chevron has a substructure of crescents, which are discrete layers rich in inclusions. These crescents are just visible in Fig. 40(d). At high concentrations, the ice becomes completely spongy with liquid inclusions.

At present, none of these phenomena are quantitatively described by linear stability theories for the onset of icicle ripples (Ogawa and Furukawa, 2002; Ueno *et al.*, 2010; Worster, 2024). These theories assume complete wetting and do not treat the role of impurities at all. When generalized to include impurities (Ladan and Morris, 2021), they fail to predict the wave-length of the ripples. The rippling instability appears to depend on the impurity dependence of the non-equilibrium partial wetting of the ice, a process that is very poorly understood (Huerre *et al.*, 2024). The process by which impurities are trapped to become inclusions is also not understood. A linear stability theory of ripples on stalactites has been proposed (Camporeale and Ridolfi, 2012), which uses an analogous assumption of complete wetting, but much less is known about stalactite growth dynamics. Sectioned stalactites do not exhibit anything analogous to the pattern of inclusions in icicles. It would be interesting to examine the path of water descending an actively growing stalactite using a dye tracer to probe the role of wetting in that case. While icicles and stalactites are superficially similar, they differ in many important details.

T. Stylolites

Stylolites (Park and Schot, 1968), Fig. 41, are self-organized features (Merino, 1992) that result from pressure dissolution, a process in which minerals dissolve at grain contacts under high-pressure conditions and reprecipitate in areas of lower stress. This causes the formation of irregular, wavy, or undulating surfaces along the mineral boundaries (Toussaint *et al.*, 2018). Stylolites can be observed as an interpenetration of dissolution surfaces into neighboring grains or as serrated surfaces in the rock. The mechanism behind stylolite formation is the differential stress distribution within a rock. Pressure is not uniformly distributed; some areas experience higher pressures, leading to enhanced dissolution. Soluble minerals dissolve under this high-pressure environment, and the dissolved material migrates and reprecipitates in areas of lower stress; a form of fingering instability (Sec. V.J). Their evolution can be mathematically modelled with elasticity and surface energy, leading to establishment of a scaling law in the morphology of the surfaces and determination of paleostress on a sample from its morphology (Rolland *et al.*, 2012). Stylolites can act as conduits for fluid migration, influencing fluid flow and replacement reactions (Koehn *et al.*, 2016), helping transport fluids and precipitating minerals in the fractures (Bruna *et al.*, 2019; Heap *et al.*, 2014).

U. Solution pipes, wormholes, and replacement fingers

Solution pipes (Fig. 42) are vertical, finger-like structures found in the epikarst zone of porous calcareous rocks. They vary in size, from a few centimeters to a few meters in diameter, but are generally less than 1 meter in diameter with variable depths, the deepest reaching 100 meters. They also vary in shape - some are more conical, tapering slowly towards the tip, whereas others are strongly elongated, with almost constant cross-section



FIG. 42 Solution pipes: A - pipes in Cretaceous chalk (Swanscombe, UK) - the photo by J. Rhodes (courtesy of British Geological Survey), B - pipes in Quaternary calcarenite (Cape Bridgewater, Australia), C, E-G - pipes in Miocene calcarenite, (Smerdyna quarry, Poland); D - pipes in Neogene calcarenite (Guilderton quarry, Australia); H - pipe in Pleistocene calcarenite at Cape Perron, Perth, Australia. Photos B and D–H are by Piotr Szymczak. Photo (C) is courtesy of Dr. Łukasz U'zarowicz (Warsaw University of Life Sciences - SGGW, Poland)

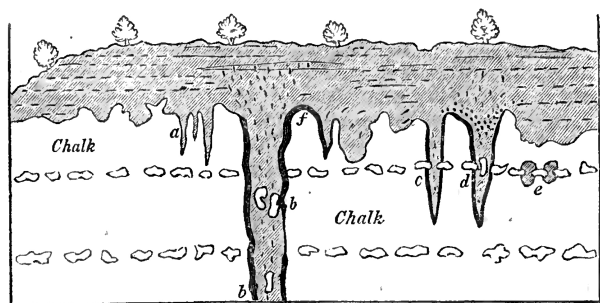


FIG. 43 Solution pipes in the chalk at Eaton near Norwich, UK, as sketched by Lyell (1839).

and a cigar-shaped termination. Their cross-sections are almost perfectly circular and very smooth (Fig. 42E-H), giving the impression that they were artificially drilled rather than formed by natural processes.

One of the first to describe in detail the morphology of solution pipes was Charles Lyell, the father of modern geology. His 1839 paper “On the tubular cavities filled with gravel and sand called sand-pipes in the chalk near Norwich” (Lyell, 1839) remains to this day a great example of deductive reasoning based on observations from nature. Lyell describes a group of solution pipes in chalk strata (see Fig. 43), and observes that they are elongated (with lengths up to 20 meters) and round in cross-section. He also comments that they do not merge and tend to stay separated from one another and that they are not guided by the fractures. When the smaller pipes cross the horizontal layers of flint nodules (c & d in the figure), the nodules tend to stay in place, sticking out of the pipe, whereas in larger pipes (b) the nodules are found somewhat lower than their original position. All of that leads him to the hypothesis that the pipes are solutional in origin, that the chalk has been removed by the corroding action of water charged with acid, in which the flint nodules, being insoluble, were left in situ in the smaller pipes after the calcareous matrix had been dissolved. He also concludes from the manner in which the large detached flints were dispersed through the contents of the widest pipes that the excavation and filling of the pipe were gradual and contemporaneous processes. He further comments that the fact that piping always proceeds under the cover of sand or gravel and never on the exposed rock may be related to the fact that these upper layers provide space for the water to focus.

Not all researchers agreed with Lyell. In particular, Trimmer (1845) expressed the opinion that pipes originate from the mechanical action of water, similar to potholes near waterfalls. However, as argued by Prestwich (1855), this would imply that they were empty during their formation, and thus all the insoluble material (like the flint nodules of Fig. 43) should be found at their base, which is not the case. Additionally, the pipes do not

seem to contain grinding tools required for pothole erosion (e.g., resistant pebbles). Furthermore, some of the pipes have a huge aspect ratio (even 100:1), much larger than any known potholes, making it hard to imagine the vertices of such an elongation actively carving pipes.

The pipes in tropical and Mediterranean climates differ from those in temperate regions, as they feature hard rims cemented with calcite (Fig. 42B). In some areas, the eroded matrix around the pipes reveals a reversed landscape, resembling a forest of vertical pipes standing closely together. The resemblance of these pipes to tree trunks has historically led to their misidentification as petrified trees (Boutakoff, 1963; Bretz, 1960). This model suggested that decaying tree trunks, rapidly buried by aeolian sand, could form conduits for groundwater, leading to the precipitation of calcite and forming a solid cast around the original trunk.

However, this hypothesis was challenged by several researchers (Grimes, 2004; Herwitz, 1993), who noted that the close spacing of the pipes (less than 0.5 m in some places) is too dense for a forest, the bases of the pipes are rounded hemispheres without paleosol horizons or branching root structures (Grimes, 2004), and some pipes reach depths up to 20 m and are unbranched vertical cylinders, which would imply rather peculiar, column-like trees. Despite these objections, interpretive signs erected at Cape Bridgewater (Fig. 42B) in the early 2000s still described this as a petrified forest (Grimes, 2004).

Nevertheless, it seems that the only hypothesis that has withstood scrutiny posits that the rimmed pipes in tropical climates are solutional in origin (De Waele *et al.*, 2011; Lipar *et al.*, 2021, 2015; Lundberg and Taggart, 1995), i.e., their genesis is similar to that postulated by Lyell for the chalk pipes in England, with the only difference being the rim cementation triggered by high evaporation rates in tropical climates. Formation of the pipes would then link with the reactive-infiltration instability (Sec. V.J): small inhomogeneities in the porous matrix tend to focus the flow, which is followed by enhanced dissolution, which eventually transforms initial inhomogeneities into mature pipe.

A question remains regarding the sources of the large masses of water that carved the pipes. While most researchers suggest that it is CO₂-charged rainwater acting over millennia, an alternative hypothesis exists for pipes formed in colder areas, which links their formation with deglaciation. Morawiecka and Walsh (1997), Walsh and Morawiecka-Zacharz (2001) and Dobrowolski and Mroczek (2015) studied pipes in Miocene calcarenite in Poland that could have formed subglacially under the cover of a continental glacier till. Piping there is restricted to areas beneath a till cover, and pipes did not develop where till is absent. This links the formation of the pipes to the deglaciation at the end of the Elsterian period, when large volumes of cold water were suddenly released into the fully saturated subglacial aquifer. In

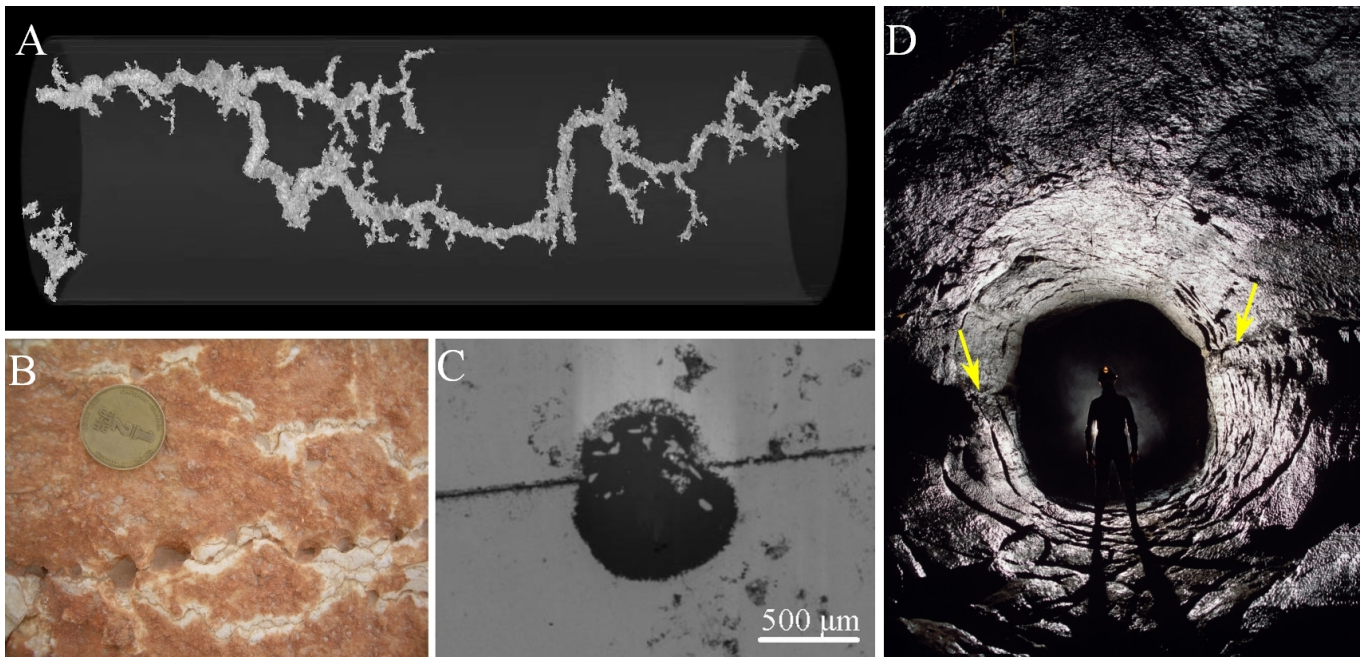


FIG. 44 Wormhole formation in porous rocks and fractures. (A) tomographic image of a wormhole etched by carbonic acid in limestone core (Cooper *et al.*, 2023). (B) A dissolutionally enlarged stylolite with several wormholes in a limestone wall of Mitzpe Ramon quarry, Israel. (C) Wormhole at the outlet of a fractured limestone core. (D) A conduit in a phreatic cave in Dan yr Ogof, Swansea Valley, South Wales. The white arrows mark the initial fissure. Panel B courtesy of Pawel Kondratiuk, University of Warsaw. Panel C courtesy of Maria Garcia Rios and Linda Luquot, Technical University of Catalonia. Panel D courtesy of Brendan Marris, Dudley Caving Club.

such conditions karstification becomes very intense (Lauritzen and Skoglund, 2013).

An interesting problem related to the formation of solution pipes, and more broadly, to the formation of self-organized structures in geological systems, is whether every structure necessarily needs a precursor. A geologist would naturally lean towards an affirmative answer to this question: since something is here now, there must have been a cause for it to form here, rather than elsewhere. Physics, on the other hand, points to positive feedback mechanisms underlying the onset of instabilities, which can produce ordered structures from any small disturbance. In the case of solution pipes, this discussion has been ongoing for several decades. Many studies suggested that pre-existing heterogeneities in rock or soil have caused the flow to focus in a particular spot. The factors invoked included animal burrows (Devitt and Smith, 2002; Doerr *et al.*, 2000), surface hollows, potholes or cracks (Coetzee, 1975; De Waele *et al.*, 2011; Grimes, 2004, 2009; Lipar *et al.*, 2015; Lundberg and Taggart, 1995), stemflow and rootflow (Herwitz, 1993; Johnson and Lehmann, 2006; Lipar *et al.*, 2015; Mitchell *et al.*, 1995). On the other hand, the numerical models (Lipar *et al.*, 2021; Petrus and Szymczak, 2016; Upadhyay *et al.*, 2015) suggest that the dissolution patterns are largely insensitive to the initial conditions in the rock matrix. Inhomogeneities do impact the time-scale and length-scale

over which the channels are first observed (Cheung and Rajaram, 2002; Hanna and Rajaram, 1998; Kalia and Balakotaiah, 2009; Maheshwari and Balakotaiah, 2013; Maheshwari *et al.*, 2013), however in a large enough system naturally growing instability eventually overwhelms any local perturbation (Upadhyay *et al.*, 2015).

Another manifestation of reactive-infiltration instability are wormholes, which dissolution fingers create when the pressurized reactive solution is pushed through porous or fractured rock. The distinction between wormholes and solution pipes is somewhat arbitrary, but in general the term solution pipes is used for gravity-driven dissolution fingers formed in the vadose zone near the surface and extending downwards whereas wormholes appear in fully saturated flow driven by external pressure gradients.

They are relatively easy to obtain in experiments (Fig. 44A), and they have been used for at least 100 years by petroleum engineers to enhance oil and gas production by increasing the permeability of the rock. The shapes of the wormholes formed during acidization depend strongly on the flow rate, with more conical, smoother wormholes forming at lower flow rates, and highly ramified, tortuous wormholes appearing at high flow rates. Long, thin (dominant) wormholes, formed at intermediate flow rates, are the most effective for petroleum engineering, since they minimize the acid required for a given increase



FIG. 45 Replacement fingers. A: A dolomite finger (marked with white dashed line) in limestone outcrop (Sharp *et al.*, 2010) B: Uranium roll with uraninite precipitation around its tip. Photograph by C. L. Van Alstine (U. S. Atomic Energy Commission), courtesy of Dr. Robert Gregory (Wyoming State Geological Survey), C: Terra Rossa fingers over limestone at Greatstone Winery near Coonawarra, South Australia. The photo is courtesy of Les Sampson (Claremont Wines, South Australia). D: Closeup of one of the pipes, showing the terra rossa layer (dark red) and more recent siliceous sands overlying it. Photograph by Piotr Szymczak.

in permeability.

Estimates of wormhole growth rates and, in particular, the so-called breakthrough time, the moment when the longest wormhole reaches the outlet of the system, are crucial for a number of geotechnical problems. These include risk assessment of potential leakage of sequestered carbon dioxide, safety of dam sites in soluble rocks, risk of catastrophic ground subsidence due to solutional widening of fractures, and the danger of water seepage into

toxic waste repositories.

Natural wormholes in porous media, except for solution pipes, are relatively rare, since large flow rates are needed to trigger the instability, which are not easily obtained under typical pressure gradients in subsurface flows. It is different in the case of rock fractures, where the permeability, and thus possible fluid velocity, is much greater.

Instabilities in fracture dissolution were first discovered

by numerical simulations (Hanna and Rajaram, 1998) and later confirmed by experiments (Detwiler *et al.*, 2003; Gouze *et al.*, 2003). Linear stability analysis shows that fractures are even more unstable to dissolution than porous media (Szymczak and Ladd, 2011), where a minimum wave-length is needed for unstable growth (Ortolova *et al.*, 1987a). However, fracture dissolution is almost always unstable (Starchenko *et al.*, 2016; Szymczak and Ladd, 2012), and intense wormholing is to be expected (see Sec. V.D). The onset of a reactive-infiltration instability has been observed in a microfluidic fracture system, with very good agreement with theoretical predictions of the wave-length of the initial instability (Osselin *et al.*, 2016).

Wormholing is the driving force behind cave formation in karst systems (Dreybrodt, 1990; Hanna and Rajaram, 1998; Szymczak and Ladd, 2011), and cave conduits are beautiful manifestations of nonuniform dissolution. Caves are initiated along fractures and bedding planes, which have a quasi two-dimensional structure, while the mature cave is almost always a system of pipe-like conduits (Fig. 44D). Wormholes are formed across a range of length-scales. Fig. 44B shows cm-size wormholes growing along a stylolite in a limestone block, while Fig. 44C shows a mm-scale wormhole emerging in fracture dissolution experiments.

Wormholes provide a way in which aggressive solutions can penetrate deeply into limestone formations. A simple estimate of the penetration length in uniform fractures gives $l_p < 1$ m, meaning limestone caves should not exist at all (White and Corwin, 1961). One possible resolution of this paradox is the sharp drop in the dissolution rate of CaCO_3 near saturation (White, 1977). However, wormhole formation offers a simpler explanation (Szymczak and Ladd, 2011); flow in the spontaneously formed conduits (Fig. 44) is several orders of magnitude larger than the initially uniform flow across the fracture width, and the penetration length increases accordingly. Numerical simulations (Starchenko *et al.*, 2016) show that highly unsaturated solutions can penetrate deeply into wormholes etched in fracture surfaces.

While solution pipes and wormholes are associated with the dissolution of the rock, replacement fingers are connected with dissolution-precipitation processes, where the primary mineral is replaced by a secondary one (Kondratiuk *et al.*, 2017; Korzhinskii, 1968; Putnis, 2009). Examples include dolomitization (Fig. 45A), which involves the replacement of limestone (calcium carbonate) with dolomite (calcium magnesium carbonate). Since the molar volume of dolomite is less than that of calcite, the primary mineral in limestone, dolomitization can create additional pore space if the process is not accompanied by significant compaction or cementation. The higher permeability of the dolomite then triggers instability, which can lead to the formation of dolomite fingers (Centrella *et al.*, 2021; Koeshidayatullah *et al.*, 2020; Merino and

Canals i Sabaté, 2011). Another example is the formation of uranium rolls (Fig. 45B), in which uraninite precipitates at the redox front that separates oxidized rock from reduced rock. The oxidized rock is more porous than the reduced one because the redox reactions produce sulfuric acid that dissolves potassium feldspars. Increased porosity again results in instability leading to the formation of characteristic fingers with a thin band (Dewynne *et al.*, 1993). Finally, Figs. 45C & D show the terra-rossa fingers above limestone. An intriguing hypothesis on their genesis has been put forward by (Merino and Banerjee, 2008). They proposed that terra-rossa is formed by authigenic replacement of the underlying limestone at a reaction front. The hydrogen ions produced in such a reaction further dissolve the rock matrix, triggering a reactive-infiltration instability which should result in intense piping (Kondratiuk *et al.*, 2017).

Wormholing is dissolution channel formation in fractures (Fig. 44). The structures form due to a reactive-infiltration instability. Fracture dissolution is almost always unstable, and intense channeling is to be expected. Wormholing is the driving force behind cave formation in karst systems, and cave conduits are classical manifestations of nonuniform dissolution. Caves are initiated along fractures and bedding planes, which have quasi-2D structure (Fig. 44a), while a mature cave is almost always a system of pipe-like conduits (Fig. 44d).

V. Mud volcanoes, pockmarks and seeps

Submarine seeps and mud volcanoes are structures that form part of the Earth's fluid venting systems. These structures expel fluids, including liquids, principally water but also hydrocarbons, and gases such as carbon dioxide and methane, from the subsurface to the seafloor (Judd and Hovland, 2009) or land surface (Kopf, 2002). Cold seeps are associated with the slow seepage of hydrocarbons, methane, and other fluids at or near ambient seafloor temperatures. Hot seeps involve the expulsion of warmer fluids, often associated with hydrothermal systems. Pockmarks are shallow depression features formed by the escape of fluids and gases from the seabed, resulting in crater-like depressions. Submarine mud volcanoes occur on the seafloor and are often linked to deep-seated overpressure zones, faulting, or hydrocarbon reservoirs. Terrestrial mud volcanoes are found on land and often associated with tectonic plate boundaries or sedimentary basins with high fluid pressure.

Submarine seeps typically involve the upward migration of fluids through vertical conduits, such as fractures, faults, or permeable sedimentary layers. Mud volcanoes, both submarine and terrestrial, are characterized by the upward movement of fluidized sediments, mud, and gases through a central vertical conduit. These conduits allow fluids to move from deep subsurface reser-



FIG. 46 Tubular concretions of authigenic carbonates, Pobiti Kamani, Varna, Bulgaria, preserve the subsurface plumbing network of an Early Eocene methane seep system in the Balkanides foreland (De Boever *et al.*, 2009) (image: Diego Delso, CC-BY-SA-4.0).

voirs to the seafloor or land surface. The vertical conduits of mud volcanoes are typically associated with high-pressure environments, where fluid overpressure exceeds the strength of overlying sediments, leading to the formation of fractures and the eruption of materials. The process is driven by buoyancy forces, where lighter fluids like hydrocarbons and gases rise through denser surrounding sediments, but also by osmotic pressure (Cardoso and Cartwright, 2016). In some cases, fluids may migrate laterally along permeable layers before reaching the seafloor (Rocha *et al.*, 2021). Horizontal migration is influenced by geological structures like unconformities or bedding planes, as well as by self-capping processes (Hovland, 2002).

Submarine seeps and mud volcanoes often lead to the precipitation of carbonate minerals, forming distinctive authigenic carbonate structures, such as mounds, tubes, or chimneys (Fig. 46). The expelled materials from mud volcanoes, such as mud and brecciated rock fragments, can lithify over time, forming mudstone or breccia deposits. These rocks serve as evidence of past mud volcanic activity. Mud volcanoes may leave behind diatreme-like structures or intrusive bodies of mudstone that cut through surrounding sediments, providing clues to the ancient venting processes (Brown, 1990). In some cases, large carbonate structures known as chemoherms can form around seeps due to the activity of chemosynthetic organisms (Teichert *et al.*, 2005). These features are preserved in the rock record and indicate past fluid seepage events (Conti and Fontana, 1999).

W. Hydrothermal vents

Hydrothermal vents form by the precipitation of minerals from hydrothermal fluids as they mix with the surrounding seawater. (As hotter, mineral-rich water exits the vent and encounters the colder seawater having a different pH, minerals precipitate out forming characteristic structures (Fig. 47).

There exist different varieties of vent (Tivey, 2007). Hotter black smokers emit dark, particle-rich, acidic plumes primarily composed of iron and sulfide minerals. Cooler white smokers emit lighter-colored plumes, often rich in barium, calcium, and silicon. A third category, discovered more recently, are cool alkaline vents first seen at Lost City hydrothermal field in the mid-Atlantic (Kelley *et al.*, 2005). These differences are reflected in differing physical growth mechanisms (Cardoso and Cartwright, 2017).

Hydrothermal vents present certain characteristic patterns, particularly chimneys and flanges, Fig. 47. The primary structures at vents are chimneys: tall, tubular structures formed by the precipitation of minerals forming a structure around the fluid plume as it emerges from the seabed. Thus chimneys grow over time and can reach many tens of meters in height. Their internal structure may consist of a single conduit through which the mineral-laden water flows, or it may be much more complex, formed of a multitude of micro- or nano-scale channels allowing slower, more diffuse flow through a porous medium. Such flows are likely to display chaotic advec-

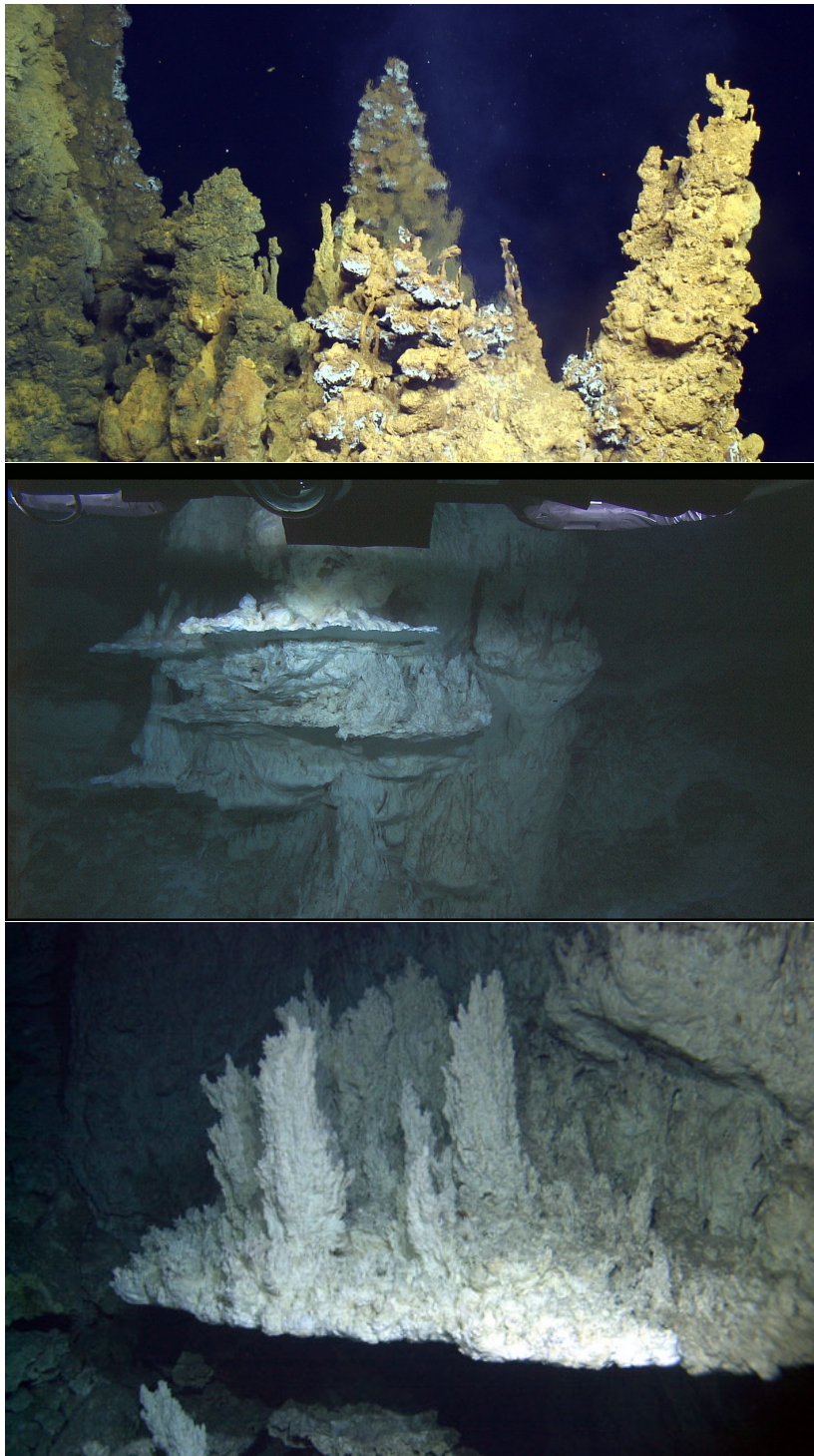


FIG. 47 Hydrothermal vent structures: chimneys and flanges (images: Submarine Ring of Fire 2014 - Ironman, NSF/NOAA, CC-BY-SA-2.0; NOAA, public domain; NSF, public domain).

tion (Sec. V.K). Flanges are horizontal structures that extend out from the sides of chimneys, creating ledge-like features from which secondary chimneys may also extend upwards. Flanges also form from the deposition of minerals as hydrothermal fluids cool and precipitate

minerals. They often trap pockets of superheated water beneath them (Turner, 1995).

Hydrothermal vents are geological versions of chemical laboratory experiments called chemical gardens (Barge *et al.*, 2015b). In a chemical-garden experiment, a solu-

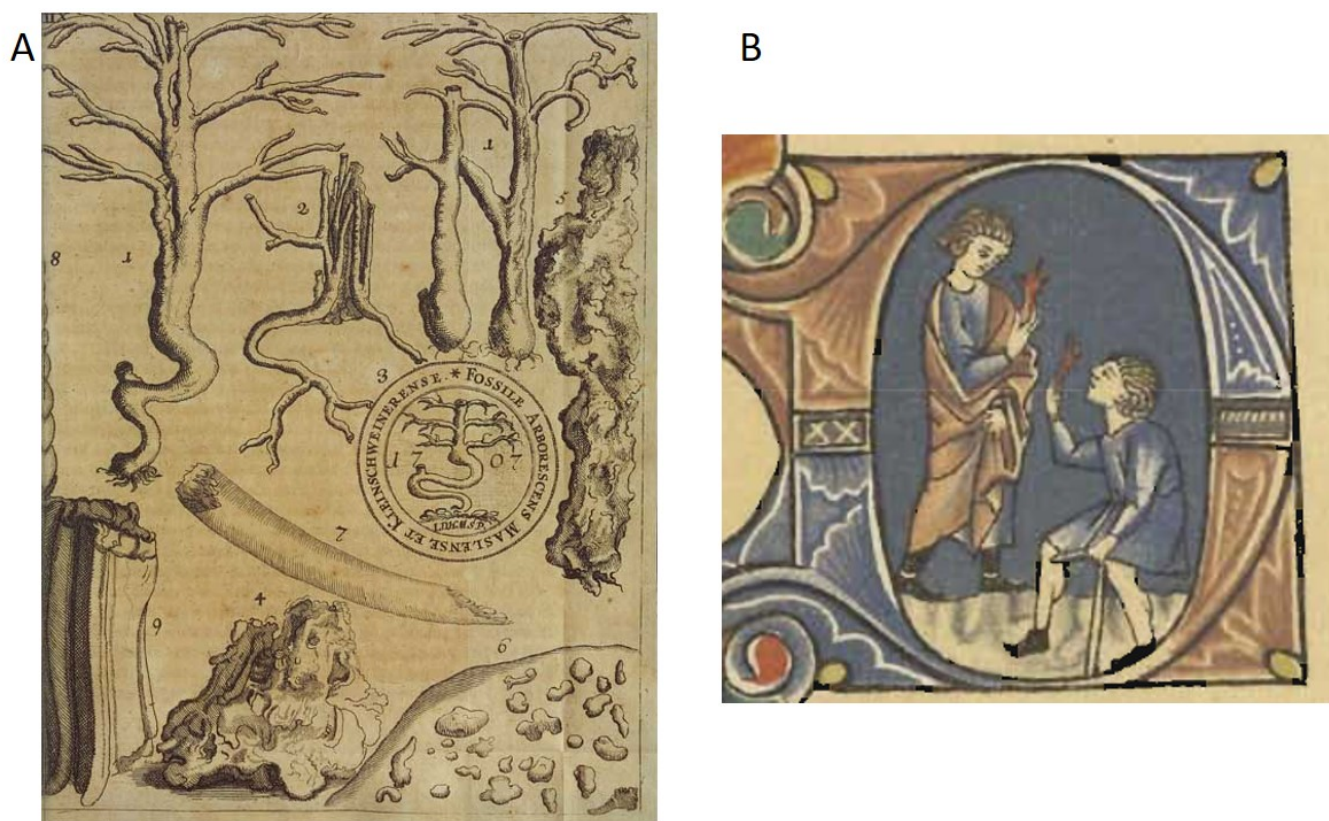


FIG. 48 A) Fulgurite illustrations from the book written by Hermann (1711). B) Illustration of the lapidary of Alfonso X El Sabio (Alfonso X and Fernandez Montana, 1881), where there can be seen rocks with an arborescent aspect that resemble fulgurites.

ble metal salt solution pumped into a solution containing a different anion, often silicate or carbonate, precipitates the insoluble metal salt resulting from the reaction (Cartwright *et al.*, 2011). The precipitate forms a cohesive solid membrane, which templates around the fluid flow while at the same time permitting chemical reaction to continue through the passage of ions across the membrane (Cartwright *et al.*, 2002).

Hydrothermal vents, specifically those of the Lost City type emitting cool alkaline fluids associated with serpentinization (Kelley *et al.*, 2005; Sainz-Díaz *et al.*, 2018), have been suggested as candidate sites for where the first life on Earth may have arisen (Cartwright and Russell, 2019; Martin and Russell, 2007; Russell and Hall, 1997). The hypothesis is that micro-compartments in submarine alkaline hydrothermal vents separated by mineral membranes (see Fig. 7) may have been where the first proto-bio-chemistry emerged (Sander and Koschinsky, 2011; Sojo *et al.*, 2016). As well as the deep ocean site of Lost City, similar vents have been found in shallow waters at Strytan, Iceland (Gutiérrez-Ariza *et al.*, 2024; Stanulla *et al.*, 2017) and at Prony Bay, New Caledonia (Monnin *et al.*, 2014).

X. Fulgurites

Fulgurites are hollow glass tubes formed in sand, soil or rock by electrical discharges, with lengths varying from centimeters to meters; the smallest ones being the most common due their fragility (Grapes, 2010; Pasek and Pasek, 2018). According to several authors, the first description of fulgurites was made by Hermann (1711) in the early 18th century (Fig. 48A) (Carter *et al.*, 2010; Gailliot, 1980; Petty, 1936). Other authors suggest that the first mention of fulgurites dates back to the 13th century (Garcia-Guinea *et al.*, 2009; Martín-Ramos *et al.*, 2019), as they appear in the lapidary of Alfonso X *El Sabio*, King of Spain, under the name of mazintarincan (Fig. 48B) (Alfonso X and Fernandez Montana, 1881).

Fulgurites are glasses formed by the rapid heating of the ground when it is impacted by an electric current of high intensity (Pasek *et al.*, 2012; Pasek and Pasek, 2018). These electric currents may be natural (i.e., lightning) or artificial; and the ground on which they form may be sand, clay soil, caliche, rock or anthropogenic material (Pasek *et al.*, 2012; Pasek and Pasek, 2018). Although some differences can be observed between natural and anthropogenic/artificial fulgurites (Figs. 49 and 50), no distinction will be made between them and the clas-

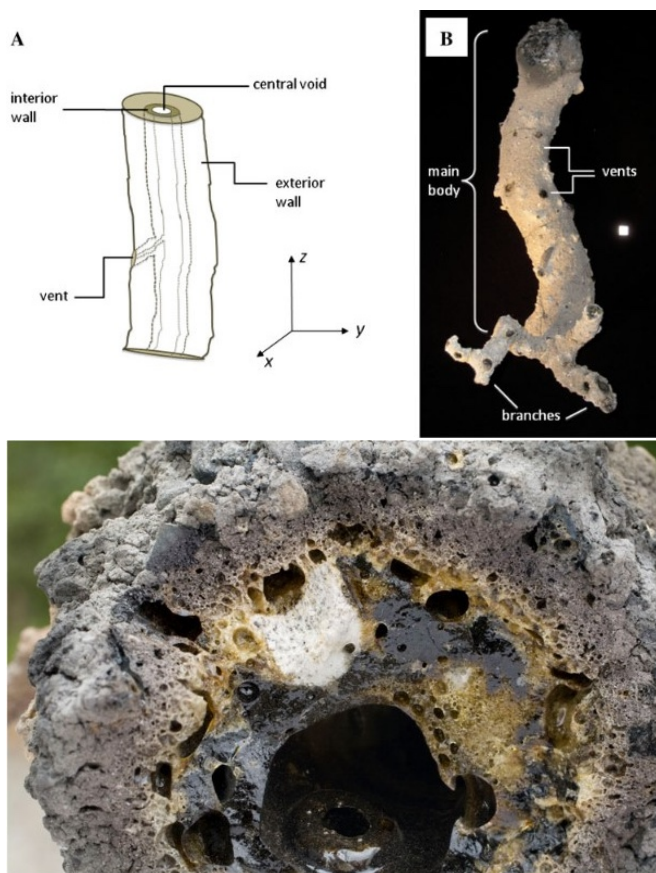


FIG. 49 Natural fulgurites. A) Scheme of fulgurite structure. B) Lateral view of a fulgurite. C) Fulgurite cross-section. Figure from Pasek *et al.* (2012).

sification made by Pasek *et al.* (2012) will be used. For a comprehensive review on artificial fulgurites the reader is referred to the review by Pasek and Pasek (2018).

Fulgurites are formed when, after the electric current hits the ground, the ground heats up rapidly, producing voids and vesicles along the path followed by the lightning, which allow volatiles to escape. This heating and the escape of gases produce a glassy silica wall with cylindrical or elongated conical, usually hollow, shapes. This vitreous inner wall is surrounded by a rough outer layer in which melted or unmelted grains can be found (Fig. 49) (Pasek *et al.*, 2012). The inner hollow had been classically explained to be formed by the expansion of gas, which presses and fuses the sand as lightning travels through the ground (Petty, 1936), and, more recently, by sand vaporization along the lightning path (Pasek and Pasek, 2018). This central hole, which may be single or multiple (formed by a multitude of closely spaced voids), is aligned along the direction in which the lightning has moved (z -direction in Fig. 49). From this main structure, new branches can grow. The main branch can be distinguished from the secondary branches because it has the greatest width, although it is not usually wider than a

few centimeters (Pasek *et al.*, 2012).

Fulgurites have been divided into 4 categories, depending on the ground composition (Pasek *et al.*, 2012). Type I, sand fulgurites, are mainly composed of silica glass, which formed a thin wall (interior wall in Fig. 49A). If present, the external wall will be also composed mainly of silica glass with traces of Al and Fe oxides. Type II, clay fulgurites, are formed in soils composed by clays, sand and/or small rock fragments. Interior and exterior walls are clearly visible in these fulgurites. This type is wider and have larger glassy regions than type I. Type III, caliche fulgurites, are formed in desert hardpan or caliche. Silica glass is not the main phase (<10%) and is surrounded by calcite. Type IV, rock fulgurites, form in rock, causing the glass walls to be surrounded by unmelted rock. They can be found on the rock surface forming narrow tubes.

In addition, a subcategory has also been proposed for exogenic/droplet fulgurites (type V) (Pasek *et al.*, 2012). This type of fulgurite is formed when, after a very powerful lightning strike, > 100 GW, some of the ground material is melted and ejected into the atmosphere, solidifying in the air. This rapid cooling in air causes their morphology to be amorphous, droplet or bubble-shaped, and they are generally greenish in color (Martín-Ramos *et al.*, 2019; Pasek *et al.*, 2012). These fulgurites are mainly composed of glass and are common as a consequence of type II and IV fulgurites (Pasek *et al.*, 2012).

It has been proposed that the phosphide mineral schreibersite, $(\text{Fe,Ni})_3\text{P}$, which forms as spherulites in fulgurites, would have provided an important source of prebiotic phosphorus on the early Earth, potentially facilitating the synthesis of phosphorus-bearing organic compounds (Hess *et al.*, 2021).

Within a solid insulating material, a Lichtenberg figure is generated by dielectric breakdown. Lichtenberg figures refer to intricate branching electric discharge patterns that can form on the surface or within the volume of insulating materials such as wood, acrylic, or glass when subjected to high-voltage electrical discharges. These patterns typically resemble fern-like structures, tree branches, or lightning bolts, and can vary in complexity and size. They are caused by the path of least resistance that the electrical current takes through the insulating material, leaving behind permanent marks or indentations that follow the electric discharge patterns. The discharge can occur either on the surface or within the material, depending on its properties and the intensity of the electric field.

Y. Seismites

The term *seismite* was coined in 1969 by Seilacher to describe the origin of structures observed in the Miocene Monterey Formation at Santa Barbara, California, USA

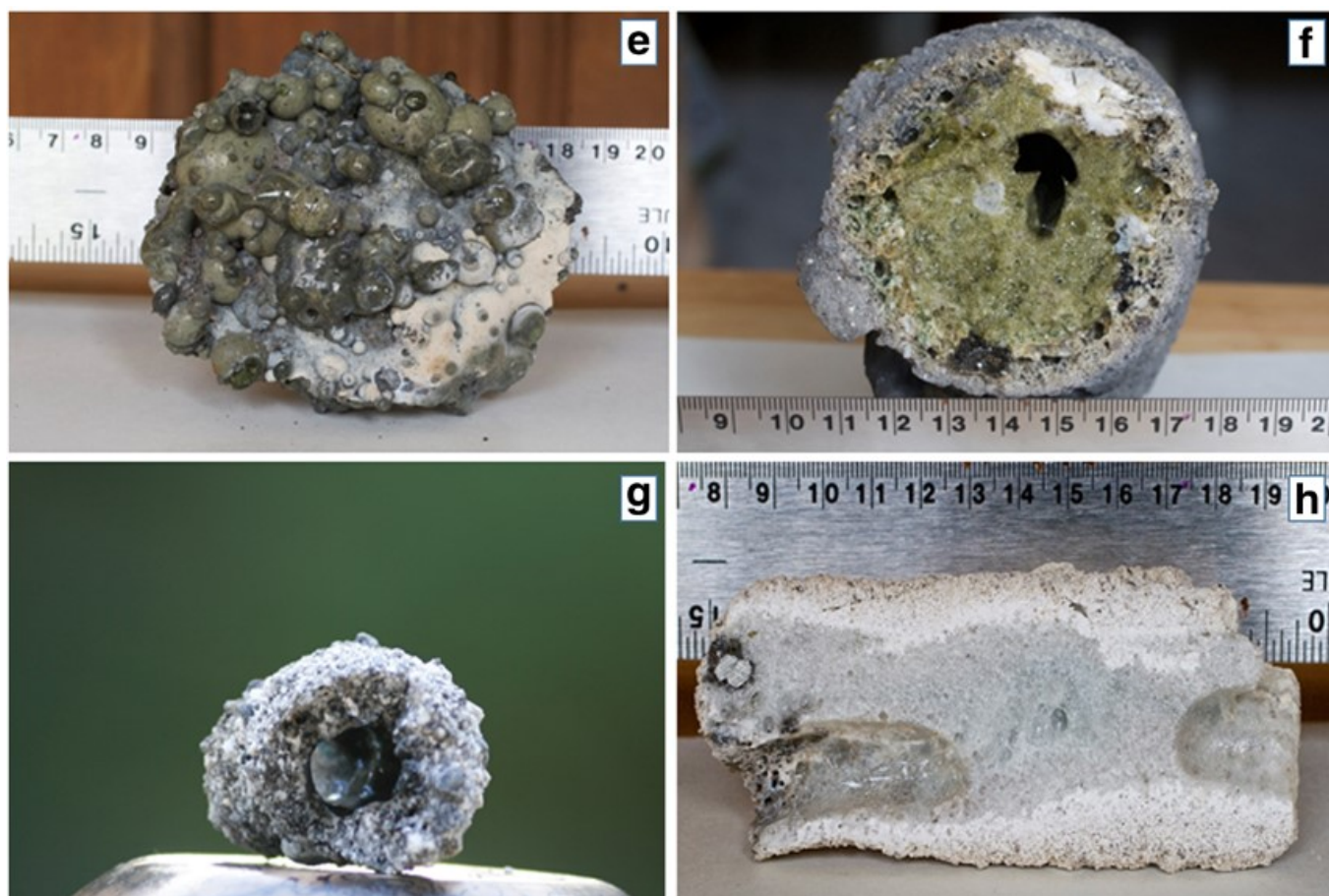


FIG. 50 Fulgurites of ambiguous (natural or artificial/anthropogenic) origin. e) Exogenic fulgurite. f-h) Fulgurites showing a hollow tube in the inner part. Figure from Pasek and Pasek (2018).

(Seilacher, 1969). This outcrop was described as a regular structural sequence of (from above) a liquefied zone, debris zone, and step zone, with gradational contacts between these zones and the bottom, but with a sharp boundary at the top. Seilacher 1969 interpreted this sequence as having been produced by earthquakes. Since then, numerous authors have used the term seismites to denote earthquake-generated sedimentary structures (Alfaro *et al.*, 2010, 1997; Montenat *et al.*, 2007; Moretti and Ronchi, 2011). However, this term seems to be currently under discussion since many of the described seismites structures are produced by liquefaction of sediments (Shanmugam, 2016), and this liquefaction can be produced by different triggering mechanisms (up to 21, including, e.g., earthquakes, sediment loading, salt tectonics and volcanic activity). Therefore, it has been proposed to refer to these structures as soft-sediment deformation structures (SSDS) (Shanmugam, 2016). Criticizing and taking a position on the use or not of the word seismite is not the aim of this review, nor is an exhaustive review of the different SSDS (e.g., Shanmugam's work 2016 lists 27 different structures). In this review, therefore, structures that have been reported as originat-

ing from seismic events will be described, and they will be referred to as seismites.

In the work of Rodriguez-Pascua *et al.* 2000, focused on the Miocene basins of the Prebetic Zone (Spain), the different SSDS found in the region are described and related to the magnitude of the earthquakes. These authors indicate that in this region, the seismites can be categorized into those produced without liquefaction and those produced after the liquefaction of the sediments. The former are produced by earthquakes of magnitude less than 5 and the latter by earthquakes greater than 5. The structures described without liquefaction include (Rodriguez-Pascua *et al.*, 2000): loop bedding, disturbed varved lamination, and mixed layers without fluidization (centimetric structures, which appeared in deep lake areas with varved sediments). In this region, the structures produced after liquefaction of the sediments are (Rodriguez-Pascua *et al.*, 2000): mushroom-like silts protruding into laminites, mixed layers with fluidification, and pseudonodules (centimetric structures, which appeared in deep lake areas with varved sediments); sand dykes, pillow structures, and intruded and fractured gravels (metric structures, which appeared in shallow



FIG. 51 Seismites. Above: giant seismites of Galera, Granada, Spain; on the left an overview of the pillow-like structures, on the right a detail of one of the pillows, about two meters across (images: Julyan Cartwright). Below: seismites in Lake Lisan (Pleistocene Dead Sea) sediments, Israel (images: Piotr Szymczak).

lake areas with detrital sediments). Among these soft-sediment deformation structures, the most impressive structures are the pillow structures, of which an extraordinary example can be found in the Baza Basin, Spain (Fig. 51). These pillow structures appeared in deformed beds with thickness varying from a few centimeters to 2.5 m, the best examples being 1.5–2 m thick and 2–4 m in width (Alfaro *et al.*, 2010). These structures were generated because a lower density unit (clays and silt) was deposited in this region, followed by a higher density unit (fine-grained and coarse-grained sand). When an earthquake occurs, the fluidification of the clays causes them to rise upwards, breaking the overlying layer, generating escape structures and giving the sand unit the pillow-like morphology (Alfaro *et al.*, 2010) in a geological example of the Rayleigh–Taylor instability (Sec. V.F).

Although in this review we have focused on a very specific example in Spain, because it is a clear seismitite example and also one of the few examples called giants, seismitites can be found all over the world, e.g., in Israel (Fig. 51, Kagan *et al.* (2018)), USA (Jewell and Ettensohn, 2004; Seilacher, 1969) and Germany (Bachmann and Aref, 2005), just to name a few.

Z. Menilites

Menilites are a type of botroidal-looking rocks composed mainly of opal (Sec. IV.C) and dolomite (Molina Grande and Molina García, 1980; Pimentel *et al.*, 2024). They occur mainly in simple centimetric forms such as spheres, dumbbells or rods (Fig. 52A). However, the most interesting are the larger ones (> 5 cm) with more complex shapes (Fig. 52B). Recently, it has been proposed that the formation of these rocks may be related to the paleoearthquakes that affected in past geological epochs the regions where these rocks appear and that occurred during the formation of these rocks (Pimentel *et al.*, 2024). In the formation of these rocks, a fluid phase is involved. A fluid phase is formed by having a porous medium above the water table, a medium that can be fluidized by earthquakes that force the water to move upwards. The different density in the composition of these nodules (opaline, not very dense) and the bedrock (marls and limestones, denser) implies, when the environment is wet, a difference in osmotic pressure (Sec. V.L) if the opal-carbonate interface is considered as a membrane (i.e., as a surface with elasticity). If the



FIG. 52 Menilites with simple (A) and complex (B) shapes (image: Pimentel *et al.* (2024)).

water entering the nodules breaks this membrane, the internal fluid under pressure extrudes, forming the characteristic shapes of this type of rock.

AA. Clathrites

Clathrites, Fig. 53, are methane-derived precipitates derived from the transformation of clathrates into carbonates. Clathrates, clathrate hydrates, or gas hydrates are partially solid structures composed of water molecules arranged in closed crystals. Within these structures, small molecules, usually non-polar gases are confined within the icy shells. Clathrates can evolve into clathrites over time. This evolution is directly linked to the transformation of clathrates into carbonates, while partially preserving and mirroring their patterns and mesoscale structure. Kennett and Fackler-Adams (2000) coined the term chlathrite in 2000 to describe the mesoscale structures exhibiting an association of soft-sediment deformation that resulted from gas hydrate formation or dissociation. These structures are found directly inside massive gas hydrate layers and sometimes exhibit surface morphologies created by a direct mirroring of clathrates bubble-structure. Examples of sites where clathrites have been observed include the Gulf of Mexico (Smith and Coffin, 2014; Suess, 2014), North Italian Apennines (Argentino *et al.*, 2019), Mediterranean Sea mud volcanoes (Aloisi *et al.*, 2000), and Cascadia (North West America) (Greinert *et al.*, 2001).

AB. Sedimentary crack patterns

Fracture propagation associated with the expansion, contraction, and shear of geological soft matter, whether

granular, gelatinous or otherwise, can produce a wide variety of crack patterns, Fig. 54. When sedimentary layers, particularly those in a drying environment, are subjected to expansion, contraction, or shear forces, they develop a network of fractures that propagate through the material (Weinberger, 1999).

Crack patterns in sedimentary environments can vary widely. They range from simple polygonal networks, such as hexagonal or rectangular arrangements, to more intricate, branched structures. The formation of these patterns is dependent on factors such as the sediment's composition, moisture content, and the environmental conditions during drying (Plummer and Gostin, 1981).

Scaling laws can explain the geometric characteristics of crack patterns. The geometry of these cracks can often follow predictable scaling laws, which help explain their formation and resulting shapes. Such scaling laws describe how the stress distribution within the drying sediment influences the size, spacing, and complexity of the crack network (Bonnet *et al.*, 2001).

In sediments, one of the most common examples of these patterns can be seen in dried mud (Fig. 54a). As water evaporates from the sediment, the surface shrinks, leading to the formation of cracks. These cracks grow progressively as the sediment continues to dry and contract (Zhao *et al.*, 2014). A further typical instance of sedimentary cracking is seen in Fig. 54b: ice wedge polygons in permafrost (Lachenbruch, 1962).

AC. Basalt columns

Appearing as a striking pattern of roughly hexagonal pillars of rock, columnar joints are famous from landscapes like those of the Giant's Causeway in Northern Ireland, and the Devil's Postpile in California. At these

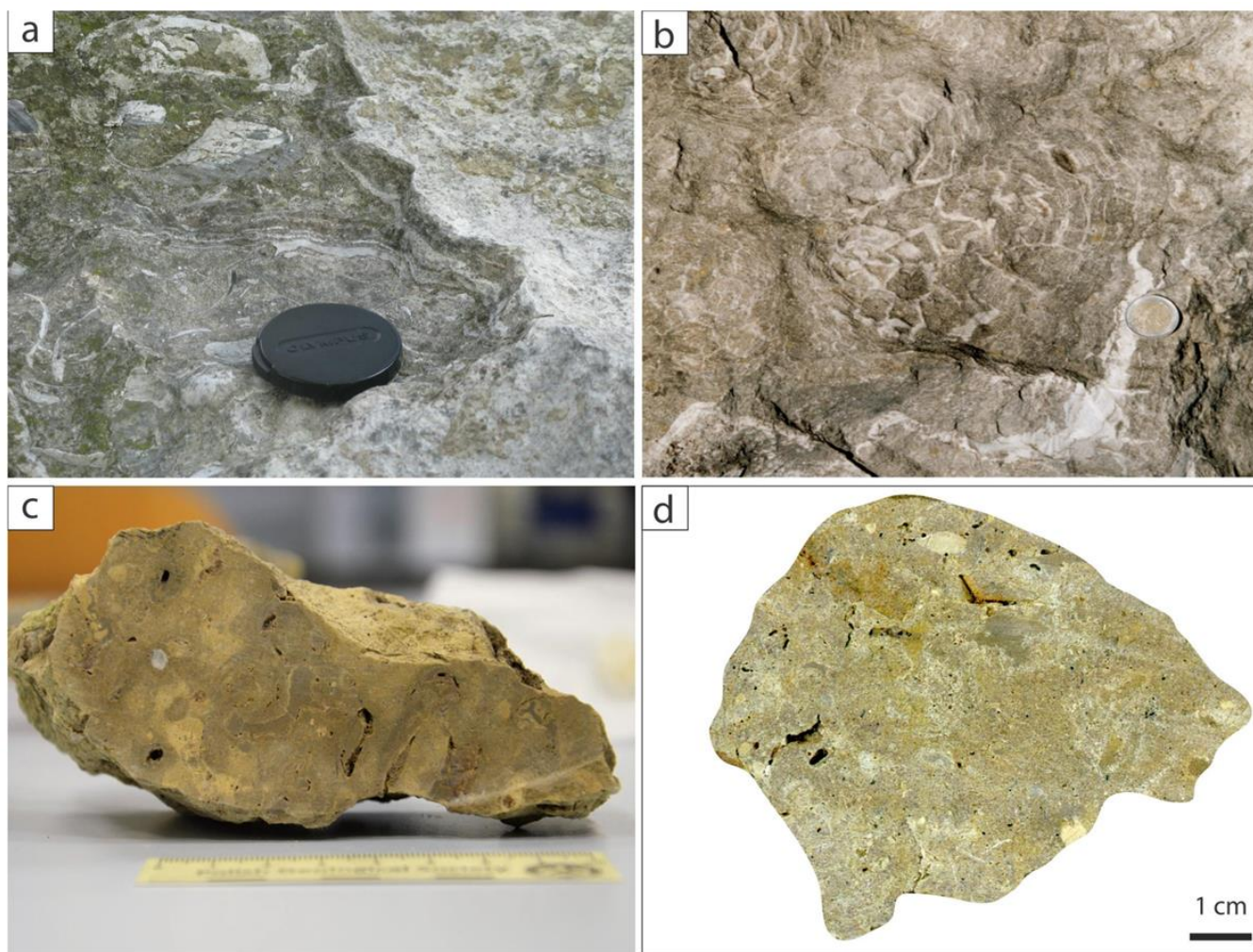


FIG. 53 Clathrite structures. (a) Thin layered structures surrounding a carbonate breccia with shell fragments. (b) Irregular network (mainly radial to concentric) of carbonate-filled veins. (c,d) Vacuolar, spongy and vuggy-like fabrics: cavities have various shapes, empty or filled with carbonate cements and/or coarser sediments and coquina debris. From Argentino *et al.* (2019).

places, basalt has broken into a colonnade consisting of regular, prismatic columns of rock, each a few tens of centimeters across. The cracks that delimit the edges of these columns were formed as the basalt cooled from molten lava, millions of years ago. Subsequently exposed by erosion, the evocative scenery of columnar jointing, as shown in Fig. 55, has attracted scientific attention for centuries (Foley and Molyneux, 1694). The origins of columnar joints in the thermal contraction of a cooling lava flow have been recognized since at least the 19th century (Mallet, 1875), and recent research has focused on explaining the origins of the regular pattern of cracks that form the joints, as well as the physics that determines the size of the columns.

Although best known in the form of columnar basalt (Aydin and DeGraff, 1988; Goehring and Morris, 2008; Long and Wood, 1986; Phillips *et al.*, 2013; Ryan and

Sammis, 1978), columnar joints occur in a wide variety of materials. They are common in other lava types, including rhyolite and andesite (DeGraff and Aydin, 1987; Spry, 1962), and have been reported in igneous rocks on Mars (Milazzo *et al.*, 2009, 2012) and the moon (Basilevsky *et al.*, 2015; Xiao *et al.*, 2014). Columns can also be found in sandstone (Summer and Ayalon, 1995) and chalk (Weinberger and Burg, 2019) where they are thought to result from the cooling and contraction after some intense thermal treatment, for example by the invasion of a nearby dyke or sill; for similar reasons, columns are sometimes found in smelter slag, coal, and rapidly quenched glass (DeGraff and Aydin, 1987; French, 1925).

Columnar joints in lava typically form when a lava flow cools slowly over time. The lava could be emplaced as a massive flood basalt, covering thousands of square kilometers (DeGraff and Aydin, 1987; Goehring and Morris,



FIG. 54 Sedimentary cracking patterns: desiccation cracks in dried sludge (image: Hannes Grobe, CC-BY-SA-2.5); ice-wedge polygons in permafrost (image: Brocken Inaglory, CC-BY-SA-3.0).

2008; Long and Wood, 1986) or as a pond or stream that formed after a smaller volcanic eruption, as is common in Hawaii (Peck and Minakami, 1968; Ryan and Sammis, 1978). As the initially fluid lava cools, it solidifies. The details of this process will depend on the specific chemistry of a lava, with a series of distinct minerals crystallizing from the melt over a range of temperatures. However, to a good approximation, there will be a change from a fluid-like to a solid-like rheology, corresponding to a glass transition or liquidus-solidus transition around 800–900°C (Gottsmann *et al.*, 2004; Lamur *et al.*, 2018; Lore *et al.*, 2001; Peck and Minakami, 1968). Below this temperature, the lava will behave as an elastic solid, and accumulate tensile stress due to thermal contraction. This situation sets up a stress gradient in the lava, mirroring the thermal gradient, which drives fracture.

Since a molten lava flow will cool inwards from its boundaries, the initial cracks will appear at the surfaces of the flow. This process has been observed, for example, in the cooling of fresh lava lakes from the Kilauea volcano (Peck and Minakami, 1968). As time and cooling proceed, the cracks from the surface will grow deeper. They will develop into a network of crack tips following just behind the solidification front, where the cooling lava supports an elastic stress. This crack network effectively carves out the columnar features as it advances (Mallet, 1875; Spry, 1962). The motions of the crack tips are not smooth, however, but rather the cracks that will form the column faces advance intermittently. When any crack grows, its active tip will move into warmer conditions. As a result, the tensile forces driving the fracture become weaker, and it will soon slow down and halt. After sufficient thermal stress has then had time to build up again, the crack can be reactivated, grow forward, and halt once more. As shown in Fig. 55(c), this stick-slip motion is recorded by a roughly periodic banding

along the faces of the columns, features called striae that look similar to chisel marks (Ryan and Sammis, 1978). Within each band, the crack surface is smoothest under the more brittle conditions of the crack initiation, and becomes rougher as the crack advances into warmer rock and slows down (DeGraff and Aydin, 1987; Ryan and Sammis, 1978). Combined with slight mismatches in the orientation of subsequent striae, and with plumose markings—faint feathery lines that develop perpendicular to the direction of crack propagation—these periodic variations in texture can be used to determine the direction in which a colonnade developed (Budkewitsch and Robin, 1994; DeGraff and Aydin, 1987; Goehring and Morris, 2008; Ryan and Sammis, 1978). For further details, Pollard and Aydin (1988) review the geology and petrology of columnar joints, and explain how to interpret the surface features (striae, plumose, hackle) on column faces.

The directional growth of columnar joints also provides the route for columns to take on well-ordered polygonal shapes. Near the flow margin, the fracture network that defines the columns looks similar to the contraction cracks that can be seen in dried mud or clay (Aydin and DeGraff, 1988; Budkewitsch and Robin, 1994; Peck and Minakami, 1968). This pattern is dominated by cracks intersecting at T-shaped junctions, which is the result of the sequential fragmentation of the surface: later cracks will curve to intersect earlier ones at right angles, to maximize their energy release rate (Bohn *et al.*, 2005). As the columns grow, the incremental advances that leave the striae features allow the crack network to change: each crack advance can be slightly misaligned with the previous step. Over time, the crack intersections that form the corners of the columns will then shift, towards Y-shaped junctions. In lava flows, this can be seen within the first 1–2 meters of a flow margin (Aydin and DeGraff, 1988). The Y-junctions are energetically favored in situ-

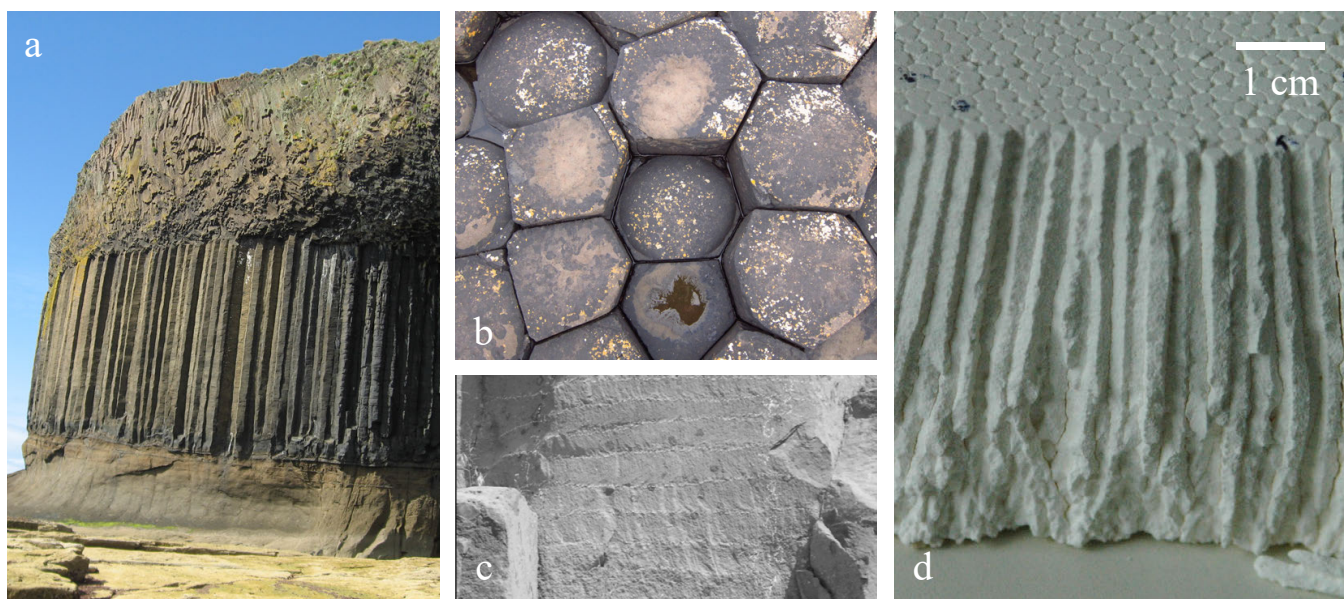


FIG. 55 Columnar jointing in lava and starch. (a) At Staffa, Scotland, a well-formed columnnade sits atop an ash layer, and is surmounted by an entablature of thinner, more disordered columns. The columnnade cooled from the ash-contact upwards, while the entablature cooled from above. (b) A cross-section of columns at the Giant's Causeway, N. Ireland, highlights their polygonal shape. (c) Striae, appearing as short bands on the face of any column, record the stick-slip motion of the column's formation. Plumose (left/right-leaning feathery lines, marked by arrows) also indicate the direction in which each crack advance occurred. (d) When a slurry of corn starch is dried, it also cracks into columnar joints. The sample here is shown inverted, with the base of the columnnade exposed, to better display the hexagonal pattern that developed. (images a-d: Lucas Goehring).

ations where the advancing cracks are guided or triggered by the locations of previous features, but where the sequence in which the cracks form becomes randomized in each cycle of fracture growth (Goehring, 2013). Goehring and Morris (2014) review this process of the ordering of hexagonal fracture patterns in more detail.

The manner in which a columnnade grows means that it records how a lava flow cools. In particular, the columns extend along the direction of cooling, and perpendicular to isotherms at the cracking front, near to the solidus or glass transition temperature (Budkewitsch and Robin, 1994; Kattenhorn and Schaefer, 2008; Mallet, 1875; Spry, 1962). Some common structures formed in this way include fans of columns, rosettes and chevrons, in addition to the more typical horizontal columnnade (Spry, 1962). A fan can form as columns radiate away from a strong cooling site, for example. The fracture network of a developing columnnade is highly permeable, allowing water and gas to circulate within the cracks, enhancing cooling (Budkewitsch and Robin, 1994; Goehring and Morris, 2008; Hardee, 1980; Lamur *et al.*, 2018; Long and Wood, 1986). Clear evidence for this comes from bore-hole measurements in the cooling Kilauea Iki lava lake (Hardee, 1980), which for many years maintained a near-constant 100°C temperature from the surface to within about ten meters of the still-molten regions of the lake. It is thought that water percolating through the cracks

boils near the molten lava, then flows away as steam to condense near the flow margins (Budkewitsch and Robin, 1994; Goehring and Morris, 2008; Hardee, 1980; Ryan and Sammis, 1981). The efficiency of this two-phase convective mechanism means that a relatively constant cooling rate can be maintained over the long periods of time that a regular columnnade takes to develop.

A large lava flow will tend to spread out into a thin but wide layer, which cools simultaneously from above and below. This leads to the common arrangement of an upper columnnade, which cooled from the top down, and a lower columnnade, which cooled from the bottom up. In many landscapes multiple flow units, each from a different volcanic event, can be layered on top of each other; there are at least four such layers visible in the cliffs above the Giant's Causeway, for example (Tomkeieff, 1940). More complex, multi-tiered structures have also been reported within a single flow unit, such as at the Columbia Plateau (DeGraff and Aydin, 1987; Long and Wood, 1986). Finally, the upper columnnade is frequently replaced by a layer of narrow and much more randomly oriented columns, a structure called entablature—as in the top layer of Fig. 55(a). It is still not clear why or how entablature forms, although it has been implicated with enhanced and localized cooling (Forbes *et al.*, 2014; Long and Wood, 1986): Hamada and Toramaru (2020) give a recent, detailed discussion of this curious open problem.

The rate at which the lava cools also affects the size of the columns, with faster cooling generally leading to smaller columns (Budkewitsch and Robin, 1994; Goehring and Morris, 2008; Goehring *et al.*, 2009; Grossenbacher and McDuffie, 1995; Ryan and Sammis, 1978). The striae provide the best evidence of this connection, which is also supported by analysis of the crystal texture (Long and Wood, 1986). In particular, the thickness or height of the striae provide insight into the cooling rate of the lava, and there is a strong correlation between the size of the striae, and the size of the columns on which they appear (DeGraff and Aydin, 1993; Goehring and Morris, 2008; Grossenbacher and McDuffie, 1995; Lamur *et al.*, 2018). This would be the case if the column size is inversely proportional to the cooling rate of the lava when the columns formed.

The understanding of columnar joint formation which has been described above has been greatly aided by analogue experiments, involving colonnades produced in drying starch—see Fig. 55(d). The interpretation of such studies relies on the exact mathematical analogy between the theories of poroelasticity and thermoelasticity, i.e. the equivalence between the elastic stresses generated by drying and by cooling, respectively (Goehring *et al.*, 2009). The first detailed experiments of Muller (1998) highlighted the value of this analogue system, although there are occasional mentions of it in earlier literature (French, 1925; Huxley, 1881). Müller’s work was followed by a series of quantitative studies that showed how to control column size by adjusting the drying rate of the starch (Toramaru and Matsumoto, 2004); tracked how the pattern ordered with depth (Goehring and Morris, 2005); and linked column growth to the passage of a sharp drying front (Mizuguchi *et al.*, 2005). Plumose structures on the larger joints of dried starch (Müller and Dahm, 2000) and other pastes (Sakaguchi *et al.*, 2022) confirm the interpretation of their appearance in lava joints. Three-dimensional images of dried starch colonnades, obtained by X-ray tomography (Crostack *et al.*, 2012; Goehring *et al.*, 2006; Goehring and Morris, 2005; Hamada and Toramaru, 2020; Mizuguchi *et al.*, 2005; Muller, 1998), also confirm how columns grow normal to the direction of drying (analogous to cooling), and led to the current appreciation of how the column size depends inversely on the drying (cooling) rate. These analogue experiments, and the mathematical analogy between cooling and drying that enables a strong interpretation of their results, are reviewed in detail in Chapter 7 of Bacchin *et al.* (2018), and Chapter 9 of Goehring *et al.* (2015).

More recently, research on columnar jointing has progressed into a number of promising additional areas. Detailed mapping of the topology and geometry of columnar joints has led to the development of simple, low-dimensional metrics that can distinguish between a wide variety of crack patterns with distinct origins (Domokos

et al., 2020; Domokos and Regös, 2024; Roy *et al.*, 2022). The origins of entablature remain enigmatic, but innovative lines of experiment (Hamada and Toramaru, 2020) have begun to unravel their nature. The related concept of ‘master cracks’, or joints that enable faster local cooling, is also being explored (Akiba *et al.*, 2021; Forbes *et al.*, 2014; Hamada and Toramaru, 2020; Moore, 2019). With more practical aims, research has been made into how the strongly anisotropic texture of columnar joints affects their hydrological and mechanical properties, such as their relative permeability to flow along different directions (Chao *et al.*, 2020; Niu *et al.*, 2023; Vasseur and Wadsworth, 2019), and their strength and resistance to deformation (Que *et al.*, 2023). These applications address questions such as the use of basalt formations for carbon geosequestration (Jayne *et al.*, 2019; Wu *et al.*, 2021),

V. PHYSICAL MECHANISMS UNDERLYING GEOLOGICAL SELF-ORGANIZATION

We hope to have convinced the reader with the geological examples we have presented that soft matter is a helpful physical classification applicable to a range of geological systems. What common underlying physical mechanisms behind the patterns are operating in these geological systems? The reader should note that—as with the list of geological examples—this list is not exhaustive; there can be mechanisms we do not cover. Our aim here as we ‘round up the usual suspects’ is to indicate the wide range of physical mechanisms involved in geological self organization. For more details we refer the reader to the physics literature.

A. Reaction–diffusion systems

Reaction–diffusion systems describe processes where substances spread out in space (diffuse) and interact with each other through chemical reactions. Often, we associate diffusion with the smoothing of concentration gradients over time, leading to a uniform homogenized soup, as substances move from regions of high concentration to low concentration. However, introducing chemical reactions into these systems, may disrupt uniformity and drive the spontaneous formation of complex spatial structures. Such systems occur in various physical, chemical, and biological settings.

At the core of pattern formation is the concept of Turing instability. In 1952, Alan Turing (Turing, 1952) demonstrated that diffusion, In 1952, Alan Turing (Turing, 1952) demonstrated that diffusion, when combined with nonlinear chemical reactions involving two interacting species, can spontaneously break the symmetry of an initially uniform mixture of chemical compounds.

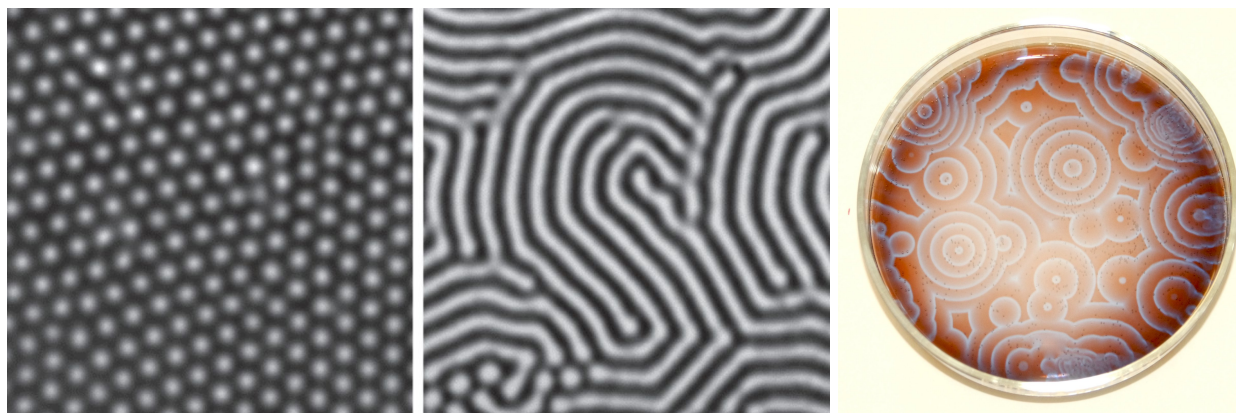


FIG. 56 Reaction–diffusion systems. a,b) Turing patterns. Courtesy of Jacques Boissonade and Patrick De Kepper, University of Bordeaux. c) Belousov-Zhabotinsky target and spiral patterns. Stephen Morris.

In the simplest case of a Turing model, one species acts as an activator (promoting its own production) while the other functions as an inhibitor (suppressing the activator’s growth). Both diffuse, but the inhibitor has a larger diffusion coefficient than the activator. Through the coupling of diffusion and reactions, small perturbations from uniformity can grow, leading to the spontaneous appearance of spatial patterns. Depending on the parameters, a Turing system can generate spots, stripes, or even labyrinthine patterns, reflecting the self-organizing capacity of reaction-diffusion dynamics (Fig. 56A,B).

The mechanism behind pattern formation in such systems was creatively explained by James Murray in his book on *Mathematical Biology* (Murray, 1989) with an analogy of “sweating grasshoppers”. Imagine a dry grassy field with grasshoppers scattered throughout. If a fire starts in one part of the field, it will naturally spread, burning everything in its path. However, grasshoppers, sensing the approaching flames, react by moving ahead of the fire and sweating profusely, which dampens the grass and prevents it from burning. In this analogy, the fire is the “activator”, spreading destruction, while the grasshoppers are the “inhibitors”, stopping the fire from spreading by moistening the grass. The key to the pattern’s emergence is that the grasshoppers react faster than the fire spreads, creating a non-uniform, repeating pattern of charred and uncharred areas, similar to the spotted patterns on animal coats. Two mechanisms are key to the creation of a pattern: self-activation (a short-range positive feedback loop), where small perturbations in the uniform state tend to grow over time (similar to fire spreading), and screening (long-range inhibition), where the formation of a structure at one point reduces the likelihood of similar structures appearing nearby. In the grasshopper example, this corresponds to grasshoppers surrounding the fire and stopping its spread. This balance of opposing forces or processes mirrors how many natural patterns emerge.

This is akin to how many natural patterns

form—through a balance of opposing forces or processes. Geological examples include patterns in sand (Fig. 11) “As a ridge gets bigger, it enhances its own growth by capturing more sand from the moving air. But in doing so it acts as a sink, removing sand from the wind and suppressing the formation of other ripples nearby. The balance between these two processes establishes a roughly constant mean distance between ripples” (Ball, 2015); honeycomb weathering (Fig. 38) (McBride and Picard, 2004); and travertine patterning (Hammer *et al.*, 2008)

A further related type of reaction–diffusion system is termed an excitable medium (Meron, 1992). In these systems a small perturbation leads only to a small transient effect; however a perturbation above a certain threshold excites the system, which then remains in its excited state for some time before returning to quiescence, and upon this return has a refractory period during which it cannot be excited a second time. A classic example is the Belousov–Zhabotinsky (BZ) reaction (Zhabotinsky, 1991). Geologically relevant examples of excitable media include the example of crystal growth mentioned above, which may be seen as an excitable medium (Cartwright *et al.*, 2012). Earthquake dynamics, as modeled by the Burridge-Knopoff model (Burridge and Knopoff, 1967) describing a chain of blocks connected by springs and pulled over a surface, may also be viewed as a type of excitable medium with elastic rather than the usual diffusive coupling (Cartwright *et al.*, 1997). Also in the temporal domain, it has been suggested that the oceanic carbon cycle may be excitable, and that mass extinction events may correspond to large perturbations that excite the system (Rothman, 2019). As for spatio-temporal patterns, an excitable model for the coupled evolution of ice-surface temperature and elevation produces spiral waves similar to those observed in the Martian north polar ice cap (Pelletier, 2004).

Reaction–diffusion systems remain an active area of research in both biological and geological pattern for-

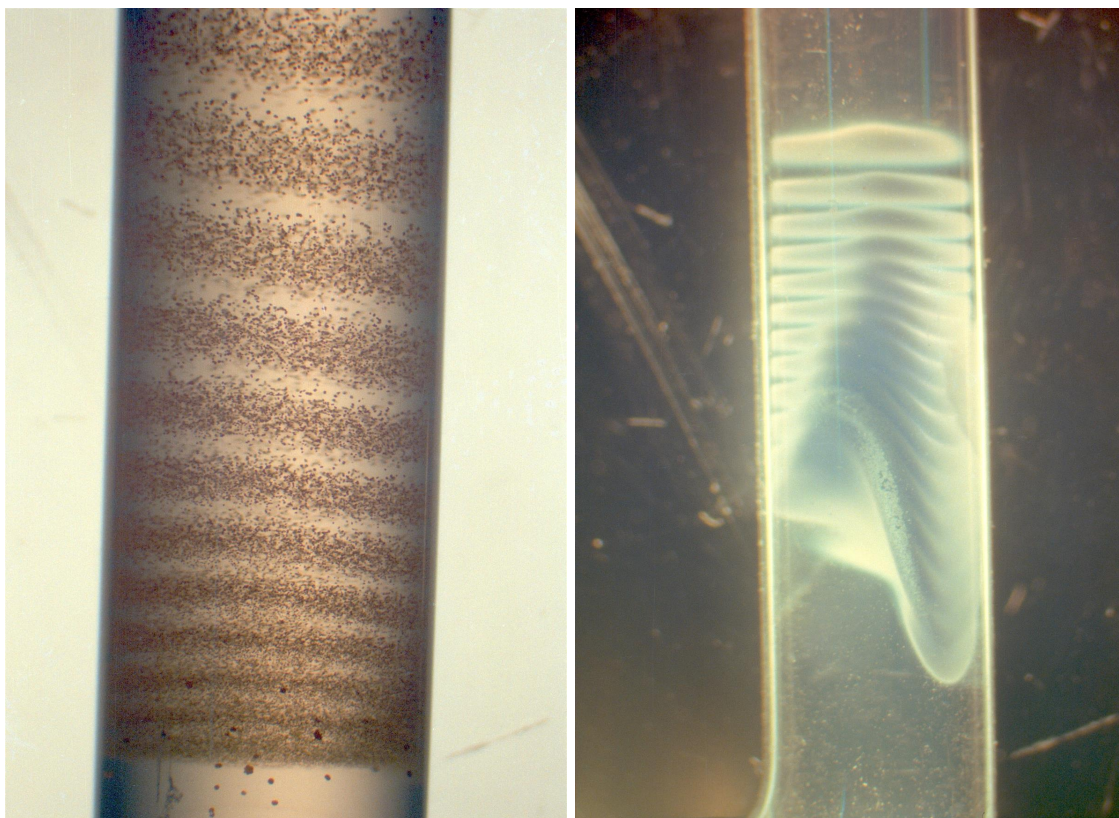


FIG. 57 Liesegang bands in laboratory experiments (images: Julyan Cartwright).

mation. While the complexity of biological systems often makes it difficult to identify the specific morphogens responsible for a given pattern, geological systems are usually much simpler, involving just a handful of chemicals. Examples such as zebra rock (Fig. 28) or target patterns in sandstone rocks (Fig. 23) strongly suggest a reaction-diffusion origin, although other banded patterns, like striped flints (Fig. 25) or sphalerites (Fig. 26) elude such a simple description. However, there are two important factors to consider when thinking about geological systems. First, in order for a reaction-diffusion pattern to survive the millenia, it needs to be literally frozen, sculpted into the rock (Jamtveit and Hammer, 2012). This means that not only bulk reactions need to be involved but also surface reactions, such as precipitation. The second key factor is the importance of fluid flow. For large enough system size L , the advective timescale, $\tau_a = L/v$, is always shorter than the diffusive timescale, $\tau_d = L^2/D$. Thus, it is invariably advection—usually through fractures, joints, and bedding planes—that brings reactants to rock strata, leading to its chemical transformation. Diffusion can be a controlling factor, particularly on smaller spatial scales, such as in the cracks observed in Fig. 23A. We shall discuss fluid-flow-mediated instabilities from Sec. V.D onwards.

B. Liesegang patterns

One particular reaction-diffusion system is Liesegang banding (Fig. 57). Liesegang band formation is a rhythmic precipitation phenomenon that occurs when one solute diffuses through a gel and reacts with another solute, resulting in distinct bands or rings. The spacing of these bands increases geometrically as one moves outward from the point of diffusion (Jabłczyński, 1926; Matalon and Packter, 1955). Although the phenomenon was initially reported by Runge (1855) and Ord (1879), it became more widely known after the systematic experiments conducted by Liesegang (1896). In his experiments, Liesegang observed the diffusion of silver nitrate in a gelatin layer containing potassium dichromate, leading to visually striking periodic precipitates with bands oriented parallel to the diffusion front. Rings are formed in a radial geometry, while bands exhibit a linear geometry. Often, these structures are referred to as periodic precipitation structures (Henisch, 2014), which is somewhat misleading; the primary defining characteristic of Liesegang structures is that they are generally not simple periodic patterns but instead have aperiodic spacings that follow some geometric series. To complicate matters further, the term “Liesegang” is frequently found in geological publications to describe any banding observed in

rocks. Here we must try to disentangle this mess.

Despite the phenomenon being known for well over a century, the mechanism of the Liesegang band formation is still a matter of discussion. Two main groups of theories have been proposed, termed pre- and post-nucleation models, differentiated by the timing of precipitate nucleation in the system (L'Heureux and Fowler, 1999; Nabika *et al.*, 2019).

In the pre-nucleation models, following Ostwald (1897) and Prager (1956), bands are proposed to result from a feedback loop between nucleation and diffusion. Precipitation starts at a specific value of supersaturation (the nucleation threshold) and subsequently depletes the solute around it, preventing it from reaching the nucleation threshold in adjacent regions. This process is followed by renewed nucleation farther from the initial band, resulting in a rhythmic pattern that regularly obeys precise quantitative spacing laws.

In contrast, post-nucleation models consider the interaction between growth, diffusion, and surface tension effects. The pattern is generated through Lifshitz–Slyozov instability (Lifshitz and Slyozov, 1961b), which demonstrates how homogeneous systems with uniformly distributed precipitate particles may become unstable due to Ostwald ripening. Smaller particles tend to dissolve because their surface energy is higher due to their curvature. The dissolved material then diffuses through the surrounding matrix and redeposits onto larger particles, which have a lower surface energy. This process results in the growth of larger particles over time at the expense of smaller ones. In an initially non-uniform system, this can generate bands that evolve through coarsening after the nucleation phase is over (Boudreau, 1995). In contrast to the pre-nucleation models, post-nucleation models can generate patterns even in the absence of an initial concentration gradient.

It is possible that both these mechanisms may be found in nature. Experiments and simulations show examples of various different morphologies beyond the classical bands and rings, including spirals, rods and spots (Dayeh *et al.*, 2014; Krug and Brandtstädter, 1999; Papp *et al.*, 2020) as well as bands of two crystalline phases (Cartwright *et al.*, 1999b).

One of our aspirations with this review is to eradicate the indiscriminate use of the term *Liesegang* pattern in geology for any spatial oscillation; as we show here, there is a variety of physical mechanisms that can produce banding, both periodic and aperiodic.

C. Oscillatory zoning

Oscillatory zoning is another reaction–diffusion system seen in geological systems. Three different zoning patterns have been described in crystals depending on the formation conditions, known as normal, inverse and oscil-

latory zoning (Ginibre *et al.*, 2007). Normal and inverse zoning show a change of the system in one direction. In normal zoning, the center is a less evolved phase than the outer zone. In a magmatic mineral, it would indicate, for example, a decrease in the temperature of the magma chamber. In reverse zoning, minerals show an involution of formation conditions. As in the example above, a magmatic mineral with reverse zoning would indicate an increase in the temperature of the magma chamber. Oscillatory zoning is a repetitive, concentric zoning of the crystal. It is this latter pattern that may be of interest for a geochemobionics review.

For natural crystals showing oscillatory zoning, extrinsic and intrinsic mechanisms have been described (Shore and Fowler, 1996). Extrinsic mechanisms are those related to physical and chemical changes within the whole system (e.g., fluid mixing, change in pressure or temperature). Intrinsic mechanisms are related to crystal growth and local phenomena (Shore and Fowler, 1996). Oscillatory zoned minerals are fairly common in nature, although it is difficult to determine what extrinsic or intrinsic factors promote their formation. Extrinsic mechanisms are not of the interest of geochemobionics and, therefore, it will be of interest to focus these lines in the synthesis of minerals in the laboratory, where all the parameters are determined and the oscillatory zoning is driven by intrinsic mechanisms and, in consequence, can be considered as an example of self-organization during crystal growth.

Two mechanisms have been put forward to explain the formation of oscillatory zoning.

In the first one, it is proposed that the zoning is caused by the reduction of the growth rate with the incorporation of the new ion and the effect of the growth rate on the partition coefficient of such an ion (Reeder *et al.*, 1990). This effect has been described for manganese-enriched calcites. Mn reduces the growth rate of calcite, which increases the partition coefficient of Mn and its absorption into the calcite structure. This results in a decrease of the Mn concentration in the solution, which increases the calcite growth rate and decreases the Mn partition coefficient. The cycle starts again by increasing the partition coefficient of Mn in the solution, which leads to oscillatory zoning (Fig. 58A).

The second mechanism described invokes the difference in solubility of the end members of the solid solution to describe the formation of the oscillatory zoning (Prieto *et al.*, 1997). If that difference is large enough, the more insoluble phase will grow first, until it is undersaturated by the drop on the concentration of one of the ions, after which the second phase will begin to grow, until, again, the drop on the concentration of the other ion in the solid solution allows the first phase to grow. This effect has been described for the solid solution (Cd,Ca)CO₃. In this case, the otavite crystallizes first, when the Cd concentration drops, the calcite crystallizes until the Ca concentra-

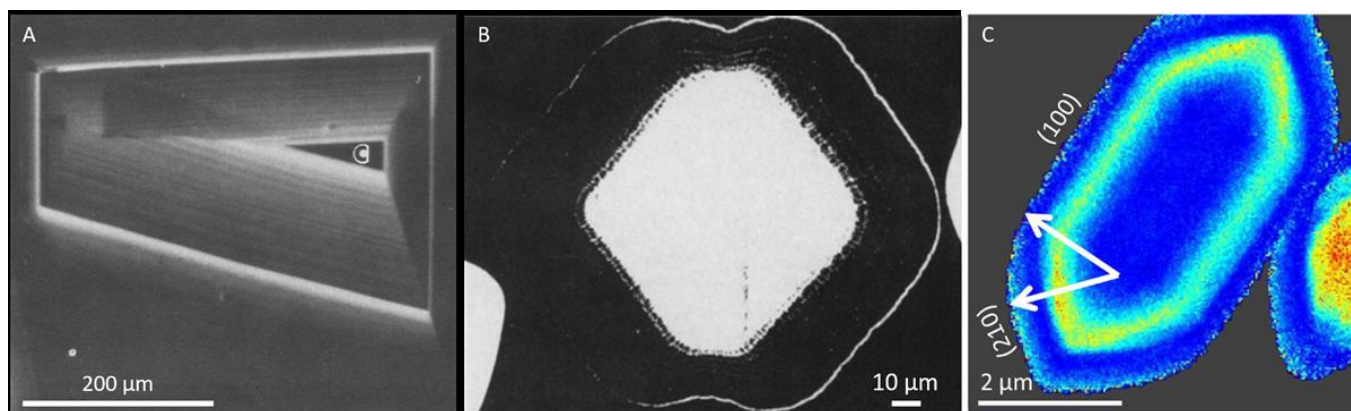


FIG. 58 Oscillatory zoning. Examples of synthetic crystals showing oscillatory zoning: a) Calcite crystal with white areas enriched in Mn (Reeder *et al.*, 1990). b) $(\text{Ca,Cd})\text{CO}_3$ crystal, white areas are enriched in Ba (Prieto *et al.*, 1997). c) $\text{Ba}(\text{SO}_4,\text{HAsO}_4)$ crystal, blueish areas are depleted in As, while yellowish-greenish areas are enriched (Ling *et al.*, 2018).

tion drops to allow the formation of a new otavite layer (Fig. 58B). This mechanism has also been described for anionic solid solutions, e.g., $\text{Ba}(\text{SO}_4,\text{HAsO}_4)$ (Fig. 58C).

These experiments were performed in closed systems, so that the observed oscillatory zoning can be considered as occurring due to causes intrinsic to the system and are, therefore, an example of chemical self-organisation.

Normal, classical crystallization itself is the self-organization of condensed matter. Is classical crystal growth from the melt or the solution an example of soft matter? It might be counted as such, since it does already lead to structures at intermediate, mesoscopic length scales: growth steps that can form target and spiral patterns. What is indubitably soft matter is the more complicated forms of crystal growth that lead to mesoscale patterns, such as oscillatory zoning.

D. Fluid-flow instabilities and convective processes

Because of the long time-scale and low speed of many geological processes, these can be modelled successfully as viscous fluids (e.g., Fletcher (1977) and Wollkind and Alexander (1982)). A common mechanism for geological self-organization is physical instability resulting from fluid interactions. These may be categorized in terms of the instability acting.

E. Rayleigh–Bénard convection

Rayleigh–Bénard instability, or buoyancy- (density)-driven convection, occurs when a fluid layer is heated from below and cooled from above, leading to the formation of convection cells as the fluid moves (convects) under this forcing (Bodenschatz *et al.*, 2000; Getling, 1998).

On a large scale, the Rayleigh–Bénard instability is a key process in the Earth’s thermal evolution and the

dynamics of fluid movement within geological settings (Busse, 1989). It provides a framework for understanding how heat is transported in the Earth’s interior, influencing everything from plate tectonics (Anderson, 2002) to the cooling of magmatic bodies and the circulation of fluids in hydrothermal systems.

The RB instability plays a significant role in the formation of layered geological structures, particularly within igneous bodies like plutons and layered intrusions. These structures are formed as a result of the convective processes driven by temperature gradients in magma chambers or large igneous bodies. Layered intrusions are large, sheet-like bodies of igneous rock that exhibit distinct layers with different mineral compositions formed as a result of the cooling and crystallization of magma within a magma chamber. In a magma chamber, RB instability creates convective currents as the hotter, less dense magma at the base of the chamber rises while the cooler, denser magma near the top sinks. As the magma cools, different minerals begin to crystallize out of the melt at different temperatures, a process known as fractional crystallization. Minerals like olivine and pyroxene, which crystallize at higher temperatures, form early and sink to the bottom, while plagioclase, which crystallizes at lower temperatures, may form later and be concentrated in upper layers. Thus the convective motion caused by RB instability results in a stratified structure within the magma chamber. As minerals crystallize and settle out of the magma, they can form distinct layers, each representing a different stage of crystallization. These layers can be highly regular, with sharp boundaries, or they may show more complex patterns depending on the dynamics of the convective currents and the rate of cooling. The layers often contain different proportions of minerals, leading to variations in color, texture, and chemical composition. In some layered intrusions, cyclic layering occurs, where similar sequences of mineral layers are repeated at different levels within the in-



FIG. 59 Rayleigh–Bénard convection seen in an experimental set up with a rigid boundary condition at the transparent top wall ($Ra = 2490$) (image: Sarah Chang TREND REU Media Project).

trusion. This cyclicity can result from periodic changes in the conditions within the magma chamber, such as fluctuations in temperature or the input of new magma (magma recharge). One of the most famous examples of a layered intrusion, the Bushveld Complex contains extensive layers of chromite, magnetite, and other minerals. RB instability is believed to have played a role in the formation of these layers by driving the convection that facilitated the differentiation of the magma. The Skaergaard Intrusion (Greenland) is a classic example of a layered intrusion showing well-defined layers of gabbro, with distinct bands of different minerals. The RB instability in the cooling magma chamber led to the formation of these layers as the magma differentiated and solidified.

RB instability also influences smaller-scale and lower-temperature geological processes. During the early stages of diagenesis, the process by which sediments are lithified into rock, RB instability can drive the movement of pore fluids in unconsolidated sediments. For example, in fine-grained sediments like clay or silt, heating from below, such as from underlying geothermal gradients, can cause the upward migration of warmer, less dense fluids, while cooler, denser fluids sink. This can result in the formation of layering or deformation features, such as load casts or convolute bedding. In permafrost regions, RB instability can occur in the active layer, the layer of soil above the permafrost that thaws and freezes seasonally. RB instability can drive the mixing of soils, leading to the formation of patterned ground, such as stone circles or stripes, the result of the convective movement of water and soil particles within the active layer. Fluid venting structures that we have discussed above as giving rise to geological patterns, like mud volcanoes, hydrothermal vents, cold seeps, are driven by RB convection.



FIG. 60 Rayleigh–Taylor instability, seen here between two different viscous soap solutions of slightly different densities, the denser overlying the lighter (image: Thermoskanne).

F. Rayleigh–Taylor instability

The Rayleigh–Taylor (RT) instability occurs when a denser fluid is accelerated into a lighter fluid, leading to the formation of complex patterns as the fluids mix (Kull, 1991); Fig. 60.

In geology, this instability is observed in processes where materials of different densities interact under the influence of gravity. In seismites (Sec. IV.Y), it is seismic movement that causes RT instability. The RT instability is relevant in the context of mantle plumes, where buoyant, hot mantle material rises through denser, cooler mantle rock (Whitehead Jr and Luther, 1975). The interface between these two regions can become unstable, leading to the formation of mushroom-shaped plumes that are a hallmark of the RT instability. In evaporite basins, where layers of salt and other minerals accumulate, RT instability can cause the salt layers to pierce through overlying strata, leading to the formation of salt diapirs (domes) (Trusheim, 1957). Here, less dense, buoyant salt layers buried under denser sedimentary rock rise, creating dome-shaped structures that can trap oil and gas, making them important in petroleum geology.

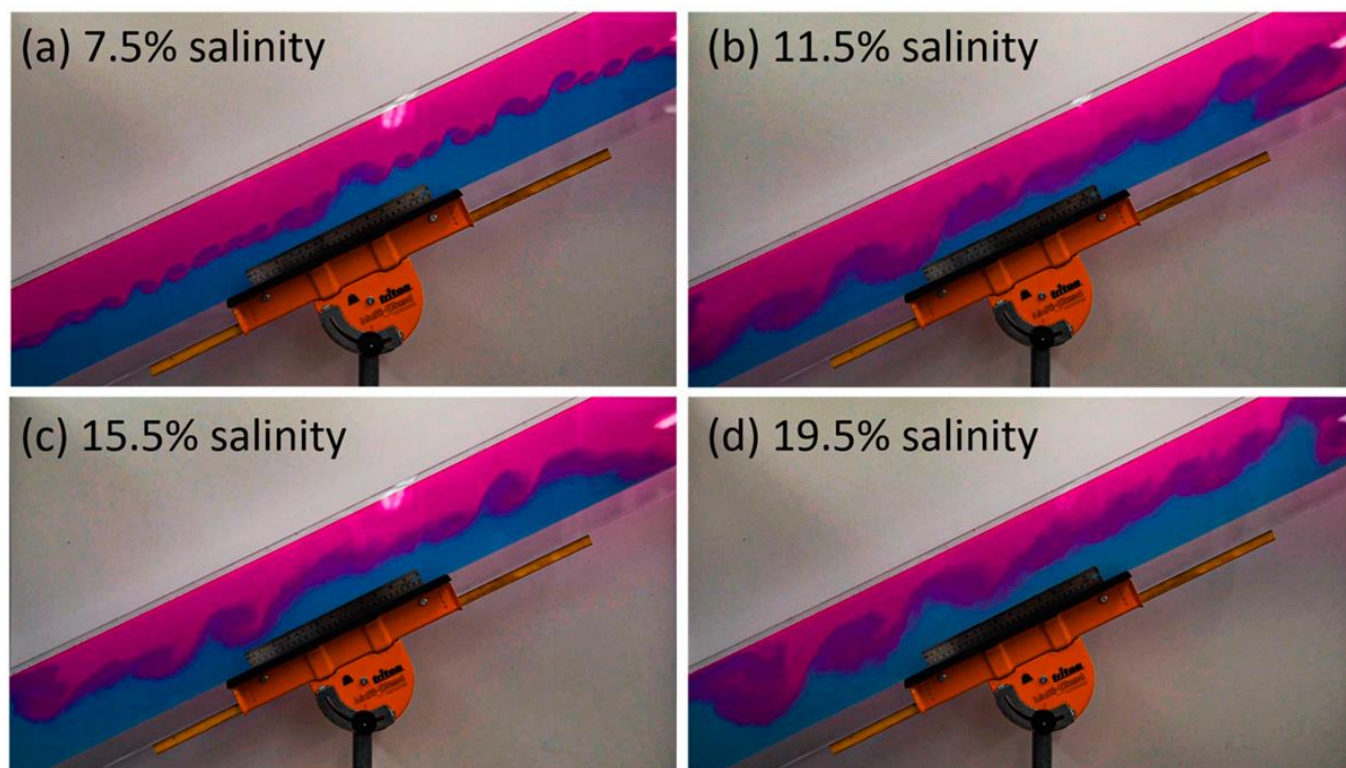


FIG. 61 Kelvin–Helmholtz instabilities shown developing in a laboratory experiment in which the interface between the two fluids is sheared by tilting the container (Gibbons *et al.*, 2023).

G. Kelvin–Helmholtz instability

Kelvin–Helmholtz, a lateral shear instability often seen in the atmosphere and ocean (De Silva *et al.*, 1996), is not rare in large-scale geological structures, due to the parallel displacement of soft sediment layers, and is often associated with earthquakes (e.g., Heifetz *et al.* (2005)). On a much smaller scale, a similar process has been suggested as driver for meso-scale rock folding (Fig. 10b). Wollkind and Alexander (1982) introduced surface tension to previously established folding laboratory models, resulting in onset conditions similar to those of RH instability. Their model successfully explained the observed characteristic wavy patterns observed in anhydrite and limestone layers from the Castille Formation of Southern New Mexico (see figure 1 in Wollkind and Alexander (1982)). A lava coil is a spiral lava pattern found when a relatively low viscosity lava solidifies along a slow-moving shear zone in the flow producing a Kelvin–Helmholtz instability. They have been identified on Mars as well as on Earth (Ryan and Christensen, 2012). At the border between biological and geological soft matter, KH instability has been applied to explain the formation of the (pseudo)fossil *Kinneyia* (Herminghaus *et al.*, 2016; Thomas *et al.*, 2013). Passive deformation of a viscoelastic bacterial biofilm under flowing shallow water results in the formation of ripple corrugations (Fabbri *et al.*, 2017)

that later get diagenetically preserved.

H. Bénard–Marangoni convection

The Bénard–Marangoni convection, or Marangoni flow, occurs when surface tension gradients drive fluid motion (Craster and Matar, 2009; Schatz and Neitzel, 2001), Fig. 62. This instability typically arises in systems where temperature or concentration gradients at a fluid’s surface lead to variations in surface tension, causing fluid to flow from regions of low surface tension to regions of high surface tension. The Bénard–Marangoni instability is also present in geology. It plays a role in the segregation of basaltic lithologies in the Earth’s lower mantle (Baron *et al.*, 2022). In a recent study it has been suggested that clay floating on a lake surface and subject to Marangoni flow when the lake becomes very shallow near the shore are what leads to complex patterns, described as Suminagashi-like, precipitated on the shore line (Rouwet and Iorio, 2017).

I. Capillary flow and coffee-ring instabilities

Salt dissolution in water enables long-distance transport of ions, with subsequent crystal precipitation occurring upon evaporation or cooling. This process manifests

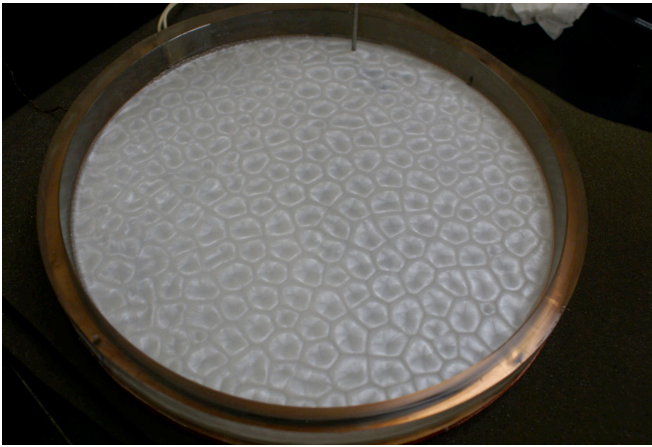


FIG. 62 Bénard-Marangoni convection seen in the same experimental set-up as seen in Fig. 59, but with a free liquid surface (image: Sarah Chang TREND REU Media Project).

itself in various scenarios, such as capillary rise of groundwater to soil surfaces or from rocks and evaporation near salt lakes. Crystal precipitation generally occurs in regions where evaporation is highest and ions are advected by liquid flow. The increase in ions concentration in these areas increases the probability of crystal nucleation. This is quite similar to the coffee ring effect, which refers to the pattern left behind when a particle-laden liquid droplet dries, characterized by a ring-like deposit of particles along the perimeter of the original droplet (Craster and Matar, 2009; Shahidzadeh *et al.*, 2015). The latter occurs because evaporation occurs more rapidly at the droplet's edges, and liquid from the center of the droplet flows outward to replenish the evaporating edges. This outward flow carries suspended particles to the droplet's perimeter, and as evaporation completes, particles are concentrated at the edge, forming a ring.

In the case of salt solutions, the accumulation of ions induces multiple nucleation at the evaporation front. This generates salt creeping, a self-amplifying process leading to the formation of three-dimensional porous crystalline networks at considerable distances from the original salt solution source (Qazi *et al.*, 2019a). While salt creeping occurs on flat surfaces, a similar process known as salt efflorescence takes place on the surface of porous materials like soil or stones, mostly due to capillary flow of the salt solution towards the evaporative region at the top of the porous media. Studies show that ion concentration near a receding liquid meniscus within the pores is influenced by evaporation and can be quantified by the Peclet number. This dimensionless number is relevant in the study of transport phenomena in a continuum and is defined as the ratio of the rate of advection of ions by the flow to the rate of diffusion of these ions driven by an appropriate gradient (Wijnhorst *et al.*, 2024). When Pe is higher than one, the advection of ions will lead to crystal precipitation. The

first precipitating large crystals at the evaporation front create large pores between them, enabling smaller crystals to nucleate afterward within these spaces, which in turn will form smaller pores, and so on. In addition, the spreading ability of the salt solution by its precipitated crystals increases the invasion area of the salt solution by capillarity. Overall, Marangoni flows are negligible in salt creeping dynamics mainly because: (a) the concentration gradient between the bulk salt solution and the liquid film in contact with precipitated crystals at the evaporative front is small, preventing high supersaturation and leading to immediate secondary nucleation of crystals.

Figure 63 illustrates the dynamic nature of salt creeping and efflorescence formation and its ability to propagate well beyond its initial boundaries (Fig. 63a). Scanning electron microscopy (SEM) images of sodium chloride (NaCl) creeping efflorescence consist of porous polycrystalline structures and show that this phenomenon covers many orders of magnitude in length scales so that it indeed appears fractal (Wijnhorst *et al.*, 2024). In turn, this new crystalline porous structure, with different pore size distributions due to different sizes of crystals, allows salt water to be sucked in by capillary pumping. Consequently, crystallization continues even further at the top of the efflorescence. The rate of evaporation plays a critical role in the development of salt creeping, efflorescence, and salt pillar formation (Desarnaud *et al.*, 2015). For creeping to occur, the evaporation rate should be high enough to induce multiple nucleation processes at the evaporation front ($Pe > 1$). This can be achieved with air flow (wind), low relative humidity, or high-temperature during evaporation. On the contrary, slow evaporation rate induces the precipitation of less nuclei which grow larger in size and towards their equilibrium shape; this can suppress the creeping phenomenon. Very low Relative humidity, can also suppress the salt creeping process as the kinetics of salt precipitation can completely change at a very high evaporation rate leading to crust formation (Desarnaud *et al.*, 2015). Another important parameter remains the properties of the porous media or surface on which salt precipitation occurs, as this can also affect the final deposition morphology (Qazi *et al.*, 2019a).

J. Saffman–Taylor instability, viscous fingering and reactive-infiltration instability

Whenever a more mobile fluid is rapidly injected into a less mobile one, the interface between them becomes unstable. This occurs because the fluid tends to flow along the path of least resistance. Therefore, if there is a protrusion on the advancing interface, it will focus the flow, leading to a faster growth of the protrusion and transforming it into a finger of the more mobile phase propagating within the less mobile phase.

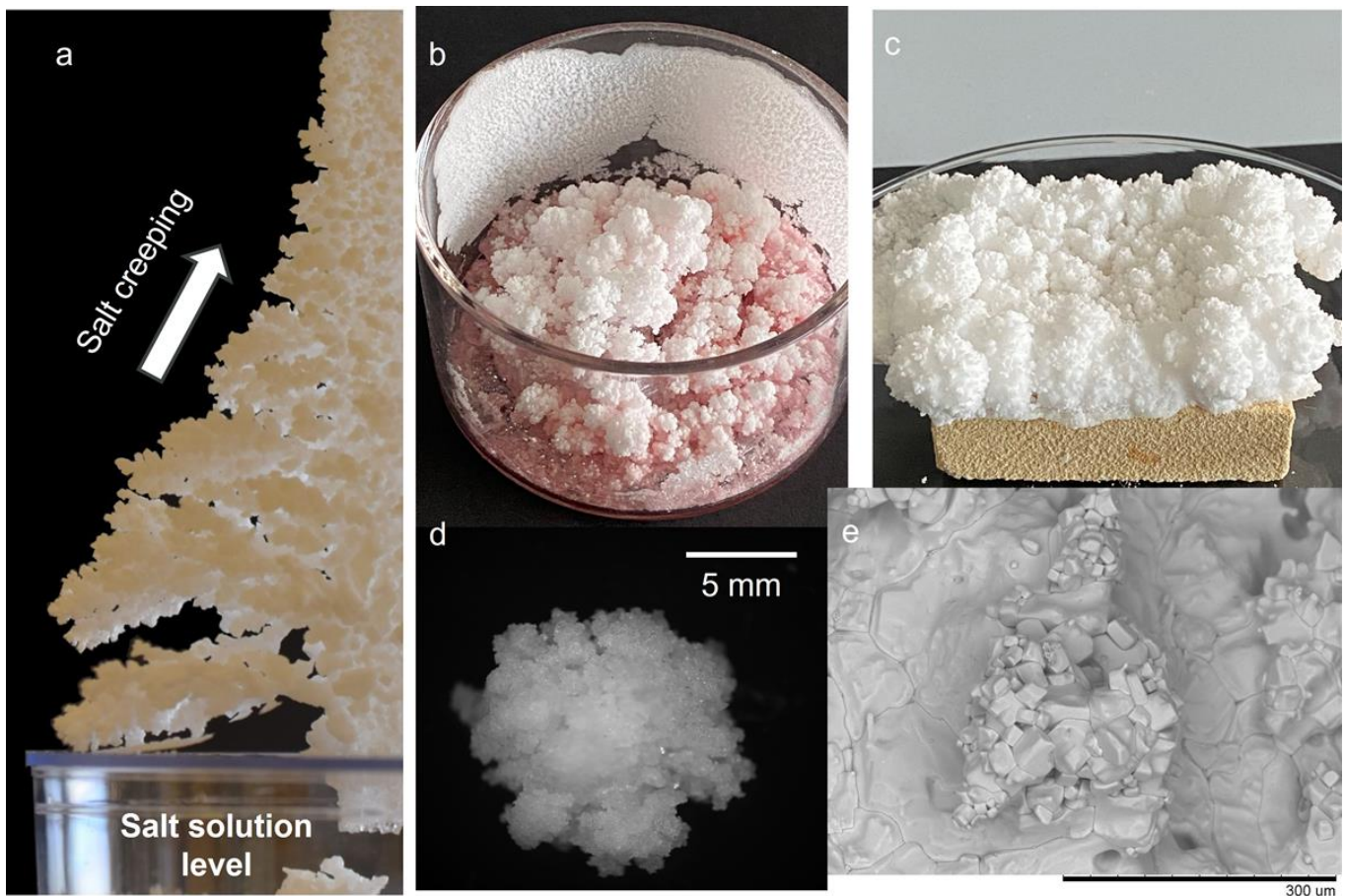


FIG. 63 NaCl crystallization patterns at different scales. (a) laboratory experiment of salt creeping on a cylindrical glass rod (flat surface) far from the evaporative salt solution in the petri dish. (b) salt crystallization as efflorescence on large NaCl crystals and creeping on glass wall of the NaCl solution evaporating in a beaker (laboratory scale experiment of the drying of a salty lake). (c) Salt Efflorescence on the top of piece of Limestone (d) zoom on the morphology of salt efflorescence unit with the porous structure (d-e) SEM images of the porous structure of the efflorescence at the microscale showing an assembly of microcrystals. @copyright N.Shahidzadeh -UvA.

Examining Darcy's law, which relates the flow rate to the pressure gradient in a porous medium

$$\mathbf{u} = -M\nabla p = -\frac{K(\phi)}{\eta}\nabla p,$$

we see that mobility M can be controlled in two ways: by altering the viscosity of the fluid η or by changing the permeability of the medium K , which depends on the porosity ϕ . The first approach leads to the viscous fingering phenomenon (Chuoke *et al.*, 1959; Hill, 1952; Saffman and Taylor, 1958), where less viscous fluid penetrates the medium in narrow, finger-like channels, displacing the more viscous fluid.

The second method can be achieved by dissolving the porous medium using a chemically active fluid that reacts with the pore surfaces. This is so-called reactive-infiltration instability (Hinch and Bhatt, 1990; Ortoleva *et al.*, 1987a; Szymczak and Ladd, 2012, 2014). A classic

example here are karst processes, initiated by the dissolution of limestone by CO_2 saturated water. Flow focusing due to the reactive-infiltration instability impacts the cave system formation (Groves and Howard, 1994; Hanna and Rajaram, 1998; Szymczak and Ladd, 2011) and surface karst features such as solution pipes (Lipar *et al.*, 2021). In industrial applications, much stronger acids, like HCl or HF, are used for stimulation of petroleum reservoirs (Economides and Nolte, 2000; Fredd and Fogler, 1998; Hoefner and Fogler, 1988) or sustaining fluid circulation in geothermal systems (Charalambous, 2021; Sutra *et al.*, 2017). A similar instability of an initially flat propagating dissolution front is seen in stylolites (Toussaint *et al.*, 2018).

It is interesting to note what happens to the initial protrusions on the unstable front during the course of evolution. As they grow larger, they transform into fingers which begin to interact with each other. Two pro-

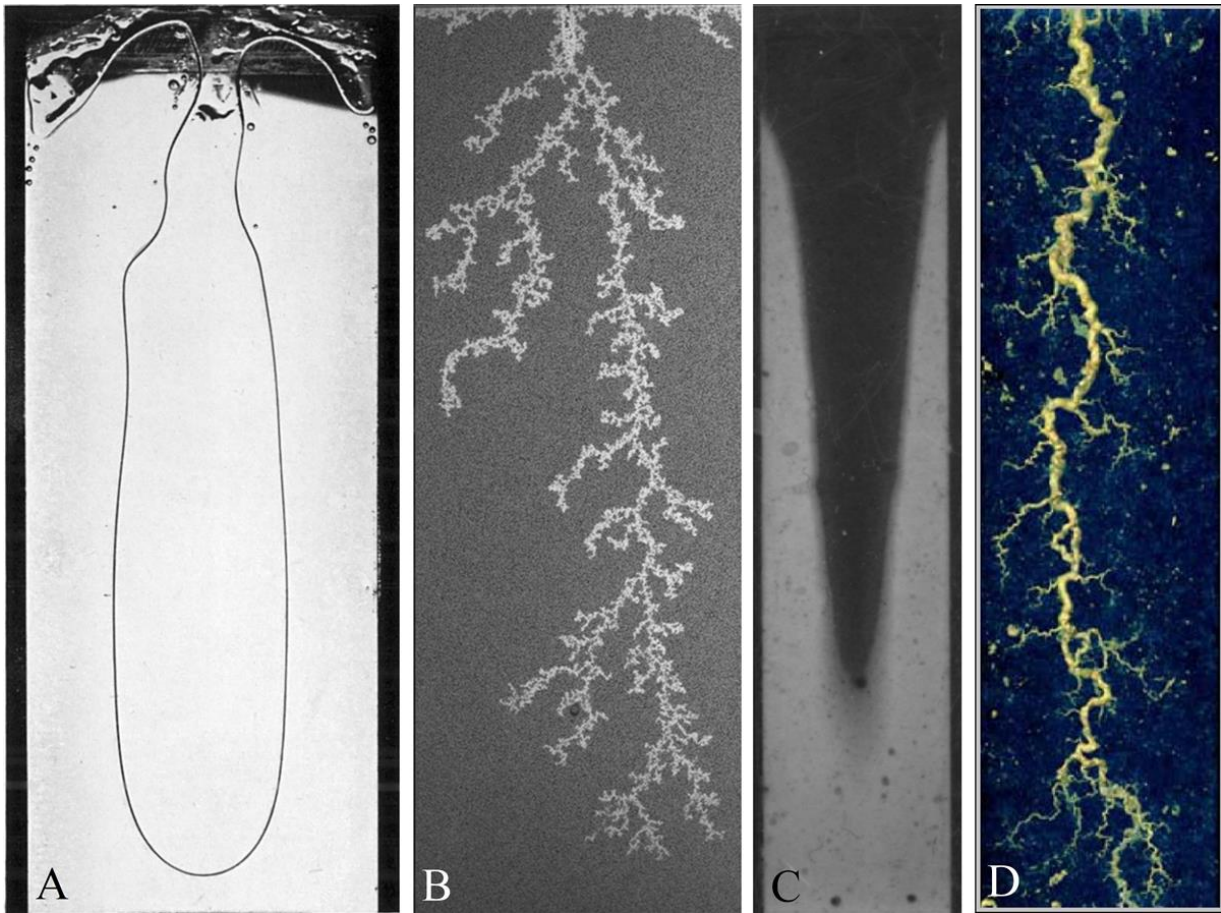


FIG. 64 A; The Saffman-Taylor finger which appears in the long-time limit in the viscous fingering experiment (Saffman and Taylor, 1958). B: The irregular, fractal finger formed in viscous fingering experiment in porous medium, where air was displacing glycerine in a Hele-Shaw cell filled with glass beads (Løvoll *et al.*, 2004). C: A smooth dissolution finger arising in a Hele-Shaw cell with a soluble bottom (Osselin *et al.*, 2016). D: A fractal dissolution finger (wormhole) formed during acidization of limestone rock (McDuff *et al.*, 2010).

cesses take place here: one is the competition of the fingers for the flow, causing the longer ones to advance ahead of the shorter ones. The other is the merging of the fingers, reducing their total number. As a result, as shown, the pattern coarsens, and eventually, a single finger emerges. In the theory of viscous fingering such a final, stable finger-like structure is known as the Saffman-Taylor finger (Fig. 64A). Interestingly, if the Saffman-Taylor experiment is conducted in a Hele-Shaw cell filled with glass beads (Fig. 64B), mimicking a porous medium, the finger appearing in the system has a highly ramified, fractal structure, not unlike diffusion-limited aggregates (Witten Jr and Sander, 1981). This is due to the fact that the local interface curvature controlling the capillary pressure drop depends on the local pore geometry and is thus sensitive to the frozen disorder associated with the structure of this system (Løvoll *et al.*, 2004).

A similar situation occurs in the case of reactive-infiltration instability. If we conduct experiments in a homogeneous system, such as a Hele-Shaw cell with a

soluble bottom, we end up with relatively regular fingers, which merge and transform into a single dissolution finger in the long-time limit (Fig. 64C), not unlike the solution pipes of Fig. 42. On the other hand, in the dissolution of porous rocks, twisted and ramified wormholes form (Fig. 64D, see also Sec. IV.U).

K. Chaotic advection

Chaotic advection is a phenomenon in fluids recognized in the 1980s (Aref, 1984), that chaotic dynamics that appears in deterministic nonlinear systems, when applied to fluid dynamics, implies that fluid flow can be chaotic (Cartwright *et al.*, 1999a). Chaotic advection can give rise to intricate fractal structures from stretching and folding in a fluid; these structures promote mixing in the fluid, with consequent enhancements in heat transfer and chemical reaction. Chaotic advection is a different phenomenon to complex turbulent flow in fast-flowing fluids, known for centuries. Chaotic dynamics, as opposed to

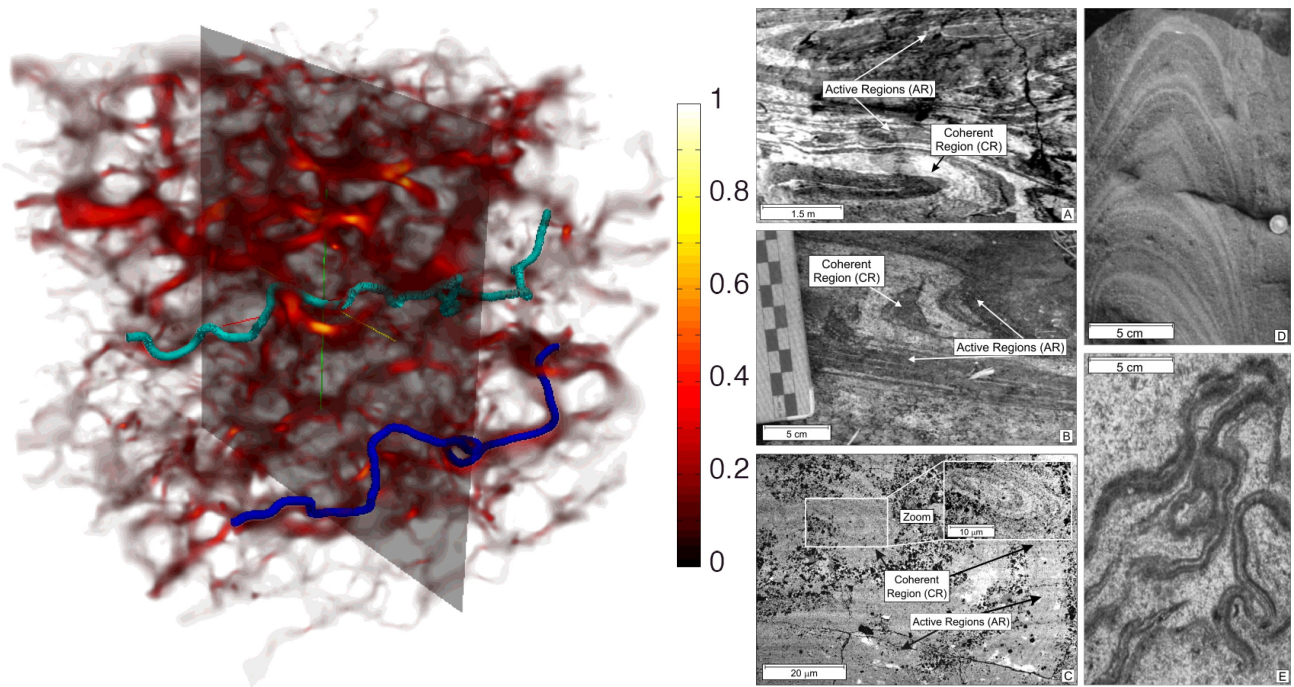


FIG. 65 Chaotic advection. (a) Digital reconstruction of the 3D flow field through a Berea sandstone block (1.6 mm cube). The normalized velocity magnitude is rendered according to the color bar; yellow zones indicate high velocity bursts. Two flow paths (blue and cyan) show evidence of branch and merge behavior. Adapted from Kang *et al.* (2014). (b) Examples of magma mixing structures in lava flows from the islands of Lesbos (A–C), Vulcano (D) and Salina (E). The dark flow structures consist of B magmas dispersed through light colored A magmas. In all lava flows mixing structures have the same patterns at many scales of magnification. Adapted from Perugini *et al.* (2003).

turbulence, occurs in slow flows, or low-Reynolds-number flows, in the terminology of fluid mechanics (Aref *et al.*, 2017).

Since a considerable fraction of geophysical fluid flows are slow, chaotic advection has a number of important consequences in geological systems. One application is to fluid flow at the scale of the pores through which water flows in rocks (Fig. 65a). A series of works have addressed this question and shown its importance for macroscopic heat- and solute-transport phenomena (Kang *et al.*, 2014; Lester *et al.*, 2016a,b; Metcalfe *et al.*, 2010). Lester *et al.* (2012) indicate how fluid mixing and chemical reactions have important impacts in the mechanics of hydrothermal systems (Trefry *et al.*, 2019) discuss how temporal fluctuations together with poroelasticity generate chaotic advection in natural groundwater systems. Schoofs *et al.* (1999) show that for typical geological parameters, thermohaline flow in the Earth’s crust is intrinsically chaotic. This dynamics impacts heat transport at mid-ocean ridges, ore genesis, metasomatism and metamorphic petrology, and the diagenetic history of sediments in subsiding basins. Oberst *et al.* (2018) propose that feedbacks between thermo-chemical and deformation processes should be of importance for the deposition of vein-filling minerals such as pyrite and gold. A further series of works have looked into chaotic advection at the

larger scale of the flow of magma in the mantle, its role in mixing, and its effects on the timescales of cooling and crystallization of magma (Fig. 65b) (De Campos, 2015; Perugini *et al.*, 2008, 2003; Petrelli *et al.*, 2016; Yuen and Malevsky, 1992).

L. Osmotic processes

Osmosis is a phenomenon induced by the differential mobility of different species in a fluid. In the simplest case, if a solvent species, a water molecule, can pass through an obstacle, a membrane, but a solute species, say a metal ion, cannot, then those ions, rebounding from the barrier, create a pressure, osmotic pressure. In this case we term the membrane semipermeable. Such a barrier to movement can be through pore size alone, but also through chemical affinities and electrical potentials.

Osmosis and osmotic pressure are ubiquitous in biology, since cells have membranes, and are subjected to, adapted to, and make use of these forces. But osmosis is present in geological systems, too. Where there is water plus a porous medium, a substrate with pores that give semipermeability; this pressure will be present (Cardoso and Cartwright, 2014). Clays and shales are some instances of geological semipermeable porous me-

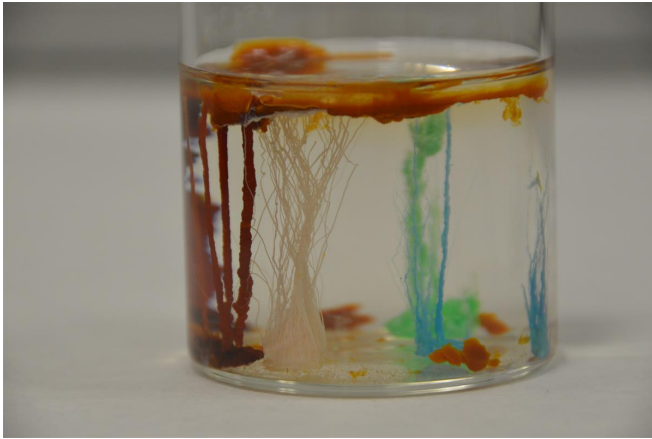


FIG. 66 Osmotic processes. A chemical garden depends on osmotic forces for its growth (image: Julyan Cartwright).

dia (Neuzil, 2000a). Osmosis, as well as buoyancy forces, may be driving the convective processes of submarine mud volcanoes and seeps (Cardoso and Cartwright, 2016; Rocha *et al.*, 2021). It has recently been shown through modelling that osmosis may be at the root of permafrost explosions producing large craters in the High Arctic of Siberia (Morgado *et al.*, 2024)

Chemical gardens are biomimetic structures forming tubular solids twisted in multiple forms imitating plants. This process has fascinated many researchers during centuries from Glauber in 1646 (Glauber, 1646) until now. Their formation starts from adding a solid seed crystal of a metal salt into a solution, often silicate, but also carbonate, phosphate, etc. This liquid phase dissolves partially the surface of the seed creating a semipermeable membrane. The external solvent enters inside the membrane by osmosis. The entrance of external solvent provokes an increase of volume stressing the membrane until breaking it. Then, the internal solution exits under osmotic and buoyancy forces. When the internal components of this solution contact with the external solution a precipitation reaction occurs forming the walls of the tubes. These forces of osmosis and buoyancy together with the precipitation reaction yield structures with constantly changing direction and morphology that mimic biological gardens. This phenomenon is a self-organized non-equilibrium process of chemical reaction under fluid advection dynamics (Barge *et al.*, 2015b).

Many studies on this phenomenon have been performed at laboratory scale (Fig. 66). However, chemical gardens can be found also in nature as geological structures. Though the length- and time-scales are clearly different, the same components and driven forces can occur in nature, such as, semipermeable membranes, osmotic pressure, concentration gradient, pH gradient, buoyancy pressure, fluid dynamics, and precipitation. Some examples of geological chemical gardens are hydrothermal vents on the sea-floor (Cardoso and Cartwright,

2017; Cartwright and Russell, 2019; Sainz-Díaz *et al.*, 2018), brinicles in sea-water (Cartwright *et al.*, 2013; Testón-Martínez *et al.*, 2024) and on other celestial bodies (Vance *et al.*, 2019). Besides, these structures, in particular in the form of alkaline submarine hydrothermal vents, are today viewed as one of the prime candidates for where life may have evolved on Earth (Cardoso *et al.*, 2020; Cartwright and Russell, 2019; Russell and Hall, 1997; Russell *et al.*, 1994), within inorganic pores and vesicles (Ding *et al.*, 2024, 2019), in a process embedding patterns and information between two mineral phases (Cartwright *et al.*, 2024, 2016; Cartwright and Mackay, 2012).

M. Diffusion-limited aggregation

Diffusion-limited aggregation (DLA; Witten and Sander (1981, 1983)) is a numerical model that describes how complex, disordered structures, often fractal-like in nature, form through the random movement and attachment of particles to a growing cluster. The simulation starts with a seed or nucleation site, and particles are added one at a time via random walk paths starting outside the region occupied by the cluster. If a particle comes close to the cluster, it attaches to its perimeter, contributing to its growth. This process is repeated, and over time, the cluster develops a complex, ramified structure.

DLA can be a good model for aggregation from solution, provided that certain conditions are met. First, it assumes that diffusion of the particles is the slowest process shaping the cluster, while the attachment process is faster. Second, since only one random walker is released at a time, the model corresponds to the infinite dilution limit of the particles. In such a limit, the cluster growth timescale is much longer than the relaxation time of the particle concentration to the stationary profile. Finally, the aggregation itself is considered to be irreversible, and the cluster does not interact with the incoming particles. Many generalizations of the DLA model exist, which relax one or more of these assumptions (Erlebacher *et al.*, 1993; Garik, 1985; Meakin, 1983, 1998), thereby extending the applicability of these models to a broader range of phenomena.

The origin of the complexity of the DLA aggregates lies in the competition between different regions of the growing cluster. A branch extending from the center is able to capture more particles since random walkers tend to stick to the first part of the cluster they encounter. Between the growing branches, there are regions that remain shielded from incoming particles, known as fjords, which become more pronounced as the branches extend.

The limited penetration of the fjords results from a strong screening effect (Meakin, 1998). Particles following random walk paths tend to become trapped along the

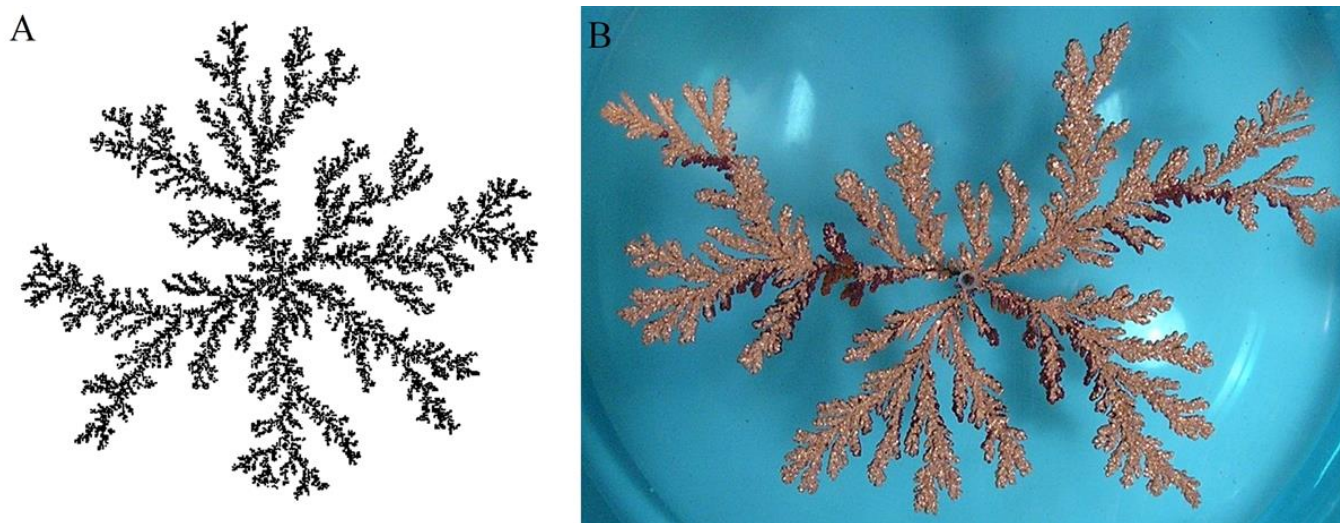


FIG. 67 A: A cluster created by the diffusion-limited aggregate (DLA) model. B: A dendritic copper aggregate, produced through electrodeposition from a copper sulfate solution, which can be described by the DLA model. Kevin R. Johnson CC-BY-2.5.

edges of the fjords, making it highly unlikely for them to reach the interior of the cluster. This phenomenon is analogous to the screening of a Laplacian field, with absorbing boundary conditions applied to the surface of the DLA fractal, resulting in an exponentially small probability of penetration as a function of the penetration depth.

Similar screening mechanisms apply to other fields, such as pressure fields or electric potentials, leading to a resemblance between diffusion-limited aggregates and other fractal growth patterns, such as viscous fingers or electrodeposition structures.

Although DLA is widely used to model far-from-equilibrium growth in physical and biological systems, it remains a theoretical challenge to fully describe its structure using scaling models. Most approaches assume a self-similar fractal pattern, but this does not fully capture the complexity of DLA (Halsey, 2000; Meakin, 1998). In fact, the mathematical structure underlying DLA, as well as more general Laplacian growth models, is quite involved, with the link to the theory of integrable systems and even quantum gravity models (Mineev-Weinstein *et al.*, 2000, 2008), providing further evidence that a simple model can indeed generate complex structures.

N. Piezoelectricity

Piezoelectricity, the generation of electric charge by the application of mechanical stress, is a less commonly discussed mechanism of pattern formation. The piezoelectric effect is an outcome of symmetry breaking in nature. It is seen in non-centrosymmetric (not having a centre of symmetry) crystals, and is related to having an electric dipole moment associated with their unit cell. Quartz is a particularly common geological instance (Fig. 68).

Piezoelectricity is used in engineering applications for forming patterned thin films through piezoelectric printing (Khan *et al.*, 2016) and in functional soft matter (Pishvar and Harne, 2020). As we have described in Sec. IV.O, it may be involved in concentrating gold nanoparticles into nuggets (Voisey *et al.*, 2024).

O. Ostwald ripening

The Ostwald ripening process was first described in the late 19th century by Wilhelm Ostwald 1897, after whom it is named. In this process, the dissolution and crystal growth of a phase occurs simultaneously under the same conditions, with the only difference being the size of the crystals. The dissolution affects the smaller crystals, which may disappear, while the larger crystals grow at the expense of the former (Fig. 69). The physical mechanisms affecting Ostwald ripening are relatively well understood, since two papers were published in 1961 describing a theory to explain the dynamics of the last stage of first-order phase transitions (Lifshitz and Slyozov, 1961a; Wagner, 1961). This theory predicted the existence of a stationary regime in which the particle size distribution evolves in a self-similar fashion by rescaling with some characteristic length scale (i.e., particle size). This characteristic length scale is scaled linearly with time, thus determining the growth dynamics. These growth dynamics vary depending on which of the processes involved is the slowest, the diffusion of the material (Lifshitz and Slyozov, 1961a) or the attachment and detachment of atoms or molecules (Wagner, 1961). These characteristics have been qualitatively determined experimentally. However, there is still no agreement between theory and experiments, so Ostwald ripening is still being

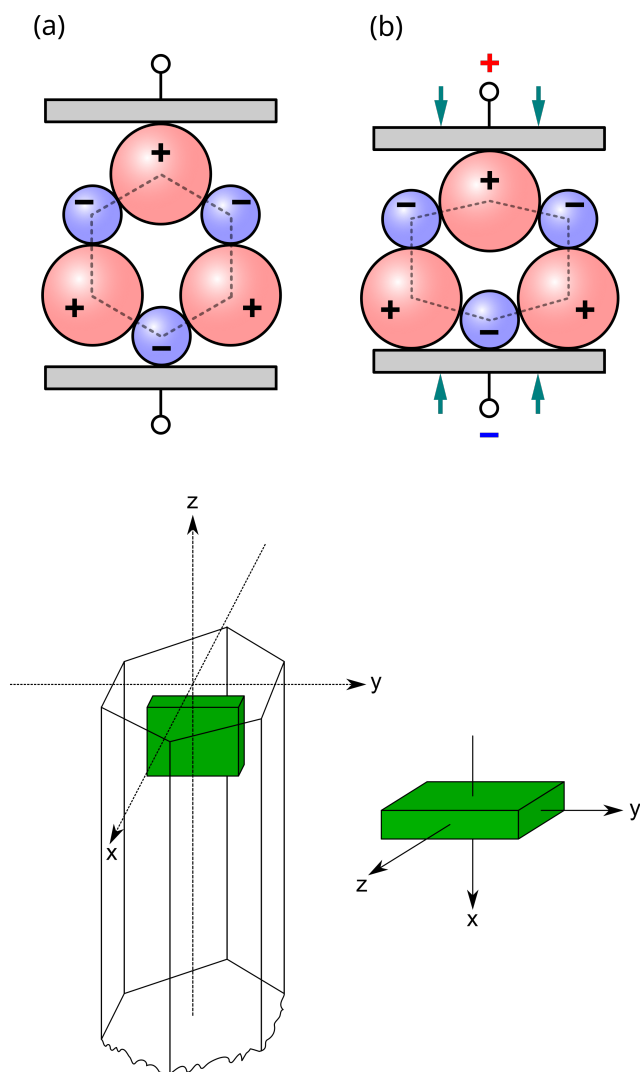


FIG. 68 Piezoelectricity: (a) simplified model of a quartz (SiO_2) crystal between two electrodes. (b) Mechanical pressure shifts the positive and negative centers of charge. This creates an electrical dipole inducing an voltage at the electrodes (image: MikeRun, CC-BY-SA-4.0). (c) Part of a quartz crystal with marked crystallographic axes and a piezoelectric plate (Curie cut) cut from it (image: CLI, CC-Zero).

studied today (van Westen and Groot, 2018).

Geologically-relevant instances of Ostwald ripening include in clays and metamorphic minerals (Eberl *et al.*, 1990), mineral paragenesis in sediments (Morse and Casey, 1988), olivine and plagioclase in magmas (Cabane *et al.*, 2005), coarsening of gold nanoparticles (Hastie *et al.*, 2021) and advection-mediated chiral autocatalysis in which complete chiral symmetry breaking is attained from an initially unbiased mixture of seed crystals (Cartwright *et al.*, 2007).

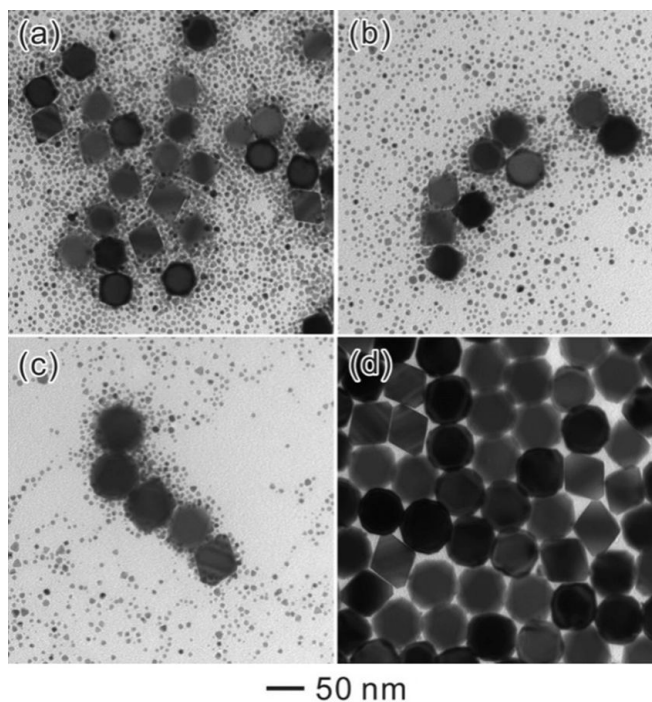


FIG. 69 Ostwald ripening process in palladium nanoparticles in formaldehyde. In the image (a) it can be seen that there are two populations of particles with different sizes. Along the reaction time (i.e., (b) and (c)), it can be seen that the smaller particles are dissolving in favor of the growth of the larger ones. Until the end (d), when only the population of larger crystals remains, which has increased in size. (Image: CC-BY, Zhang *et al.* (2015)).

P. Fracture processes

When a material is subjected to stress, the forces within the material can exceed its internal strength, causing it to fracture (Anderson, 2017). The way a material fractures is governed by both the material's properties and the external conditions applied to it, leading to various types of patterns.

Fracture begins with the formation of a crack (Broberg, 1999), which then propagates through the material. The path of this crack is influenced by the distribution of stress within the material. As a crack advances, it relieves stress in its immediate vicinity but can concentrate stress at its tip which can cause the crack to branch or change direction, depending on the material homogeneity and the external loading conditions. For example, in brittle materials like glass, cracks tend to propagate in straight lines under uniform stress, whereas in more ductile materials, they might follow more tortuous paths, creating complex patterns.

Several mechanisms contribute to the pattern formation observed in fractured materials. One such mechanism is the interaction between multiple cracks (Meyer and Brückner-Foit, 2000). When multiple cracks propa-

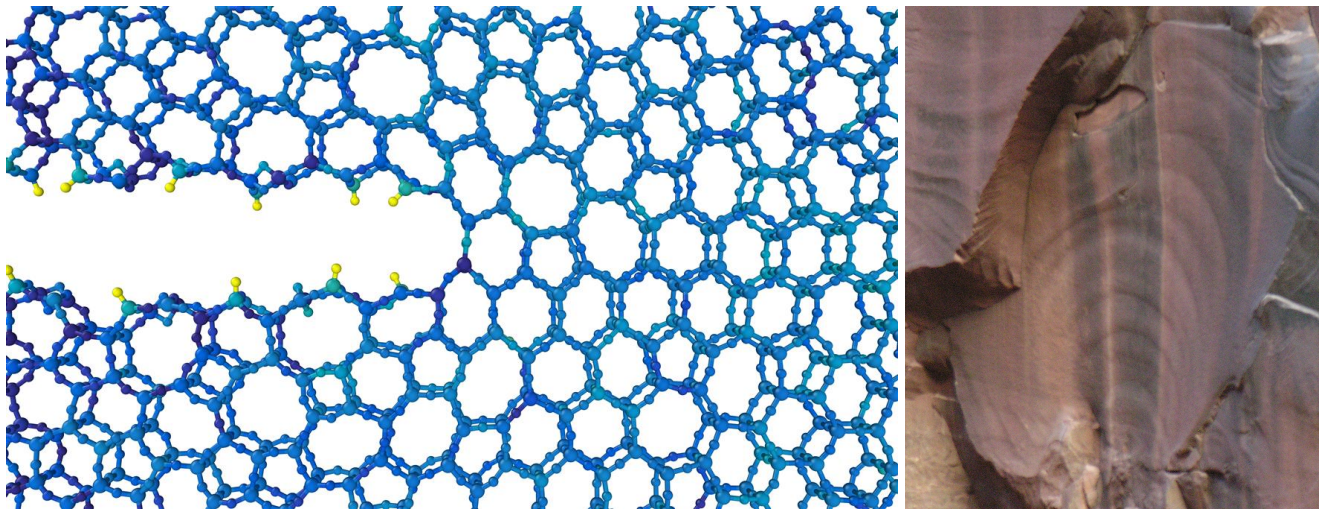


FIG. 70 Fracture processes. (a) SiO_2 fracture. Crack propagation in a two-dimensional bilayer of amorphous silicon dioxide modeled with a polarizable interatomic potential (Caccin *et al.*, 2015). Atoms are colored by their local potential energy on a scale normalized from dark blue, lowest energy, to yellow, highest energy. (Image credit: Marco Caccin and Alessandro De Vita, King's College London; James Kermode, University of Warwick. CC-BY-NC-SA-2.0). (b) Plumose fracture patterns in sandstone, North Canyon, Arizona, USA (image: Awickert, CC-BY-SA-3.0).

gate simultaneously, their paths can intersect or influence each other, leading to branching (Sun *et al.*, 2021) and the formation of intricate networks of cracks. Another important mechanism is the anisotropy of the material (Hakim and Karma, 2005), which can cause cracks to preferentially propagate along certain directions, resulting in directional patterns.

Fracture patterns often exhibit self-similarity (Shcherbakov and Turcotte, 2003; Tarasovs and Ghassemi, 2014), meaning that they look similar at different scales. This self-similarity is governed by scaling laws that describe how the fracture process operates similarly across different size scales (Bažant, 1993). For example, the branching patterns in a shattered windscreen or the cracks in dried mud both exhibit fractal characteristics, where smaller branches or cracks resemble the larger overall pattern. These scaling laws highlight the universal nature of fracture processes, showing how similar patterns can emerge in different materials under varying conditions.

Chemical processes significantly influence the development of fracture patterns in geological materials, a factor that has often been underestimated. This review highlights the intricate relationship between mechanical and geochemical processes, suggesting that advancements in understanding fracture patterns in geological contexts will require a closer integration of these two domains (Laubach *et al.*, 2019).

Mineral replacement processes are common in various geological settings and involve the transformation of one mineral into another, often under specific conditions that result in changes to the volume of the material. These

volume changes, often resulting from chemical reactions, generate stresses within the mineral structure. These stresses can lead to fracturing of the original mineral, thereby influencing the development of replacement minerals (Jamtveit *et al.*, 2009).

VI. SUMMARY AND OUTLOOK

The physical mechanisms that we have described in Section V underlie the mesoscale geological patterns of Section IV. They operate upon the types of materials that we noted in Section III, and these material types correspond to those studied in the context of soft matter, as we described in Section II. Thus mesoscale geological pattern-forming systems are instances of geological soft matter.

Matter in the universe self organizes and self assembles at all scales, from the clusters and filaments of galaxies forming the large-scale structure of the universe to the quarks and gluons within nucleons. In the middle of this scale range comes what we think of as the geology or Earth sciences. Here too there is self organization and self-assembly on different scales, from plate tectonics to the molecular composition of rocks. Mesoscale geological pattern-forming systems are instances of geological soft matter (Fig. 71), where because the building blocks are intermediate in size between atoms and the macroscale, the structure is soft when it forms. It is important to comprehend their formation mechanisms to understand geological self-organization. Understanding the mechanisms behind their formation can shed light on

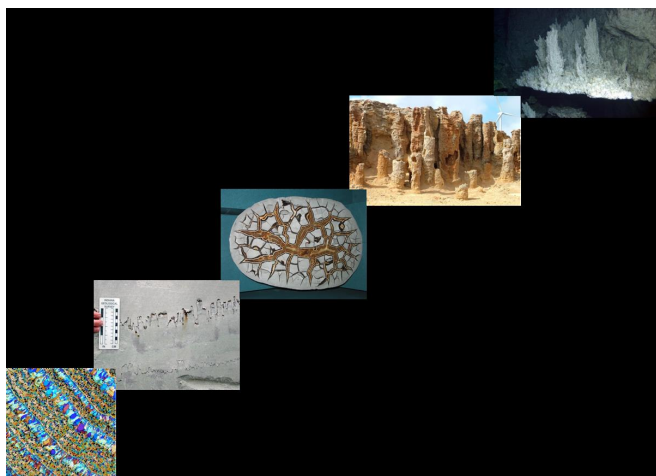


FIG. 71 Different patterns shown in this review ordered by size from smallest to largest. The sizes of these patterns may vary, with structures appearing only on one scale and others presenting a wide variety of sizes.

the physicochemical and mechanical conditions in the environments within which these patterns originated. This information is critical for unraveling Earth’s past environmental conditions and geodynamic processes as well as separating complex patterns formed abiotically from those that are evidence of life, especially when evidence is sought for ancient life on Earth and potentially life on other planets.

One key aspect is *self* organization, i.e., organization coming from within the system being studied. Of course *the system* in itself is something that can be redefined to make anything self-organized, but we usually are thinking of a small a system as possible, so for geological self-organization here we are considering the Earth and its drivings as external.

Although Earth scientists have long studied such geological paradigms of pattern formation, they might not have explicitly termed them ‘self-organized.’ An oscillatory mesoscale pattern formation mechanism was first brought forward by Harloff (1927), Plemister (1934) and Hills (1936) to explain the observed zoning of plagioclase. However, it was during the 1970s–80s that the studies by Fisher (1973) and Fraser (1977) and Ortoleva (1984) and Ortoleva *et al.* (1987b) clearly attributed the formation of some of the geological patterns found in rocks/minerals to geochemical self-organization processes. Ever since the application of nonlinear dynamics in explaining geological pattern formation was extended from crystals and rocks to a variety of geologic systems. Recently, self-organization in geological settings has gained interest for two main reasons: i) more and more studies suggest that geochemical self-organization might have played a catalytic role in the transition from geochemistry to biology (Cardoso *et al.*, 2020; García-Ruiz *et al.*, 2020; Hanczyc

et al., 2007; Kotopoulou, 2020; Kotopoulou *et al.*, 2021; McGlynn *et al.*, 2012; Russell *et al.*, 1994), ii) the precipitation of abiotic self-organized structures known as silicate-carbonate biomorphs, although of little geological relevance, demonstrated that inorganic features may be easily misinterpreted as cell relics owing to their life-like morphology (García-Ruiz *et al.*, 2003).

Overall, by studying these rhythmic patterns from a nonlinear dynamical systems point of view, researchers can gain valuable insights into the environmental and geodynamic conditions during pattern formation. This insight will be a powerful ally not only in the understanding of the geological history and past environmental dynamics of our planet, but also in distinguishing abiotic from biologically-influenced mesoscale pattern formation. We aspire that this review might assist towards this direction.

ACKNOWLEDGMENTS

This review paper originated at the workshop “Geochemobionics: Self-Organization in Geological Systems” organized by Sean McMahon at the University of Edinburgh in 2022. The workshop was funded by the European COST (Cooperation in Science and Technology) program, action number CA17120, Chemobionics.

EK acknowledges funding from the European Union’s Horizon 2020 research and innovation program under the Marie Skłodowska-Curie grant agreement No 101031812 ‘NanoBioS’.

REFERENCES

- Akiba, Y, A. Takashima, A. Inoue, H. Ishidaira, and H. Shima (2021), “Geometric attributes of polygonal crack patterns in columnar joints,” *Earth Space Sci.* **8** (5), e2020EA001457.
- Alfaro, Pedro, Luis Gibert, Massimo Moretti, Francisco J. García-Tortosa, Carlos Sanz de Galdeano, Jesus Galindo-Zaldivar, and Angel C. Lopez-Garrido (2010), “The significance of giant seismites in the Plio-Pleistocene Baza palaeolake (S Spain),” *Terra Nova* **22** (3), 172–179.
- Alfaro, Pedro, Massimo Moretti, and Jesús M. Soria (1997), “Soft-sediment deformation structures induced by earthquakes (seismites) in Pliocene lacustrine deposits (Guadix-Baza Basin, Central Betic Cordillera),” *Eclogae Geologicae Helvetiae* **90**, 531–540.
- Alfonso X., and Jose Fernandez Montana (1881), *Lapidario del Rey D. Alfonso X: código original* ([s.n.]).
- Aloisi, Giovanni, Catherine Pierre, Jean-Marie Rouchy, Jean-Paul Foucher, John Woodside, and the MEDINAUT Scientific Party (2000), “Methane-related authigenic carbonates of eastern mediterranean sea mud volcanoes and their possible relation to gas hydrate destabilisation,” *Earth and Planetary Science Letters* **184** (1), 321–338.
- Anderson, Don L (2002), “Plate tectonics as a far-from-

- equilibrium self-organized system,” *Plate Boundary Zones* **30**, 411–425.
- Anderson, Ted L (2017), *Fracture mechanics: fundamentals and applications*, 4th ed. (CRC press).
- Andreotti, Bruno, Yoël Forterre, and Olivier Pouliquen (2013), *Granular media: between fluid and solid* (Cambridge University Press).
- Aref, Hassan (1984), “Stirring by chaotic advection,” *Journal of Fluid Mechanics* **143**, 1–21.
- Aref, Hassan, John R Blake, Marko Budišić, Silvana S S Cardoso, Julyan H E Cartwright, Herman J H Clercx, Kamal El Omari, Ulrike Feudel, Ramin Golestanian, Emmanuelle Gouillart, Gert-Jan F. van Heijst, Tatyana S. Krasnopol'skaya, Yves Le Guer, Robert S. MacKay, Vyacheslav V. Meleshko, Guy Metcalfe, Igor Mezić, Alessandro P. S. de Moura, Oreste Piro, Michel F. M. Speetjens, Rob Sturman, Jean-Luc Thiffeault, and Idan Tuval (2017), “Frontiers of chaotic advection,” *Reviews of Modern Physics* **89** (2), 025007.
- Argentino, Claudio, Stefano Conti, Chiara Fioroni, and Daniela Fontana (2019), “Evidences for paleo-gas hydrate occurrence: What we can infer for the miocene of the northern apennines (italy),” *Geosciences* **9** (3), 134.
- Arne, Dennis C, L. W. Curtis, and S. A. Kissin (1991), “Internal zonation in a carbonate-hosted Zn-Pb-Ag deposit, Nanisivik, Baffin Island, Canada,” *Economic Geology* **86**, 699–717.
- Aydin, Atilla, and James M. DeGraff (1988), “Evolution of polygonal fracture patterns in lava flows,” *Science* **239**, 471–476.
- Bacchin, Patrice, David Brutin, Anne Davaille, Erika Di Giuseppe, Xiao Dong Chen, Ioannis Gergianakis, Frédérique Giorgiutti-Dauphiné, Lucas Goehring, Yannick Hallez, Rodolphe Heyd, Romain Jeantet, Cécile Le Floch-Fouéré, Martine Meireles, Eric Mittelstaedt, Céline Nicloux, Ludovic Pauchard, and Marie-Louise Saboungi (2018), “Drying colloidal systems: Laboratory models for a wide range of applications,” *Eur. Phys. J. E* **41**, 94.
- Bachmann, Gerhard H, and Mahmoud A.M. Aref (2005), “A seismite in triassic gypsum deposits (grabfeld formation, ladinian), southwestern germany,” *Sedimentary Geology* **180** (1-2), 75–89.
- Balitsky, V S, T. M. Bublikova, S. L. Sorol'zjna, L. V. Balitskaya, and A. S. Shteinberg (1987), “Man-made jewelry malachite,” *Gems & Gemology* **23**, 152–157.
- Ball, Philip (2015), “Forging patterns and making waves from biology to geology: a commentary on turing (1952)‘the chemical basis of morphogenesis’,” *Philosophical Transactions of the Royal Society B: Biological Sciences* **370** (1666), 20140218.
- Barbey, P, F. Faure, J. L. Paquette, K. Pistre, C. Delangle, and J. P. Gremilliet (2019), “Skeletal quartz and dendritic biotite: Witnesses of primary disequilibrium growth textures in an alkali-feldspar granite,” *Lithos* **348–349**.
- Barge, Laura M, Yeghegis Abedian, Michael J Russell, Ivria J Doloboff, Julyan H E Cartwright, Richard D Kidd, and Isik Kanik (2015a), “From chemical gardens to fuel cells: generation of electrical potential and current across self-assembling iron mineral membranes,” *Angewandte Chemie International Edition* **54** (28), 8184–8187.
- Barge, Laura M, Silvana S S Cardoso, Julyan H E Cartwright, Geoffrey J T Cooper, Leroy Cronin, Anne De Wit, Ivria J Doloboff, Bruno Escibano, Raymond E Goldstein, Florence Haudin, David E. H. Jones, Alan L. Mackay, Jerzy Maselko, Jason J. Pagano, J. Pantaleone, Michael J. Russell, C. Ignacio Sainz-Díaz, Oliver Steinbock, David A. Stone, Yoshifumi Tanimoto, and Noreen L. Thomas (2015b), “From chemical gardens to chemobionics,” *Chemical Reviews* **115** (16), 8652–8703.
- Baron, Marzena A, Guillaume Fiquet, Guillaume Morard, Francesca Miozzi, Imène Esteve, Béatrice Doisneau, Anna S Pakhomova, Yanick Ricard, and François Guyot (2022), “Melting of basaltic lithologies in the earth's lower mantle,” *Physics of the Earth and Planetary Interiors* **333**, 106938.
- Basilevsky, AT, A.M. Abdrakhimov, J.W. Head, C.M. Pieters, Yunzhao Wu, and Long Xiao (2015), “Geologic characteristics of the Luna 17/Lunokhod 1 and Chang'E-3/Yutu landing sites, Northwest Mare Imbrium of the Moon,” *Planetary Space Sci.* **117**, 385–400.
- Bassler, Ray Smith (1908), *The formation of geodes with remarks on the silicification of fossils*, Vol. 35 (US Government Printing Office).
- Bážant, Zdeněk P (1993), “Scaling laws in mechanics of failure,” *Journal of Engineering Mechanics* **119** (9), 1828–1844.
- Bell, T H, and M D Bruce (2007), “Progressive deformation partitioning and deformation history: Evidence from millipede structures,” *Journal of Structural Geology* **29** (1), 18–35.
- Benedetto, Rancesco Di, Gian Piero Bernardini, Pilar Costagliola, David Plant, and David J Vaughan (2005), “Compositional zoning in sphalerite crystals,” *American Mineralogist* **90** (8-9), 1384–1392.
- Bertenthal, Alyse (2021), “Scaling the baseline: Technicalities and environmental regulation in owens valley, california,” *Law & Policy* **43** (1), 30–50.
- Biot, Maurice Anthony (1961), “Theory of folding of stratified viscoelastic media and its implications in tectonics and orogenesis,” *Geological Society of America Bulletin* **72** (11), 1595–1620.
- Bodenschatz, Eberhard, Werner Pesch, and Guenter Ahlers (2000), “Recent developments in rayleigh-bénard convection,” *Annual review of fluid mechanics* **32** (1), 709–778.
- Boggs Jr, Sam (2009), *Petrology of sedimentary rocks* (Cambridge university press).
- Bogush, G H, M. A. Tracy, and C. F. Zukoski (1988), “Preparation of monodisperse silica particles: Control of size and mass fraction,” *Journal of Non-Crystalline Solids* **104** (1), 95–106.
- Bohn, S, L. Pauchard, and Y. Couder (2005), “Hierarchical crack pattern as formed by successive domain divisions. I. Temporal and geometrical hierarchy,” *Phys. Rev. E* **71**, 046214.
- Bonnet, Eric, Olivier Bour, Noelle E Odling, Philippe Davy, Ian Main, Patience Cowie, and Brian Berkowitz (2001), “Scaling of fracture systems in geological media,” *Reviews of geophysics* **39** (3), 347–383.
- Bons, P D, M. W. Jessell, A. Griera, and C. Fay (2009), “Porphyroblast rotation versus nonrotation: Conflict resolution!,” *COMMENT*,
- Borhara, Krishna, and Charles M Onasch (2020), “Evidence for silica gel and its role in faulting in the tuscarora sandstone,” *Journal of Structural Geology* **139**, 104140.
- Boswell, PGH (1951), “The trend of research on the rheotropy of geological materials,” *Science Progress* (1933-) **39** (156), 608–622.
- Boudreau, AE (1995), “Crystal aging and the formation of fine-scale igneous layering,” *Mineralogy and Petrology*

- 54 (1), 55–69.
- Boutakoff, N (1963), “The geology and geomorphology of the portland area,” Geological Survey of Victoria Memoir **22**, 1–172.
- Breitkreuz, Christoph (2013), “Spherulites and lithophysae—200 years of investigation on high-temperature crystallization domains in silica-rich volcanic rocks,” Bulletin of Volcanology **75**, 1–16.
- Bretz, J Harlen (1960), “Bermuda: A partially drowned, late mature, pleistocene karst,” Geological Society of America Bulletin **71** (12), 1729–1754.
- Briere, P R (2000), “Playa, playa lake, sabkha: Proposed definitions for old terms,” J. Arid Environ. **45** (1), 1–7.
- Bringedal, Carina, Theresa Schollenberger, G. J. M. Pieters, C. J. van Duijn, and Rainer Helmig (2022), “Evaporation-Driven Density Instabilities in Saturated Porous Media,” Transp. Porous Med. **143**, 297–341.
- Broberg, K Bertram (1999), *Cracks and fracture* (Elsevier).
- Brocx, M, and V Semeniuk (2010), “The geoheritage significance of crystals,” Geology Today **26** (6), 216–225.
- Brown, Kevin M (1990), “The nature and hydrogeologic significance of mud diapirs and diatremes for accretionary systems,” Journal of Geophysical Research: Solid Earth **95** (B6), 8969–8982.
- Bruna, Pierre-Olivier, Arthur P C Lavenu, Christophe Mantoni, and Giovanni Bertotti (2019), “Are stylolites fluid-flow efficient features?” Journal of Structural Geology **125**, 270–277.
- Brunn, P O (1976), “Slow motion of a sphere in a second-order fluid,” Rheol. Acta **15**, 163–171.
- Bryan, WH (1963), “The later history of expanded spherulites,” Journal of the Geological Society of Australia **10** (1), 141–149.
- Budkewitsch, Paul, and Pierre-Yves Robin (1994), “Modelling the evolution of columnar joints,” J. Volcanol. Geotherm. Res. **59**, 219–239.
- Burnley, PC (2013), “The importance of stress percolation patterns in rocks and other polycrystalline materials,” Nature Communications **4** (1), 2117.
- Burridge, Robert, and Leon Knopoff (1967), “Model and theoretical seismicity,” Bulletin of the seismological society of america **57** (3), 341–371.
- Busse, FH (1989), “Fundamentals of thermal convection mantle convection, plate tectonics and global dynamics ed wr peltier,”.
- Butt, C R M, R M Hough, and M Verrall (2020), “Gold nuggets: the inside story,” Ore and Energy Resource Geology **4**, 100009.
- Cabane, Hugues, Didier Laporte, and Ariel Provost (2005), “An experimental study of ostwald ripening of olivine and plagioclase in silicate melts: implications for the growth and size of crystals in magmas,” Contributions to Mineralogy and Petrology **150**, 37–53.
- Caccin, Marco, Zhenwei Li, James R Kermode, and Alessandro De Vita (2015), “A framework for machine-learning-augmented multiscale atomistic simulations on parallel supercomputers,” International Journal of Quantum Chemistry **115** (16), 1129–1139.
- Cady, SL, H-R Wenk, and M. Sintubin (1998), “Microfibrillar quartz varieties: characterization by quantitative x-ray texture analysis and transmission electron microscopy,” Contributions to Mineralogy and Petrology **130**, 320–335.
- Camporeale, Carlo, and Luca Ridolfi (2012), “Hydrodynamic-driven stability analysis of morphological patterns on stalactites and implications for cave paleoflow reconstructions,” Phys. Rev. Lett. **108**, 238501.
- Cardoso, Silvana S S, and Julyan H E Cartwright (2014), “Dynamics of osmosis in a porous medium,” Royal Society Open Science **1** (3), 140352.
- Cardoso, Silvana S S, and Julyan H E Cartwright (2016), “Increased methane emissions from deep osmotic and buoyant convection beneath submarine seeps as climate warms,” Nature communications **7** (1), 13266.
- Cardoso, Silvana S S, and Julyan H E Cartwright (2017), “On the differing growth mechanisms of black-smoker and lost city-type hydrothermal vents,” Proceedings of the Royal Society A: Mathematical, Physical and Engineering Sciences **473** (2205), 20170387.
- Cardoso, Silvana S S, Julyan H E Cartwright, Jitka Čejková, Leroy Cronin, Anne De Wit, Simone Giannerini, Dezső Horváth, Alfrío Rodrigues, Michael J Russell, C Ignacio Sainz-Díaz, and Á. Tóth (2020), “Chemobionics: From self-assembled material architectures to the origin of life,” Artificial Life **26** (3), 315–326.
- Carter, Elizabeth A, Michael D. Hargreaves, Terence P. Kee, Matthew A. Pasek, and Howell G. M. Edwards (2010), “A Raman spectroscopic study of a fulgurite,” Philosophical Transactions: Mathematical, Physical and Engineering Sciences **368** (1922), 3087–3097.
- Cartwright, Julyan H E, Jitka Čejková, Elena Fimmel, Simone Giannerini, Diego Luis Gonzalez, Greta Goracci, Clara Grácio, Jeanine Houwing-Duistermaat, Dragan Matić, Nataša Mišić, *et al.* (2024), “Information, coding, and biological function: The dynamics of life,” Artificial Life **30** (1), 16–27.
- Cartwright, Julyan H E, Antonio G Checa, Bruno Escibano, and C Ignacio Sainz-Díaz (2012), “Crystal growth as an excitable medium,” Philosophical Transactions of the Royal Society A: Mathematical, Physical and Engineering Sciences **370** (1969), 2866–2876.
- Cartwright, Julyan H E, Bruno Escibano, Diego L. Gonzalez, C. Ignacio Sainz-Díaz, and Idan Tuval (2013), “Bricicles as a case of inverse chemical gardens,” Langmuir **29** (25), 7655–7660.
- Cartwright, Julyan H E, Bruno Escibano, and C Ignacio Sainz-Díaz (2011), “Chemical-garden formation, morphology, and composition. i. effect of the nature of the cations,” Langmuir **27** (7), 3286–3293.
- Cartwright, Julyan H E, Mario Feingold, and Oreste Piro (1999a), “An introduction to chaotic advection,” Mixing: Chaos and turbulence , 307–342.
- Cartwright, Julyan H E, Juan Manuel García-Ruiz, María Luisa Novella, and Fermín Otálora (2002), “Formation of chemical gardens,” Journal of colloid and interface science **256** (2), 351–359.
- Cartwright, Julyan H E, Juan Manuel García-Ruiz, and Ana I Villacampa (1999b), “Pattern formation in crystal growth: Liesegang rings,” Computer physics communications **121**, 411–413.
- Cartwright, Julyan H E, Simone Giannerini, and Diego L González (2016), “Dna as information: at the crossroads between biology, mathematics, physics and chemistry,” Philosophical Transactions of the Royal Society A: Mathematical, Physical and Engineering Sciences **374** (2063), 20150071.
- Cartwright, Julyan H E, Emilio Hernández-García, and Oreste Piro (1997), “Burridge-knopoff models as elastic excitable media,” Physical Review Letters **79** (3), 527.

- Cartwright, Julyan H E, and Alan L Mackay (2012), “Beyond crystals: the dialectic of materials and information,” *Philosophical Transactions of the Royal Society A: Mathematical, Physical and Engineering Sciences* **370** (1969), 2807–2822.
- Cartwright, Julyan H E, Oreste Piro, and Idan Tuval (2007), “Ostwald ripening, chiral crystallization, and the common-ancestor effect,” *Physical review letters* **98** (16), 165501.
- Cartwright, Julyan H E, and Michael J. Russell (2019), “The origin of life: the submarine alkaline vent theory at 30,” *Interface Focus* **9**.
- Cathles, L M, and A. T. Smith (1983), “Thermal constraints on the formation of mississippi valley-type lead-zinc deposits and their implications for episodic basin dewatering and deposit genesis,” *Economic Geology* **78** (5), 983–1002.
- Centrella, Stephen, Nicolas E Beaudoin, Hannelore Derluyin, Geoffrey Motte, Guilhem Hoareau, Pierre Lanari, Francesca Piccoli, Christophe Pecheyran, and Jean Paul Callot (2021), “Micro-scale chemical and physical patterns in an interface of hydrothermal dolomitization reveals the governing transport mechanisms in nature: Case of the layens anticline, pyrenees, france,” *Sedimentology* **68** (2), 834–854.
- Chan, M A, Jens Ormö, A J Park, Michael Stich, Virginia Souza-Egipsy, and Goro Komatsu (2007), “Models of iron oxide concretion formation: field, numerical, and laboratory comparisons,” *Geofluids* **7** (3), 356–368.
- Chao, Zhiming, Guotao Ma, Xiewen Hu, and Gang Luo (2020), “Research on anisotropic permeability and porosity of columnar jointed rock masses during cyclic loading and unloading based on physical model experiments,” *Bull. Eng. Geol. Env.* **79**, 5433—5454.
- Charalambous, Andreas N (2021), “Water well acidization revisited: includes oil and geothermal well perspectives,” *Quarterly Journal of Engineering Geology and Hydrogeology* **54** (3), qjeh2020–071.
- Chen, Antony S-H, John Ladan, and Stephen W. Morris (2006), “Icicle atlas run 120906,” .
- Chen, Antony Szu-Han, and Stephen W. Morris (2011), “Experiments on the morphology of icicles,” *Phys. Rev. E* **83**, 026307.
- Chen, Antony Szu-Han, and Stephen W Morris (2013), “On the origin and evolution of icicle ripples,” *New Journal of Physics* **15** (10), 103012.
- Cheung, W, and H. Rajaram (2002), “Dissolution finger growth in variable aperture fractures: Role of the tip-region flow field,” *Geophys. Res. Lett.* **29**, 2075.
- Chopard, B, HJ Herrmann, and T Vicsek (1991), “Structure and growth mechanism of mineral dendrites,” *Nature* **353** (6343), 409–412.
- Christiansen, F W (1963), “Polygonal fracture and fold systems in the salt crust, Great Salt Lake Desert, Utah,” *Science* **139** (3555), 607–609.
- Chuoque, RL, P Van Meurs, and C_ van der Poel (1959), “The instability of slow, immiscible, viscous liquid-liquid displacements in permeable media,” *Transactions of the AIME* **216** (01), 188–194.
- Cicconi, Maria Rita, and Daniel R Neuville (2019), “Natural glasses,” *Springer handbook of glass* , 771–812.
- Cöelfen, H, and M. Antonietti (2008), *Mesocrystals and Non-classical Crystallization* (Wiley).
- Coetzee, F (1975), “Solution pipes in coastal aeolianites of zululand and mozambique,” *Trans. Geol. Soc. S. Afr.* **78**, 323–333.
- Conti, Stefano, and Daniela Fontana (1999), “Miocene chemohorms of the northern apennines, italy,” *Geology* **27** (10), 927–930.
- Cooke, RU, and IJ Smalley (1968), “Salt weathering in deserts,” *Nature* **220** (5173), 1226–1227.
- Cooper, Max P, Rishabh P Sharma, Silvana Magni, Tomasz P Blach, Andrzej P Radlinski, Katarzyna Drabik, Alessandro Tengattini, and Piotr Szymczak (2023), “4d tomography reveals a complex relationship between wormhole advancement and permeability variation in dissolving rocks,” *Advances in Water Resources* **175**, 104407.
- Coward, Andrew J, Anja C Slim, Joël Brugger, Sasha Wilson, Tim Williams, Brad Pillans, and Anton Maksimenko (2023), “Mineralogy and geochemistry of pattern formation in zebra rock from the east kimberley, australia,” *Chemical Geology* **622**, 121336.
- Coward, Andrew Jeremy (2022), *How the zebra rock got its stripes: the formation of hematite banding in Western Australian siltstones*, thesis (Monash University).
- Craster, Richard V, and Omar K Matar (2009), “Dynamics and stability of thin liquid films,” *Reviews of modern physics* **81** (3), 1131–1198.
- Craw, Dave, and Kat Lilly (2016), “Gold nugget morphology and geochemical environments of nugget formation, southern new zealand,” *Ore Geology Reviews* **79**, 301–315.
- Crostack, H-A, J. Nellesen, G. Fischer, M. Hofmann, H.-G. Rademacher, and W. Tillmann (2012), “Analysis of crack patterns in drying corn starch by in-situ radiography and x-ray computer tomography,” *Exp. Mech.* **532**, 912–932.
- Cullimore, D Roy, and Lori A. Johnston (2008), “Microbiology of concretions, sediments and mechanisms influencing the preservation of submerged archaeological artifacts,” *International Journal of Historical Archaeology* **12**, 120–132.
- Cunningham-Craig, E H (1916), “The origin of oil-shale,” *Proceedings of the Royal Society of Edinburgh* **36** (1-2), 44–86.
- Curtis, Neville J, Jason R. Gascooke, Martin R. Johnston, and Allan Pring (2019), “A Review of the Classification of Opal with Reference to Recent New Localities,” *Minerals* **9** (5), 299, number: 5.
- Curtis, Neville J, Jason R. Gascooke, and Allan Pring (2021), “Silicon-Oxygen Infrared and Raman Analysis of Opals: The Effect of Sample Preparation and Measurement Type,” *Minerals* **11** (2), 173, number: 2 Publisher: Multidisciplinary Digital Publishing Institute.
- Davidovits, Joseph (1994), “Geopolymers: man-made rock geosynthesis and the resulting development of very early high strength cement,” *Journal of Materials education* **16**, 91–91.
- Davidson, Patrick, and Jean-Christophe P Gabriel (2005), “Mineral liquid crystals,” *Current opinion in colloid & interface science* **9** (6), 377–383.
- D’Avino, G, M. A. Hulsen, F. Slijkens, and J. Vermant (2008), “Rotation of a sphere in a viscoelastic liquid subjected to shear flow. Part I: Simulation results,” *J. Rheol.* **52**, 1331–1346.
- Dayeh, Malak, Manal Ammar, and Mazen Al-Ghoul (2014), “Transition from rings to spots in a precipitation reaction–diffusion system,” *RSC Advances* **4** (104), 60034–60038, publisher: The Royal Society of Chemistry.
- De Boever, Eva, Daniel Birgel, Volker Thiel, Philippe Muechez, Jörn Peckmann, Lyubomir Dimitrov, and Rudy Swennen (2009), “The formation of giant tubular concretions triggered by anaerobic oxidation of methane as revealed by archaeal molecular fossils (lower eocene, varna, bul-

- garia,” *Palaeogeography, Palaeoclimatology, Palaeoecology* **280** (1-2), 23–36.
- De Campos, Cristina P (2015), “Chaotic flow patterns from a deep plutonic environment: a case study on natural magma mixing,” *Pure and applied geophysics* **172**, 1815–1833.
- De Gennes, Pierre-Gilles (1992), “Soft matter,” *Science* **256** (5056), 495–497.
- De Silva, I P D, H J S Fernando, F Eaton, and D Hebert (1996), “Evolution of kelvin-helmholtz billows in nature and laboratory,” *Earth and Planetary Science Letters* **143** (1-4), 217–231.
- De Waele, Jo, Stein-Erik Lauritzen, and Mario Parise (2011), “On the formation of dissolution pipes in quaternary coastal calcareous arenites in mediterranean settings,” *Earth Surf. Processes Landforms* **36** (2), 143–157.
- De Yoreo, James J, Pupa UPA Gilbert, Nico AJM Sommerdijk, R Lee Penn, Stephen Whitelam, Derk Joester, Hengzhong Zhang, Jeffrey D Rimer, Alexandra Navrotsky, Jillian F Banfield, Adam F. Wallace, F. Marc Michel, Fiona C. Meldrum, Helmut Cölfen, and Patricia M. Dove (2015), “Crystallization by particle attachment in synthetic, biogenic, and geologic environments,” *Science* **349** (6247), aaa6760.
- DeGraff, James M, and Atilla Aydin (1987), “Surface morphology of columnar joints and its significance to mechanics and direction of joint growth,” *Geol. Soc. Am.* **99**, 605–617.
- DeGraff, James M, and Atilla Aydin (1993), “Effect of thermal regime on growth increment and spacing of contraction joints in basaltic lava,” *J. Geophys. Res.* **98**, 6411–6430.
- Demmenie, Menno, Lars Reus, Paul Kolpakov, Sander Woutersen, Daniel Bonn, and Noushine Shahidzadeh (2023), “Growth and form of rippled icicles,” *Phys. Rev. Appl.* **19**, 024005.
- Desarnaud, Julie, Hannelore Derluyn, Luisa Molari, Stefano de Miranda, Veerle Cnudde, and Noushine Shahidzadeh (2015), “Drying of salt contaminated porous media: Effect of primary and secondary nucleation,” *Journal of Applied Physics* **118** (11).
- Detwiler, R L, R. J. Glass, and W. L. Bourcier (2003), “Experimental observations of fracture dissolution: The role of Péclet number in evolving aperture variability,” *Geophys. Res. Lett.* **30**, 1648.
- Devitt, Dale A, and Stanley D Smith (2002), “Root channel macropores enhance downward movement of water in a mojave desert ecosystem,” *J. Arid Environ.* **50** (1), 99–108.
- Dewynne, J N, A. C. Fowler, and P. S. Hagan (1993), “Multiple reaction fronts in the oxidation/reduction of iron-rich uranium ores,” *Siam J. Appl. Math.* **53**, 971–989.
- Ding, Yang, Silvana S S Cardoso, and Julyan H E Cartwright (2024), “Dynamics of the osmotic lysis of mineral protocells and its avoidance at the origins of life,” *Geobiology* **22** (4), e12611.
- Ding, Yang, Julyan H E Cartwright, and Silvana S S Cardoso (2019), “Intrinsic concentration cycles and high ion fluxes in self-assembled precipitate membranes,” *Interface Focus* **9** (6), 20190064.
- Dixon, John C (2009), “Aridic Soils, Patterned Ground, and Desert Pavements,” in *Geomorphology of Desert Environments* (Springer Netherlands, Dordrecht) pp. 101–122.
- Dobrowolski, Radosław, and Przemysław Mroczek (2015), “Clay cortex in epikarst forms as an indicator of age and morphogenesis—case studies from lublin–volhynia chalkland (east poland, west ukraine),” *Geomorphology* **247**, 66–75.
- Doehne, Eric (2002), “Salt weathering: a selective review,” *Geological society, London, special publications* **205** (1), 51–64.
- Doerr, SH, RA Shakesby, and RPDm Walsh (2000), “Soil water repellency: its causes, characteristics and hydrogeomorphological significance,” *Earth Sci. Rev.* **51** (1-4), 33–65.
- Domokos, Gábor, Douglas J. Jerolmack, Ferenc Kun, and János Török (2020), “Plato’s cube and the natural geometry of fragmentation,” *Proc. Nat. Acad. Sci.* **117** (31), 18178–18185.
- Domokos, Gábor, and Krisztina Regös (2024), “A discrete time evolution model for fracture networks,” *Cent. Eur. J. Oper. Res.* **32**, 83–94.
- Dreybrodt, W (1990), “The role of dissolution kinetics in the development of karst aquifers in limestone: A model simulation of karst evolution,” *J. Geol.* **98**, 639–655.
- Eberl, Dennis D, Jan Šrodoň, Martin Kralik, Bruce E Taylor, and Zell E Peterman (1990), “Ostwald ripening of clays and metamorphic minerals,” *Science* **248** (4954), 474–477.
- Economides, M J, and K. G. Nolte (2000), *Reservoir Stimulation* (Wiley, Chichester, UK).
- Emmanuel, Simon, and Brian Berkowitz (2007), “Effects of pore-size controlled solubility on reactive transport in heterogeneous rock,” *Geophysical Research Letters* **34** (6).
- Erlebacher, J, P. C. Searson, and K. Sieradzki (1993), “Computer simulation of dense-branching patterns,” *Physical Review Letters* **71**, 3311–3314.
- Evans, Robert, Daan Frenkel, and Marjolein Dijkstra (2019), “From simple liquids to colloids and soft matter,” *Physics Today* **72** (2), 38–39.
- Fabbri, Stefania, Jian Li, Robert P Howlin, Amir Rmaile, Bart Gottenbos, Marko De Jager, E Michelle Starke, Marcelo Aspiras, Marilyn T Ward, Nicholas G Cogan, and Paul Stoodley (2017), “Fluid-driven interfacial instabilities and turbulence in bacterial biofilms,” *Environmental microbiology* **19** (11), 4417–4431.
- Fallick, AE, J Jocelyn, T Donnelly, M Guy, and C Behan (1985), “Origin of agates in volcanic rocks from scotland,” *Nature* **313** (6004), 672–674.
- Farrington, Oliver Cummings, and Berthold Laufer (1927), *Agate: physical properties and origin, archaeology and folklore* (Field Museum of Natural History).
- Fay, C, and T. H. Bell (2008), “Porphyroblast rotation versus nonrotation: Conflict resolution!” *Geology*.
- Feeney, R, SL Schmidt, P Strickholm, J Chadam, and P Ortoleva (1983), “Periodic precipitation and coarsening waves: Applications of the competitive particle growth model,” *The Journal of Chemical Physics* **78** (3), 1293–1311.
- Fisher, George W (1973), “Nonequilibrium thermodynamics as a model for diffusion-controlled metamorphic processes,” *American Journal of Science* **273** (10), 897–924.
- Fitzner, Bernd, Kurt Heinrichs, and Dennis La Bouchardiere (2003), “Weathering damage on pharaonic sandstone monuments in luxor-egypt,” *Building and Environment* **38** (9-10), 1089–1103.
- Flatt, Robert J, Francesco Caruso, Asel Maria Aguilar Sanchez, and George W. Scherer (2014), “Chemomechanics of salt damage in stone,” *Nat. Commun.* **5**, 4823.
- Fletcher, Raymond C (1977), “Folding of a single viscous layer: exact infinitesimal-amplitude solution,” *Tectonophysics* **39** (4), 593–606.
- Foley, Sam, and T. Molyneux (1694), “An account of the Giants Caus-Way in the North of Ireland: by the Reverend

- Dr. Sam. Foley," *Phil. Trans. R. Soc. Lond.* **18**, 170–182.
- Fontboté, Lluís (1993), "Self-organization fabrics in carbonate-hosted ore deposits: the example of diagenetic crystallization rhythmites (dcrs)," in *Current research in geology applied to ore deposits. Proceedings of the Second Biennial SGA Meeting, Granada, Spain*, pp. 11–14.
- Fontbote, Lluís, and Hendrik Gorzawski (1990), "Genesis of the mississippi valley-type Zn-Pb deposit of San Vicente, central Peru; geologic and isotopic (Sr, O, C, S, Pb) evidence," *Economic Geology* **85** (7), 1402–1437.
- Forbes, A E S, S. Blake, and H. Tuffen (2014), "AEntablature: fracture types and mechanisms," *Bull. Volcanol.* **76**, 820.
- Fowler, A D, H. E. Stanley, and G. Daccord (1989), "Dis-equilibrium silicate mineral textures: Fractal and non-fractal features," *Nature* **341**, 134–138.
- Fraser, Donald G (1977), *Thermodynamics in Geology: Proceedings of the NATO Advanced Study Institute Held in Oxford, England, September 17–27, 1976*, Vol. 30 (Springer Science & Business Media).
- Fredd, C N, and H. S. Fogler (1998), "Influence of transport and reaction on wormhole formation in porous media," *AIChE Journal* **44**, 1933–1949.
- French, J W (1925), "The fracture of homogeneous media," *Trans. Geol. Soc. Glasgow* **17**, 50–68.
- French, MW, RH Worden, and DR Lee (2013), "Electron backscatter diffraction investigation of length-fast chalcidony in agate: implications for agate genesis and growth mechanisms," *Geofluids* **13** (1), 32–44.
- Fritz, Steven J (1986), "Ideality of clay membranes in osmotic processes: a review," *Clays and clay minerals* **34**, 214–223.
- Fron-del, C (1985), "Systematic compositional zoning in the quartz fibers of agates," *American Mineralogist* **70** (9–10), 975–979.
- Fron-del, Clifford (1978), "Characters of quartz fibers," *American Mineralogist* **63** (1–2), 17–27.
- Gabriel, Jean-Christophe P, Clément Sanchez, and Patrick Davidson (1996), "Observation of nematic liquid-crystal textures in aqueous gels of smectite clays," *The Journal of physical chemistry* **100** (26), 11139–11143.
- Gailliot, Mary Patricia (1980), "Petrified lightning," *Rocks & Minerals* **55** (1), 13–17.
- Gaillou, Eloïse, Emmanuel Fritsch, Bertha Aguilar-Reyes, Benjamin Rondeau, Jeffrey Post, Alain Barreau, and Mikhail Ostroumov (2008), "Common gem opal: An investigation of micro- to nano-structure," *American Mineralogist* **93** (11–12), 1865–1873.
- Gao, Weihong, Muriel Rigout, and Huw Owens (2016), "Facile control of silica nanoparticles using a novel solvent varying method for the fabrication of artificial opal photonic crystals," *Journal of Nanoparticle Research* **18** (12), 387.
- Garcia-Guinea, J, M. Furio, M. Fernandez-Hernan, M. A. Bustillo, E. Crespo-Feo, V. Correcher, L. Sanchez-Munoz, and E. Matesanz (2009), "The quartzofeldspathic fulgurite of bustaviejo (madrid): Cathodoluminescence and raman emission," *AIP Conference Proceedings* **1163** (1), 128–134.
- García-Ruiz, Juan M, Fermín Otálora, Antonio Sanchez-Navas, and Francisco J Higes-Rolando (1994), "The formation of manganese dendrites as the mineral record of flow structures," *Fractals and dynamic systems in geoscience*, 307–318.
- Garcia-Ruiz, Juan Manuel, Stephen T Hyde, AM Carnerup, AG Christy, MJ Van Kranendonk, and NJ Welham (2003), "Self-assembled silica-carbonate structures and detection of ancient microfossils," *Science* **302** (5648), 1194–1197.
- García-Ruiz, Juan Manuel, Mark A Van Zuilen, and Wolfgang Bach (2020), "Mineral self-organization on a lifeless planet," *Physics of Life Reviews* **34**, 62–82.
- Garik, Peter (1985), "Anisotropic growth of diffusion-limited aggregates," *Physical Review A* **32**, 1275–1278.
- Gauthier, F, H. L. Goldsmith, and S. G. Mason (1971), "Particle motions in non-Newtonian media I. Couette flow," *Rheol. Acta* **10**, 344–364.
- Getling, Alexander V (1998), *Rayleigh-Bénard convection: structures and dynamics*, Vol. 11 (World Scientific).
- Gibbons, Melissa M, Dillon Muldoon, and Imane Khalil (2023), "Demonstrating the kelvin-helmholtz instability using a low-cost experimental apparatus and computational fluid dynamics simulations," *Fluids* **8** (12), 318.
- Ginibre, Catherine, Gerhard WÄ¶rner, and Andreas Kronz (2007), "Crystal zoning as an archive for magma evolution," *Elements* **3** (4), 261–266.
- Glauber, Johann Rudolf (1646), *Furni novi philosophici, sive Descriptio artis distillatoriae novae; nec non spirituum, olcorum, florum, aliorumque medicamentorum illis beneficio, facilimā quādam & perculiari viā è vegetabilibus, animalibus & mineralibus conficiendorum & quidem magno cum lucro; agens quoque de illorum usu tam chymico quam medico, edita & publicata in gratiam veritatis studiosorum* (prostant apud J. Janssonium, Amsterdamam) oCLC: 5515255.
- Goehring, L (2013), "Evolving fracture patterns: columnar joints, mud cracks and polygonal terrain," *Phil. Trans. R. Soc. A* **371** (20120353–20120353).
- Goehring, L, and S.W. Morris (2008), "Scaling of columnar joints in basalt," *J. Geophys. Res.* **113**, B10203.
- Goehring, Lucas, Zhenquan Lin, and Stephen W. Morris (2006), "An experimental investigation of the scaling of columnar joints," *Phys. Rev. E* **74**, 036115.
- Goehring, Lucas, L. Mahadevan, and Stephen W. Morris (2009), "Nonequilibrium scale selection mechanism for columnar jointing," *Proc. Nat. Acad. Sci.* **106**, 387–392.
- Goehring, Lucas, and Stephen W. Morris (2005), "Order and disorder in columnar joints," *Europhys. Lett.* **69**, 739–745.
- Goehring, Lucas, and Stephen W. Morris (2014), "Cracking mud, freezing dirt and breaking rocks," *Phys. Today* **67**, 39–44.
- Goehring, Lucas, Akio Nakahara, Tapati Dutta, So Kitsunezaki, and Sujata Tarafdar (2015), *Desiccation cracks and their patterns: Formation and Modelling in Science and Nature* (Wiley-VCH, Singapore).
- Gogoi, Bibhuti, and Ashima Saikia (2019), "The genesis of emulsion texture owing to magma mixing in the ghan-sura felsic dome of the chotanagpur granite gneiss complex of eastern india," *The Canadian Mineralogist* **57** (3), 311–338.
- Goodchild, JG (1899), "On the genesis of some scottish minerals," *Proc. Royal Phys. Soc. Edinburgh* **14**, 181–220.
- Gottsmann, Joachim, Andrew J. L. Harris, and Donald B. Dingwell (2004), "Thermal history of hawaiian pahoehoe lava crusts at the glass transition: implications for flow rheology and emplacement," *Earth Planetary Sci. Lett.* **228**, 343–353.
- Götze, J, R. Möckel, and Y. Pan (2020), "Mineralogy, geochemistry and genesis of agate—A review," *Minerals* **10** (11), 1037.
- Gouze, P, C. Noiriél, C. Bruderer, and D. Loggia (2003), "X-ray tomography characterization of fracture surfaces during dissolution," *Geophys. Res. Lett.* **30**, 1267.

- Grapes, Rodney (2010), *Pyrometamorphism*, 2nd ed. (Springer-Verlag Berlin Heidelberg).
- Gravish, Nick, and Daniel I. Goldman (2016), "Entangled granular media," in *Fluids, Colloids and Soft Materials*, Chap. 17 (John Wiley & Sons, Ltd) pp. 341–354.
- Greiner, Jens, Gerhard Bohrmann, and Erwin Suess (2001), "Gas hydrate-associated carbonates and methane-venting at hydrate ridge: classification, distribution and origin of authigenic lithologies," *Geophysical Monograph-American Geophysical Union* **124**, 99–114.
- Griffiths, Ross W (2000), "The dynamics of lava flows," *Annual review of fluid mechanics* **32** (1), 477–518.
- Grimes, K G (2004), "Solution pipes or petried forests? drifting sands and drifting opinions!" *Vic. Nat.* **121** (1), 14–22.
- Grimes, K G (2009), "Solution pipes and pinnacles in syngenetic karst," in *Karst Rock Features. Karren Sculpturing* (Karst Research Institute) pp. 513–526.
- Groeneveld, D, J. Huntington, and D. Barz (2010), "Floating brine crusts, reduction of evaporation and possible replacement of fresh water to control dust from Owens Lake bed, California," *J. Hydrol.* **392**, 211–218.
- Groom, Kaelin M, Casey D Allen, Lisa Mol, Thomas R Paradise, and Kevin Hall (2015), "Defining tafoni: Re-examining terminological ambiguity for cavernous rock decay phenomena," *Progress in Physical Geography* **39** (6), 775–793.
- Grossenbacher, Kenneth A, and Stephen M. McDuffie (1995), "Conductive cooling of lava: columnar joint diameter and stria width as functions of cooling rate and thermal gradient," *J. Volcanol. Geotherm. Res.* **69**, 95–103.
- Groves, C G, and A. D. Howard (1994), "Early development of karst systems. I. Preferential flow path enlargement under laminar flow," *Water Resources Research* **30**, 2837–2846.
- Gutiérrez-Ariza, Carlos, Laura M Barge, Yang Ding, Silvana S S Cardoso, Shawn Erin McGlynn, Ryuhei Nakamura, Donato Giovanelli, Roy Price, Hye Eun Lee, F Javier Huertas, C. Ignacio Sainz-Díaz, and Julyan H. E. Cartwright (2024), "Magnesium silicate chimneys at the strytan hydrothermal field, iceland, as analogues for prebiotic chemistry at alkaline submarine hydrothermal vents on the early earth," *Progress in Earth and Planetary Science* **11** (1), 11.
- Haidinger, W (1848), "Über die metamorphose der gebirgsarten," *Ber. über die Mittheilungen von Freunden der Naturwissenschaften in Wien* **4**, 103–134.
- Hakim, Vincent, and Alain Karma (2005), "Crack path prediction in anisotropic brittle materials," *Physical review letters* **95** (23), 235501.
- Halsey, Thomas C (2000), "Diffusion-limited aggregation: A model for pattern formation," *Physics Today* **53** (11), 36–41.
- Hamada, Ai, and Atsushi Toramaru (2020), "Analogue experiments on morphological transition from columnnade to entablature of columnar joints," *J. Volcanol. Geotherm. Res.* **402**, 106979.
- Hammer, Ø, DK Dysthe, B Lelu, H Lund, P Meakin, and B Jamtveit (2008), "Calcite precipitation instability under laminar, open-channel flow," *Geochimica et Cosmochimica Acta* **72** (20), 5009–5021.
- Hanczyc, Martin M, Sheref S Mansy, and Jack W Szostak (2007), "Mineral surface directed membrane assembly," *Origins of Life and Evolution of Biospheres* **37**, 67–82.
- Hanna, R B, and H. Rajaram (1998), "Influence of aperture variability on dissolutional growth of fissures in karst formations," *Water Resour. Res.* **34**, 2843–2853.
- Hardee, Harry C (1980), "Solidification in Kilauea Iki lava lake," *J. Volcanol. Geotherm. Res.* **7**, 211–223.
- Harloff, C (1927), "Zonal structure in plagioclases: Leidsche geol.,"
- Harris, Chris (1989), "Oxygen-isotope zonation of agates from karoo volcanics of the skeleton coast, namibia," *American Mineralogist* **74** (3-4), 476–481.
- Hastie, ECG, M Schindler, DJ Kontak, and B Lafrance (2021), "Transport and coarsening of gold nanoparticles in an orogenic deposit by dissolution–reprecipitation and ostwald ripening," *Communications Earth & Environment* **2** (1), 57.
- Heaney, PJ, and A.M. Davis (1995), "Observation and origin of self-organized textures in agates," *Science* **269** (5230), 1562–1565.
- Heap, Michael J, Patrick Baud, Thierry Reuschlé, and Philip G Meredith (2014), "Stylolites in limestones: Barriers to fluid flow?" *Geology* **42** (1), 51–54.
- Heide, Klaus, and Gerhard Heide (2011), "Vitreous state in nature—origin and properties," *Geochemistry* **71** (4), 305–335.
- Heifetz, Eyal, Amotz Agnon, and Shmuel Marco (2005), "Soft sediment deformation by kelvin helmholtz instability: A case from dead sea earthquakes," *Earth and Planetary Science Letters* **236** (1-2), 497–504.
- Heinrichs, Kurt (2008), "Diagnosis of weathering damage on rock-cut monuments in petra, jordan," *Environmental Geology* **56**, 643–675.
- Henisch, Heinz K (2014), *Periodic precipitation* (Elsevier).
- Hermann, Leonhard David (1711), *Maslographia Oder Beschreibung Des Schlesischen Massel Im Oelß-Bernstädtischen Fürstenthum mit seinen Schauwürdigkeiten: Theils Unterschiedlicher so wohl Heydnischer, als Christlicher Antiquiteten, Monumenten und Epitaphien, Theils Auf dem so genau [n] ten Töppelberge gefundener Sonderbahren Reliquien, von Urnis oder Todten-Gefässen, Fibulis, Stylis, Nadeln oder Grieffeln, Messern, Müntzen, Donnerkeilen [et] c. Theils In, und als auch umb Massel In Regno Animalis, Vegetabili, und Minerali befindlicher Naturalien, versteinter Muscheln, oder Muschel-Steinen, auch anderen figurirten Stein-Wesens, geschliffenen, und polirten Steinen, wunderbahren Brunnen, Erd-Baum-und Feld-Gewächsen, Nebst Dazu gehörigen Kupffer-Stücken* (Brachvogel).
- Herminghaus, Stephan, Katherine Ruth Thomas, Saeedeh Aliaskarisohi, Hubertus Porada, and Lucas Goehring (2016), "Kinneyia: a flow-induced anisotropic fossil pattern from ancient microbial mats," *Frontiers in Materials* **3**, 30.
- Herwitz, S R (1993), "Stemflow influences on the formation of solution pipes in bermuda eolianite," *Geomorphology* **6** (3), 253–271.
- Hess, Benjamin L, Sandra Piazzolo, and Jason Harvey (2021), "Lightning strikes as a major facilitator of prebiotic phosphorus reduction on early Earth," *Nature Communications* **12** (1), 1535.
- Hewitt, DR (2020), "Vigorous convection in porous media," *Proc. R. Soc. A* **476**, 20200111.
- Hill, S (1952), "Channeling in packed columns," *Chemical Engineering Science* **1** (6), 247–253.
- Hills, Edwin Sherbon (1936), "Reverse and oscillatory zoning in plagioclase feldspars," *Geological Magazine* **73** (2), 49–56.
- Hinch, E J, and B. S. Bhatt (1990), "Stability of an acid front moving through porous rock," *J. Fluid Mech.* **212**, 279–288.

- Hird, Robert, and Malcolm D Bolton (2016), "Migration of sodium chloride in dry porous materials," *Proceedings of the Royal Society A: Mathematical, Physical and Engineering Sciences* **472** (2186), 20150710.
- Hoefner, M L, and H. S. Fogler (1988), "Pore evolution and channel formation during flow and reaction in porous media," *AIChE Journal* **34**, 45–54.
- Hou, Zhaoliang, Dawid Woś, Cornelius Tschegg, Anna Rogowitz, A Hugh N Rice, Lutz Nasdala, Florian Füsseis, Piotr Szymczak, and Bernhard Grasmann (2023), "Three-dimensional mineral dendrites reveal a nonclassical crystallization pathway," *Geology*.
- Hovland, Martin (2002), "On the self-sealing nature of marine seeps," *Continental Shelf Research* **22** (16), 2387–2394.
- Howard, Charles Brian, and Avinoam Rabinovitch (2018), "A new model of agate geode formation based on a combination of morphological features and silica sol-gel experiments," *European Journal of Mineralogy* **30** (1), 97–106.
- Hsu, Tao, and Andrew Lucas (2016), "Fordite from the corvette assembly plant," *Gems & Gemology* **52** (1).
- Huang, Bin-Juine, and Jen-Chi Huang (1976), "Creeping-film phenomenon of potassium chloride solution," *Nature* **261** (5555), 36–38.
- Huang, Ming, Fei Li, Fan Dong, Yu Xin Zhang, and Li Li Zhang (2015), "Mno 2-based nanostructures for high-performance supercapacitors," *Journal of Materials Chemistry A* **3** (43), 21380–21423.
- Huerre, Axel, Christophe Josserand, and Thomas Séon (2024), "Freezing and capillarity," *Annual Review of Fluid Mechanics*.
- Huinink, H Pel, L Pel, and K Kopinga (2004), "Simulating the growth of tafoni," *Earth Surface Processes and Landforms: The Journal of the British Geomorphological Research Group* **29** (10), 1225–1233.
- Huppert, Herbert E, and J. Stewart Turner (1981), "Double-diffusive convection," *J. Fluid Mech.* **106**, 299–329.
- Huxley, T H (1881), *Physiography: An Introduction to the Study of Nature* (MacMillan and Co., London).
- Hwang, W R, and M. A. Hulsen (2011), "Structure Formation of Non-Colloidal Particles in Viscoelastic Fluids Subjected to Simple Shear Flow," *Macromol. Materials Eng.* **296**, 321–330.
- Ibne Haque, Ruhul Amin, Atish Jyoti Mitra, and Tapati Dutta (2024), "Three-dimensional modeling of polygonal ridges in salt playas," *Langmuir* **40** (33), 17311–17319.
- Iler, R K (1965), "Formation of precious opal," *Nature* **207** (4996), 472–473.
- Jablczyński, K (1926), "Über Liesegang-Ringe," *Kolloid-Zeitschrift* **40** (1), 22–28.
- Jackson, Brian (2003), "Structures and micro-structures in Scottish agates," in *Symposium on Agate and Cryptocrystalline Quartz, Golden, Colorado*, pp. 89–94.
- Jamtveit, B, and Ø. Hammer (2012), "Sculpting of rocks by reactive fluids," *Geochemical Perspectives* **1** (3), 341–481.
- Jamtveit, Bjørn, Christine V Putnis, and Anders Malthesørensen (2009), "Reaction induced fracturing during replacement processes," *Contributions to Mineralogy and Petrology* **157**, 127–133.
- Jamtveit, Bjørn, and Paul Meakin (1999), *Growth, Dissolution and Pattern Formation in Geosystems* (Springer, Dordrecht).
- Jaupart, Claude, and Sylvie Vergnolle (1989), "The generation and collapse of a foam layer at the roof of a basaltic magma chamber," *Journal of Fluid Mechanics* **203**, 347–380.
- Jayne, Richard S, Hao Wu, and Ryan M. Pollyea (2019), "Geologic co2 sequestration and permeability uncertainty in a highly heterogeneous reservoir," *Int. J. Greenhouse Gas Control* **83**, 128–139.
- Jerolmack, Douglas J, and Karen E. Daniels (2019), "Viewing earth's surface as a soft-matter landscape," *Nature Reviews Physics*.
- Jewell, Helen E, and Frank R. Effensohn (2004), "An ancient seismite response to taconian far-field forces," *Journal of Geodynamics* **37** (3-5), 487–511.
- Johnson, M S, and J. Lehmann (2006), "Double-funneling of trees: Stemflow and root-induced preferential flow," *Ecoscience* **13** (3), 324–333, cited By :102 Export Date: 18 July 2018.
- Jones, Francis T (1952), "Iris agate," *American Mineralogist: Journal of Earth and Planetary Materials* **37** (7-8), 578–587.
- Jones, J B, J. V. Sanders, and E. Ralph Segnit (1964), "Structure of opal," *Nature* **204** (4962), 990–991.
- Judd, Alan, and Martin Hovland (2009), *Seabed fluid flow: the impact on geology, biology and the marine environment* (Cambridge University Press).
- Kadau, Dirk, Hans J Herrmann, José S Andrade, Ascânio D Araújo, Luiz J C Bezerra, and Luis P Maia (2009), "Living quicksand," *Granular Matter* **11**, 67–71.
- Kagan, Elisa, Mordechai Stein, and Shmuel Marco (2018), "Integrated paleoseismic chronology of the last glacial lake lisan: From lake margin seismites to deep-lake mass transport deposits," *Journal of Geophysical Research: Solid Earth* **123** (4), 2806–2824.
- Kalia, N, and V. Balakotaiah (2009), "Effect of medium heterogeneities on reactive dissolution of carbonates," *Chem. Eng. Sci.* **64** (2), 376–390.
- Kang, Peter K, Pietro De Anna, Joao P Nunes, Branko Bijeljic, Martin J Blunt, and Ruben Juanes (2014), "Pore-scale intermittent velocity structure underpinning anomalous transport through 3-d porous media," *Geophysical Research Letters* **41** (17), 6184–6190.
- Katsev, S, I. L'Heureux, and A. D. Fowler (2001), "Mechanism and duration of banding in Mississippi Valley-type sphalerite," *Geophysical Research Letters* **28** (23), 4643–4646.
- Katsev, Sergey, and Ivan L'Heureux (2001), "Two-dimensional model of banding pattern formation in minerals by means of coarsening waves: Mississippi valley-type sphalerite," *Physics Letters A* **292**, 66–74.
- Kattenhorn, Simon A, and Conrad J. Schaefer (2008), "Thermal-mechanical modeling of cooling history and fracture development in inflationary basalt lava flows," *J. Volcanol. Geotherm. Res.* **170** (3), 181–197.
- Kawahara, Hirokazu, Hidekazu Yoshida, Koshi Yamamoto, Nagayoshi Katsuta, Shoji Nishimoto, Ayako Umemura, and Ryusei Kuma (2022), "Hydrothermal formation of Fe-oxide bands in zebra rocks from northern Western Australia," *Chemical Geology* **590**, 120699.
- Kelka, Ulrich, Manolis Veveakis, Daniel Koehn, and Nicolas Beaudoin (2017), "Zebra rocks: compaction waves create ore deposits," *Scientific Reports* **7** (1), 14260.
- Keller, PC (1990), *Gemstones and Their Origin* (Springer).
- Kelley, Deborah S, Jeffrey A Karson, Gretchen L Fruh-Green, Dana R Yoerger, Timothy M Shank, David A Butterfield, John M Hayes, Matthew O Schrenk, Eric J Olson, Giora Proskurowski, Mike Jakuba, Al Bradley, Ben Lar-

- son, Kristin Ludwig, Deborah Glickson, Kate Buckman, Alexander S. Bradley, William J. Brazelton, Mitch J. Elend, Kevin Roe, Adélie Delacour, Stefano M. Bernasconi, Marvin D. Lilley, John A. Baross, Roger E. Summons, and Sean P. Sylva (2005), “A serpentinite-hosted ecosystem: the lost city hydrothermal field,” *Science* **307** (5714), 1428–1434.
- Kennett, James P, and Benjamin N Fackler-Adams (2000), “Relationship of clathrate instability to sediment deformation in the upper neogene of california,” *Geology* **28** (3), 215–218.
- Kenngott, JGA (1851), “Über die Achatmandeln in den Melaphyren, namentlich über die von Theiss in Tirol,” *Naturwiss. Abh. gesammelt und durch Subscription herausgeg. von W. Haidinger* **4**, 71–104.
- Khaldoun, A, E Eiser, G H Wegdam, and Daniel Bonn (2005), “Liquefaction of quicksand under stress,” *Nature* **437** (7059), 635–635.
- Khan, Asif, Zafar Abas, Heung Soo Kim, and Il-Kwon Oh (2016), “Piezoelectric thin films: an integrated review of transducers and energy harvesting,” *Smart Materials and Structures* **25** (5), 053002.
- Kharaka, Yousif K, and Frederick A P Berry (1973), “Simultaneous flow of water and solutes through geological membranes—i. experimental investigation,” *Geochimica et Cosmochimica Acta* **37** (12), 2577–2603.
- Kile, Daniel E (2002), “Occurrence and genesis of thunder eggs containing plume and moss agate: from the del norte area, saguache county, colorado,” *Rocks & Minerals* **77** (4), 252–268.
- Kim, Daeik, Hsuan-Ting Lai, George V Chilingar, and Teh Fu Yen (2006), “Geopolymer formation and its unique properties,” *Environmental geology* **51**, 103–111.
- Kirkpatrick, JD, CD Rowe, JC White, and EE Brodsky (2013), “Silica gel formation during fault slip: Evidence from the rock record,” *Geology* **41** (9), 1015–1018.
- Klose, Martina, Thomas E. Gill, abnd Vicken Etyemezian, George Nikolich, Zahra Ghodsi Zadeh, Nicholas P. Webb, and R. Scott Van Pelt (2019), “Dust emission from crusted surfaces: Insights from field measurements and modelling,” *Aeolian Res.* **40**, 1–14.
- Knauth, L Paul (1994), “Chapter 7. Petrogenesis of Chert,” in *Silica. Physical Behavior, Geochemistry, and Materials Applications*, edited by Peter J. Heaney, Charles T. Pre-witt, and Gerald V. Gibbs (De Gruyter, Berlin, Boston) pp. 233–258.
- Koehn, Daniel, Margaret P Rood, Nicolas Beaudoin, Peter Chung, Paul D Bons, and Enrique Gomez-Rivas (2016), “A new stylolite classification scheme to estimate compaction and local permeability variations,” *Sedimentary Geology* **346**, 60–71.
- Koeshidayatullah, Ardiansyah, Hilary Corlett, Jack Stacey, Peter K Swart, Adrian Boyce, and Cathy Hollis (2020), “Origin and evolution of fault-controlled hydrothermal dolomitization fronts: A new insight,” *Earth and Planetary Science Letters* **541**, 116291.
- Kok, Jasper F, Trude Storelvmo, Vlassis A. Karydis, Adeyemi A. Adebisi, Natalie M. Mahowald, Amato T. Evan, Cenlin He, and Danny M. Leung (2023), “Mineral dust aerosol impacts on global climate and climate change,” *Nature Reviews Earth and Environment* **4**, 71–86.
- Kondratiuk, Paweł, Hanna Tredak, Virat Upadhyay, Anthony J. C. Ladd, and Piotr Szymczak (2017), “Instabilities and finger formation in replacement fronts driven by an oversaturated solution,” *J. Geophys. Res. Solid* **122**, 5972—5991.
- Kopf, Achim J (2002), “Significance of mud volcanism,” *Reviews of geophysics* **40** (2), 2–1.
- Korzhinskii, D S (1968), “The theory of metasomatic zoning,” *Miner. Deposita* **231**, 222–231.
- Kotopoulou, Electra (2020), *Mineral self-organization in extreme geochemical environments: implications for prebiotic chemistry and life detection*, Ph.D. thesis (Universidad de Granada).
- Kotopoulou, Electra, Antonio Delgado Huertas, Juan Manuel Garcia-Ruiz, Jose M Dominguez-Vera, Jose Maria Lopez-Garcia, Isabel Guerra-Tschuschke, and Fernando Rull (2019), “A polyextreme hydrothermal system controlled by iron: the case of dallol at the afar triangle,” *ACS Earth Space Chemistry* **3** (1), 90–99.
- Kotopoulou, Electra, Miguel Lopez-Haro, Jose Juan Calvino Gamez, and Juan Manuel García-Ruiz (2021), “Nanoscale anatomy of iron-silica self-organized membranes: implications for prebiotic chemistry,” *Angewandte Chemie International Edition* **60** (3), 1396–1402.
- Krinsley, D (1970), “A geomorphological and paleoclimatological study of the playas of Iran. Part 1,” *U.S. Geol. Survey CP* **70-800**.
- Krug, H J, H. Brandstädter, and K. H. Jacob (1996), “Morphological instabilities in pattern formation by precipitation and crystallization processes,” *Geologische Rundschau* **85**, 19–28.
- Krug, Hans-Jürgen, and Hermann Brandtstädter (1999), “Morphological Characteristics of Liesegang Rings and Their Simulations,” *The Journal of Physical Chemistry A* **103** (39), 7811–7820, publisher: American Chemical Society.
- Kucha, H, E. Schroll, J. Raith, and S. Hałas (2010), “Microbial sphalerite formation in carbonate-hosted zn-pb ores, bleiberg, austria: Micro- to nanotextural and sulfur isotope evidence,” *Economic Geology* **105**, 1005–1023.
- Kull, Hans-Jörg (1991), “Theory of the rayleigh-taylor instability,” *Physics reports* **206** (5), 197–325.
- Lachenbruch, Arthur H (1962), *Mechanics of thermal contraction cracks and ice-wedge polygons in permafrost*, Vol. 70 (Geological Society of America).
- Ladan, John, and Stephen W. Morris (2021), “Experiments on the dynamic wetting of growing icicles,” *New Journal of Physics* **23** (12), 123017.
- Ladan, John, and Stephen W. Morris (2022), “Pattern of inclusions inside rippled icicles,” *Phys. Rev. E* **106**, 054211.
- Lahti, Seppo I, Paula Raivio, and Ilkka Laitakari (2005), *Orbicular rocks in Finland* (Geological Survey of Finland).
- Lamur, Anthony, Yan Lavallée, Fiona E. Iddon, Adrian J. Hornby, Jackie E. Kendrick, Felix W. von Aulock, and Fabian B. Wadsworth (2018), “Disclosing the temperature of columnar jointing in lavas,” *Nat. Commun.* **9**, 1432.
- Landmesser, Michael (1984), “Das problem der achatgenese,” *Mitt. Pollichia* **72**, 5–137.
- Langer, JS (1989), “Dendrites, viscous fingers, and the theory of pattern formation,” *Science* **243** (4895), 1150–1156.
- Larcombe, C O G (1925), “Rock specimens from Ord River and Oakover River respectively,” *Annual Progress Report of the Geological Survey of Western Australia* , 122.
- Larcombe, C O G (1927), “Some rocks from four miles east of Argyle Station, Ord River, King district, Kimberley division,” *Annual Progress Report of the Geological Survey of Western Australia* , 139–140.
- Lasser, J, M. Ernst, and L. Goehring (2021), “Stability and

- dynamics of convection in dry salt lakes,” *J. Fluid Mech.* **917**, A14.
- Lasser, J, J. M. Nield, M. Ernst, V. Karius, G. F. S. Wiggs, M. R. Threadgold, C. Beaume, and L. Goehring (2023), “Salt Polygons and Porous Media Convection,” *Phys. Rev. X* **13**, 011025.
- Lasser, J, J. M. Nield, and L. Goehring (2020), “Surface and subsurface characterisation of salt pans expressing polygonal patterns,” *Earth Syst. Sci. Data* **12** (4), 2881–2898.
- Laubach, Stephen E, RH Lander, Louise J Criscenti, Lawrence M Anovitz, JL Urai, Ryan M Pollyea, John N Hooker, Wayne Narr, Mark A Evans, Sebastien N Kerisit, J. E. Olson, T. Dewers, D. Fisher, R. Bodnar, B. Evans, P. Dove, L. M. Bonnell, M. P. Marder, and L. Pyrak-Nolte (2019), “The role of chemistry in fracture pattern development and opportunities to advance interpretations of geological materials,” *Reviews of Geophysics* **57** (3), 1065–1111.
- Lauritzen, S E, and R. Ø. Skoglund (2013), “Glacier ice-contact speleogenesis in marble stripe karst,” in *Proceedings of the 16th International Congress of Speleology, July 21–28, Brno*, Vol. 3 (Academic Press San Diego) pp. 363–396.
- Lester, Daniel R, Marco Dentz, and Tanguy Le Borgne (2016a), “Chaotic mixing in three-dimensional porous media,” *Journal of Fluid Mechanics* **803**, 144–174.
- Lester, Daniel R, Alison Ord, and Bruce E Hobbs (2012), “The mechanics of hydrothermal systems: Ii. fluid mixing and chemical reactions,” *Ore geology reviews* **49**, 45–71.
- Lester, DR, MG Trefry, and Guy Metcalfe (2016b), “Chaotic advection at the pore scale: Mechanisms, upscaling and implications for macroscopic transport,” *Advances in water resources* **97**, 175–192.
- Leveson, David J (1966), “Orbicular rocks: a review,” *Geological Society of America Bulletin* **77** (4), 409–426.
- L’Heureux, Ivan (2000), “Origin of banded patterns in natural sphalerite,” *Physical Review E* **62**, 3234–3245.
- Li, Dongyan, Jun Yang, Wenxiang Tang, Xiaofeng Wu, Lianqi Wei, and Yunfa Chen (2014), “Controlled synthesis of hierarchical mno 2 microspheres with hollow interiors for the removal of benzene,” *RSC Advances* **4** (51), 26796–26803.
- Liesegang, M, and R. Milke (2014), “Australian sedimentary opal-a and its associated minerals: Implications for natural silica sphere formation,” *American Mineralogist* **99** (7), 1488–1499.
- Liesegang, Raphael E (1896), “Über einige eigenschaften von gallerten,” *Naturwissenschaft Wochenschr* **11**, 353–362.
- Liesegang, RE (1910), “Die entstehung der achate,” *Zentralblatt für Mineralogie* **11**, 593–597.
- Liesegang, RE (1914), *Die Achate* (Springer).
- Lifshitz, I M, and V. V. Slyozov (1961a), “The kinetics of precipitation from supersaturated solid solutions,” *Journal of Physics and Chemistry of Solids* **19** (1), 35–50.
- Lifshitz, Ilya M, and Vitaly V Slyozov (1961b), “The kinetics of precipitation from supersaturated solid solutions,” *Journal of physics and chemistry of solids* **19** (1-2), 35–50.
- Ling, Florence T, Heather A. Hunter, Jeffrey P. Fitts, Catherine A. Peters, Alvin S. Acerbo, Xiaojing Huang, Hanfei Yan, Evgeny Nazaretski, and Yong S. Chu (2018), “Nanospectroscopy captures nanoscale compositional zonation in barite solid solutions,” *Scientific Reports* **8** (1), 13041.
- Lipar, Matej, Piotr Szymczak, Susan Q White, and John A Webb (2021), “Solution pipes and focused vertical water flow: Geomorphology and modelling,” *Earth-Science Reviews* **218**, 103635.
- Lipar, Matej, John A Webb, Susan Q White, and Ken G Grimes (2015), “The genesis of solution pipes: Evidence from the Middle–Late Pleistocene Bridgewater Formation calcarenite, southeastern Australia,” *Geomorphology* **246**, 90–103.
- Liu, Chong, Victor M. Calo, Klaus Regenauer-Lieb, and Manman Hu (2023a), “Coefficients of Reaction-Diffusion Processes Derived From Patterns in Rocks,” *Journal of Geophysical Research: Solid Earth* **128** (5), e2022JB026253.
- Liu, Xiaocheng, Chenming Zhang, Yue Liu, Congrui Li, Chengji Shen, Pei Xin, Ling Li, and David A. Lockington (2023b), “Processes controlling formation of salt efflorescence in coastal salt flats,” *Water Resources Research* **59** (12), e2022WR034279, e2022WR034279 2022WR034279.
- Long, Philip E, and Bernard J. Wood (1986), “Structures, textures and cooling histories of Columbia River basalt flows,” *Geol. Soc. Am. Bull.* **97**, 1144–1155.
- Lore, J, A. Aydin, and K. Goodson (2001), “A deterministic methodology for prediction of fracture distribution in basaltic multiflows,” *J. Geophys. Res.* **106**, 6447–6459.
- Loughnan, F C, and F. I. Roberts (1990), “Composition and origin of the ‘zebra rock’ from the East Kimberley region of Western Australia,” *Australian Journal of Earth Sciences* **37** (2), 201–205.
- Løvoll, Grunde, Yves Méheust, Renaud Toussaint, Jean Schmittbuhl, and Knut Jørgen Måløy (2004), “Growth activity during fingering in a porous hele-shaw cell,” *Phys. Rev. E* **70**, 026301.
- Lowenstein, T K, and L. A. Hardie (1985), “Criteria for the recognition of salt-pan evaporites,” *Sedimentology* **32** (5), 627–644.
- Lugli, Stefano, José Torres-Ruiz, Giorgio Garuti, and Fernando Olmedo (2000), “Petrography and Geochemistry of the Eugui Magnesite Deposit (Western Pyrenees, Spain): Evidence for the Development of a Peculiar Zebra Banding by Dolomite Replacement,” *Economic Geology* **95** (8), 1775–1791.
- Lundberg, J, and B. E. Taggart (1995), “Dissolution pipes in northern Puerto Rico: An exhumed paleokarst,” *Carbonates Evaporites* **10** (2), 171–183.
- Lyell, Charles (1839), “On the tubular cavities filled with gravel and sand called “Sand-pipes,” in the chalk near Norwich,” *Phil. Mag.* **15** (96), 257–266.
- L’Heureux, Ivan, and Anthony D Fowler (1999), “Branching and oscillatory patterns in plagioclase and mississippi-valley type sphalerite deposits,” in *Growth, Dissolution and Pattern Formation in Geosystems* (Springer) pp. 85–108.
- Ma, Chi, Jennifer Gresh, George R Rossman, Gene C Ulmer, and Edward P Vicenzi (2001), “Micro-analytical study of the optical properties of rainbow and sheen obsidians,” *The Canadian Mineralogist* **39** (1), 57–71.
- Macalady, Jennifer L, Daniel S. Jones, and Ezra H. Lyon (2007), “Extremely acidic, pendulous cave wall biofilms from the frasassi cave system, italy,” *Environmental Microbiology* **9** (6), 1402–1414.
- Maheshwari, P, and V. Balakotaiah (2013), “Comparison of carbonate HCl acidizing experiments with 3D simulations,” *SPE Prod. Oper.* **28**, 402–413.
- Maheshwari, P, R. R. Ratnakar, N. Kalia, and V. Balakotaiah (2013), “3-d simulation and analysis of reactive dissolution and wormhole formation in carbonate rocks,” *Chem. Eng.*

- Sci. **90**, 258–274.
- Makkonen, Lasse (1988), “A Model of Icicle Growth,” *Journal of Glaciology* **34** (116), 64–70.
- Mallet, Robert (1875), “On the origin and mechanism of production of the prismatic (or columnar) structure of basalt,” *Phil. Mag.* **50**, 122–135 and 201–226.
- Marshall, Jim D, and Duncan Pirrie (2013), “Carbonate concretions—explained,” *Geology today* **29** (2), 53–62.
- Martin, William, and Michael J. Russell (2007), “On the origin of biochemistry at an alkaline hydrothermal vent,” *Philosophical transactions of the Royal Society of London. Series B, Biological sciences* **362**, 1887–1925.
- Martín-Ramos, Pablo, Francisco PSC Gil, Francisco J Martín-Gil, and Jesús Martín-Gil (2019), “Characterization of exogenic fulgurites from an archaeological site in Tiedra, Valladolid, Spain,” *Geological Magazine* **156** (8), 1455–1462.
- Matalon, R, and A Packter (1955), “The liesegang phenomenon. i. sol protection and diffusion,” *Journal of colloid science* **10** (1), 46–62.
- Mathiesen, Joachim, Itamar Procaccia, Harry L Swinney, and Matthew Thrasher (2006), “The universality class of diffusion-limited aggregation and viscous fingering,” *Europhysics Letters* **76** (2), 257.
- Matthes, Gerard H (1953), “Quicksand,” *Scientific American* **188** (6), 97–104.
- Mattievich, Enrico, J Chadwick, John D Cashion, John Frank Boas, MJ Clark, and RD Mackie (2003), “Macroscopic ferro-nematic liquid crystals determine the structure of kimberley zebra rock,” in *27th ann. cond. matt. phys. meet. conf. handb.*
- McBride, Antar Abdel-Wahab, and Ahmed Reda M El-Younsy (1999), “Origin of spheroidal chert nodules, drunks formation (lower eocene), egypt,” *Sedimentology* **46** (4), 733–755.
- McBride, Earle F, and M Dane Picard (2004), “Origin of honeycombs and related weathering forms in oligocene macigno sandstone, tuscan coast near livorno, italy,” *Earth Surface Processes and Landforms* **29** (6), 713–735.
- McDuff, D R, C. E. Shuchart, S. K. Jackson, D. Postl, and J. S. Brown (2010), “Understanding wormholes in carbonates: Unprecedented experimental scale and 3-D visualization,” *J. Petrol. Technol.* **62**, 78–81.
- McGlynn, Shawn E, Isik Kanik, and Michael J Russell (2012), “Peptide and rna contributions to iron–sulphur chemical gardens as life’s first inorganic compartments, catalysts, capacitors and condensers,” *Philosophical Transactions of the Royal Society A: Mathematical, Physical and Engineering Sciences* **370** (1669), 3007–3022.
- Meakin, Paul (1983), “Diffusion-controlled flocculation: The effects of attractive and repulsive interactions,” *Journal of Chemical Physics* **79**, 2426–2429.
- Meakin, Paul (1998), *Fractals, Scaling and Growth Far from Equilibrium* (Cambridge University Press, Cambridge, UK).
- Meakin, Paul, and Bjørn Jamtveit (2010), “Geological pattern formation by growth and dissolution in aqueous systems,” *Proceedings of the Royal Society A: Mathematical, Physical and Engineering Sciences* **466** (2115), 659–694.
- Mendes da Costa, E (1757), *A Natural History of Fossils* (L. Davis and C. Reymers).
- Merino, E, and A. Banerjee (2008), “Terra Rossa genesis, implications for Karst, and Eolian dust: A geodynamic thread,” *J. Geol.* **116**, 62–75.
- Merino, E, A. Canals, and R. C. Fletcher (2006), “Genesis of self-organized zebra textures in burial dolomites: Displacive veins, induced stress, and dolomitization,” *Geologica Acta* **4**, 383–394.
- Merino, Enrique (1992), “Self-organization in stylolites,” *American Scientist* **80** (5), 466–473.
- Merino, Enrique, and Àngels Canals i Sabaté (2011), “Self-accelerating dolomite-for-calcite replacement: Self-organized dynamics of burial dolomitization and associated mineralization,” *American Journal of Science*, 2011, vol. 311, p. 573–607.
- Meron, Ehud (1992), “Pattern formation in excitable media,” *Physics reports* **218** (1), 1–66.
- Metcalfe, Guy, Daniel Lester, Alison Ord, Pandurang Kulkarni, Mike Trefry, Bruce E Hobbs, Klaus Regenauer-Lieb, and Jeffery Morris (2010), “A partially open porous media flow with chaotic advection: towards a model of coupled fields,” *Philosophical Transactions of the Royal Society A: Mathematical, Physical and Engineering Sciences* **368** (1910), 217–230.
- Meyer, D, and M. Brückner-Foit (2000), “Crack interaction modelling,” *Fatigue & Fracture of Engineering Materials & Structures* **23** (4), 315–323.
- Michele, J, R. Pätzold, and R. Donis (1977), “Alignment and aggregation effects in suspensions of spheres in non-Newtonian media,” *Rheol. Acta* **16**, 317–321.
- Michot, Laurent J, Isabelle Bihannic, Solange Maddi, Sérgio S Funari, Christophe Baravian, Pierre Levitz, and Patrick Davidson (2006), “Liquid–crystalline aqueous clay suspensions,” *Proceedings of the National Academy of Sciences* **103** (44), 16101–16104.
- Migaszewski, Zdzisław M, Agnieszka Gałuszka, Tomasz Durkiewicz, and Ewa Starnawska (2006), “Middle Oxfordian–Lower Kimmeridgian chert nodules in the Holy Cross Mountains, south-central Poland,” *Sedimentary Geology* **187** (1–2), 11–28.
- Migaszewski, Zdzisław M, Agnieszka Gałuszka, and Andrzej Migaszewski (2022), “Geochemistry and petrology of striped chert as a provenance tool for artefacts from the krzemionki neolithic mining area (poland),” *Archaeometry* **64** (5), 1093–1109.
- Milazzo, MP, L.P. Keszthelyi, W.L. Jaeger, M. Rosiek, S. Mattson, C. Verba, R.A. Beyer, P.E. Geissler, A.S. McEwen, and the HiRISE Team (2009), “Discovery of columnar jointing on Mars,” *Geology* **37** (2), 171–174.
- Milazzo, MP, D. K. Weiss, B. Jackson, and J. Barne (2012), “Columnar jointing on Mars: Earth analog studies,” *43rd Lunar Planet. Sci. Conf.*, 2726.
- Mineev-Weinstein, M, P. B. Wiegmann, and A. Zabrodin (2000), “Theory of diffusion-limited aggregation,” *Physical Review Letters* **84** (24), 5106–5109.
- Mineev-Weinstein, Mark, Mihai Putinar, and Razvan Teodorescu (2008), “Random matrices in 2d, laplacian growth and operator theory,” *Journal of Physics A: Mathematical and Theoretical* **41** (26), 263001.
- Mitchell, A R, T. R. Ellsworth, and B. D. Meek (1995), “Effect of root systems on preferential flow in swelling soil,” *Commun. Soil Sci. Plan.* **26** (15–16), 2655–2666, cited By :63 Export Date: 18 July 2018.
- Mizuguchi, Tsuyoshi, Akihiro Nishimoto, So Kitsunozaki, Yoshihiro Yamazaki, and Ichio Aoki (2005), “Directional crack propagation of granular water systems,” *Phys. Rev. E* **71**, 056122.
- Molina Grande, M A, and J. Molina García (1980), “Ídolos naturales de piedra en el bronce del Sureste Peninsular,”

- Murgetana **59**, 5–36.
- Monecke, Thomas, T James Reynolds, Tadsuda Taksavasu, Erik R Tharalson, Lauren R Zeeck, Mario Guzman, Garrett Gissler, and Ross Sherlock (2023), “Natural growth of gold dendrites within silica gels,” *Geology*.
- Monnin, C, V Chavagnac, C Boulart, B Ménez, Martine Gérard, E Gérard, C Pisapia, Marianne Quemeneur, Gaël Erauso, Anne Postec, L. Guentas-Dombrowski, C Payri, and B. Pelletier (2014), “Fluid chemistry of the low temperature hyperalkaline hydrothermal system of prony bay (new caledonia),” *Biogeosciences* **11** (20), 5687–5706.
- Montenat, Christian, Pascal Barrier, Philippe Ott d’Estevou, and Christian Hibschi (2007), “Seismites: An attempt at critical analysis and classification,” *Sedimentary Geology Deformation of soft sediments in nature and laboratory*, **196** (1), 5–30.
- Moore, James G (2019), “Mini-columns and ghost columns in columbia river lava,” *Journal of Volcanology and Geothermal Research* **374**, 242–251.
- Morawiecka, I, and P. Walsh (1997), “A study of solution pipes preserved in the miocene limestones (staszow, poland),” *Acta Carsologica* **20**, 337–350.
- Moretti, M, and A. Ronchi (2011), “Liquefaction features interpreted as seismites in the Pleistocene fluvio-lacustrine deposits of the Neuquén Basin (Northern Patagonia),” *Sedimentary Geology Recognising triggers for soft-sediment deformation: Current understanding and future directions*, **235** (3), 200–209.
- Morgado, Ana M O, Luis A M Rocha, Julyan H E Cartwright, and Silvana S S Cardoso (2024), “Osmosis drives explosions and methane release in siberian permafrost,” *Geophysical Research Letters* **51** (18), e2024GL108987.
- Morris, F K (1930), “Amygdules and pseudo-amygdules,” *Bulletin of the Geological Society of America* **41** (3), 383–404.
- Morrow, David W (2014), “Zebra and boxwork fabrics in hydrothermal dolomites of northern Canada: Indicators for dilational fracturing, dissolution or in situ replacement?” *Sedimentology* **61** (4), 915–951.
- Morse, John W, and William H Casey (1988), “Ostwald processes and mineral paragenesis in sediments,” *American Journal of Science* **288** (6), 537–560.
- Moxon, T, and G. Palyanova (2020), “Agate genesis: A continuing enigma,” *Minerals* **10** (11), 953.
- Muller, G (1998), “Experimental simulation of basalt columns,” *J. Volcanology and Geothermal Res.* **86**, 93–96.
- Müller, G, and T. Dahm (2000), “Fracture morphology of tensile cracks and rupture velocity,” *J. Geophys. Res.* **105** (B1), 723–738.
- Murray, James D (1989), *Mathematical Biology: I. An Introduction* (Springer).
- Mustoe, George E (1982), “The origin of honeycomb weathering,” *Geological Society of America Bulletin* **93** (2), 108–115.
- Mylius, G F (1709), *Memorabilium Saxoniae Subterraneae* (F. Groschuff).
- Nabika, Hideki, Masaki Itatani, and István Lagzi (2019), “Pattern formation in precipitation reactions: The liesegang phenomenon,” *Langmuir* **36** (2), 481–497.
- Nacken, R (1948), “Über die nachbildung von chalcedonmandeln,” *Natur Folk* **78**, 2–8.
- Neelamma, MK, Sowmya R Holla, M Selvakumar, P Akhil Chandran, and Shounak De (2022), “Bentonite clay liquid crystals for high-performance supercapacitors,” *Journal of Electronic Materials* **51** (5), 2192–2202.
- Neuzil, C E (2000a), “Osmotic generation of ‘anomalous’ fluid pressures in geological environments,” *Nature* **403** (6766), 182–184.
- Neuzil, CE (2000b), “Osmotic generation of ‘anomalous’ fluid pressures in geological environments,” *Nature* **403** (6766), 182–184.
- Nield, Donald A, and Adrian Bejan (2017), *Convection in Porous Media*, 7th ed. (Springer Cham).
- Nield, J M, R. G. Bryant, G. F.S. Wiggs, J. King, D. S.G. Thomas, F. D. Eckardt, and R. Washington (2015), “The dynamism of salt crust patterns on playas,” *Geology* **43** (1), 31–34.
- Niu, Zihao, Zhende Zhu, Xiangcheng Que, Yanxin He, and Xinghua Xie (2023), “Hydromechanical behaviour of columnar jointed rock masses under true triaxial conditions: An experimental and theoretical investigation,” *Geoenergy Sci. Eng.* **224**, 211623.
- Noeggerath, J (1849), “Sendschreiben an den k.k. wirklichen Bergrath und Prof., Herrn W. Haidinger in Wien, über die Achat Mandeln in den Melaphyren,” *Verh. naturhist. Vereins preuss. Rheinlande u. Westphalens*, 243–260.
- Norris, D J, E. G. Arlinghaus, L. Meng, R. Heiny, and L. E. Scriven (2004), “Opaline photonic crystals: How does self-assembly work?” *Advanced Materials* **16** (16), 1393–1399.
- Nova, Nicolas, Nicolas Maigret, and Maria Roszkowska (2021), *The Bestiary of the Anthropocene* (Onomatopée).
- Oberst, Sebastian, Robert K Niven, Daniel R Lester, Alison Ord, Bruce Hobbs, and Norbert Hoffmann (2018), “Detection of unstable periodic orbits in mineralising geological systems,” *Chaos: An Interdisciplinary Journal of Nonlinear Science* **28** (8).
- Oehler, John H (1976), “Hydrothermal crystallization of silica gel,” *Geological Society of America Bulletin* **87** (8), 1143–1152.
- Oehler, John H, and J William Schopf (1971), “Artificial microfossils: experimental studies of permineralization of blue-green algae in silica,” *Science* **174** (4015), 1229–1231.
- Oen, I S, P. Kager, and C. Kieft (1980), “Oscillatory zoning of a discontinuous solid-solution series: sphalerite-stannite,” *American Mineralogist* **65**, 1220–1232.
- Ogawa, Naohisa, and Yoshinori Furukawa (2002), “Surface Instability of Icicles,” *Physical Review E* **66** (4), 041202.
- Ord, W M (1879), *On the Influence of Colloids upon Crystalline Form and Cohesion* (E. Stanford, London).
- Ortoleva, P (1984), “From nonlinear waves to spiral and speckle patterns:: Nonequilibrium phenomena in geological and biological systems,” *Physica D: Nonlinear Phenomena* **12** (1-3), 305–320.
- Ortoleva, P, J. Chadam, E. Merino, and A. Sen (1987a), “Geochemical self-organization II: The reactive-infiltration instability,” *Am. J. Sci.* **287**, 1008–1040.
- Ortoleva, P, E. Merino, Craig Moore, and John Chadam (1987b), “Geochemical self-organization i; reaction-transport feedbacks and modeling approach,” *American Journal of science* **287** (10), 979–1007.
- Ortoleva, P J (1994), *Geochemical Self-Organization* (Oxford University Press, New York).
- Osselin, F, A. Budek, O. Cybulski, P. Kondratiuk, P. Garstecki, and P. Szymczak (2016), “Microfluidic observation of the onset of reactive infiltration instability in an analog fracture,” *Geophys. Res. Lett.* **43**, 6907–6915.
- Ostwald, Wilhelm (1897), “Besprechung der arbeit von liesegangs „a-linien“,” *Z. Phys. Chem.* **22**, 289–330.
- Pabian, Roger K, and Andrejs Zarins (1994), *Banded Agates*,

- Origins and Inclusions* (University of Nebraska-Lincoln).
- Pal, Rajinder (2003), "Rheological behavior of bubble-bearing magmas," *Earth and Planetary Science Letters* **207** (1-4), 165–179.
- Papineau, D (2020), "Chemically oscillating reactions in the formation of botryoidal malachite," *Am. Mineral.* **105** (4), 447–454.
- Papp, P, B. Bohner, Ágota Tóth, and D. Horváth (2020), "Fine tuning of pattern selection in the cadmium-hydroxide-system," *The Journal of Chemical Physics* **152** (9), 094906.
- Park, Charles Frederick (1938), "Dolomite and jasperoid in the Metaline District, northeastern Washington," *Economic Geology* **33**, 709–729.
- Park, Won C, and Erik H Schot (1968), "Stylolites; their nature and origin," *Journal of Sedimentary Research* **38** (1), 175–191.
- Pasek, M A, Kristin Block, and Virginia Pasek (2012), "Fulgurite morphology: a classification scheme and clues to formation," *Contributions to Mineralogy and Petrology* **164** (3), 477–492.
- Pasek, Matthew A, and Virginia D. Pasek (2018), "The forensics of fulgurite formation," *Mineralogy and Petrology* **112** (2), 185–198.
- Paschier, Cees W, John S Myers, and Alfred Kröner (2012), *Field geology of high-grade gneiss terrains* (Springer Science & Business Media).
- Peck, Dallas L, and Takeshi Minakami (1968), "The formation of columnar joints in the upper part of Kilauean lava lakes, Hawaii," *Geol. Soc. Am. Bull.* **79**, 1151–1168.
- Pelletier, Jon D (2004), "How do spiral troughs form on mars?" *Geology* **32** (4), 365–367.
- Perugini, Diego, Maurizio Petrelli, and Giampiero Poli (2008), "A virtual voyage through 3d structures generated by chaotic mixing of magmas and numerical simulations: a new approach for understanding spatial and temporal complexity of magma dynamics," *Visual Geosciences* **13** (1), 1–24.
- Perugini, Diego, Giampiero Poli, and Roberto Mazzuoli (2003), "Chaotic advection, fractals and diffusion during mixing of magmas: evidence from lava flows," *Journal of Volcanology and Geothermal Research* **124** (3-4), 255–279.
- Petrelli, Maurizio, Kamal El Omari, Yves Le Guer, and Diego Perugini (2016), "Effects of chaotic advection on the timescales of cooling and crystallization of magma bodies at mid crustal levels," *Geochemistry, Geophysics, Geosystems* **17** (2), 425–441.
- Petrov, TG, E.N. Protopopov, and A.V. Shuyskiy (2013), "Decorative grown malachite. nature and technology," *Russ. J. Earth Sci.* **13**, ES2001.
- Petrus, K, and P. Szymczak (2016), "Influence of Layering on the Formation and Growth of Solution Pipes," *Front. Phys.* **3**, 92.
- Petty, Julian J (1936), "The origin and occurrence of fulgurites in the Atlantic Coastal Plain," *American Journal of Science* **s5-31** (183), 188–201.
- Phemister, James (1934), "Zoning in plagioclase feldspar," *Mineralogical magazine and journal of the Mineralogical Society* **23** (145), 541–555.
- Phillips, J C, M. C. S. Humphreys, K. A. Daniels, R. J. Brown, and F. Witham (2013), "The formation of columnar joints produced by cooling in basalt at Staffa, Scotland," *Bull. Volcanol.* **75**, 715.
- Philpotts, John, and John R Evans (1991), "Rare earth minerals in "thunder eggs" from zarembo island, southeast alaska," *US Geological Survey Bulletin* **2041**, 98.
- Pimentel, Carlos, Carlos Gutiérrez-Ariza, Antonio G. Checa, C. Ignacio Sainz-Díaz, and Julyan H. E. Cartwright (2024), "Mineralogical description and hypothesis on the formation of menilites from Galera, Granada (Spain)," *Physics and Chemistry of Minerals* **51** (1), 7.
- Pishvar, Maya, and Ryan L Harne (2020), "Foundations for soft, smart matter by active mechanical metamaterials," *Advanced science* **7** (18), 2001384.
- Pitman, Michael G, and André Läuchli (2002), "Global impact of salinity and agricultural ecosystems," *Salinity: environment-plants-molecules* **3**, 20.
- Pliny the Elder, (77), "Naturalis Historia."
- Plummer, P S, and V A Gostin (1981), "Shrinkage cracks; desiccation or synaeresis?" *Journal of Sedimentary Research* **51** (4), 1147–1156.
- Pollard, DD, and A. Aydin (1988), "Progress in understanding jointing over the past century," *Geol. Soc. Am. Bull.* **100**, 1181–1204.
- Potter, Russel M, and George R Rossman (1979), "Mineralogy of manganese dendrites and coatings," *American mineralogist* **64** (11-12), 1219–1226.
- Prager, S (1956), "Periodic precipitation," *J. Chem. Phys.* **25** (2), 279–283.
- Prestwich, Joseph (1855), "On the origin of the sand-and gravel-pipes in the chalk of the london tertiary district," *Quarterly Journal of the Geological Society* **11** (1-2), 64–84.
- Prieto, M, A. Fernández-González, A. Putnis, and L. Fernández-Díaz (1997), "Nucleation, growth, and zoning phenomena in crystallizing (ba,sr)CO₃, (ba, sr)SO₄, and (cd,ca)CO₃ solid solutions from aqueous solutions," *Geochimica et Cosmochimica Acta* **61** (16), 3383–3397.
- Prospero, Joseph M (2002), "Environmental characterization of global sources of atmospheric soil dust identified with the NIMBUS 7 Total Ozone Mapping Spectrometer (TOMS) absorbing aerosol product," *Rev. Geophys.* **40** (1).
- Putnis, A (2009), "Mineral Replacement Reactions," *Rev. Mineral. Geochem.* **70** (1), 87–124.
- Qazi, M J, H. Salim, C. A. W. Doorman, E. Jambon-Puillet, and N. Shahidzadeh (2019a), "Salt creeping as a self-amplifying crystallization process," *Science Advances* **5** (12), eaax1853.
- Qazi, Mohsin J, Daniel Bonn, and Noushine Shahidzadeh (2019b), "Drying of salt solutions from porous media: Effect of surfactants," *Transport in Porous Media* **128**, 881–894.
- Que, Xiangcheng, Zhende Zhu, Yanxin He, Zihao Niu, and Haonan Huang (2023), "Strength and deformation characteristics of irregular columnar jointed rock mass: A combined experimental and theoretical study," *J. Rock Mech. Geotech. Eng.* **15** (2), 429–441.
- Raiswell, R, and QJ Fisher (2000), "Mudrock-hosted carbonate concretions: a review of growth mechanisms and their influence on chemical and isotopic composition," *Journal of the Geological Society* **157** (1), 239–251.
- Rakovan, John (2017), "Word to the wise: Geode (and friends)," *Rocks & Minerals* **92** (1), 85–91.
- Reeder, Richard J, Richard O. Fagioli, and William J. Meyers (1990), "Oscillatory zoning of Mn in solution-grown calcite crystals," *Earth-Science Reviews* **29** (1), 39–46.
- Retallack, GJ (2021), "Zebra rock and other ediacaran pale-

- osols from western australia,” *Australian Journal of Earth Sciences* **68** (4), 532–556.
- Reusch, E (1864), “Über den Agat,” *Ann. Phys. Chem.* **123**, 94–114.
- Rocha, Luis A M, Carlos Gutiérrez-Ariza, Carlos Pimentel, Isabel Sánchez-Almazo, C Ignacio Sainz-Díaz, Silvana S S Cardoso, and Julyan H E Cartwright (2021), “Formation and structures of horizontal submarine fluid conduit and venting systems associated with marine seeps,” *Geochemistry, Geophysics, Geosystems* **22** (11), e2021GC009724.
- Rodríguez-Navarro, Carlos, Eric Doehne, and Eduardo Sebastian (1999), “Origins of honeycomb weathering: The role of salts and wind,” *Geological Society of America Bulletin* **111** (8), 1250–1255.
- Rodríguez-Pascua, MA, JP Calvo, G De Vicente, and D Gómez-Gras (2000), “Soft-sediment deformation structures interpreted as seismites in lacustrine sediments of the Prebetic Zone, SE Spain, and their potential use as indicators of earthquake magnitudes during the Late Miocene,” *Sedimentary Geology* **135**, 117–135.
- Rolland, Alexandra, Renaud Toussaint, Patrick Baud, Jean Schmittbuhl, Nathalie Conil, Daniel Koehn, Francois Renard, and Jean-Pierre Gratier (2012), “Modeling the growth of stylolites in sedimentary rocks,” *Journal of Geophysical Research: Solid Earth* **117** (B6).
- Roots, Robert D (1952), “Thunder eggs,” *Rocks & Minerals* **27** (5-6), 234–236.
- Rothman, Daniel H (2019), “Characteristic disruptions of an excitable carbon cycle,” *Proceedings of the National Academy of Sciences* **116** (30), 14813–14822.
- Rouwet, Dmitri, and Marta Iorio (2017), “The sedimentation of suminagashi-like floating clay patterns at el chichón crater lake (chiapas, mexico),” *Geological Society, London, Special Publications* **437** (1), 153–161.
- Roy, A, R. A. I. Haque, A. J. Mitra, S. Tarafdar, and T. Dutta (2022), “Combinatorial topology and geometry of fracture networks,” *Phys. Rev. E* **105**, 034801.
- Rubin, Allan M (1993), “Dikes vs. diapirs in viscoelastic rock,” *Earth and Planetary Science Letters* **117** (3-4), 653–670.
- Runge, Friedlieb Ferdinand (1855), *Der Bildungstrieb der Stoffe : veranschaulicht in selbstständig gewachsenen Bildern (Fortsetzung der Musterbilder)* (Selbstverlag, Oranienburg).
- Russell, M J, and A. J. Hall (1997), “The emergence of life from iron monosulphide bubbles at a submarine hydrothermal redox and ph front,” *Journal of the Geological Society* **154**, 377–402.
- Russell, Michael J, Roy M Daniel, Allan J Hall, and John A Sherringham (1994), “A hydrothermally precipitated catalytic iron sulphide membrane as a first step toward life,” *Journal of Molecular Evolution* **39**, 231–243.
- Ryan, A J, and Philip R Christensen (2012), “Coils and polygonal crust in the athabasca valles region, mars, as evidence for a volcanic history,” *Science* **336** (6080), 449–452.
- Ryan, Michael P, and Charles G. Sammis (1978), “Cyclic fracture mechanisms in cooling basalt,” *Geol. Soc. Am. Bull.* **89**, 1295–1308.
- Ryan, Michael P, and Charles G. Sammis (1981), “The glass transition in basalt,” *J. Geophys. Res.* **86**, 9519–9535.
- Saffman, P G, and Geoffrey Taylor (1958), “The penetration of a fluid into a porous medium or ele-shaw cell containing a more viscous liquid,” *Proc. R. Soc. Lon. Ser-a.* **245** (1242), 312–329.
- Sainz-Díaz, C Ignacio, Elizabeth Escamilla-Roa, and Julyan H E Cartwright (2018), “Growth of self-assembling tubular structures of magnesium oxy/hydroxide and silicate related with seafloor hydrothermal systems driven by serpentinization,” *Geochemistry, Geophysics, Geosystems* **19** (8), 2813–2822.
- Sakaguchi, Hidetsugu, Kazuki Yamada, and Michiko Shimokawa (2022), “Observation and a simple model of plumose pattern on fracture surfaces of drying pastes,” *Europhys. Lett.* **138** (1), 16002.
- Sander, Sylvia G, and Andrea Koschinsky (2011), “Metal flux from hydrothermal vents increased by organic complexation,” *Nature Geoscience* 2011 4:3 **4**, 145–150.
- Saunders, James A (1994), “Silica and gold textures in bonanza ores of the sleeper deposit, humboldt county, nevada; evidence for colloids and implications for epithermal ore-forming processes,” *Economic Geology* **89** (3), 628–638.
- Saunders, James A (2022), “Colloids and nanoparticles: Implications for hydrothermal precious metal ore formation,” *SEG Discovery* (130), 15–21.
- Saunders, James A, and Michelle Burke (2017), “Formation and aggregation of gold (electrum) nanoparticles in epithermal ores,” *Minerals* **7** (9), 163.
- Saunders, James A, Michelle Burke, and Matthew E Brueseke (2020), “Scanning-electron-microscope imaging of gold (electrum) nanoparticles in middle miocene bonanza epithermal ores from northern nevada, usa,” *Mineralium Deposita* **55**, 389–398.
- Schalm, O, K Proost, K De Vis, S Cagno, K Janssens, F Mees, P Jacobs, and J Caen (2011), “Manganese staining of archaeological glass: the characterization of mn-rich inclusions in leached layers and a hypothesis of its formation,” *Archaeometry* **53** (1), 103–122.
- Schatz, Michael F, and G Paul Neitzel (2001), “Experiments on thermocapillary instabilities,” *Annual Review of Fluid Mechanics* **33**, 93–127.
- Scheuchzer, J J (1700), “Dissertatio epistolica acarnanis de dendritis aliisque lapidibus, qui in superficie sua plantarum, foliorum, florum figuras exprimunt,” *Miscellanea Curiosa Sive Ephemeridum Medico-Physicarum Germanicarum Academiae Caesareo-Leopoldinae Naturae Curiosorum Decuriae III. Annus Quintus Et Sextus, Anni M. DC. XCVII & XCVIII. Continens Celeberrimorum Virorum Tum Medicorum tum aliorum Eruditorum in Germania & extra eam Observationes Medico-Physico-Anatomico-Botanico-Mathematicas Cum Appendice & Privilegio Sac. Caes. Majestatis.* , 57–80.
- Schlossmacher, K (1960), “Die Entstehung der Achate, Teil II,” *Z. deutsch. Ges. Edelsteinkde.* **33**, 11–16.
- Schmitt, Raymond W (1995), “The ocean’s salt fingers,” *Sci. Am.* **272** (5), 70–75.
- Schoenly, Paul A, and James A Saunders (1993), “Natural gold dendrites from hydrothermal au-ag deposits: characteristics and computer simulations,” *Fractals* **1** (03), 585–593.
- Schoofs, Stan, Frank J Spera, and Ulrich Hansen (1999), “Chaotic thermohaline convection in low-porosity hydrothermal systems,” *Earth and Planetary Science Letters* **174** (1-2), 213–229.
- Scirocco, R, J. Vermant, and J. Mewis (2004), “Effect of the viscoelasticity of the suspending fluid on structure formation in suspensions,” *J. Non-Newtonian Fluid Mech.* **117**, 183–192.
- Sederholm, J J (Jakob Johannes) (1928), *On orbicular granites, spotted and nodular granites, etc., and on the Rapakivi*

- texture*, Bulletin de la Commission Géologique de Finlande No. 83 (Government Press).
- Seilacher, Adolf (1969), "Fault-Graded Beds Interpreted as Seismites," *Sedimentology* **13** (1-2), 155–159.
- Seilacher, Adolf (2001), "Concretion morphologies reflecting diagenetic and epigenetic pathways," *Sedimentary Geology* **143** (1-2), 41–57.
- Shah, Syed Zahid, Mohammad Sayab, Domingo Aerden, and M. Asif Khan (2011), "Foliation intersection axes preserved in garnet porphyroblasts from the swat area, nw himalaya: A record of successive crustal shortening directions between the indian plate and kohistan–ladakh island arc," *Tectonophysics* **509** (1-2), 14–32.
- Shahidzadeh, Noushine, Marthe F. L. Schut, Julie Desarnaud, Marc Prat, and Daniel Bonn (2015), "Salt stains from evaporating droplets," *Scientific Reports* **5** (1).
- Shahidzadeh-Bonn, Noushine, Julie Desarnaud, François Bertrand, Xavier Chateau, and Daniel Bonn (2010), "Damage in porous media due to salt crystallization," *Physical Review E* **81** (6), 066110.
- Shalev, Eyal, and Vladimir Lyakhovskiy (2012), "Viscoelastic damage modeling of sinkhole formation," *Journal of Structural Geology* **42**, 163–170.
- Shanmugam, G (2016), "The seismite problem," *Journal of Palaeogeography* **5** (4), 318–362.
- Sharp, Ian, P Gillespie, D Morsalnezhad, C Taberner, Ridvan Karpuz, Jaume Vergés, A Horbury, N Pickard, J Garland, and D Hunt (2010), "Stratigraphic architecture and fracture-controlled dolomitization of the cretaceous khami and bangestan groups: an outcrop case study, zagros mountains, iran," Geological Society, London, Special Publications **329** (1), 343–396.
- Shcherbakov, R, and D L Turcotte (2003), "Damage and self-similarity in fracture," *Theoretical and applied fracture mechanics* **39** (3), 245–258.
- Shore, Mark, and Anthony D. Fowler (1996), "Oscillatory zoning in minerals; a common phenomenon," *The Canadian Mineralogist* **34** (6), 1111–1126.
- Short, M B, J. C. Baygents, J. W. Beck, D. A. Stone, R. S. Toomey, and R. E. Goldstein (2005), "Stalactite growth as a free-boundary problem: A geometric law and its platonic ideal," *Physical Review Letters* **94** (1), 018501.
- Smith, Joseph P, and Richard B Coffin (2014), "Methane flux and authigenic carbonate in shallow sediments overlying methane hydrate bearing strata in alaminos canyon, gulf of mexico," *Energies* **7** (9), 6118–6141.
- Snijkers, F, G. D'Avino, P. L. Maffettone, and F. Greco (2009), "Rotation of a sphere in a viscoelastic liquid subjected to shear flow. Part II. Experimental results," *J. Rheol.* **53**, 459–480.
- Sojo, Victor, Barry Herschy, Alexandra Whicher, Eloi Camprubí, and Nick Lane (2016), "The origin of life in alkaline hydrothermal vents," *Astrobiology* **16**, 181–197.
- Sowerby, James (1804), *British Mineralogy* (London: R. Taylor).
- Spry, Alan (1962), "The origin of columnar jointing, particularly in basalt flows," *J. Geol. Soc. Aust.* **8** (2), 191–216.
- Stanulla, Richard, Christiane Stanulla, Erlendur Bogason, Thomas Pohl, and Broder Merkel (2017), "Structural, geochemical, and mineralogical investigation of active hydrothermal fluid discharges at strýtan hydrothermal chimney, akureyri bay, eyjafjörður region, iceland," *Geothermal Energy* **5**, 1–11.
- Starchenko, V, C. J. Marra, and A. J. C. Ladd (2016), "Three-dimensional simulations of fracture dissolution," *J. Geophys. Res. Solid* **121**, 6421–6444.
- Stevens, Joel D, John M. Sharp Jr., Craig T. Simmons, and T.R. Fenstemaker (2009), "Evidence of free convection in groundwater: Field-based measurements beneath wind-tidal flats," *J. Hydrol.* **375**, 394–409.
- Stewart, AM, Lewis T. Chadderton, and Brian R. Senior (2010), "Self-assembly in the growth of precious opal," *Journal of Crystal Growth* **312** (3), 391–396.
- Stöber, Werner, Arthur Fink, and Ernst Bohn (1968), "Controlled growth of monodisperse silica spheres in the micron size range," *Journal of Colloid and Interface Science* **26** (1), 62–69.
- Suess, Erwin (2014), "Marine cold seeps and their manifestations: geological control, biogeochemical criteria and environmental conditions," *International Journal of Earth Sciences* **103**, 1889–1916.
- Summer, Neil S, and Avner Ayalon (1995), "Dike intrusion into unconsolidated sandstone and the development of quartzite contact zones," *J. Struct. Geol.* **17** (7), 997–1010.
- Sun, Yanan, Michael G Edwards, Bin Chen, and Chenfeng Li (2021), "A state-of-the-art review of crack branching," *Engineering Fracture Mechanics* **257**, 108036.
- Sutra, Emilie, Matteo Spada, and Peter Burgherr (2017), "Chemicals usage in stimulation processes for shale gas and deep geothermal systems: a comprehensive review and comparison," *Renewable and Sustainable Energy Reviews* **77**, 1–11.
- Swennen, R, V. Vandeginste, and R. Ellam (2003), "Genesis of zebra dolomites (Cathedral Formation: Canadian-Cordillera Fold and Thrust Belt, British Columbia)," *Journal of Geochemical Exploration Proceedings of Geofluids IV*, **78-79**, 571–577.
- Szymczak, P, and A. J. C. Ladd (2011), "The initial stages of cave formation: Beyond the one-dimensional paradigm," *Earth Planet. Sci. Lett.* **301**, 424–432.
- Szymczak, P, and A. J. C. Ladd (2012), "Reactive infiltration instabilities in rocks. Fracture dissolution," *J. Fluid Mech.* **702**, 239–264.
- Szymczak, P, and A. J. C. Ladd (2014), "Reactive infiltration instabilities in rocks. Part 2. Dissolution of a porous matrix," *J. Fluid Mech.* **738**, 591–630.
- Tarasovs, Sergejs, and Ahmad Ghassemi (2014), "Self-similarity and scaling of thermal shock fractures," *Physical Review E* **90** (1), 012403.
- Teichert, Barbara MA, Gerhard Bohrmann, and Erwin Suess (2005), "Chemoherms on hydrate ridge—unique microbially-mediated carbonate build-ups growing into the water column," *Palaeogeography, Palaeoclimatology, Palaeoecology* **227** (1-3), 67–85.
- Testón-Martínez, Sergio, Laura M Barge, Jan Eichler, C Ignacio Sainz-Díaz, and Julyan H E Cartwright (2024), "Experimental modelling of the growth of tubular ice brinicles from brine flows under sea ice," *The Cryosphere* **18** (5), 2195–2205.
- Theeuwes, Felix (1975), "Elementary osmotic pump," *Journal of pharmaceutical sciences* **64** (12), 1987–1991.
- Thomas, Katherine, Stephan Herminghaus, Hubertus Porada, and Lucas Goehring (2013), "Formation of kinneyia via shear-induced instabilities in microbial mats," *Philosophical Transactions of the Royal Society A: Mathematical, Physical and Engineering Sciences* **371** (2004), 20120362.
- Tivey, Margaret Kingston (2007), "Generation of seafloor hy-

- drothermal vent fluids and associated mineral deposits," *Oceanography* **20** (1), 50–65.
- Tomkeieff, S I (1940), "The basalt lavas of the Giant's Causeway district of Northern Ireland," *Bull. Volcanol.* **6**, 89–146.
- Toramaru, A, and T. Matsumoto (2004), "Columnar joint morphology and cooling rate: A starch-water mixture experiment," *J. Geophys. Res.* **109**, B02205.
- Toussaint, Renaud, Einat Aharonov, Daniel Koehn, J-P Gratier, Martin Ebner, Patrick Baud, Alexandra Rolland, and Francois Renard (2018), "Stylolites: A review," *Journal of Structural Geology* **114**, 163–195.
- Trainer, Jr, David W (1931), "'Zebra' Rock," *American Mineralogist* **16** (5), 221–225.
- Trefry, Michael G, Daniel R Lester, Guy Metcalfe, and Junhong Wu (2019), "Temporal fluctuations and poroelasticity can generate chaotic advection in natural groundwater systems," *Water Resources Research* **55** (4), 3347–3374.
- Trimmer, Joshua (1845), "On the pipes or sand-galls in the chalk and chalk-rubble of Norfolk," *Quarterly Journal of the Geological Society* **1** (1), 300–317.
- Trivedi, R, and W Kurz (1994), "Dendritic growth," *International Materials Reviews* **39** (2), 49–74.
- Trusheim, Ferdinand (1957), "Über halokinese und ihre bedeutung für die strukturelle entwicklung norddeutschlands," *Zeitschrift der deutschen geologischen Gesellschaft*, 111–151.
- Turing, Alan Mathison (1952), "The chemical basis of morphogenesis," *Phil. Trans. R. Soc. Lond. B* **237**, 37–72.
- Turner, JS (1995), "Laboratory models of growing flanges, and a comparison with other growth mechanisms of "black smoker" chimneys," *Earth and Planetary Science Letters* **134** (3-4), 491–499.
- Tyler, SW, S. Kranz, M.B. Parlange, J. Albertson, G.G. Katul, G.F. Cochran, B.A. Lyles, and G. Holder (1997), "Estimation of groundwater evaporation and salt flux from Owens Lake, California, USA," *J. Hydrol.* **200** (1), 110–135.
- Ueno, K, M Farzaneh, S Yamaguchi, and H Tsuji (2010), "Numerical and experimental verification of a theoretical model of ripple formation in ice growth under supercooled water film flow," *Fluid Dynamics Research* **42** (2), 025508.
- Upadhyay, Virat K, Piotr Szymczak, and Anthony J. C. Ladd (2015), "Initial conditions or emergence: What determines dissolution patterns in rough fractures?" *J. Geophys. Res. Solid Earth* **120** (9), 6102–6121.
- Van Dam, Remke L, Craig T. Simmons, David W. Hyndman, and Warren W. Wood (2009), "Natural free convection in porous media: First field documentation in groundwater," *Geophysical Research Letters* **36** (11).
- Van Straaten, LMJU (1978), "Dendrites," *Journal of the Geological Society* **135** (1), 137–151.
- Vance, Steven D, Laura M Barge, Silvana S S Cardoso, and Julyan H E Cartwright (2019), "Self-assembling ice membranes on Europa: brinicle properties, field examples, and possible energetic systems in icy ocean worlds," *Astrobiology* **19** (5), 685–695.
- Vasseur, Jérémie, and Fabian B. Wadsworth (2019), "The permeability of columnar jointed lava," *J. Geophys. Res.: Solid Earth* **124** (11), 11305–11315.
- Vasseur, Jérémie, Fabian B Wadsworth, and Donald B Dingwell (2020), "Permeability of polydisperse magma foam," *Geology* **48** (6), 536–540.
- Veran-Tissoires, Stéphanie, Manuel Marcoux, and Marc Prat (2012), "Discrete salt crystallization at the surface of a porous medium," *Physical review letters* **108** (5), 054502.
- Vernon, RH (1985), "Possible role of superheated magma in the formation of orbicular granitoids," *Geology* **13** (12), 843–845.
- Veveakis, Manolis, and Thomas Poulet (2021), "A note on the instability and pattern formation of shrinkage cracks in viscoplastic soils," *Geomechanics for Energy and the Environment* **25**, 100198.
- Voigtländer, Anne, Morgane Houssais, Karol A Bacik, Ian C Bourg, Justin C Burton, Karen E Daniels, Sujit S Datta, Emanuela Del Gado, Nakul S Deshpande, Olivier Devauchelle, *et al.* (2024), "Soft matter physics of the ground beneath our feet," *Soft Matter* **20** (30), 5859–5888.
- Voisey, Christopher R, Nicholas JR Hunter, Andrew G Tomkins, Joël Brugger, Weihua Liu, Yang Liu, and Vladimir Luzin (2024), "Gold nugget formation from earthquake-induced piezoelectricity in quartz," *Nature Geoscience*, 1–6.
- Wagner, Carl (1961), "Theorie der Alterung von Niederschlägen durch Umlösen (Ostwald-Reifung)," *Zeitschrift für Elektrochemie, Berichte der Bunsengesellschaft für physikalische Chemie* **65** (7-8), 581–591.
- Walger, Eckart, Georgvon Mattheß, Volker Seckendorff, and Friedrich Liebau (2009), "The formation of agate structures: models for silica transport, agate layer accretion, and for flow patterns and flow regimes in infiltration channels," *Neues Jahrbuch für Mineralogie-Abhandlungen*, 113–152.
- Wallace, Malcolm W, and Ashleigh v. S. Hood (2018), "Zebra textures in carbonate rocks: Fractures produced by the force of crystallization during mineral replacement," *Sedimentary Geology* **368**, 58–67.
- Walsh, P, and I. Morawiecka-Zacharz (2001), "A dissolution pipe palaeokarst of mid-pleistocene age preserved in miocene limestones near staszow, poland," *Palaeogeography, Palaeoclimatology, Palaeoecology* **174** (4), 327–350.
- Wang, Yifeng, and Enrique Merino (1990), "Self-organizational origin of agates: Banding, fiber twisting, composition, and dynamic crystallization model," *Geochimica et Cosmochimica Acta* **54** (6), 1627–1638.
- Washburn, Edward R (2002), "The creeping of solutions," *The Journal of Physical Chemistry* **31** (8), 1246–1248.
- Weinberger, R, and A. Burg (2019), "Reappraising columnar joints in different rock types and settings," *J. Struct. Geol.* **125**, 185–194.
- Weinberger, Ram (1999), "Initiation and growth of cracks during desiccation of stratified muddy sediments," *Journal of structural geology* **21** (4), 379–386.
- Wellman, H W, and A T Wilson (1965), "Salt weathering, a neglected geological erosive agent in coastal and arid environments," *Nature* **205** (4976), 1097–1098.
- Welsch, B, F. Faure, V. Famin, A. Baronnet, and P. Bachèlery (2013), "Dendritic crystallization: A single process for all the textures of olivine in basalts?" *Journal of Petrology* **54**, 539–574.
- van Westen, Thijs, and Robert D. Groot (2018), "Effect of Temperature Cycling on Ostwald Ripening," *Crystal Growth & Design* **18** (9), 4952–4962.
- White, JF, and J.F. Corwin (1961), "Synthesis and origin of chalcedony," *American Mineralogist: Journal of Earth and Planetary Materials* **46** (1-2), 112–119.
- White, W B (1977), "Role of solution kinetics in the development of karst aquifers," *Mem. Int. Assoc. Hydrogeol.* **12**, 503–517.
- Whitehead Jr, John A, and Douglas S Luther (1975), "Dy-

- namics of laboratory diapir and plume models,” *Journal of Geophysical Research* **80** (5), 705–717.
- Wijnhorst, R, M. Prat, and N. Shahidzadeh (2023), “The self-organized structure of salt efflorescence,” to be submitted.
- Wijnhorst, R, F. Van der Sloot, L. Pel, and N. Shahidzadeh (2024), “Effect of evaporative surface area on salt efflorescence and subflorescence formation in a given porous material,” *Physical Review Applied* **21** (6).
- Witten, Thomas A, and Leonard M Sander (1981), “Diffusion-limited aggregation, a kinetic critical phenomenon,” *Physical review letters* **47** (19), 1400.
- Witten, Thomas A, and Leonard M Sander (1983), “Diffusion-limited aggregation,” *Physical review B* **27** (9), 5686.
- Witten Jr, TA, and Leonard M Sander (1981), “Diffusion-limited aggregation, a kinetic critical phenomenon,” *Physical review letters* **47** (19), 1400.
- Wollkind, David J, and J Iwan D Alexander (1982), “Kelvin–helmholtz instability in a layered newtonian fluid model of the geological phenomenon of rock folding,” *SIAM Journal on Applied Mathematics* **42** (6), 1276–1295.
- Won, D, and C. Kim (2004), “Alignment and aggregation of spherical particles in viscoelastic fluid under shear flow,” *J. Non-Newtonian Fluid Mech.* **117**, 141–146.
- Wooding, R A (1960), “Rayleigh instability of a thermal boundary layer in flow through a porous medium,” *J. Fluid Mech.* **9** (2), 183–192.
- Wooding, R A, S. W. Tyler, and I. White (1997a), “Convection in groundwater below an evaporating Salt Lake: 1. Onset of instability,” *Water Resour. Res.* **33** (6), 1199–1217.
- Wooding, R A, Scott W. Tyler, Ian White, and P. A. Anderson (1997b), “Convection in groundwater below an evaporating Salt Lake: 2. Evolution of fingers or plumes,” *Water Resour. Res.* **33** (6), 1219–1228.
- Woodward, S P (1864), “On the nature and origin of banded flints,” *Geological Magazine* **1** (4), 145–149.
- Worster, M Grae (2024), “On icicle ripples,” *Journal of Engineering Mathematics* **145**, 15–45.
- Wu, Hao, Richard S. Jayne, Robert J. Bodnar, and Ryan M. Pollyea (2021), “Simulation of CO₂ mineral trapping and permeability alteration in fractured basalt: Implications for geologic carbon sequestration in mafic reservoirs,” *Int. J. Greenhouse Gas Control* **109**, 103383.
- Wurtsbaugh, Wayne A, Craig Miller, Sarah E. Null, R. Justin DeRose, Peter Wilcock, Maura Hahnenberger, Frank Howe, and Johnnie Moore (2017), “Decline of the world’s saline lakes,” *Nature Geosci.* **10**, 816.
- Xiao, Zhiyong, Zuoxun Zeng, Zhiyong Li, David M. Blair, and Long Xiao (2014), “Cooling fractures in impact melt deposits on the moon and mercury: Implications for cooling solely by thermal radiation,” *J. Geophys. Res. Planets* **119** (7), 1496–1515.
- Yardley, BWD, C.A. Rochelle, A.C. Barnicoat, and G.E. Lloyd (1991), “Oscillatory zoning in metamorphic minerals: an indicator of infiltration metasomatism,” *Mineralogical Magazine* **55** (379), 357–365.
- Yariv, Shmuel, and Harold Cross (1979), *Geochemistry of colloid systems: For earth scientists* (Springer Science & Business Media).
- Yuen, David A, and Andrei V Malevsky (1992), “Strongly chaotic newtonian and non-newtonian mantle convection,” in *Chaotic processes in the geological sciences* (Springer) pp. 71–88.
- Zhabotinsky, Anatol M (1991), “A history of chemical oscillations and waves,” *Chaos: An Interdisciplinary Journal of Nonlinear Science* **1** (4), 379–386.
- Zhang, Zhaorui, Zhenni Wang, Shengnan He, Chaoqi Wang, Mingshang Jin, and Yadong Yin (2015), “Redox reaction induced Ostwald ripening for size- and shape-focusing of palladium nanocrystals,” *Chemical Science* **6** (9), 5197–5203.
- Zhao, Zhen-yu, Yan-ru Guo, WANG Yan, LIU Hong, and Qing Zhang (2014), “Growth patterns and dynamics of mud cracks at different diagenetic stages and its geological significance,” *International Journal of Sediment Research* **29** (1), 82–98.
- Zheng, Hu, Wenqing Niu, Wuwei Mao, Lihui Li, Fawu Wang, and Yu Huang (2021), “Mechanics of granular material and the application in engineering geology,” *Journal of Engineering Geology* **29** (1), 12–24.
- Zhu, Chuanwei, S. Liao, Wei Wang, Yuxu Zhang, Tao Yang, H. Fan, and H. Wen (2018), “Variations in Zn and S isotope chemistry of sedimentary sphalerite, Wusihe Zn–Pb deposit, Sichuan province, China,” *Ore Geology Reviews* **95**, 639–648.
- Zieg, Michael J, and Bruce D Marsh (2005), “The Sudbury igneous complex: Viscous emulsion differentiation of a superheated impact melt sheet,” *Geological Society of America Bulletin* **117** (11–12), 1427–1450.
- Zöcher, H (1925), “Über freiwillige Strukturbildung in Solen,” *Z. anorg. Chem* **147**, 91–110.